NRF2 Confers Disease Tolerance to Bloodstream Infections

Ana Martins Ribeiro

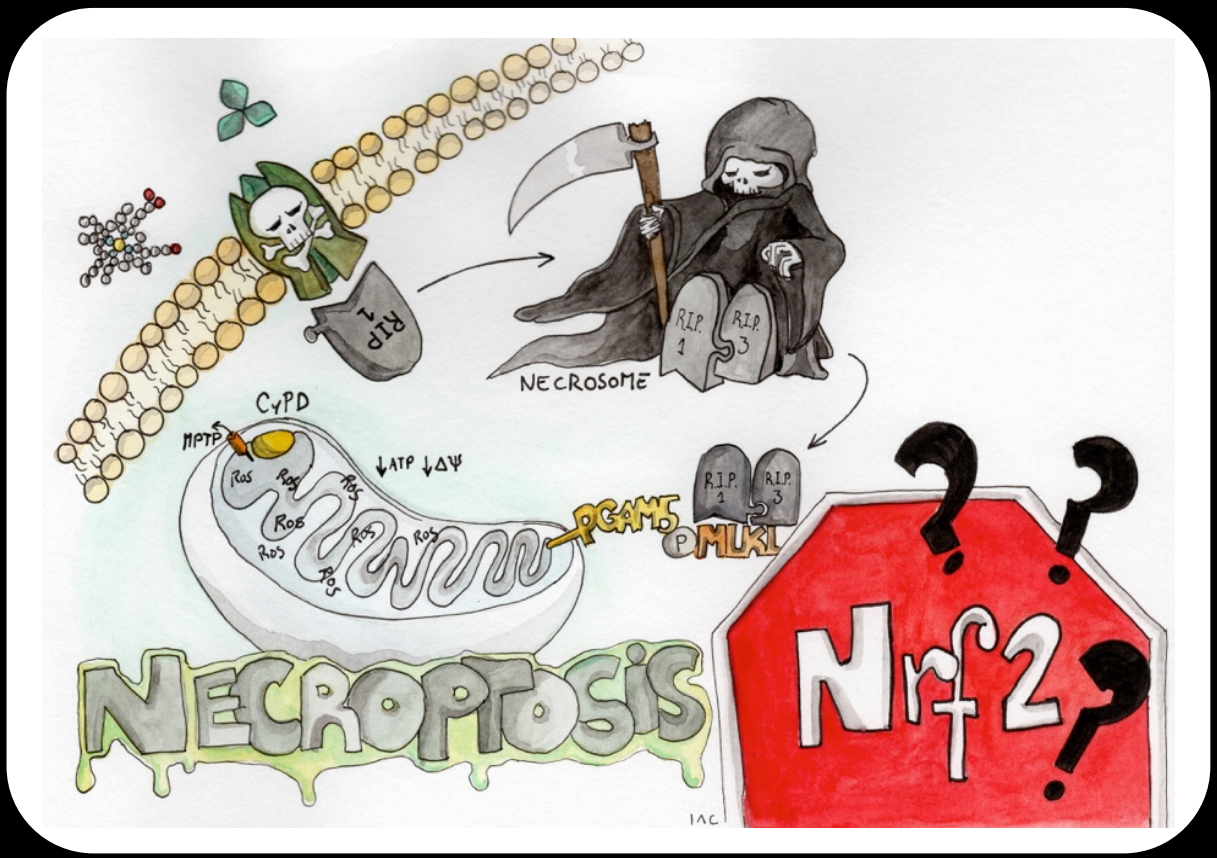

Dissertation presented to obtain the Ph.D degree in Immunology

Instituto de Tecnologia Química e Biológica António Xavier | Universidade Nova de Lisboa

Oeiras,
June, 2017

UNIVERSIDADE NOVA DE LISBOA

Nrf2 Confers Disease Tolerance to Bloodstream Infections

Ana Martins Ribeiro

Dissertation presented to obtain the Ph.D degree in Immunology

Instituto de Tecnologia Química e Biológica António Xavier | Universidade Nova de Lisboa

Research work coordinated by:

FUNDAÇÃO CALOUSTE GULBENKIAN
Instituto Gulbenkian de Ciência

Oeiras, June 2017

Nrf2 Confers Disease Tolerance to Bloodstream Infections

Ana Martins Ribeiro

Supervisor: Doctor Miguel P. Soares

PhD Fellowship financed by
Fundação para a Ciência e Tecnologia, SFRH/BD/51877/2012

Oeiras, June 2017

FUNDAÇÃO CALOUSTE GULBENKIAN
Instituto Gulbenkian de Ciência

Acknowledgements

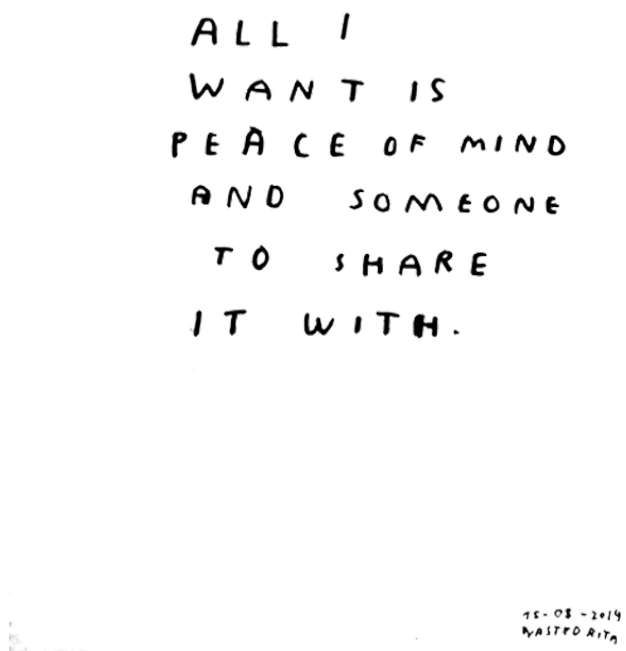

I would like to thank my supervisor, Miguel Soares, for welcoming me in his lab. I acknowledge all the lessons he gave me on how to be a critical thinker, a thorough researcher and an enthusiastic performer. Under his supervision I have learned what it is to be a good scientist and a better person.

I also want to express my most profound gratitude to Raffaella Gozzelino, who trusted me the project she had started. With her I have learned extremely valuable lessons from TNF-dependent cell death to how to survive in this complicated multicellular, multiorganismal, multipersonality world of science. Thank you for your friendship and for believing in me the way you did – it changed

the way I see myself and it definitely changed my life. “Friendship always comes first”, you said. I will never forget it and you will always have a special place in my heart as a friend for life.

A big “thank you” to all my former and present colleagues from the Inflammation lab. Wherever I go next, it will be very difficult to have such a friendly, helpful and fun environment like the one we had together. During these past years, I spent most time of my life in this big house that is the IGC and I can proudly and happily call you my “IGC family”.

A very special thanks to the people who are (or once were) my colleagues at the inflammation lab and will forever be much more than that: Susana Ramos, Bahtiyar Yilmaz, Birte Blankenhaus, Sebastian Weis, Sílvia Cardoso, Patricia Bastos, Vital Domingues and Rita Carlos. Thank you for always being there for me when I needed (with experiments or just with the right words at the right moment) and for making me feel safe during the hard times. Also, thank you for the good moments – we had a few ones and those are the ones I will always keep.

I cannot forget to mention the “collaborators” in this project: Pedro Elias Marques and Damian Trujillo. We had a great time togetstrher with beer and pastéis de nata. In the end, the friendship stayed (and so did the cool data!).

To my PIBS 2011 friends Ana Stankovich, Marta Marialva, Rita Aires, Sandra Tavares, Inês Pais and Rômulo Areal, a big hug. We have started this journey together as “little kids” and it was great to grow up next to you. I admire all of you and I know you will have a lot of success in your lives, no matter what you choose to do with it.

My “IGC family” includes very special friends who were extremely important during this expedition and will remain with me forever: Inês Cabral (who draw the cover of this thesis – you are awesome, Inezinha!), Pedro Alves, Ana Regalado, Joana Loureiro, Luciana de

Moraes, Zoé Enderlin, Vânia Silva, Elvira Lama and Erik Van Bergen. Thank you for all the laughs we've shared, all the beers we've drank and all the tears you've cleaned. You made my days lighter and shinier.

A big "thank you" to Sofia Tavares, Tatiana Rocha, Gabriel Martins and João Madureira. Practical questions related to your daily duties led me to talk more with you and discover great personalities. I am very thankful for what you have done for me.

Because I still had 10% of the time to dedicate to my life outside of the PhD, I want to mention my friends who were always there for me: Luís Marques, Tatiana Rodrigues, Rita Ferreira and Inês Santarino. You know how important you are for me. I miss spending more time with you and I enjoy every second of it when life allows us. Without those moments, these past few years would have been much harder. Of course I have to mention Inês' PhD work: thank you for trusting my knowledge and for including me in your work and your paper – I am very happy to share it with you and that's another connection we will always keep.

I would also like to thank Josina Côrte-Real, my singing teacher, for being such an amazing professional and for letting me believe I can have an alternative career. I love every class with you and that unique feeling of lightness that only appears after singing.

My most special acknowledgement goes to my family: Caetano Souto Maior (I'll try not to go romantic on this), I love you and it is because of you that I never fell off the rope, you make my life a better place every day; and my parents, without whom I would not be here.

I thank my thesis committee Luís Teixeira and Moisés Mallo for the yearly discussions about my work. Thank you Thiago Carvalho and Élio Sucena for choosing me to be part of the IGC community in the first place and for hearing me when I needed.

I would like to thank all the members of the jury: Helena Vieira, Cecília Rodrigues, Luís Ferreira Moita and Colin Adrain for kindly accepting to review this thesis and spend some time discussing my work on *the big day*.

Finally, a very special “thank you” to Iqbal Hamza who believed some day I would finish my thesis with enough success to join his lab. Your kind support was very important for me and contributed immensely to this work. Thank you for trusting me, I will not let you down.

Abstract

Described originally in plants, disease tolerance is a defense strategy against infection, which protects the host by sustaining homeostasis without exerting a direct negative impact on pathogens. This is enforced by a myriad of stress and damage responses conferring tissue damage control and preventing *"damage to functions and structures"*, fully operational in animals, including flies, mice and humans.

Production of cytotoxic levels of reactive oxygen species (ROS) is a common resistance mechanism against infection as it mediates pathogen killing. However, there is a clear trade-off in the activation of this defense strategy in that ROS can lead to oxidative stress in host parenchymal cells, eventually leading to programmed cell death, tissue dysfunction and damage. The stress response to oxidative insults is mastered by the transcription factor Nuclear Factor E2-Related Factor-2 (NRF2). Under homeostasis, NRF2 binds to the Kelch-like ECH-associated protein 1 (KEAP1), a redox sensor constitutively associated with the Cul3–Rbx1 E3 ubiquitin ligase complex, which ubiquitinates and targets Nrf2 for degradation by the 26s proteasome. Oxidative stress impairs KEAP1 binding to the Cul3–Rbx1 complex, sparing NRF2 from degradation and allowing for the *de novo* synthetized NRF2 to undergo nuclear translocation. Inside the nucleus, this transcription factor binds to Antioxidant Responsive Elements (AREs), promoting the transcription of genes encoding for cytoprotective proteins mediating metabolic adaptation and detoxification, allowing the return to homeostasis.

Bloodstream infections are associated with varying levels of hemolysis and therefore with the generation of extracellular

hemoglobin, which releases its heme prosthetic groups upon oxidation. When released from extracellular oxidized hemoglobin, labile heme can sensitize parenchyma cells to undergo programmed cell death in response to a variety of inflammatory agonists, such as Tumor Necrosis Factor (TNF). This deleterious effect is driven to a large extent by the generation of ROS, leading to mitochondrial dysfunction and programmed cell death. As a consequence, released Damage Associated Molecular Patterns (DAMPs) from damaged tissues sustain inflammation and cellular stress. Many of these pathogenic effects are countered by the stress-response regulated by NRF2 and involve the expression of a variety of effector genes, including the heme-catabolizing enzyme HO-1 (Heme Oxygenase-1) and the iron sequestering protein Ferritin Heavy Chain (FtH), which are essential to establish disease tolerance to bloodstream infections.

In this PhD thesis we hypothesized that the mechanism via which the stress-response regulated by NRF2 confers tissue damage control and establishes disease tolerance to bloodstream infections involves the inhibition of programmed cell death by necroptosis. Here, we demonstrate that NRF2 is activated in response to labile heme both *in vivo* and *in vitro,* and protects parenchyma cells from undergoing necroptosis triggered by heme and TNF. This protective effect is mediated by a mechanism preserving mitochondrial function downstream of the signal transduction pathway comprising Receptor-Interacting serine/threonine-Protein Kinase 1 (RIPK1), Receptor-Interacting serine/threonine-Protein Kinase 3 (RIPK3), Mixed lineage kinase domain like pseudokinase (MLKL) and Phosphoglycerate Mutase Family Member 5 (PGAM5). In the specific case of *Plasmodium* infection, this cytoprotective effect also targets the participation of Cyclophilin D (CYPD), presumably on the

regulation of the mitochondrial permeability transition pore (MPTP) leading to necrosis.

Our work demonstrates that NRF2 is essential to confer tissue damage control and establish disease tolerance to bloodstream infectious diseases associated with hemolysis, such as malaria and sepsis. We propose that manipulation of signal transduction pathways that modulate the cellular redox status might unravel a general mechanism for tissue damage control and disease tolerance in different inflammation models accompanied by the accumulation of labile heme.

Sumário

Descrita originalmente em plantas, a tolerância à doença é uma estratégia de defesa contra infecções que protege o hospedeiro através da manutenção da homeostasia sem exercer qualquer efeito negativo directo nos agentes patogénicos. Esta estratégia é reforçada por uma miríade de respostas ao stress e dano, conferindo controlo de danos no tecido e prevenindo *"danos a funções e estruturas"*, encontrando-se integralmente operacional em animais, incluindo moscas, ratinhos e humanos.

A produção de níveis citotóxicos de espécies reactivas de oxigénio é uma estratégia comummente utilizada como parte de um mecanismo de resistência contra infecções, na medida em que contribui para a morte do agente patogénico. Porém, existe um claro *trade-off* na activação desta estratégia de defesa uma vez que as espécies reactivas de oxigénio induzem stress oxidativo, culminando na disfunção e dano tecidular. A resposta a stress induzida por agentes pro-oxidantes é regulada pelo factor de transcrição Nuclear Factor E2-Related Factor-2 (NRF2). Em condições de homeostasia, esta proteína liga-se ao Kelch-like ECH-associated protein 1 (KEAP1), um sensor redox constitutivamente associado ao complexo Cul3–Rbx1 E3 ubiquitin ligase, levando à ubiquitinação do NRF2 e ao seu direccionamento para degradação pelo proteasoma 26s. O stress oxidativo impede a ligação do KEAP1 ao complexo Cul3–Rbx1 e permite que o NRF2 sintetizado *de novo* seja translocado para o núcleo. Uma vez no núcleo, o NRF2 liga-se ao um grupo de promotores denominados Elementos de Resposta Antioxidante, promovendo a transcrição de genes codificantes para proteínas citoprotectoras responsáveis pela adaptação metabólica e detoxificação do sistema, promovendo o retorno à homeostasia.

Infecções da corrente sanguínea estão associadas a diferentes graus de hemólise e, por conseguinte, à acumulação de hemoglobina no meio extracelular, o que promove a sua oxidação e libertação dos seus grupos prostéticos (heme). Quando libertado da hemoglobina extracelular oxidada, o heme lábil pode induzir a morte celular programada de células do parênquima, quando na presença de agonistas inflamatórios como o Tumor Necrosis Factor (TNF). Este efeito deletério é promovido maioritariamente pela geração de espécies reactivas de oxigénio, o que leva à disfunção mitocondrial e morte celular programada. Como consequência, a libertação de *Damage Associated Molecular Patterns (DAMPs)* dos tecidos lesados sustém a inflamação e stress celular.

Os efeitos deletérios do heme lábil são contrabalançados pela resposta ao stress mediada por NRF2, envolvendo a expressão de genes efectores incluindo o gene que codifica para HO-1 (Heme Oxygenase-1) e para a proteína sequestradora de ferro FtH (Ferritin Heavy Chain), cujas funções foram já associadas ao estabelecimento de tolerância à doença em infecções da corrente sanguínea.

A nossa hipótese neste trabalho é que o mecanismo através do qual a resposta a stress mediada por NRF2 confere controlo de danos no tecido e estabelece tolerância a infecções da corrente sanguínea envolve a inibição da morte celular programada, particularmente através da via de necroptose. Os nossos resultados demonstram que o NRF2 é activado em resposta ao heme lábil tanto *in vivo* como *in vitro* e protege as células parênquimais de sofrerem necroptose em resposta ao efeito sinergístico do heme com o TNF. O nosso trabalho revela que a protecção conferida pelo NRF2 assenta num mecanismo que preserva a função mitocondrial *downstream* à via de sinalização que inclui as proteínas Receptor-Interacting serine/threonine-Protein Kinase 1 (RIPK1), Receptor-

Interacting serine/threonine-Protein Kinase 3 (RIPK3), Mixed lineage kinase domain like pseudokinase (MLKL) e Phosphoglycerate Mutase Family Member 5 (PGAM5). No caso específico da infecção causada por *Plasmodium*, o efeito citoprotector do NRF2 também tem como alvo a proteína Cyclophilin D (CYPD) e, presumivelmente, a modulação da transição de permeabilidade mitocondrial (*MPTP*) e a indução de necrose.

O nosso trabalho demonstra que o NRF2 é essencial para o controlo de danos no tecido e para estabelecer tolerância à doença no contexto de infecções da corrente sanguínea associadas a hemólise, como a malária e a sépsis. Assim, propomos que a manipulação das vias de transdução de sinal que modulam o estado *redox* das células poderá deslindar um mecanismo geral de controlo de danos no tecido e tolerância à doença em diferentes modelos de inflamação associados a condições de hemólise.

List of abbreviations

A-T: Ataxia-Telangiectasia
ABCB6: ATP Binding Cassette subfamily B member 6 (Langereis blood group)
ADP: Adenosine Diphosphate
ALIS: Aggresome-Like Induced Structure
ALT: Alanine Aminotransferase
AMP: Adenosine Monophosphate
AMPK: 5' Adenosine Monophosphate-activated Protein Kinase
APAP: Acetaminophen
AQP: Aquaporin
ARE: Antioxidant Response Element
AST: Aspartate Aminotransferase
ATF: Activating Transcription Factor
Atg: Autophagy related
ATM: Ataxia-Telangiectasia Mutated protein kinase
ATP: Adenosine Triphosphate
BMDM: Bone Marrow Derived Macrophages
Brx: Protein Kinase A-Anchoring Protein13
Casp8: Caspase 8
CAT: Catalase
cFLIP$_L$: FLICE-inhibitory protein (long form)
CFU: Colony Forming Units
cIAP: Cellular inhibitor of apoptosis
CK: Creatine Kinase
CLP: Cecal Ligation and Puncture
CO: Carbon monoxide Coactivator 1α
COI (or CoxI): Cytochrome c Oxidase Subunit I
COIII (or CoxIII): Cytochrome c Oxidase Subunit III
Con A: Concanavalin A
CS: Citrate Synthase
Cul3: Cullin 3
CypD: Cyclophilin D
Cytb: Cytochrome b
DAI: DNA-Dependent Activator of IFN-Regulatory Factors
DAMP: Damage Associated Molecular Pattern

DCFDA: 2',7'-Dichlorofluorescin Diacetate

Drp1: Dynamin-Related Protein1

ECM: Experimental Cerebral Malaria

EPO: Erythropoietin

ER: Endoplasmic Reticulum

ERAD: Endoplasmic Reticulum-Associated Protein Degradation

ETC: Electron Transport Chain

FADD: FAS Associated Death Domain

FCCP: Carbonyl cyanide-p-trifluoromethoxyphenylhydrazone

Fe^{2+}: Ferrous iron

Fe^{3+}: Ferric iron

FtH: Ferritin Heavy Chain

G6PD: Glucose 6 Phosphate Dihydrogenase

GCLM: Glutamate-Cysteine Ligase, Modifier Subunit

GPx: Glutathione Peroxidase

GSH: Reduced Glutathione

GSK-3b: Glycogen Synthase Kinase 3 Beta

GSSH: Oxidized Glutathione

GST: Glutathione S-Transferase

H&E: Hematoxilin and Eosin

H_2O_2: Hydrogen Peroxide

HIF: Hypoxia Inducible Factor

HMGB1: High Mobility Group Box1

HO-1: Heme Oxygenase-1

HOIL-1: Heme-Oxidized Iron Regulated Protein 2 (IRP2) Ubiquitin Ligase-1

Hrd1: ERAD-Associated E3 Ubiquitin-Protein Ligase

HRE: Hypoxia Response Element

HRG1: Heme Responsive Gene1

HRI: Heme-Regulated eIF2α Kinase

HSF1: Heat-Shock Factor 1

HSP: Heat-Shock Protein

HSR: Heat-Shock Response

IgG: Immunoglobulin G

IkBα: NF-kappa-B Inhibitor Alpha

IKK: Inhibitor of κB kinase

IL: Interleukin

iNOS (NOS2): Nitric Oxide Synthase

IRI: Ischemia Reperfusion Injury

IRP2: Iron Regulated Protein 2

KEAP1: Kelch-like ECH-Associated Protein1

LAP: LC3-Associated Phagocytosis

LC3: Microtubule-Associated Protein1 Light Chain 3

LDH: Lactate Dehydrogenase

LPS: Lipopolysaccharide

LUBAC: Linear Ubiquitin Chain Assembly Complex

MAPK: Mitogen-Activated Protein Kinase

MCP-1: Monocyte chemotactic protein 1

MEF: Mouse Embryonic Fibroblast

MIP: Macrophage Inflammatory Protein

MLKL: Mixed Lineage Kinase Domain-Like

MnSOD: Manganese Superoxide Dismutase

Mø: Macrophages

MPTP: Mitochondrial Permeability Transition Pore

mTOR: Mechanistic Target Of Rapamycin

MyD88: Myeloid Differentiation Primary Response Gene 88

NAC: N-Acetyl cysteine

NADPH: Nicotinamide Adenine Dinucleotide Phosphate

NBR1: Neighbor of Braca 1

Nd1: NADPH Dehydrogenase

NDP52: Nuclear Dot Protein 52

Nec-1: Necrostatin-1

NF-κB: Nuclear Factor Kappa-Light-Chain-Enhancer of Activated B Cells

NFAT5: Nuclear Factor of Activated T-cells 5

NLRP3: NACHT, LRR and PYD Domains-Containing Protein 3

NO: Nitric Oxide

NOX: NADPH Oxidase

Nqo1: NAD(P)H:Quinone Oxidoreductase-1

NRF1: Nuclear Respiratory Factor 1

NRF2: Nuclear Factor-Erythroid 2-Related Factor 2

NRF3: Nuclear Factor (Erythroid2)-Like Factor 3

O_2^-: Superoxide Anion

ORE: Osmotic Response Element

OXPHOS: Oxidative Phosphorylation

p62 (SQTM): Ubiquitin-Binding Protein p62 (Sequestosome-1)

PAMP: Pathogen Associated Molecular Pattern

Pcc*: *Plasmodium chabaudi chabaudi

PCD: Programmed Cell Death

PERK1: Proline-Rich Receptor-Like Protein Kinase

PGAM5: Phosphoglycerate Mutase Family Member 5

PGC1α: Peroxisome Proliferator-Activated Receptor γ

PHZ: Phenylhydrazine

PMI: p62-Mediated Mitophagy Inducer

PRR: Pattern Recognition Receptor

PS: Phosphatidylserine

RANKL: Receptor Activator of Nuclear Factor Kappa-B Ligand

RANTES: Regulated on Activation, Normal T Cell Expressed and Secreted

RBC: Red Blood Cell

Rbx1: Ring-Box 1

RHIM: RIP Homotypic Interaction Motif

RIPK1: Receptor Interacting Protein Kinase 1

RIPK3: Receptor Interacting Protein Kinase 3

RIRR: ROS-Induced ROS Release

RNS: Reactive Nitrogen Species

ROS: Reactive Oxygen Species

SCFβ-TrCP: Skp1 (S-Phase Kinase-Associated Protein1) - Cul1-F-Box (SCF)-β-Transducin Repeats-Containing Proteins (β-TrCP)

SEM: Standard Error of the Mean

SIRS: Systemic Inflammatory Response Syndrome

SLC: Solute Carrier Channel

sMAF: Small Musculoaponeurotic Fibrosarcoma

SOD: Superoxide Dismutase

SRXN1: Sulfiredoxin 1

STD: Standard Deviation

Tfam: Transcription Factor A, Mitochondrial

TLR: Toll-Like Receptor

TMRE: TetraMethylrRhodamine Ethyl ester

TMRM: TetraMethylRhodamine Methyl ester

TNF: Tumor Necrosis Factor

TNFR1: Tumor Necrosis Factor Receptor 1

TR: Transferin Receptor

TRADD: TNF Receptor-Associated Death Domain

TRAF: TNF Receptor Associated Factor

TRAIL: TNF-Related Apoptosis-Inducing Ligand

TRX1: Thioredoxin 1

TXNRD1: Thioredoxin Reductase 1

Ub: Ubiquitin

UCP3: Uncoupler Protein 3

UPR: Unfolded Protein Response

vATPase: Vacuolar-Type H^+ -ATPase

VHL: Ubiquitin Ligase Von Hippel–Lindau

Xbp1: X-box-Binding Protein 1

ΔΨm: Mitochondrial Membrane Potential

Table of contents

CHAPTER 1: INTRODUCTION 1

1.1. INFLAMMATION AND THE BREAKDOWN OF HOMEOSTASIS 2
1.2. HOST DEFENSE STRATEGIES AGAINST INFECTION 2
1.2.1. DISEASE TOLERANCE AND TISSUE DAMAGE CONTROL 4
1.2.2. STRESS RESPONSES UNDERLYING TISSUE DAMAGE CONTROL 5
1.2.3. DAMAGE RESPONSES UNDERLYING TISSUE DAMAGE CONTROL: THE ROLE OF NRF2 19
1.3. NRF2 IN CELLULAR REDOX HOMEOSTASIS 30
1.3.1. NRF2 , NADPH OXIDASES AND MITOCHONDRIA 31
1.3.2. NRF2 AND MITOCHONDRIAL QUALITY CONTROL 33
1.3.3. NRF2 AND MITOCHONDRIAL HOMEOSTASIS DURING INFECTION 34
1.4. NRF2 AS A CYTOPROTECTIVE MOLECULE AGAINST THE PATHOPHYSIOLOGY OF HEMOLYTIC DISORDERS 36
1.4.1. HEME AS A DANGER MOLECULE 36
1.4.2. NRF2 AND HEME CYTOTOXICITY 39
1.5. OXIDATIVE STRESS AND PROGRAMMED CELL DEATH 45
1.5.1. ROS AND TNF-DEPENDENT NECROPTOSIS 45
1.6. NRF2 AND TNF-DEPENDENT NECROPTOSIS 52
1.7. THESIS OVERVIEW 54
1.8. REFERENCES 54

CHAPTER 2: RESULTS 69

2.1. NRF2 IS ESSENTIAL TO ESTABLISH DISEASE TOLERANCE TO MALARIA. 70
2.2. NRF2 IS ESSENTIAL TO ESTABLISH DISEASE TOLERANCE TO POLYMICROBIAL SEPSIS. 77
2.3. NRF2 CONFERS TISSUE DAMAGE CONTROL AFTER STERILE HEMOLYSIS. 82
2.4. NRF2 REGULATES THE ANTI-OXIDANT RESPONSE TARGETING THE MITOCHONDRIA. 87
2.5. LABILE HEME SENSITIZES HEPATOCYTES TO UNDERGO TNF-DEPENDENT NECROPTOSIS. 94
2.6. NRF2 REGULATES A CYTOPROTECTIVE RESPONSE THAT INHIBITS NECROPTOSIS. 97
2.7. REFERENCES 108

CHAPTER 3: DISCUSSION 111

REFERENCES 118

EXPERIMENTAL PROCEDURES 123

APPENDIX 1 137

APPENDIX 2 **179**

List of figures

FIGURE 1.1. DISEASE TOLERANCE TO INFECTION ACTS IN TWO DISTINCT WAYS..... 4
FIGURE 1.2. TISSUE DAMAGE CONTROL IN HOST-MICROBE INTERACTIONS. 4
FIGURE 1.3. CONTROL OF NRF2 ACTIVATION BY DIFFERENT E3 UBIQUITIN LIGASE COMPLEXES. 9
FIGURE 1.4. OUTCOMES OF NRF2 ACTIVATION. 11
FIGURE 1.5. HIF-1A AND NRF2 MEDIATE THE STRESS RESPONSE TO PATHOPHYSIOLOGICAL O_2 LEVELS. 15
FIGURE 1.6. AMPK AND NRF2 PROTECT AGAINST METABOLIC IMBALANCE. 16
FIGURE 1.7. NRF2 AS A PLAYER IN THE OSMOTIC STRESS RESPONSE. 18
FIGURE 1.8. CROSSTALK BETWEEN THE OXIDATIVE STRESS RESPONSE, THE HEAT SHOCK RESPONSE AND THE UNFOLDED PROTEIN RESPONSE. 22
FIGURE 1.9. CROSSTALK BETWEEN THE OXIDATIVE STRESS RESPONSE AND THE DNA DAMAGE RESPONSE. 24
FIGURE 1.10. CROSSTALK BETWEEN THE OXIDATIVE STRESS RESPONSE AND THE DAMAGE RESPONSE AGAINST LIPID PEROXIDATION. 27
FIGURE 1.11. CROSSTALK BETWEEN THE OXIDATIVE STRESS RESPONSE AND THE AUTOPHAGY DAMAGE RESPONSE. 29
FIGURE 1.12. THE ROLE OF NRF2 IN CELLULAR REDOX STATE. 32
FIGURE 1.13. HEME CATABOLISM 37
FIGURE 1.14. THE PATHOPHYSIOLOGY OF HEMOLYTIC INFLAMMATORY DISEASES. 44
FIGURE 1.15. TNF-DEPENDENT PROGRAMMED CELL DEATH MACHINERY. 52
FIGURE 2.1. NRF2 CONFERS DISEASE TOLERANCE TO MALARIA INFECTION. 72
FIGURE 2.2. NRF2 PROTECTS AGAINST MULTI-ORGAN DAMAGE/DYSFUNCTION IN MALARIA INFECTION 73
FIGURE 2.3. NRF2 PROVIDES TISSUE DAMAGE CONTROL TO MALARIA INFECTION. 73
FIGURE 2.4. NRF2 PREVENTS DAMP RELEASE AND OXIDATIVE STRESS IN MALARIA INFECTION 75
FIGURE 2.5. NRF2 COUNTERS INFLAMMATION IN MALARIA INFECTION 76
FIGURE 2.6. NRF2 PROVIDES DISEASE TOLERANCE TO POLYMICROBIAL SEPSIS. 78
FIGURE 2.7. NRF2 CONFERS TISSUE DAMAGE CONTROL IN POLYMICROBIAL SEPSIS 80
FIGURE 2.8. NRF2 PROVIDES TISSUE DAMAGE CONTROL MAINLY IN THE LIVER UPON POLYMICROBIAL SEPSIS 80
FIGURE 2.9. NRF2 COUNTERS INFLAMMATION UPON POLYMICROBIAL SEPSIS 81
FIGURE 2.10. NRF2 PROTECTS AGAINST LETHALITY ASSOCIATED WITH SEVERE ACUTE HEMOLYSIS 83
FIGURE 2.11. NRF2 PROVIDES TISSUE DAMAGE CONTROL AFTER ACUTE STERILE HEMOLYSIS 84
FIGURE 2.12. NRF2 PROTECTS AGAINST THE CYTOTOXIC EFFECTS OF LABILE HEME. 86
FIGURE 2.13. NRF2 SPECIFICALLY PROTECTS AGAINST HEMOLYSIS, NOT RBC DEPLETION. 87
FIGURE 2.14. HEME SYNERGIZES WITH TNF TO INDUCE NRF2 EXPRESSION BUT NOT TRANSCRIPTIONAL ACTIVITY. 88
FIGURE 2.15. NRF2 PROTECTS AGAINST MITOCHONDRIAL DYSFUNCTION, MITOCHONDRIAL ROS PRODUCTION AND CELL DEATH IN RESPONSE TO HEME AND TNF. 90

FIGURE 2.16. NRF2 PROTECTS AGAINST HEME AND TNF-MEDIATED CYTOTOXICITY VIA A MECHANISM ASSOCIATED WITH REDUCED PRODUCTION/ACCUMULATION OF MITOCHONDRIAL ROS. 92
FIGURE 2.17. HEME AND TNF SYNERGIZE TO PRODUCE MITOCHONDRIAL ROS AND MITOCHONDRIAL DYSFUNCTION, LEADING TO CELL DEATH. 93
FIGURE 2.18. LABILE HEME SYNERGIZES WITH TNF TO TRIGGER RIPK3-DEPENDENT NECROPTOSIS AND MITOCHONDRIAL DYSFUNCTION IN HEPATOCYTES. 95
FIGURE 2.19. LABILE HEME SYNERGIZES WITH TNF TO TRIGGER MLKL AND PGAM5-DEPENDENT MITOCHONDRIAL DYSFUNCTION AND CELL DEATH IN HEPATOCYTES. 97
FIGURE 2.20. NRF2 PROTECTS AGAINST RIKP3-DEPENDENT PROGRAMMED CELL DEATH BY BLOCKING MITOCHONDRIAL ROS PRODUCTION AND MITOCHONDRIAL DYSFUNCTION IN VITRO. 98
FIGURE 2.21. NRF2 ACTS AS A CYTOPROTECTIVE MOLECULE AGAINST RIPK3-INDUCED DAMAGE IN VIVO AFTER ACUTE HEMOLYSIS AND SEPSIS 100
FIGURE 2.22. NRF2 PROTECTS AGAINST RIPK1 BUT NOT RIPK3-INDUCED LETHALITY IN VIVO AFTER MALARIA INFECTION 102
FIGURE 2.23. NRF2 DOES NOT PROTECT AGAINST CASPASE8 DEPENDENT APOPTOSIS IN VIVO AFTER MALARIA INFECTION 103
FIGURE 2.24. CYPD CONTRIBUTES TO HEME AND TNF-INDUCED PCD AND MITOCHONDRIAL DYSFUNCTION IN VITRO BUT NOT IN VIVO 104
FIGURE 2.25. NRF2 FAILS TO REVERT RIPK3 OR CYPD-MEDIATED TISSUE DAMAGE IN VIVO AFTER MALARIA INFECTION 106
FIGURE 2.26. NRF2 PROTECTS AGAINST RIPK3 AND CYPD-INDUCED LETHALITY AND TISSUE DAMAGE IN VIVO AFTER MALARIA INFECTION 108

Chapter 1:

Introduction

"In the face of such hopelessness as our eventual, unavoidable death, there is little sense in not at least trying to accomplish all of your wildest dreams in life."
(Kevin Smith)

1.1. Inflammation and the breakdown of homeostasis

It was more than 200 years ago, in the 19th century, when the idea of a stable internal environment first arose. Claude Bernard coined the term *milieu interieur* referring to biological processes present in all living beings, which maintain steady states despite variations in the external environment[1]. This concept was further explored by Walter Cannon, who crafted the term homeostasis as the equilibrium or stability in biological systems via maintenance of key physiological variables by feedback mechanisms[2]. Cannon classified any living being as an open system with automatic reactive mechanisms used to correct large fluctuations, thus maintaining each homeostatic category within narrow and constant limits[2].

The steadiness of the internal milieu is constantly subjected to different threats while the organism interacts with its environment. As such, organisms evolved adaptive responses to exogenous cues such as microbes or allergens and endogenous signals like the ones produced by stressed, damaged or malfunctioning tissues[3]. Inflammation refers to the adaptive responses which aim primarily at identifying and eliminating the source of insult, followed by repair of the damage caused in this process, as a means to reestablish an homeostatic state[4]. In the particular case of infection, i.e., invasion of an organism by a disease-causing microbe, the physiological purpose of inflammation is to defend the host by neutralizing and eliminating pathogens while triggering a tissue repair program to ultimately restore homeostasis[3].

1.2. Host defense strategies against infection

It is traditionally thought in the field of immunology that the best approach for a host to counter infection is by neutralizing, killing

and/or eliminating the infectious agent. This host defense strategy, commonly known as *resistance to infection*, aims at protecting the host by activating a number of immune-mediated mechanisms that act directly on invading microorganisms[5].

The negative impact of infectious diseases is countered, not only by the host´s capacity to limit pathogen burden, but also by its ability to tolerate the presence of pathogens, limiting their deleterious effect on host tissues[6]. This defense strategy that protects the infected host without interfering directly with the pathogen is named *disease tolerance* and is recognized as a distinct evolutionarily conserved mechanism in host-microbe interactions[5].

Immune driven resistance mechanisms likely coevolved with disease tolerance mechanisms, acting in a concerted manner to limit disease severity and maintain host homeostasis. Resistance carries a significant *trade off* as it can impose collateral damage to the host tissues (immunopathology), eventually increasing host morbidity and/or mortality. As such, disease tolerance plays a major role in counteracting the negative impact of host immunity as well as the direct deleterious effects of pathogens in host tissues[5,7] (Figure 1.1).

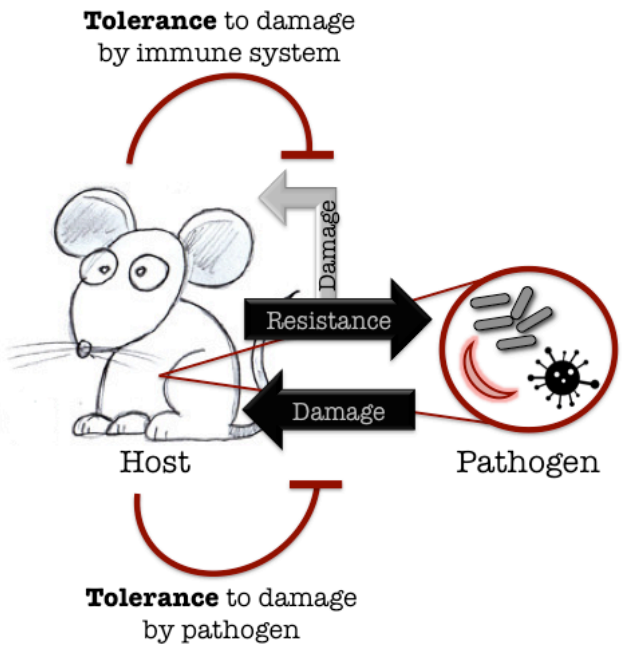

Figure 1.1. Disease tolerance to infection acts in two distinct ways.
Both pathogens and the immune response to infection can damage host tissues. Disease tolerance mechanisms protect the host from these two different forms of stress (Adapted from Medzhitov et al., 2012).

1.2.1. Disease tolerance and tissue damage control

Disease tolerance relies on tissue damage control mechanisms that encompass stress and damage responses, which act in a concerted manner to preserve the functional integrity of host tissues, thus preventing the collapse of homeostasis[8].

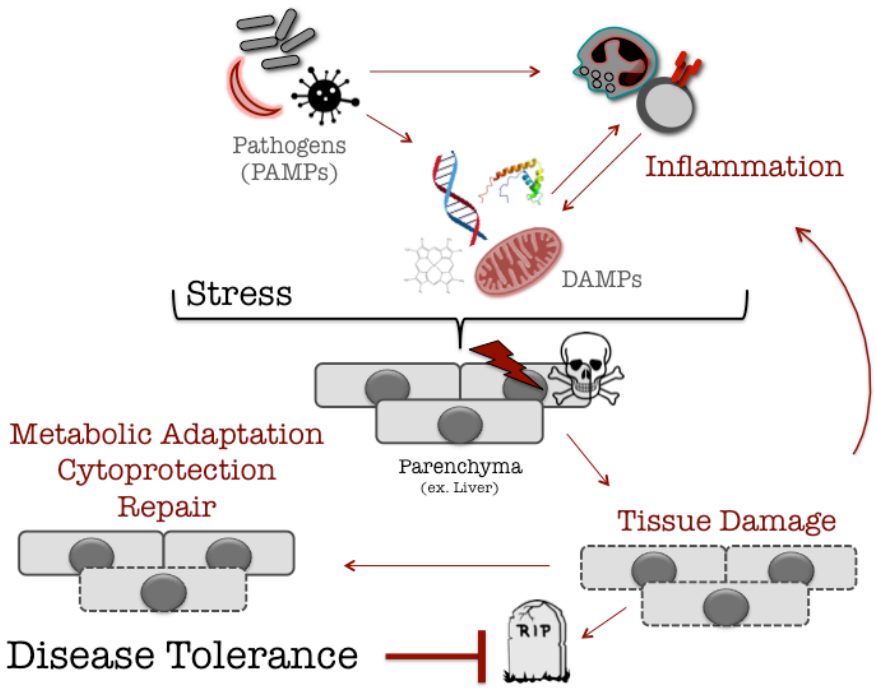

Figure 1.2. Tissue damage control in host-microbe interactions.
Two major classes of molecules can initiate inflammation: PAMPs and DAMPs. The later include mitochondrial components, heme, DNA, histones or other DNA binding proteins such as HMGB1, released to the extracellular space due to cytotoxicity imposed directly by pathogens (through toxins, for example) and/or by inflammatory mediators (immunopathology). This causes different types of stress to parenchyma cells, eventually leading to

programmed cell death and tissue damage, culminating in host death. Tissue damage fosters further DAMP release, which sustains the inflammatory response. This positive forward pathologic loop is mitigated by the activation of specific stress and damage responses that confer tissue damage control via metabolic adaptation, cytoprotection and repair as part of a disease tolerance strategy.

Inflammatory responses to infection are initiated and perpetrated through the recognition of pathogen-derived molecules [Pathogen Associated Molecular Patterns (PAMPs)] or molecules derived from damaged or dead host cells [Damage Associated Molecular Patterns (DAMPs)] by pattern recognition receptors (PRR)[9] (Figure1.2). These correspond to intracellular components such as nuclear and mitochondrial DNA, purine nucleotides (i.e., ATP, UTP), High-Mobility Group Box 1 (HMGB1) and mitochondrial N-formyl peptides, released upon plasma membrane disintegration, typical of necrotic cell death[10]. DAMP release induces an inflammatory response, which imposes stress to parenchyma cells, i.e., host cells that do not exert a direct negative impact on pathogens[7] (Figure 1.2). This is countered by the activation of specific stress and damage responses that confer tissue damage control by providing metabolic adaptation, cytoprotection and repair of damaged cells and tissues, as part of a disease tolerance strategy against infection (Figure 1.2)[7].

1.2.2. Stress responses underlying tissue damage control

Stress responses are triggered by sensors that respond to environmental cues whose variations can interfere with cellular homeostasis via, for example, deregulation of redox status, osmolarity, oxygen tension and metabolite concentration, among others[8]. The outcome of stress responses is metabolic adaptation, which allows the maintenance of core cellular processes at the expense of accessory ones, assuring cellular, tissue and organ

function under different types of stress[8]. This is achieved through the expression of immediate-early response genes regulated by specific transcription factors known as master regulators of stress responses[8]. In this section, I emphasize the association between the oxidative stress response orchestrated by NRF2, the main focus of this thesis, and other stress responses, mainly in the context of disease tolerance to infection.

The oxidative stress response

Oxidative stress resulting from the accumulation of Reactive Oxygen Species (ROS) has been widely implicated in the pathogenesis of infectious diseases[11,12]. ROS are compounds that have chemically reactive oxygen-containing functional groups with of one or more unpaired electrons, which renders these compounds highly unstable[13]. In the context of infection, innate immune cells produce ROS as part of a resistance strategy promoting the elimination of pathogens. However, the generation of these highly reactive compounds leads to oxidative stress on host cells, eventually leading to tissue damage, organ dysfunction and disease[5].

Oxidative stress is countered by the activation of an adaptive cellular response pathway induced by the transcription factor NRF2 and leading to the expression of a battery of genes with anti-oxidant and detoxifying properties[14,15,16]. Consistent with this notion, levels of ROS in NRF2-deficient cells are elevated when compared to wild-type cells[17]. This difference becomes even more significant upon exposure to pro-oxidants[18] and is directly linked to impaired activation of antioxidant programs countering the deleterious effects of ROS[19]. One of the mechanisms via which NRF2 protects against oxidative stress involves the expression of both catalytic and

regulatory subunits of γ-glutamyl cysteine ligase, the enzyme catalyzing the rate-limiting step in glutathione biosynthesis[20]. Glutathione is an evolutionarily conserved antioxidant, which in its reduced form (GSH) prevents ROS-mediated damage to cellular components, such as caused by the accumulation of free radicals, peroxides, lipid peroxides or heavy metals[21]. Moreover, the xCT subunit of x_c^-, the system that imports cystine into cells, i.e. a precursor of glutathione, is also a transcriptional target for NRF2[20]. GSH levels are maintained by glutathione reductase 1[22], another transcriptional target for NRF2 that reduces oxidized glutathione (GSSG) to GSH using reducing equivalents from Nicotinamide Adenine Dinucleotide Phosphate (NADPH). Together, these data probably explain why levels of GSH are lower in NRF2-deficient cells as compared to wild type cells, while intracellular GSH accumulates following NRF2 activation[23,24].

NRF2 also regulates the expression of thioredoxin (TRX1)[23,25] and sulfiredoxin (SRXN1)[26], essential proteins for the reduction of oxidized thiol groups[16]. Additionally, NADPH-generating enzymes such as Glucose-6-Phosphate Dehydrogenase (G6PD) and drug metabolizing enzymes that require NADPH as a cofactor, namely NAD(P)H Quinone Dehydrogenase 1 (NQO1) and thioredoxin reductase 1 (TXNRD1) are also regulated by NRF2[27,28].

Upon infection, engagement of PRRs by PAMPs activates NRF2 in innate immune cells such as monocytes/macrophages (Mø). For instance, lipopolysaccharide (LPS) recognition by Toll-Like Receptor 4 (TLR4) triggers the transcription/expression of the inducible form of nitric oxide synthase (iNOS/NOS2), via a mechanism involving the adaptor molecule Myeloid differentiation primary response gene 88 (Myd88) and the transcription factor nuclear factor kappa B (NF-κB)[29]. The TLR4–MyD88–NF-κB signal transduction pathway also triggers the transcription/expression of the phagocytic NADPH

oxidase (NOX2/gp91phox), leading to the generation of intracellular superoxide ($O_2^{\cdot -}$) anions[30]. The NO produced through iNOS activity reacts with O_2^- and produces peroxinitrate ($ONNO^-$) anions, which targets several thiol-based (S-H) redox systems, including reactive cysteines in the Kelch-like ECH-associated protein 1 (KEAP1)[16,31,32] (Figure 1.3), an adaptor for the cullin (Cul)3– RING (really interesting new gene)-box protein (Rbx)1 ubiquitin ligase complex[16]. This protein acts as a repressor of NRF2 activation under homeostasis, as it constitutively targets this transcription factor for proteolytic degradation by the 26s proteasome[16] (Figure 1.3).

Upon oxidative stress, some of the reactive cysteines of KEAP1, (Cys151) are targeted by $ONNO^-$, generating thiol oxidation products and ultimately forming disulfide (S-S) bonds[33]. These alter the tertiary structure of Keap1, inhibiting its ubiquitin ligase activity and hence NRF2 ubiquitination/degradation[16,31,32]. The newly transcribed NRF2 undergoes nuclear translocation and binds to small musculoaponeurotic fibrosarcoma (sMaf) transcription factors, including MafF, MafG and MafK[34], driving the transcription of NRF2-responsive genes containing AREs in their promoter[16] (Figure 1.3).

It is now clear that other E3 ubiquitin ligase complexes contribute to integrate NRF2 activation within different forms of cellular stress[16]. These include the Skp1 (S-phase kinase-associated protein 1)–Cul1–F-box (SCF)–β-transducin repeats-containing proteins (β-TrCP) complex (SCFβ-TrCP)[35], which recognizes the Neh6 (NRF2-ECH homology 6) domain of NRF2 when phosphorylated by the Glycogen Synthase Kinase 3β (GSK3β)[35]. NRF2 phosphorylation at the Neh6 domain allows for coupling of different forms of stress sensed by GSK3β with NRF2 ubiquitination by the SCFβ-TrCP complex and its degradation by the 26s proteasome[16,35] (Figure 1.3). The HMG (high mobility group)-coA reductase degradation 1 (HRD1) E3 ubiquitin–protein ligase involved in endoplasmic reticulum-

associated protein degradation (ERAD) also controls NRF2 activation[36]. Hrd1 targets the Nhe4–5 domain of NRF2 for ubiquitination and degradation by the 26s proteasome[36] (Figure 1.3). How Hrd1 acts in the context of other components of the endoplasmic reticulum stress response, such as the protein kinase RNA-like ER kinase 1 (PERK1)[37], to regulate NRF2 is not clear.

It is worth noting that NRF2 activity is controlled to a large extent by its rate of transcription/expression (Figure 1.3). This is regulated by several transcription factors including NF-κB[16] and NRF2 itself, as well as clock components that impose a circadian control to NRF2 activity[38] (Figure 1.3). Presumably, this is required to sustain NRF2-dependent gene expression.

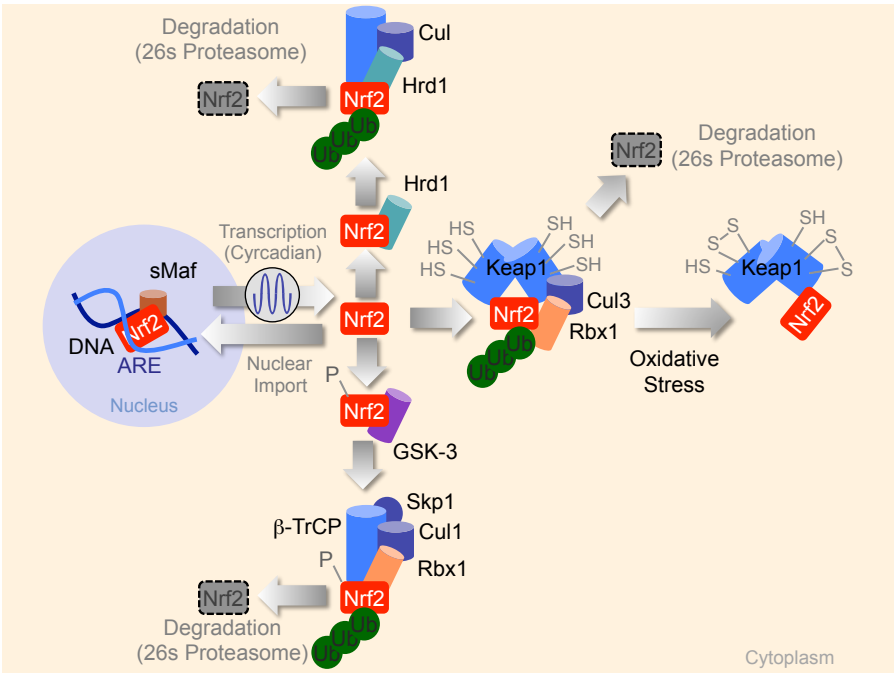

Figure 1.3. Control of NRF2 activation by different E3 ubiquitin ligase complexes.
When no longer targeted for degradation by E3 ubiquitin ligase complexes, NRF2 activity is controlled mainly by its rate of transcription, with newly transcribed NRF2 regulating gene expression. It is the Keap1–Cul3–Rbx1,

Hrd1 E3 ubiquitin ligase and SCFβ-TrCP complexes, however that underlies the stress responsive nature of NRF2 activity (From Soares & Ribeiro, 2015).

Upon infection, NRF2 acts in different cellular components to modulate both resistance and tolerance to specific pathogens (Figure 1.4). Perhaps the best demonstration that NRF2 modulates host resistance to infection is provided by the observation that deletion of *Nrf2* in mice increases viral clearance upon Marburg virus infection[39]. This effect is mediated by the Marburg virus encoded VP24 protein, which binds the Kelch domain of Keap1 and inhibits the ubiquitin ligase activity of the Keap1–Cul3–Rbx1 complex, hence inducing NRF2 activation[39,40]. Several other observations are consistent with the notion that viruses induce host NRF2 activation *in vitro*, as suggested for Kaposi's sarcoma-associated herpes virus[41], as well as for Influenza[42,43] and Dengue[44] viruses. However, the pathophysiologic relevance of these observations remains to be elucidated. Conversely, viruses such as hepatitis C virus, down-regulate NRF2 activation via a mechanism impairing its nuclear import through delocalization of sMaf proteins[45]. The impact of this phenomenon to the outcome of hepatitis C virus infection is also not clear.

Intracellular bacteria also modulate NRF2 activation, as demonstrated for *Salmonella typhimurium* infection in Mø[46]. NRF2 activation enforces the transcription/expression of Ferroportin-1 (Fpn-1), an iron exporter that decreases iron cellular content[46]. This limits *Salmonella* access to iron, restraining the proliferation of this intracellular pathogen[46]. Whether NRF2 acts under pathophysiologic conditions to promote resistance to *Salmonella* infection is likely, but this remains to be formally demonstrated. Furthermore, pharmacologic induction of NRF2 by sulforaphane promotes

resistance to *Pseudomonas aeruginosa*[47] as well as to *Plasmodium* infection in mice[48].

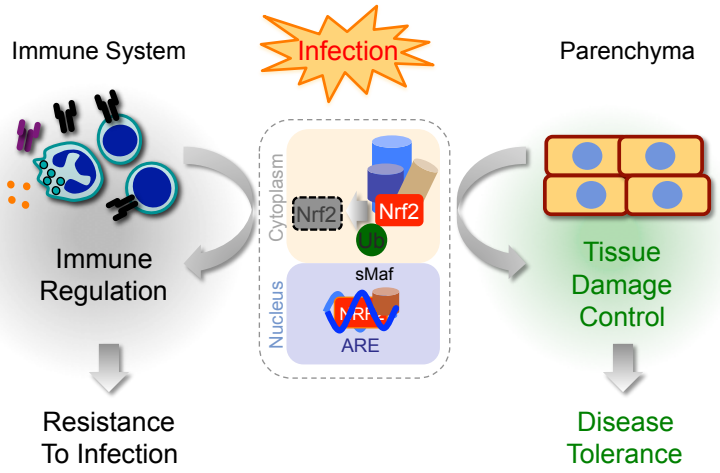

Figure 1.4. Outcomes of NRF2 activation.
Upon infection, activation of NRF2 in cellular components of the immune system acts in an immunoregulatory manner, modulating resistance to infection. Activation of NRF2 in parenchyma tissues provides tissue damage control and disease tolerance to infection. Control of NRF2 activation is illustrated in the context of a generic E3 ubiquitin ligase complex, detailed under Figure 1.3 (From Soares & Ribeiro, 2015).

The NRF2 signal transduction pathway was co-opted to confer tissue damage control and disease tolerance to systemic infections[15]. This is particularly important for *Plasmodium* infection (the causative agent of malaria), where the blood stage of the disease is associated with hemolysis and consequent accumulation of extracellular hemoglobin in plasma[49]. Upon oxidation, extracellular hemoglobin releases its heme prosthetic groups, a structure composed of a tetrapyrrole ring surrounding a single iron (Fe) atom, leading to the unfettered generation of ROS[49].

ROS and contributes to oxidative stress and cellular damage to host parenchyma tissues, eventually compromising host homeostasis and driving the pathogenesis of severe forms of

malaria[49]. The pathophysiologic relevance of this pathway is highlighted by the finding that mutations in the β-chain of hemoglobin (sickle hemoglobin) establish disease tolerance to the blood stage of *Plasmodium* infection via a mechanism that relies on the induction of NRF2-dependent HO-1 expression[50]. This enzyme catalyzes the degradation of heme via cleavage of its protoporphyrin IX ring, giving rise to biliverdin, then converted to the salutary antioxidant bilirubin, the cytoprotective CO and equimolar amounts of labile Fe^{2+} [51]. Whether this cytoprotective mechanism explains how sickle hemoglobin protects humans from malaria remains to be established, but is likely to be the case based on recent evidence from a human cohort[52].

Similarly, nitric oxide (NO) suppresses the pathogenesis of severe forms of malaria through a mechanism involving the induction of HO-1 via NRF2 and establishing disease tolerance to malaria[53]. This protective effect arises via NO-driven NRF2 activation[53], presumably through mechanisms targeting Keap1 at Cys151[16,54]. NRF2 activation induces heme catabolism by HO-1, generating CO[55], a gasotransmitter shown to establish disease tolerance to malaria[53]. This occurs via the binding of CO to the prosthetic heme group of cell free hemoglobin, preventing heme from participating in the pathogenesis of *Plasmodium* infection[50,53,56].

Presumably, the mechanism via which NRF2 confers tissue damage control and establishes disease tolerance to malaria also involves the expression of Ferritin Heavy Chain (FtH). This regulator of iron metabolism is also regulated at a transcriptional level via the activation of NRF2[57,58] and was demonstrated to play a crucial role in the establishment of disease tolerance to malaria[59].

There is circumstantial evidence to suggest that NRF2 confers disease tolerance to systemic infections, other than malaria. Namely, NRF2 is protective against endotoxic shock[60], severe sepsis

triggered by polymicrobial infection[60] and lung injury induced by *Staphylococcus aureus* infection[61] in mice. These salutary effects have been associated mainly with immunoregulation, although there is no clear evidence demonstrating a role for NRF2 in the modulation of pathogen load under these specific experimental settings[60].

In my thesis I demonstrate that NRF2 prevents the lethal outcome of malaria and polymicrobial sepsis in mice, without interfering with pathogen load. This shows that NRF2 does confer disease tolerance to infection via the induction of tissue damage control mechanisms when activated in parenchyma cells or presumably acting as an immunoregulatory transcription factor in innate immune cells, although this remains to be fully established.

NRF2 and the hypoxia stress response

Hypoxia refers to a pathophysiological condition in tissues where the O_2 concentration is lower than homeostatic levels (normoxia) due to either failure in delivery or use of O_2[62]. Alterations in O_2 tension modulate cell function by affecting intracellular NADPH levels, protein kinases, ion channels and antioxidant defenses[63]. The transcription factor Hypoxia Inducible Factor 1 alpha (HIF-1α) is the master regulator of the hypoxia stress response, leading to most changes in gene expression that allow adaptation to prolonged low oxygen tension[64].

Hypoxia is sensed by the prolyl hydroxylase (PHD2), which uses O_2 to hydroxylate two proline residues in HIF-1α[65]. This promotes the recruitment of the E3 ubiquitin ligase von Hippel–Lindau (VHL/Cul3), ubiquitinating and targeting HIF-1α for proteolytic degradation by the 26s proteasome pathway[65]. PHD2 activity is inhibited when O_2 pressure decreases below physiologic levels, releasing HIF-1α from VHL and allowing its nuclear translocation and binding to DNA

Hypoxia-Responsive Elements (HRE) in the promoters of effector genes regulating metabolic adaptation to hypoxia[65] (Figure 1.5).

One hallmark of hypoxia is the increased generation of ROS, presumably due to the shut down of the mitochondrial electron transport chain (ETC) as a consequence of the low O_2 concentration reaching the mitochondria[65]. Several lines of evidence have demonstrated that mitochondrial ROS are essential to mount a hypoxic response[66]. For instance, the activity of the hypoxia sensor PHD is highly sensitive to iron redox state and ROS accumulation, which has a profound effect on the activation of HIF-1α[67] (Figure 1.5). As such, NRF2-dependent modulation of intracellular redox status impacts on the hypoxia stress response to insure return to homeostasis under low O_2 conditions[67]. In the context of cancer, NRF2 depletion was shown sufficient to decrease HIF-1α at the post-translational level, suggesting a role of NRF2 in the regulation of PHD proteins[68] (Figure 1.5). Additionally, NQO1, encoded by a downstream target gene of NRF2, interacts physically with HIF-1α, leading to its stabilization by decreasing the interaction with PHDs[69] (Figure 1.5).

Inflammation can trigger hypoxia, leading to exacerbated generation of ROS and oxidative stress, countered by the concerted action of the transcription factors HIF-1α and NRF2[70] (Figure 1.5), as suggested for experimental models of inflammation such as alcohol-induced liver injury[70] and liver transplantation following ischemia reperfusion injury (IRI)[71].

Determining the molecular mechanisms via which the NRF2 and HIF-1α-mediated pathways communicate might provide new insights into tissue damage control mechanisms, namely under the disease tolerance strategy in the context of infection.

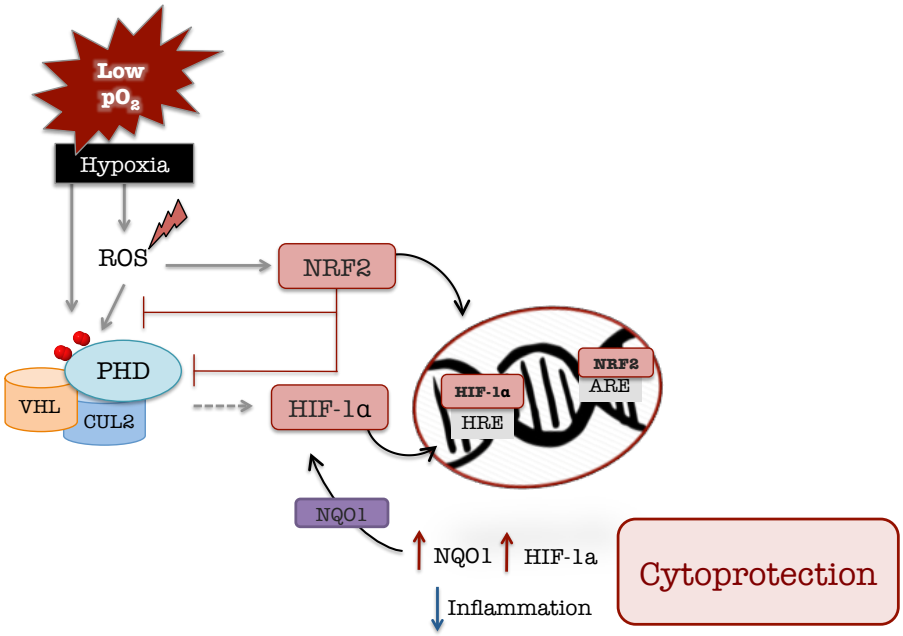

Figure 1.5. HIF-1α and NRF2 mediate the stress response to pathophysiological O_2 levels.
Low O_2 levels (hypoxia) lead to ROS production and inactivation of PHD, allowing the induction of HIF-1α. Both hypoxia and redox unbalance trigger HIF-1α stabilization and nuclear translocation. NRF2 counters ROS production/accumulation and PHD activity, impacting on HIF-1α stabilization and activation. The expression of NQO1 downstream of NRF2 activation leads to HIF-1α stabilization via direct interaction with NQO1 and the induction of the hypoxia stress response. The NRF2-dependent response ameliorates inflammation and provides cytoprotection.

NRF2 and the metabolic stress response

Infection can decrease mitochondrial ATP output and reduce its availability, compromising host homeostasis[72]. The stress response pathway orchestrated by the 5' Adenosine Monophosphate-activated Protein Kinase (AMPK) regulates cellular energy status by sensing increases in the ratios of Adenosine Monophosphate (AMP) to Adenosine Triphosphate (ATP) and Adenosine Diphosphate (ADP) to ATP (Figure 1.6)[72]. Cellular AMP, ADP and ATP concentrations are maintained by different mechanisms regulating ATP production

and consumption in the mitochondria[72]. When cellular ATP concentration decreases, the ADP:ATP ratio increases[72]. This is sensed by AMPK, which orchestrates a cellular adaptive response promoting catabolic pathways generating ATP while switching off ATP consumption[72] (Figure 1.6).

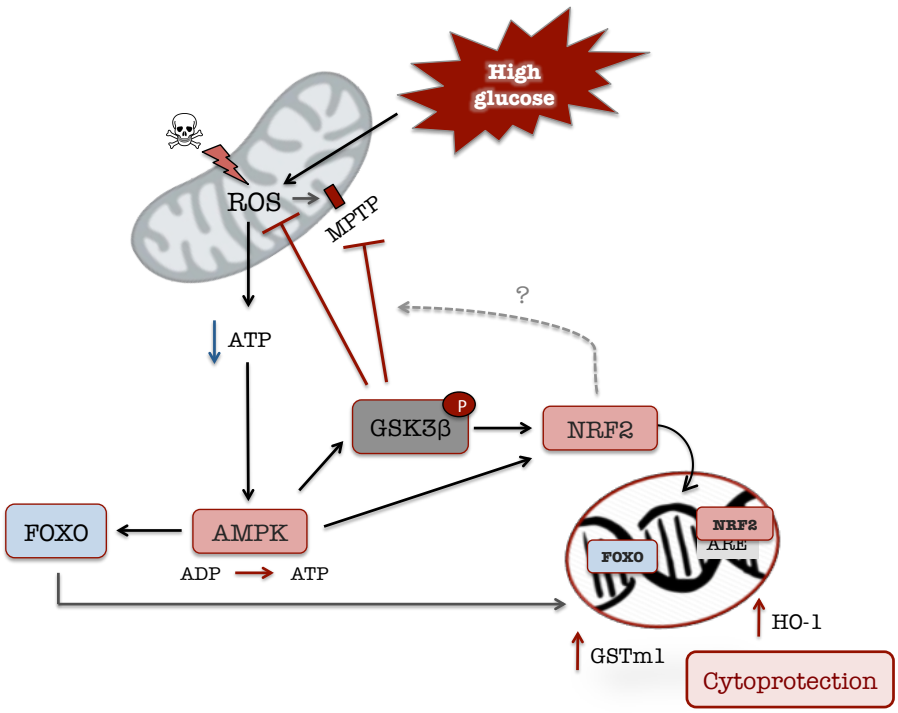

Figure 1.6. AMPK and NRF2 protect against metabolic imbalance.

The generation of ROS either due to abnormal levels of glucose (hyperglycemia) or other metabolic stresses leads to mitochondrial dysfunction and decrease in ATP production. This signals to AMPK, which in turn converts ADP in ATP to replenish the pool of ATP. AMPK activates the transcription factor Forkhead box class O (FOXO) that translocates to the nucleus where it induces the expression of the cytoprotective gene *Glutathione S-transferase Mu 1* (*Gstm1),* a gene which expression has been also shown to depend on Nrf2. The activation of AMPK induces NRF2 nuclear translocation and downstream HO-1 expression and cytoprotection. AMPK phosphorylates GSK3β, inactivating its repressor activity on NRF2 and promoting the antioxidant signal transduction pathway. GSK3β phosphorylation by AMPK protects mitochondria by blocking MPTP formation and ROS production. Whether this protection is dependent on

NRF2 via release from GSK3β-mediated degradation remains to be elucidated.

There is circumstantial evidence proposing a link between the metabolic and the oxidative stress response. For instance, AMPK activation inhibits GSK3β thus promoting NRF2 activation and downstream expression of NRF2-regulated genes preventing mitochondrial dysfunction through repression of mitochondrial permeability transition pore (MPTP) and ROS production[35,73] (Figure 1.6). Moreover, pharmacologic AMPK agonists also induce NRF2 activation and downstream expression of NRF2-regulated genes such as HO-1[74], while inhibition of AMPK blocks NRF2-dependent HO-1 expression, presumably via NRF2 inhibition[74]. Finally, transgenic expression of a constitutive active form of AMPK triggers NRF2 activation and HO-1 expression in endothelial cells[75] (Figure 1.6). Therefore, it is likely that AMPK, when induced in host parenchyma cells, synergizes with NRF2 to confer some level of tissue damage control and disease tolerance to infection but this remains to be demonstrated experimentally.

NRF2 and the osmotic stress response

Mammalian cells evolved adaptive mechanisms to compensate for increases in extracellular osmolarity, i.e., the number of solute molecules per solution volume or solution weight[76]. At the cellular level, semipermeable membranes mediate the separation of two solutions with distinct compositions[76]. Thus, the ability to regulate and preserve different intracellular and extracellular solute microenvironments is crucial in maintaining cellular and tissue homeostasis[76].

Variations in cellular volume and intracellular concentrations of inorganic ions/macromolecules lead to osmotic stress, through a

mechanism involving the aquaporin 'water channels' (AQP) and solute carrier channels (SLC)[76]. Prolonged osmotic stress is sensed by the protein kinase A-anchoring protein 13 or Brx, which activates Mitogen-Activated Protein Kinases (MAPK)[76]. These kinases include the p38 MAPK that targets the transcription factor Nuclear Factor of Activated T Cells 5 (NFAT5), known to be the master regulator of the osmotic stress response[76]. Phosphorylated NFAT5 dimerizes and translocates to the nucleus where it binds to Osmotic-Response Elements (ORE) in the promoters of osmoregulatory genes[76] (Figure 1.7).

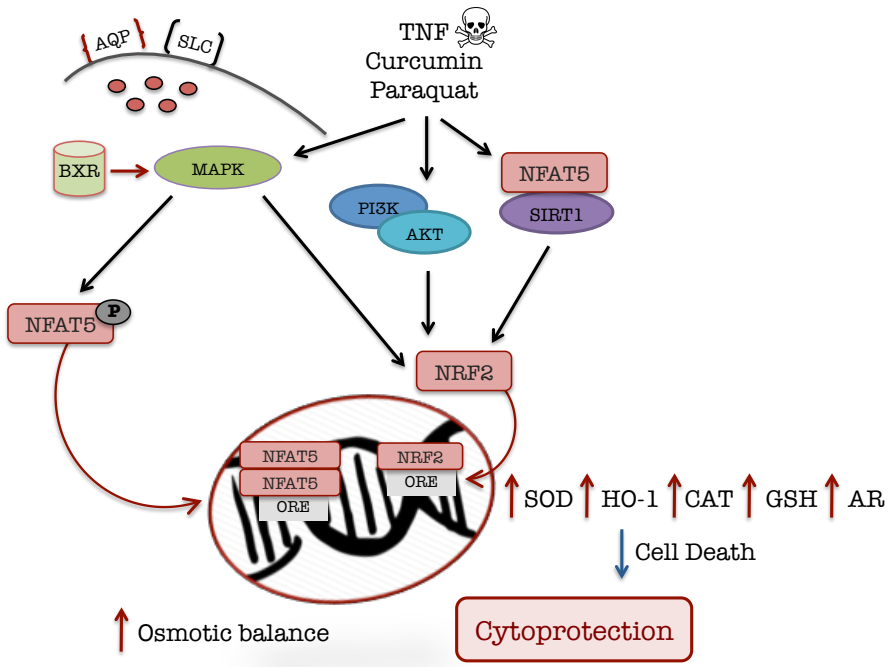

Figure 1.7. NRF2 as a player in the osmotic stress response. Osmotic stress is caused by variations in cellular volume and intracellular concentrations of inorganic ions/macromolecules via the AQP and SLC channels. This is sensed by Brx, which activates MAPK targeting NFAT5 for phosphorylation, dimerization and nuclear translocation, where it binds to OREs. Other toxic stimuli activate MAPK and PI3k/Akt, or interaction of NFAT5 with Sirt1, leading to NRF2 stabilization, nuclear translocation and

binding to ORE, where it mediates transcription of cytoprotective genes and blocks cell death.

The osmotic stress response orchestrated by NFAT5 has been previously linked to infection such as the one caused by *Leishmania major*, as it strengthens the antimicrobial barrier function of the skin and promotes host defense[77]. Moreover, the cytoprotective response mediated by NFAT5 was shown to operate in parenchyma cells during sepsis, providing tissue damage control to the kidney[78].

The oxidative response pathway controlled by NRF2 was shown to interact with the osmotic stress response[79]. Namely, Curcumin, a natural polyphenolic compound that induces NRF2 activation, upregulates the expression of aldose reductase via NRF2-dependent mechanism involving the ORE in the aldose reductase promoter[79] (Figure 1.7). The cytoprotective effect of NFAT5 promotes the SIRT1/NRF2 pathway leading to up-regulation of NRF2-regulated genes, including *Superoxide Dismutase* (*SOD*), *Catalase* (*Cat)*, *GSH* and *HMOX1*, all of which counter the induction of programmed cell death[80 81 82] (Figure 1.7).

To which extent NRF2 contributes directly to the maintenance of osmotic homeostasis downstream of NFAT5 activation to provide tissue damage control and disease tolerance still remains to be demonstrated.

1.2.3. Damage responses underlying tissue damage control: The role of NRF2

Damage responses are triggered by sensors that recognize specific macromolecular or organelle damage, acting downstream of stress responses presumably as a second layer of tissue damage control mechanisms enforcing disease tolerance. Damage responses induce repair mechanisms as a means to restore cellular

integrity and ultimately tissue function[8]. Here I focus on the connection between the oxidative stress response orchestrated by NRF2 and damage responses, mainly in the context of disease tolerance to infection.

NRF2, the heat shock response (HSR) and the unfolded protein response (UPR)

Accumulation of misfolded proteins either in the cytosol or the endoplasmic reticulum (ER) is a form of macromolecular damage associated with different types of stress[8]. This leads to the activation of two distinct damage responses: the heat-shock response (HSR) in the cytosol and the unfolded protein response (UPR) in the ER[8].

The heat shock response is a biological process activated in conditions leading to denaturation of proteins through a specific program orchestrated at the transcriptional level via activation of Heat Shock Factors (HSF) leading to the expression of a series of effector Heat Shock Proteins (HSP)[83]. One of the protective effects of HSPs comes from their ability to block TNF-dependent programmed cell death by apoptosis through a mechanism that relies on the activation of HSF[84,], presumably explaining why HSF counters endotoxic shock[85]. Of note, initiation of apoptotic programs blocks further HSF activation and HSP expression[86].

Disruption of *Hsf1* gene was shown to increase mortality and exaggerate TNF production during endotoxemia[85] and *Listeria monocytogenes* infection[87]. These data demonstrate that HSF1 is needed to prevent the overproduction of TNF and subsequent death due to septic shock that can result following high-dose challenge with bacterial pathogens[85,87].

Several studies suggest that HSF1 plays an important role in countering cellular oxidative stress/damage. Namely, HSF1 has been reported to maintain GSH cellular levels and prevent oxidative

damage to mitochondria[88] (Figure 1.8). Moreover, HSF1 and NRF2 interact functionally to control the expression of chaperones, antioxidant and drug metabolizing enzymes, proteins involved in repair of damaged macromolecules, maintenance of cell structure as well as in redox and intermediary metabolism[89]. Presumably, this is explained by the fact that NRF2 and HSF1 share transcriptional target genes encoding proteins regulating iron metabolism and oxidative stress, including the heme catabolizing enzyme HO-1 (initially named HSP32)[90,91], Transferrin Receptor (TR)[92], HSP70[93] and the nucleoporin p62[94,95]. It is possible that NRF2 and HSF1 are to some extent redundant[90] (Figure 1.8), compensating for each other's absence, as illustrated for the regulation of HSP70 expression or HO-1[96]. These observations suggest that NRF2 and HSF1 engage in crosstalk for cytoprotection, responding to a variety of stress stimuli associated with infection.

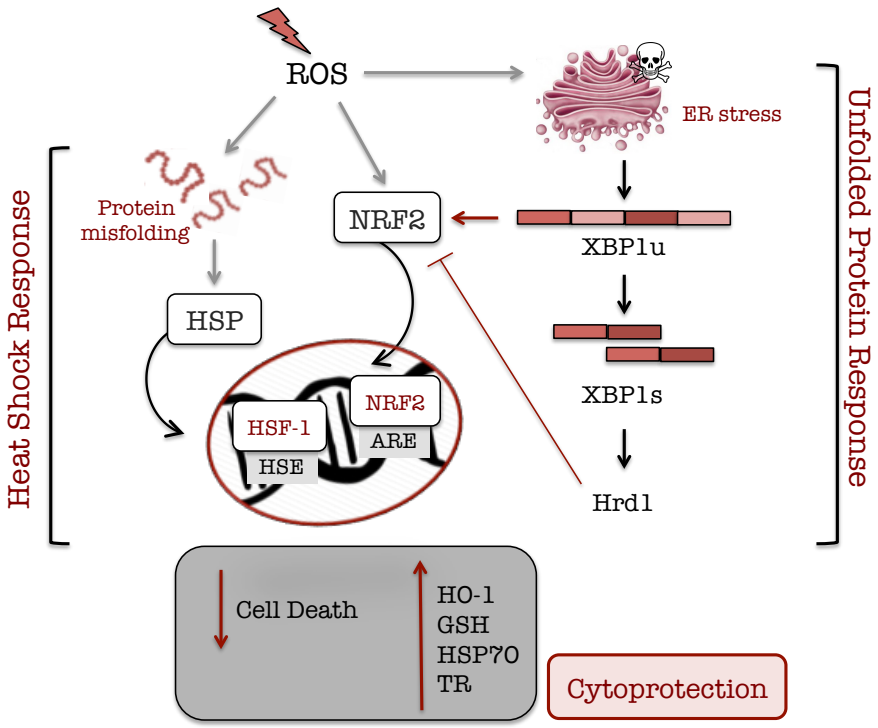

Figure 1.8. Crosstalk between the oxidative stress response, the heat shock response and the unfolded protein response. The accumulation of misfolded proteins as consequence of oxidative stress activates HSPs in the cytoplasm. In parallel, ROS production induces NRF2. The genetic programs activated by NRF2 and HSF-1 afford cytoprotection through the upregulation of detoxifying enzymes that prevent cell death, presumably as part of a disease tolerance strategy. The induction of NRF2 upon oxidative stress to the ER is most likely part of the UPR, as an important mechanism contributing to tissue damage control. The accumulation of ROS leads to the accumulation of partially/non-properly folded proteins in the ER. This in turn triggers the activation of the UPR, which relies on the expression of *Xbp1* where its unspliced form (*Xbp1u*) activates NRF2 and the oxidative stress response. The spliced form of *Xbp1* (*XBP1s)* leads to upregulation of Hrd1, a repressor of NRF2.

The oxidative environment of the ER favors correct protein folding guaranteed by specific enzymes that maintain redox homeostasis[98]. Perturbations in this fine tuned redox balance, such as those caused by external cues, trigger the UPR. This highlights the importance of oxidative stress responses in maintenance of ER homeostasis[98] (Figure 1.8). In support of this notion, the UPR modulates NRF2 activation via different mechanisms[37]: On one hand, the non-spliced form of *X-box-binding protein 1* (*XPB1u*) activates NRF2 to induce the expression of HO-1[99]; On the other hand, its spliced form (*XBP1s)* encodes for a transcription factor that modulates the expression of *ERAD-associated E3 ubiquitin-protein ligase* (*Hrd1*)[100], which interacts directly with NRF2 to inhibit its activation[36], presumably acting as a negative feed back loop avoiding the sustained activation of NRF2 (Figure 1.8).

The UPR has been clearly demonstrated to have a role in tissue damage control and disease tolerance, as it is required to sustain epithelial barrier integrity and prevent colitis[101]. Moreover, ER stress was implicated *in vitro* in *Pseudomonas aeruginosa* infection of human primary bronchial epithelial cells through the cytoprotective

induction of heme-regulated eIF2α kinase (HRI), activated by high levels of ROS[102]. In *Caenorhabditis elegans, Xbp1* is protective against *P. aeruginosa* infection by providing tissue damage control, without interfering with bacterial load[103]. Although NRF2 and the UPR play a role in providing disease tolerance it is still not clear what are the mechanisms through which these pathways act in a concerted manner to confer tissue damage control in the context of infection.

NRF2 and the DNA damage response (DDR)

Recognition of DNA damage sites and activation of repair programs are crucial to avoid the accumulation of mutations and maintain genome integrity and stability[104]. Different classes of pathogens[105] are important triggers for genomic instability, a well established hallmark of cancer[106], and damage responses such as the one orchestrated by ataxia telangiectasia mutated protein kinase (ATM) play a crucial role in sensing and repairing this type of insult[107] (Figure 1.9).

Sub-toxic levels of DNA damage inflicted by pharmacological agents which activate the response orchestrated by ATM provide a robust protection against severe polymicrobial sepsis in mice[108]. Here, ATM plays a cytoprotective role via a disease tolerance strategy by providing tissue damage control through activation of the autophagy damage response in the lung epithelium, without interfering with bacterial counts[108] (Figure 1.9).

Establishing a link between the DNA damage response and the oxidative stress response is the data showing that administration of dexamethasone, a glucocorticoid used for treatment of Ataxia Telangiectasia (A-T), improves redox state in A-T lymphoblastoid cell lines by promoting an NRF2-mediated antioxidant response[109]. This

suggests a role for NRF2 in cytoprotection against DNA damage compensating for the absence of ATM (Figure 1.9). Moreover, ATM activation and subsequent DNA repair were identified as downstream targets of HO-1 through generation of CO, suggesting a putative role of NRF2 in inducing the DDR[110]. In the context of high oxidative stress caused by heme toxicity in a model of hemolytic inflammatory diseases, the absence of ATM leads to NRF2 activation, suggesting that ATM might act in parallel with NRF2 as part of the antioxidant stress response (Rita Carlos et al., unpublished observation) (Figure 1.9).

Taken together, these data suggest a putative connection between the oxidative stress response modulated by NRF2 and the DDR dependent on ATM as regulators of tissue damage control, although the mechanisms through which these proteins interact still remains uncharacterized.

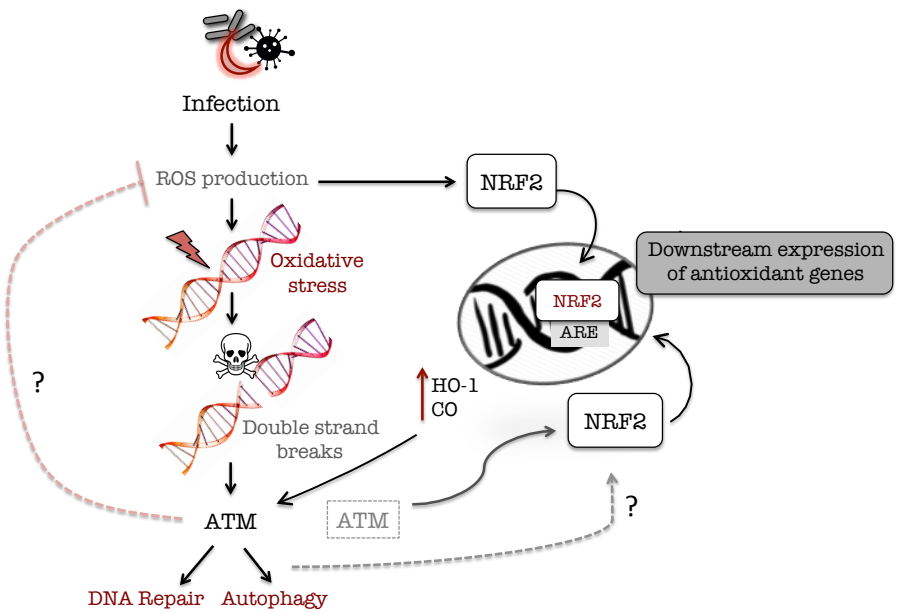

Figure 1.9. Crosstalk between the oxidative stress response and the DNA damage response.

ROS production, for example in the context of infection, leads to oxidative stress, activating NRF2. Concomitantly, it might cause damage to DNA through the generation of DNA base lesions that often lead to DNA breaks. These breaks are sensed by ATM, which activates a protective program (DDR) relying on the activation of DNA damage mechanisms, on the induction of autophagy and possibly NRF2 activation (grey arrow). The absence of ATM (grey box) is sufficient to activate NRF2. The NRF2 dependent response induces the expression of HO-1, which through CO production activates ATM. Whether ATM acts in parallel or to compensate the absence of NRF2 in the amelioration of ROS production/accumulation still remains to be understood.

NRF2 and the lipid damage response

Oxidative damage to lipids, or lipid peroxidation, is associated with a self-propagated oxidative chain reaction catalyzed by divalent metals, such as the iron contained inside the lipophilic ring of heme[111] (Figure 1.10). Labile ('loosely coordinated', 'redox-active') iron in the cytosol, mitochondrial matrix and lysosomes can catalyze the formation free radicals via Fenton reaction[112] (Figure 1.10) and trigger ferroptosis, an iron-dependent form of programmed cell death elicited by lipid peroxidation and reverted by lipophilic antioxidants[113]. Of note, the Fenton Reaction will be analyzed in detail on Section 1.3.

Members of the Glutathione Peroxidase (GPX) family of oxido-reductase enzymes play a crucial role in the detoxification of oxidized macromolecules by reducing ROS to water and oxygen utilizing glutathione as the reducing agent[114]. GPX4 is the only member of the GPX family that interacts with cell membranes and prevents uncontrolled peroxidation of phospholipids and ultimately cell death[115] (Figure 1.10). This might presumably explain why GPX4 confers tissue damage control upon *Salmonella typhimurium* infection[114]. GPX4 levels are significantly decreased in *Salmonella typhimurium* infection and inversely correlate with the rate of

neutrophil migration across mucosal surfaces, which impose a certain level of tissue damage. Moreover, overexpression of GPX4 *in vitro* decreases *Salmonella typhimurium*-induced neutrophil migration, ameliorating immunopathology[114]. The salutary effect provided by GPX4 depends on cystine supply for glutathione biosynthesis[116], which has been shown to depend on NRF2[16,27]. Recent studies have identified the NRF2-dependent gene expression as a downstream event to GPX4 specific deletion in the liver (Figure 1.10)[117] and that it plays a central role in protecting hepatocellular carcinoma cells against ferroptosis, a specific type of programmed necrosis triggered by lipid peroxidation and GPX4 depletion[118]. Moreover, liver specific NRF2 activation increases the expression of GPX4[27].

Additionally, GPX4 was shown to be activated by Hepatitis C Virus in human liver biopsies as a strategy to ameliorate lipid peroxidation and allow viral spread[119]. Together, these data suggest that the activation of NRF2 counters lipid peroxidation via a mechanism involving GPX4 and conferring cytoprotection against ferroptosis[118]. Whether the salutary effect of GPX4 as a lipophilic antioxidant against lipid peroxidation is directly related to the antioxidant nature of NRF2 activity in the context of infection remains to be further elucidated.

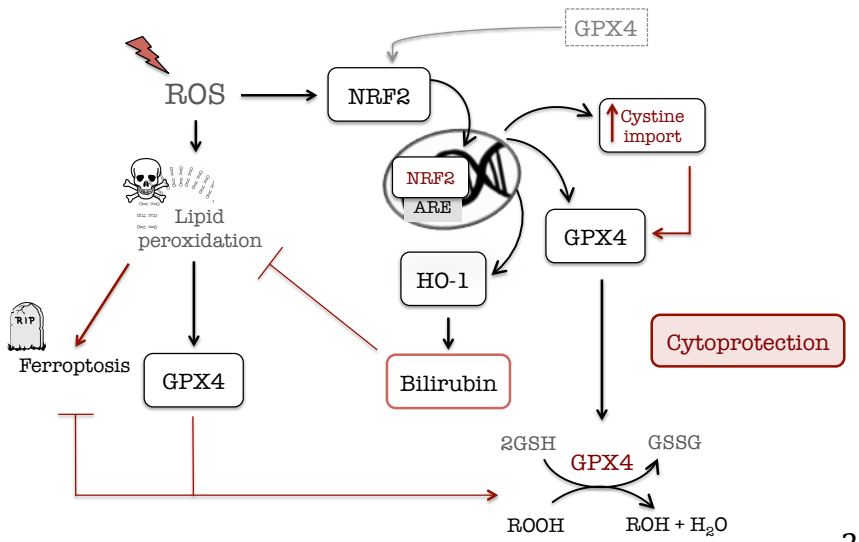

Figure 1.10. Crosstalk between the oxidative stress response and the damage response against lipid peroxidation.
The damage response to lipid peroxidation caused by ROS is orchestrated by GPX4, the enzyme that converts a hydroperoxide group (LOOH) into a hydroxyl group (ROH) and water, using GSH as a substrate. NRF2 induces the uptake of cystine leading to GPX4 detoxifying activity. NRF2 activation upon ROS production in the lipid fraction leads to *Gpx4* and *Hmox-1* expression. HO-1 produces bilirubin, a powerful lipophilic antioxidant, as by-product of heme catabolism. Both bilirubin and GPX4 act on the lipid fraction as antioxidant molecules, conferring cytoprotection. Absence of GPX4 (grey box) induces the activation of NRF2 and downstream cytoprotective response.

NRF2 and autophagy

Autophagy is a tightly regulated damage response in which the cell self-digests its own components in response to multiple forms of cellular stress including nutrient or growth factor deprivation, hypoxia, ROS, DNA damage, protein aggregates, damaged organelles or intracellular pathogens[120]. This self-degradation process not only provides nutrients to maintain vital cellular functions during fasting but can also avoid the accumulation of damaged organelles, misfolded proteins or invading microorganisms (xenophagy). As such, autophagy constitutes a major protective mechanism that ensures cell survival integrating cues from different upstream stress responses[121].

Autophagy is protective against many infectious diseases[120], a salutary effect associated mainly with resistance to infection via xenophagy[120]. More recently, however, this damage response has been shown to provide tissue damage control and establish disease tolerance in septic mice through its concerted action with the ATM-dependent DNA damage response[108].

The autophagy pathway has been functionally linked to the NRF2-dependent oxidative stress response. Namely, autophagy leads to the sequestration of Keap1-p62 complexes in autophagosomes,

resulting in lysosomal-mediated degradation of Keap1 and NRF2 activation[94]. Blocking autophagy leads to the accumulation of p62 and its binding to KEAP1, inducing prolonged NRF2 activation[94]. As such, p62 accumulation induces NRF2 in autophagy-deficient mouse livers, presumably and counter intuitively, the major cause of hepatotoxicity in autophagy-impaired livers[94].

Interestingly, NRF2 mediates the induction of p62-containing aggresome-like induced structures in response to TLR4 engagement by LPS, promoting autophagy. Similarly, heme treatment was shown to induce the formation of p62 containing aggresome-like induced structures, activating NRF2 and conferring cytoprotection against heme[122]. Presumably, this generates a positive feedback loop in which NRF2 induces p62 aggregation, which in turn amplifies NRF2 activation. Whether the formation of aggresome-like induced structures in response to heme depends on signaling through TLR4 similarly to LPS and what is the mechanism via which NRF2 is protective remains to be established.

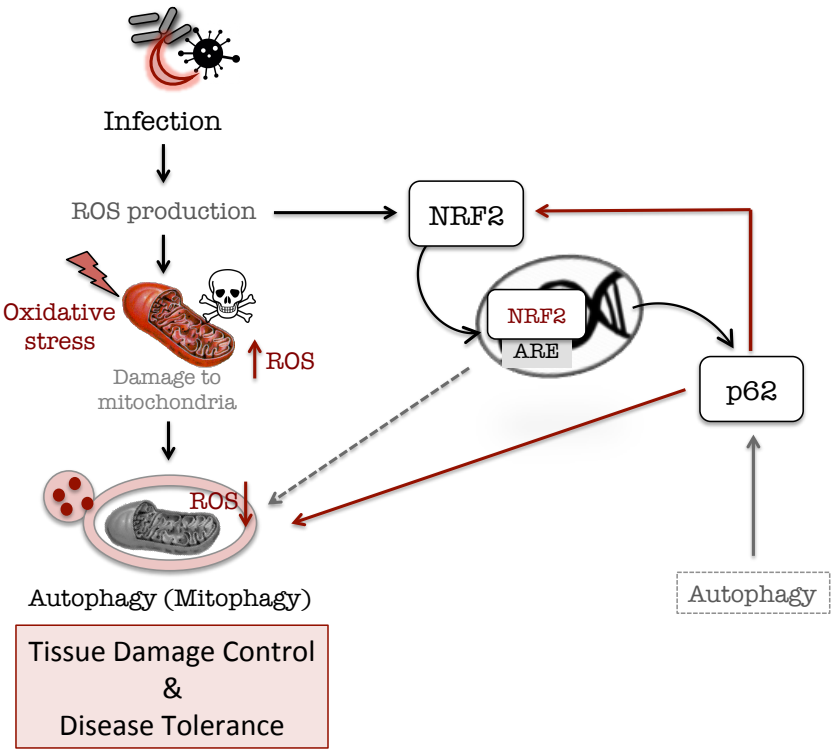

Figure 1.11. Crosstalk between the oxidative stress response and the autophagy damage response.
ROS production following recognition and elimination of pathogens, for example, induces protein oxidation on different organelles. Namely, oxidative damage to mitochondria interferes with its function and leads to increased ROS production, as these organelles are the major source of ROS in the cell. Mitochondria quality control mechanisms activate the autophagy pathway leading to its removal and destruction. NRF2 induction, as a response to oxidative stress, activates mitophagy to remove the source of ROS and the expression of p62, which stabilizes NRF2 in autophagy-deficient mice and induces mitophagy. In this context (dashed grey box), the increased levels of p62 results in the induction the expression of various cytoprotective enzymes, via NRF2 stabilization.

Exacerbated mitochondrial ROS production impairs mitochondrial function, leading to its elimination through a process called mitophagy[123] (Figure 1.11). This negative feedback regulation loop removes the source of stress and prevents oxidative damage[124].

NRF2 was suggested to have a role in redox-sensitive mitophagy in a model of *Staphylococcus aureus*-induced sepsis, as it increases autophagy of mitochondrial cargo in the lungs[125]. Furthermore, p62-mediated mitophagy inducer (PMI) upregulates p62 via stabilization of NRF2 and stimulates mitophagy[126] (Figure 1.11). *In vivo* using a model of diabetic kidney disease, it was shown that mitochondrial ROS promote tubular injury and that mitophagy promoted by NRF2 is protective against this type of insult[127]. Recently, Tomatidine, a natural compound known to inhibit age-related skeletal muscle atrophy in mice was described to have a beneficial role in *C. elegans*[128]. In this study, the authors have demonstrated that mild mitochondrial ROS production activates the NRF2 pathway, leading to salutary higher levels of mitophagy and prolonged lifespan[128].

These data argue that redox quality control programs might be targeted through NRF2 activation and consequent elimination as a means to modulate ROS levels and protect against tissue damage.

1.3. NRF2 in cellular redox homeostasis

The mechanisms involved in the maintenance of ROS-sensitive physiological functions is called redox biology[129]. Under homeostatic conditions, ROS are powerful signaling molecules, contributing to the maintenance of core physiological processes (Figure 1.12)[130]. These molecules include free radicals such as the superoxide anion (O_2^-) and the hydroxyl radical (•OH) and oxidants such as hydrogen peroxide (H_2O_2) (Figure 1.12)[131]. The O_2^- produced both by NADPH oxidases and mitochondria is rapidly converted into hydrogen peroxide (H_2O_2) by compartment-specific SODs. In the presence of highly reactive ferrous iron (Fe^{2+}), H_2O_2 is converted to hydroxyl radicals (•OH), ferric iron (Fe^{3+}) and the hydroxide anion (OH^-), the so-called Fenton Reaction. Hydroxyl radicals are extremely powerful in oxidizing DNA, proteins and lipids, leading to oxidative stress[131] (Figure 1.12).

Oxidative stress refers to the consequences of elevated intracellular levels of ROS in lipids, proteins and DNA (Figure 1.12)[130] and is linked to a plethora of pathologies such as neurodegenerative diseases, cancer, chronic inflammation or autoimmunity[132,133]. Oxidative stress elicits an adaptive response that ensures return to the normal cellular redox status[134]. The first line of defense is provided by enzymes that inactivate ROS, such as SOD and Catalase (Cat), which reduce O_2 to H_2O_2 and convert two molecules of H_2O_2 into two molecules of H_2O and O_2, respectively[135] (Figure 1.12).

Antioxidants are the second line of defense against oxidative stress (Figure 1.12). These are small molecules with redox-active properties that prevent ROS formation or remove ROS directly like bilirubin or GSH (direct antioxidants) or act indirectly like NRF2, via the induction of cytoprotective genes that recycle and/or generate

direct antioxidants[135]. Modulation of NRF2 activity may be advantageous over direct antioxidants for two reasons: First, the induction of detoxifying enzymes is a natural process and the expression of these genes will be held only when and where is needed, leaving signaling processes mediated by ROS intact; Second, the antioxidant effect is prolonged because proteins have a longer half-life than small molecule activators[136]. Additionally, antioxidants can be classified based on their source: the endogenous that are produced by the cells such as GSH and Catalase or the exogenous, which are obtained through diet, such as ascorbate[135].

1.3.1. NRF2 , NADPH oxidases and mitochondria

ROS levels are determined their rate of production, either as the main product or as a by-product of catalytic reactions as well as by the rate of ROS elimination by different antioxidant mechanisms[137].

One of the main sources of ROS are NADPH oxidases, a family of multi-subunit enzymes that transfers electrons across biological membranes (Figure 1.13)[138]. NADPH oxidases were initially discovered due to their involvement on the generation of the oxidative burst associated with bacterial clearance by phagocytes[138]. There are several NADPH oxidase isoforms that include NOX1-5 and DUOX1 and 2, which sole role appears to generate ROS in different cell types[138]. Activation of NRF2 in response to the ROS generated via NADPH oxidases[139] counters the expression of the catalytic subunits NOX2 and NOX4[137], thus acting in a negative feed back loop for the maintenance of cellular redox homeostasis (Figure 1.13).

Mitochondria are the other main source of cellular ROS generated as a natural by-product of oxidative phosphorylation through the

electron transport chain[140] (Figure 1.12). NRF2 also counters the production of mitochondrial ROS[141], acting as a negative feed back loop to maintain mitochondrial redox homeostasis. NRF2 regulates both substrate availability for mitochondrial respiration and mitochondrial ROS production[141], therefore acting as a crucial mechanism maintaining overall cellular redox homeostasis[140].

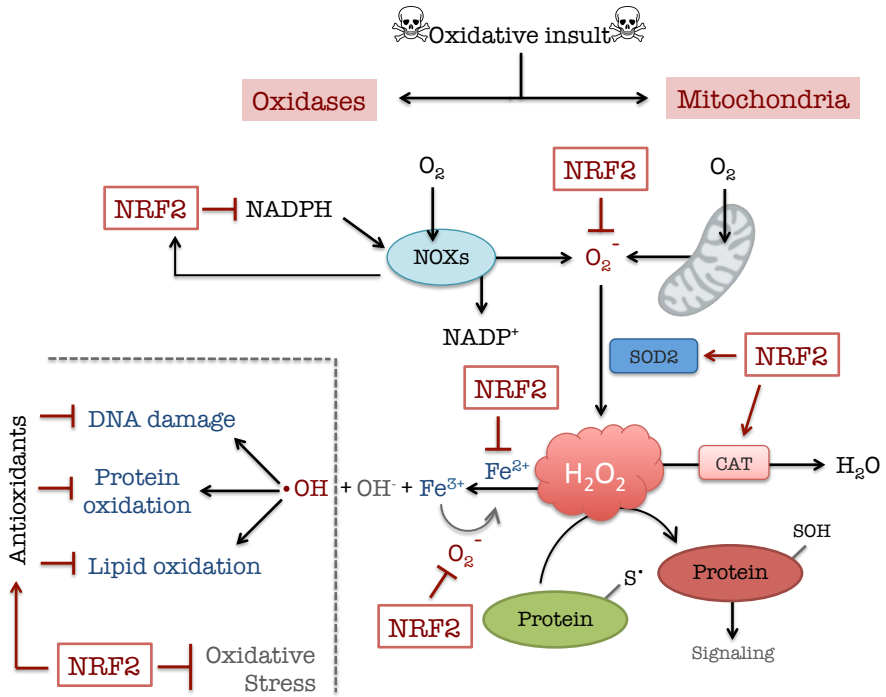

Figure 1.12. The role of NRF2 in cellular redox state.
Intracellular superoxide (O_2^-) is primarily produced by the oxidation of NADPH by NAPH oxidase enzymes (NOXs) or by electron leak from aerobic respiration in mitochondria. Superoxide is rapidly converted into hydrogen peroxide (H_2O_2) by compartment-specific superoxide dismutases (SODs). H_2O_2 is capable of oxidizing cysteine residues on proteins to initiate signaling processes. Alternatively, H_2O_2 may be converted to H_2O by cellular antioxidant proteins, such as catalase (Cat). In the presence of ferrous iron (Fe^{2+}), H_2O_2 is converted through Fenton Reaction into highly reactive hydroxyl radicals (•OH), which irreversibly damage cellular macromolecules. This reaction also produces hydroxide anions (OH^-) and ferric iron (Fe^{3+}) that, in the presence of O_2^-, provides the substrate for Fenton Reaction (Fe^{2+}) sustaining oxidative stress. NRF2 (pink rectangles)

counters cellular oxidative stress at different levels. (Adapted from Schieber M & Chandel NS, Current Biology 2014)

1.3.2. NRF2 and mitochondrial quality control

Mitochondrial membrane potential ($\Delta\psi_m$) can be disrupted by diverse pathological states and have negative consequences for mitochondrial integrity and cellular homeostasis[142]. *ROS-induced ROS release* (RIRR) in the mitochondria[143] can trigger MPTP opening[143] and the collapse of $\Delta\psi_m$ with increased ROS generation by the electron transport chain (ETC). Presumably, cytosol ROS production potentiates mitochondria RIRR, acting as a positive feedback mechanism potentially leading to mitochondrial and cellular injury[143].

Being the $\Delta\psi_m$ a universal indicator of mitochondrial health and cellular redox state, any given insult changing its amplitude has deep consequences in cellular and tissue homeostasis[144]. NRF2 activation was shown to increase the $\Delta\psi_m$ as well as the availability of substrates for respiration and ATP production[145]. Concordantly, constitutive activation of NRF2 in cells lacking the NRF2 repressor Keap1 is associated with higher rate of mitochondrial respiration, suggesting that NRF2 activation promotes mitochondrial oxidative phosphorylation and, hence, increased ROS production[137]. This is countered by NRF2-dependent gene expression, including the uncoupling protein 3 (UCP3), which increases the mitochondrial inner membrane proton conductance, decreasing superoxide production[146].

Activation of NRF2 has been linked to mitophagy, a regulated process driving the degradation and recycling of dysfunctional mitochondria[142]. This is supported by the observation that constitutive activation of NRF2 in cells lacking the NRF2 repressor Keap1 increase LC3 (an autophagossome marker) recruitment to

mitochondria[126]. Similarly, treatment with the autophagy and NRF2 inducer PMI in Keap1-knockdown or *Keap1*$^{-/-}$ cells (NRF2 over-activation) causes an increase in LC3 recruitment to mitochondria, which does not occur in *Nrf2*$^{-/-}$ cells[126]. Furthermore, induction of mitophagy with the uncoupling agent FCCP activates NRF2[147].

NRF2 has been shown to upregulate p62, a protein that facilitates the recruitment of damaged mitochondria to the phagophore[147]. A very recent study has strengthened the link between NRF2 and mitophagy demonstrating that MitoQ, a mitochondria targeted antioxidant induces mitophagy via NRF2 signaling, exerting beneficial effects on tubular injury caused by diabetic kidney disease[148].

In order to maintain cellular homeostasis, the removal of damaged mitochondria by mitophagy needs to be carefully regulated and counter-balanced by the biogenesis of new mitochondria[149]. Concordantly, it has been reported that NRF2 contributes to maintenance of liver mitochondria[150] and that several proteins involved in mitochondrial biogenesis are transcriptionally regulated by NRF2[151].

In sum, the tightly regulated processes that underlie mitochondrial quality control through mitophagy and mitochondrial biogenesis rely to some extent on the activation of NRF2.

1.3.3. NRF2 and mitochondrial homeostasis during infection

Activation of NRF2 contributes to maintain mitochondrial homeostasis and function during infection[140]. For example, endotoxic shock triggers cardiac oxidative damage, consequently damaging mitochondrial DNA (mtDNA) and decreasing its copy number, impairing mitochondrial gene transcription and protein expression[152]. On the other hand, expression of genes involved in mitochondrial

biogenesis is increased in response to oxidative stress with mitochondrial oxidative damage being necessary to trigger mitochondrial biogenesis[153].

The murine model of experimental sepsis is perhaps the model of infection in which the NRF2-dependent regulation of mitochondrial biogenesis has been more extensively investigated. For instance, using *E. coli* peritoneal injection in mice it was demonstrated that NRF2, through HO-1 up-regulation, links mitochondrial biogenesis and anti-inflammatory response programs by inducing PGC1-α and Tfam, as well as TNF and Interleukin 10 (IL-10), respectively. This cytoprotective effect acts *in vivo* against *E. coli*-induced sepsis through HO-1 activity and consequent CO production, via a NRF2-dependent mechanism[154]. In a model of *Staphylococcus aureus*-induced peritonitis, CO induces NRF2-dependent mitochondrial biogenesis, accompanied by an increase in mtDNA copy number in the liver of septic mice[155]. More recently, PGC1-α was shown to be required not only for the induction of hepatic mitochondrial biogenesis, but also for mitochondrial antioxidant enzyme induction, namely SOD2, partnering with NRF2 in *Staphylococcus aureus*-induced sepsis[156]. The protective effect of NRF2 in mediating the mitochondrial biogenesis program was corroborated in lung cells upon *Staphylococcus aureus*-induced pneumonia in mice[151].

Together, these results indicate a clear role for NRF2 in preservation of overall cellular homeostasis by maintenance of mitochondrial integrity and number.

1.4. NRF2 as a cytoprotective molecule against the pathophysiology of hemolytic disorders

Heme is an evolutionarily conserved structure that acts as a prostethic group for a variety of hemoproteins and plays a pivotal role in many essential biological processes[157]. Heme is stored mainly into hemoglobin and myoglobin, which constitutes the largest pool of bioavailable iron in RBCs and muscle cells, respectively[158]. Endogenous heme levels are tightly regulated to prevent heme-driven cytotoxicity while assuring its availability for incorporation into nascent apo-hemoproteins. This is tightly regulated through a fine tuned maintenance program of heme synthesis, transport and catabolism[49].

Under pathophysiologic conditions, damage to RBC and muscle cells can result in hemoglobin and myoglobin leakage into circulation, driving its rapid oxidation and release of heme prosthetic groups[159]. This occurs via a process converting iron from ferrous (Fe^{2+}) to ferric (Fe^{3+}) state. The end product of this reaction is labile heme, i.e., redox active loosely bound to proteins or molecules other than its normal partners, the hemoproteins[159]. Circulating labile heme is a threat to systemic homeostasis, as it creates the potential for iron cytotoxicity interfering with basic cellular functions and possibility culminating in cell death[49].

1.4.1. Heme as a danger molecule

The cytotoxic nature of labile heme is associated with its pro-oxidant activity, as Fe^{2+} catalyzes the formation of ROS via Fenton reaction (Figure 1.10, Figure 1.12)[160]. Heme degradation by HO-1 occurs via the oxidative cleavage of the protoporphyrin IX ring, giving rise to biliverdin, CO and equimolar amounts of labile Fe^{2+} (Fig. 1.13)[51]. The cytoprotective action of HO-1 resides both in the

degradation of toxic labile heme as well as in the release of cytoprotective heme degradation products: biliverdin, which is then converted by biliverdin reductase to bilirubin, a powerful lipid phase antioxidant[161]; and CO, an anti-inflammatory and cytoprotective gaseous molecule[162]. The highly reactive Fe^{2+} produced upon heme catabolism is captured by Ferritin, a protein with ferroxidase activity capable of chelating and converting iron into its non-reactive, reusable form (Fe^{3+})[200] (Fig. 1.13).

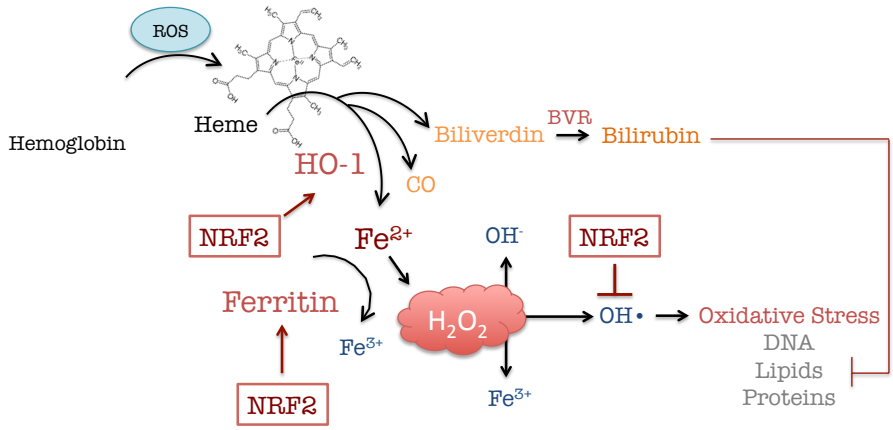

Figure 1.13. Heme catabolism.
Under hemolysis (RBC damage) or rhabdomyolysis (muscle cell damage), hemoglobin or myoglobin, respectively, are released into circulation and become oxidized, releasing its heme prosthetic groups. Labile heme is degraded by HO-1 releasing CO and biliverdin (converted to bilirubin by biliverdin reductase) as well as equimolar amounts Fe^{2+}. This iron form reacts with H_2O_2 to form hydroxyl radicals (•OH), hydroxide ions (OH^-) and Fe^{3+}. Countering this process is Ferritin, which scavenges Fe^{2+} and catalyzes its oxidation to its non-reactive form (Fe^{3+}). NRF2 modulates the cytoprotective effects of HO-1 and ferritin and blocks the deleterious effect of the hydroxyl radical.

Heme belongs to a class of molecules named alarmins that are normally intracellular and can be released, both actively by cells and

passively as a result of sterile trauma, ischemia or toxin/pathogen-induced rupture[159,165]. Such molecules are at the interface of damage and repair, inducing a robust inflammatory response causing collateral tissue damage[166,167] while promoting tissue repair, as illustrated for muscle[168], intestinal[169] and lung injuries[170].

Systemic infections are often associated with more or less severe levels of hemolysis either as an active process for acquisition of host iron[171] or as a consequence of pathogen life-cycle[172]. The effects of hemolysis can be beneficial, as extracellular hemoglobin contributes to pathogen clearance, presumably due to the peroxidase activity of heme reacting with H_2O_2 to oxidize molecules in microbes, as illustrated for bacteria[173] and protozoan parasites[174] (Figure 1.14). Moreover, labile heme released from oxidized hemoglobin synergizes with LPS to induce cytokine production in macrophages through TLR4 signaling[175,166]. Concordantly, LPS-primed macrophages by heme produce Interleukin-1 β (IL-1β) dependent on nucleotide-binding domain and leucine rich repeat containing family, pyrin domain containing 3 (NLRP3) inflammasome[176]. On the other hand, a consequence of hemolytic disorders is excessive erythrophagocytosis, which leads to macrophage apoptosis and consequently to impaired bacterial or parasite clearance[177].

Labile heme is not only cytotoxic to pathogens, but also to host cells and, if not promptly mobilized via export or catabolism, it has a strong potential to react with any cellular membrane[49,111]. Heme was recently described to have a role in the formation aggresome-like induced structures both *in vitro* in macrophages and *in vivo* in a model of acute hemolysis (Phenylhydrazine)[122]. These structures composed of p62 aggregates containing ubiquitinated proteins are storage compartments whose formation is part of the antioxidant response to excessive ROS formation by heme[122]. The formation of these aggresome-like induced structures is dependent on the NRF2

antioxidant capacity and NRF2-dependent heme degradation via HO-1 upregulation. Moreover, the iron released upon heme catabolism is sufficient to induce ALIS and, hence, FtH prevents its formation[122].

The deleterious effect of labile heme is key in the process leading to oxidative stress, cytotoxicity, tissue damage and ultimately organ failure characteristic of the pathogenesis of hemolytic immune-mediated inflammatory diseases[159].

1.4.2. NRF2 and heme cytotoxicity

Intravascular hemolysis is associated with many disorders ranging from genetic variation that compromise RBC homeostasis, such as sickle cell anemia and β-thalassemia, to infectious diseases like malaria or sepsis[49]. These hemolytic conditions have one thing in common – the accumulation of circulating labile heme, which acts as a DAMP inducing a robust pro-inflammatory response while acting as a pro-oxidant and cell death agonist[178].

Malaria

Malaria, the disease caused by the *Plasmodium spp*. protozoan is characterized by a transient liver stage in which the parasite develops inside hepatocytes, followed by a blood stage, where the parasite invades RBCs, causing hemolysis as a consequence of its replication[55]. All clinical manifestations of malaria occur at the blood-stage of infection, coinciding with the release of hemoglobin from RBC and the accumulation of labile heme in circulation[55]. To what extent the labile heme derives from hemoglobin or from the release of myoglobin subsequent to muscle damage, is not clear[179]. Several lines of evidence suggest that labile heme contributes to the pathogenesis of infectious diseases, malaria being the most clearly

established[49,53,176]. Heme sensitizes parenchyma cells, including hepatocytes, to undergo TNF-dependent programmed cell death *in vitro*[180]. The severity of *Plasmodium* infection correlates with the accumulation of cell-free hemoglobin and labile heme in the plasma of mice[56,59] and humans[181,59], eliciting the onset of severe forms of malaria[56,180]. This cytotoxic effect is countered via heme catabolism by HO-1 and the production of CO, which has cytoprotective and anti-inflammatory effects that prevent the pathologic outcome of malaria[50,53,56] (Figure 1.14). Heme catabolism generates labile iron, which is scavenged by ferritin, a multimeric protein revealed critical to restore homeostasis in both rodent and human malaria[59] (Figure 1.14). Interestingly, activation of NRF2 plays a crucial role in the induction of HO-1 and the subsequent production of CO that limits malaria severity[50,53] (Figure 1.14). Whether NRF2 also plays a crucial role in the induction of ferritin during *Plasmodium* infection remains to be elucidated.

Sepsis

Sepsis develops from an exacerbated immune response to microbial infection that leads to tissue damage, multiple organ failure and, in most cases, death[182]. Although the mechanisms underlying the pathogenesis of sepsis remain poorly understood, it is now clear that labile heme is as a crucial pathophysiological agonist for poor sepsis outcome[183]. *In vitro* studies have shown a direct physicochemical interaction of bacterial LPS with RBC membranes, resulting in RBC damage and hemolysis[184]. In mice, cecal ligation and puncture (CLP), a model of experimental sepsis, is associated with RBC deformation (poikilocytosis), accumulation of cell-free hemoglobin and labile heme, as well as decreased plasma concentrations of haptoglobin and hemopexin, the receptors for free

hemoglobin and heme, respectively[183]. Both RBC deformations[185] and decreased hemopexin[183] concentrations are found in sepsis patients, suggesting a conserved effect of labile heme in the pathogenesis of polymicrobial systemic infections (Figure 1.15). Moreover, these data show that significant amounts of hemoglobin can be released and have relevant pathological outcomes, even in the absence of overt hemolysis like the one occurring in malaria disease. Namely, deregulated plasma osmolarity[186], acidosis[187] and bacterial hemolysins[188] contribute to the increase of labile heme in circulation, which, capable of damaging RBCs by itself, enters a positive-feedback loop that contributes to further heme release into circulation[189] (Figure 1.14). Although mainly hemoglobin-derived heme has been linked to the pathogenesis of sepsis, rhabdomyolysis, a disease characterized by severe muscle damage and myoglobin release, was also associated with septic shock, suggesting a transversal role for heme in this disease, independently of the source, i.e. hemoglobin or myoglobin[190].

The deleterious effects of heme in the pathogenesis of sepsis have been liked mainly to sensitization of parenchyma cells to TNF-dependent programmed cell death[183]. More recently, heme was also show to block phagocytosis and migration of human and mouse phagocytes, by disrupting actin cytoskeletal dynamics, thus impairing bacterial clearance[191].

NRF2-dependent protection against heme toxicity has been described in the context of sepsis as artesunate, a protective molecule against this pathology, enhances NRF2 activation with downstream HO-1 upregulation and increased activity in lung tissue[161]. Whether NRF2 and the oxidative stress response protect against sepsis by preventing programmed cell death in the lung still remains to be elucidated.

Activation of NRF2 and consequent amelioration of heme toxicity via tissue damage control mechanisms countering oxidative stress may be good candidates for prevention of the pathophysiological effects of hemolysis in the context of polymicrobial infections.

Hereditary hemolytic anemias

A number of hereditary diseases associated with defects in RBC structure and function can lead to premature RBC senescence associated with increased erythrophagocytosis and hemoglobin release into circulation[49].

The most widely studied form of hereditary hemolytic anemia is sickle cell disease, caused by a single point mutation in the β chain of hemoglobin[49]. This pathology is characterized by the presence of deformed RBCs (sickle shape) with a shortened half-life and prone to hemoglobin polymerization[49]. These defects lead to heme release into circulation, which can increase RBC adhesion, hemolysis, vascular occlusion and ultimately stroke[192] (Figure 1.14). This causes ischemia-reperfusion injury (IRI) characterized by an interruption of blood supply to a given tissue followed by the abrupt delivery of O_2 that cannot be readily used for mitochondrial electron transport chain[193]. The excess O_2 is used by oxidative enzymes like NADPH oxidase to produce ROS, contributing to oxidative stress and ultimately programmed cell death[49]. As such, the NRF2-dependent antioxidant response has been implicated in the context of IRI. Namely, mice lacking NRF2 develop severe tissue damage after kidney IRI injury[194] whereas Keap1 hypomorphs that activate NRF2 constitutively are protected against this oxidative insult[195].

More recently, the connection between NRF2 and sickle cell anemia was reinforced by the finding that *Keap1*-knockout mice, with constitutive activation of NRF2, are protected against oxidative

stress and inflammation associated with sickle cell anemia[196]. Interestingly, NRF2 does not interfere with hemolysis nor stress-induced erythropoiesis during sickle cell disease, suggesting that this transcription factor protects against oxidative tissue damage and the consequent pathologic outcome, rather than preventing hemolysis[196] (Figure 1.14). Presumably, the protective effect exerted by NRF2 acts via the expression of HO-1 and the subsequent production of CO[197 198] (Figure 1.14).

In the context of infection, the mutated form of hemoglobin confers a survival advantage to human populations, when in heterozygozity, in highly endemic areas of *Plasmodium* infection[50]. This is done through constitutive expression of HO-1 via the activation of the NRF2 antioxidant pathway[50]. The CO produced through heme catabolism by HO-1 binds to cell-free hemoglobin, blocking the release of its heme prosthetic groups and countering the pathogenesis of severe forms of malaria[50] (Figure 1.14).

Autoimmune hemolytic anemia is a heterogeneous autoimmune disorder characterized by the development of antibodies directed against antigens on autologous RBCs[199]. As such, RBC are eliminated at a higher rate than the rate of bone marrow replenishment, presumably saturating the carrying capacity of hemoglobin and heme transport/catabolism systems, leading to the accumulation of labile heme in plasma[199]. The chronic accumulation of labile heme in circulation leads to regenerative immune-mediated hemolytic anemia due to increased sequestration of damaged erythrocytes, a phenotype countered by NRF2 and the oxidative stress response[200]. Furthermore, hematological analysis revealed that old mice (14 weeks) lacking NRF2 have morphologically abnormal RBCs, which are more sensitive to H_2O_2-induced hemolysis and carry higher levels of IgG bound to it in the presence

of oxidative damage, suggesting that these cells are more prone to elimination through erythrophagocytosis[200].

Overall, NRF2 plays a pivotal role in diseases associated with hemoglobin leakage from RBCs, presumably countering the deleterious effects of heme by limiting the generation/accumulation of ROS and providing tissue damage control.

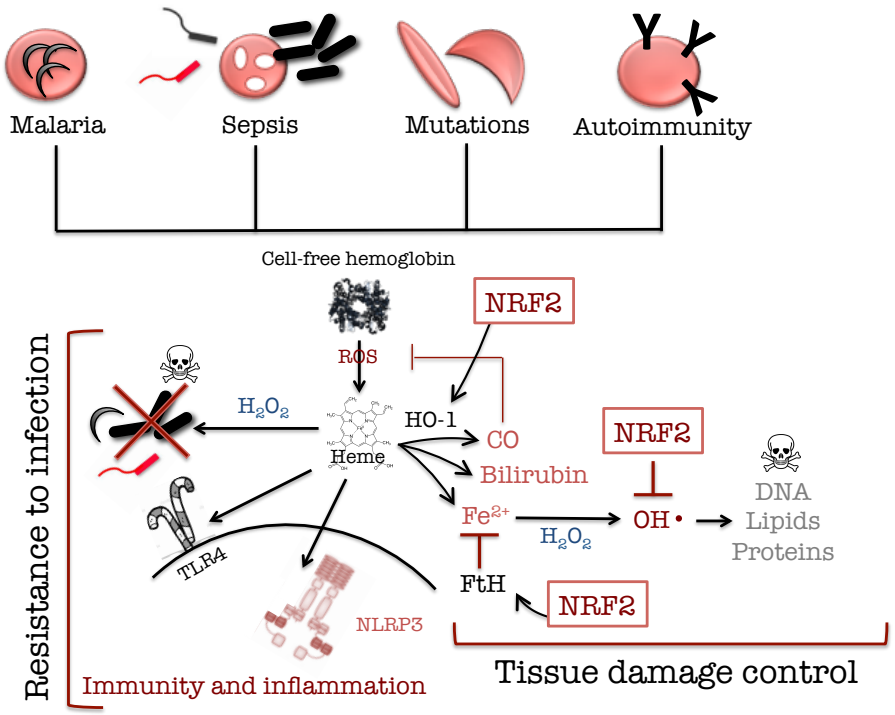

Figure 1.14. The pathophysiology of hemolytic inflammatory diseases.

Hemolytic infectious diseases such as malaria or sepsis, as well as genetically encoded hemolytic conditions such as sickle cell anemia or autoimmune hemolytic anemia are associated with the release of hemoglobin into circulation. Upon oxidation, extracellular hemoglobin releases its heme prosthetic groups, which impacts on tissue homeostasis. Heme signals via TLR-4 and NLRP3 inflammasome activation to promote inflammation. Concomitantly, heme acts directly on pathogen membranes by inducing ROS formation and subsequent killing. Heme degradation by HO-1 leads to the release of Fe^{2+}, which is sequestered and neutralized by ferritin, as to avoid the production of superoxide, leading to oxidative stress. Heme catabolism by HO-1 also generates biliverdin, converted to bilirubin

by biliverdin reductase, and CO, which binds to cell-free hemoglobin and inhibits the release of heme. The cytoprotective effect mediated by HO-1, Ferritin (FtH) and by detoxifying enzymes neutralizing superoxide formation is dependent on NRF2. Hence, NRF2 is crucial to counter oxidative stress leading to tissue damage and guarantee the return to homeostasis.

1.5. Oxidative stress and Programmed cell death

When stress and damage responses fail to sustain the functional outputs of parenchymal cells, tissues or organs, the default program shifts to programmed cell death as a means to eliminate damaged cells and return to homeostasis[201]. Cell death is an important biological process that contributes to the shaping of multicellular organisms during development as well as to maintenance of homeostasis in the adult. In the immune system, programmed cell death mechanisms play a key role in inflammation and pathogen defense[201].

The notion that oxidative stress triggers programmed cell death emerged more than 20 years ago. By that time, it was thought that cells could die exclusively through one pathway – apoptosis[202]. Nowadays, growing evidence demonstrates that cells can die through a plethora of different pathways and that ROS are key players in many of them[203]. Despite the emerging knowledge in different cell death pathways and its relevance in pathological scenarios, in this thesis I will focus on the necroptosis pathway.

1.5.1. ROS and TNF-dependent necroptosis

Regulated necrosis is a genetically controlled cell death process that results in plasma membrane permeability and leakage, cytoplasmic granulation as well as organelle and/or cellular swelling – in other words, an *ordered cellular explosion*[204]. Receptors of the

TNF superfamily were the first to be linked both to apoptosis and regulated necrosis and, although TNF-induced necrosis have been studied since the late 1980's, it was only the discovery of the crucial role played by receptor interacting protein kinase 1 and 3 (RIPK1 and RIPK3) in this pathway that captured the interest of the scientific community[203]. The term necroptosis arose to define a mode of regulated necrosis depending on both RIPK1 and RIPK3. Since then, different pathways of regulated necrosis have been described and defined based on different molecular players and the stimuli that "pull the necrotic trigger"[203].

The molecular machinery of necroptosis

Unlike apoptosis, which is carried out by caspases in a silent and in some settings anti-inflammatory fashion, necroptosis is an extremely turbulent form of programmed cell death from the point of view of the immune system[205]. This pathway may have been selected throughout evolution in the context of viral infections, as its lytic nature is inflammatory and promotes immunity[206]. Moreover, necroptosis is only activated when caspases are inhibited, which happens for example upon targeting of caspases by viral proteins, blocking the apoptotic pathway[206].

Necroptosis can be activated by death receptors such as TNF receptor 1 (TNFR1), PRR such as TLR3 or TLR4 and interferon receptors[207], as well as by intracellular DNA sensor such as the DNA-dependent activator of interferon-regulatory factors (DAI)[230] . TNFR1-dependent necroptosis is the best-characterized pathway and the one I will focus on throughout this thesis.

While death receptors such as the TNFR can trigger programmed cell death, the dominant outcome of their downstream signaling transduction pathway is to promote cell survival[207]. Engagement of

TNFR1 leads to the formation of complex I[210], composed of TNF receptor–associated death domain (TRADD), TNF receptor–associated factor 2 (TRAF2), RIPK1, cellular inhibitor of apoptosis 1 and 2 (cIAP1, cIAP2) and the linear ubiquitin chain assembly complex (LUBAC)[203] (Figure 1.15). Complex I is essential for recruitment and activation of the Inhibitor of κB Kinase (IKK) complex[203,207], which phosphorylates Inhibitor of kappa B (IκBα) leading to its degradation by the 26S proteasome pathway and subsequent nuclear translocation of NF-κB[211]. This results in the upregulation of pro-inflammatory and anti-apoptotic genes blocking the cytotoxic effects of TNF[212,213] (Figure 1.15). Activation of NF-κB induces the expression of $cFLIP_L$, a Caspase 8 heterodimer that prevents apoptosis by inhibiting its activation[212] (Figure 1.15). Unlike conventional death receptors such as FAS or Tumor Necrosis Factor-Related Apoptosis-Inducing Ligand (TRAIL), Fas-associated death domain (FADD) and Caspase 8 are not recruited to TNFR1-associated complex I[214]. Instead, rapid internalization of complex I is crucial to dock FADD and Caspase 8, the initiator caspase, forming a new cytoplasmic structure named complex IIa[201] (Figure 1.15), which leads to downstream activation of effector caspases and culminating in apoptosis (Figure 1.15). The heterodimer $cFLIP_L$ inhibits Caspase 8 proapoptotic activity but maintains cleavage capacity of the necrosis regulators RIPK1 and RIPK3, blocking apoptosis and necroptosis[201] (Figure 1.15). Active Caspase 8 in Complex IIa initiates not only the apoptotic program, but also cleaves and inactivates essential necroptosis mediators such as RIPK1 and RIPK3[215] (Figure 1.15). Hence, inhibition of Caspase-8 or its upstream adaptor FADD primes cells for necroptosis by preserving the integrity of RIPK1 and RIPK3[207]. In fact, most necroptotic stimuli described to date rely on TNFR1 stimulation and simultaneous caspase inhibition reinforced by the inhibition of IAPs, which in turn

blocks NF-κB activation[207,216]. Stabilization of RIPK1 and recruitment of RIPK3 convert Complex IIa to Complex IIb or the necrosome[217] (Figure 1.15). These two kinases interact via their RIP homotypic interaction motif (RHIM) forming an amyloid-like complex, essential for recruitment and activation of the downstream RIPK3 substrate mixed lineage kinase domain-like (MLKL)[218] (Figure 1.15). RIPK3 phosphorylates MLKL, stimulating its oligomerization and translocation to organelle and plasma membranes (Figure 1.15)[219]. The mechanism through which MLKL disrupts membrane integrity is still controversial, but recent data indicates recruitment of NADPH oxidases and ROS generation as well as disruption of calcium or sodium ion channels[219].

Mitochondria promote necroptosis, probably by aiding in the translocation of the necrosome to the mitochondria membranes. This process relies on the binding of MLKL to the mitochondrial phosphatase phosphoglycerate mutase family member 5 (PGAM5), which then triggers mitochondrial ROS production and mitochondrial damage[220] (Figure 1.15). This protein has an important role in mitochondrial homeostasis and programmed cell death through impairment of mitochondrial dynamics, leading to necroptosis[220] (Figure 1.15).

Necroptosis and infection

Because the release of DAMPs stimulates pattern recognition receptors such as TLRs, the explosive nature of necroptosis is widely accepted as part of the pathophysiology of many inflammatory diseases[221].

In viral infections, such as caused by Vaccinia virus, TNF induces RIPK1/RIPK3 activation in host tissues. Deletion of the genes encoding for these proteins renders cells resistant to necroptosis and

reduces inflammation[222,223]. As a trade-off, mice in which RIPK1/RIPK3 activation is impaired succumb to infection due to failure in controlling viral replication[222,223].

In bacterial sepsis, however, TNF is a major driver of systemic cytokine storm, tissue damage and multiorgan failure. As such, impaired RIPK1/RIPK3 activation was shown to be protective against TNF-induced Systemic Inflammatory Response Syndrome (SIRS)[224,225].

The necroptosis pathway is also implicated in the control of *Mycobacterium* infection[11]. One of the major protective functions of TNF is to promote granuloma formation, which is crucial in bacteria containment[11]. Activation of RIPK1 and RIPK3 by TNF leads to the accumulation of ROS and necroptosis of macrophages in these granulomas, allowing bacteria to be released into the growth-permissive extracellular environment. Blocking necroptosis however, leads to burst of macrophages due to excessive bacterial replication inside these cells. As a consequence of macrophage death, bacteria reach the extracellular environment, where replication is permissive[11]. Hence, unlike the situation with Vaccinia virus, one can view *Mycobacterium* as a pathogen that hijacks the host necroptosis machinery to promote its own growth and dissemination.

In parasitic diseases such as malaria, the leakage of hemoglobin and consequent release of heme into circulation leads to inflammation and oxidative stress activating TNF-dependent programmed cell death in parenchyma cells[180]. Macrophages are also prone to heme sensitization to programmed cell death via TLR4 signaling and autocrine TNF and ROS production, which synergize to induce RIPK1/RIPK3-dependent necroptosis[175]. Other cell types that are susceptible to ROS-dependent necrosis include neurons[226] and astrocytes[227].

Besides its role in infection, activation of the RIPK1/RIPK3/MLKL signaling pathway is a hallmark of sterile inflammatory conditions such as acute and chronic alcohol exposure[220] and acetaminophen (APAP)-induced liver injury[221]. Consistent with these findings, a recent study shows that MLKL is the trigger for necroptosis *in vivo* in human autoimmune hepatitis and in a model of inflammation-dependent hepatitis (Concanavalin A, Con A) where it is upregulated and activated[230]. Interestingly, in this particular context, hepatocellular necrosis is driven by a previously unrecognized RIPK3-independent function of MLKL[230]. Additionally, RIPK3 and MLKL are essential players mediating hepatocyte cell death in samples from human patients with primary biliary cholangitis, and genetic ablation of RIPK3 protects mouse hepatocytes from oxidative stress, inflammation and necrosis[231]. The tissue damage caused by IRI in several organs was also shown to be dependent on the necroptosis machinery and many of these studies unravel a role for mitochondria as key players in TNF-dependent necroptosis[232,233].

Together, these data highlight the role of the canonical necroptosis mediators RIPK3 and MLKL in promoting tissue damage in models of sterile inflammation, and may presumably act through a similar mechanism upon infection.

Mitochondria and the execution of necroptosis

Although there is some controversy as to whether mitochondria are required for necroptosis[234], vast information pointing to these organelles as key players in the execution of necroptosis was obtained in cell lines and requires backup from both primary cells and *in vivo* data. The first evidence for involvement of ROS in necroptosis arose more than 10 years ago, where it was demonstrated that triggering the formation of the necrosome after

TNFR1 engagement leads to ROS production[235]. In adition, TNF-mediated ROS generation dependent on RIPK1 derive from mitochondria[236], where suppression of the mitochondrial respiratory chain complex I is cytoprotective[237]. Presumably, the complex IIb formed by RIPK1/RIPK3/MLKL in response to TNFR1 engagement triggers necroptosis via translocation to mitochondria and subsequent mitochondrial ROS production, activation of PGAM5 and mitochondrial damage[234] (Figure 1.15).

PGAM5 regulates mitochondrial fission and mitophagy[238]. Mitochondrial fission is a result of mitochondrial stress and dysfunction characterized by the significant cristae remodeling, leading to fragmentation and disappearance of cristae membranes and a typical change in mitochondrial morphology to a spherical shape[239]. This is achieved via the recruitment of dynamin-related protein 1 (Drp1) by PGAM5, which activates Drp1 GTPase activity through its dephosphorylation, leading to mitochondrial fragmentation, an early obligatory step in necrosis execution[240,271,242]. In agreement with these findings, PGAM5 contributes to ROS production[243] downstream of RIPK3 and MLKL[243], presumably through Drp1 activation, which was shown to promote TNF-dependent necroptosis[243,244] (Figure 1.15).

MPTP is a large non-specific channel that spans in the inner mitochondrial membrane impairing oxidative phosphorylation and promoting ROS production[245]. This process leads to ATP depletion, mitochondrial swelling and rupture, culminating in necrotic cell death[245]. Cyclophilin D (CypD), a mitochondrial matrix protein encoded by the nuclear gene *Peptidylprolyl Isomerase F* (*Ppif*)[245] is a critical regulator of the MPTP opening (Figure 1.16)[246,247,248] and is involved in TNF-dependent necroptosis[217,11] probably acting downstream from RIPK1[249] but probably not RIPK3[232].

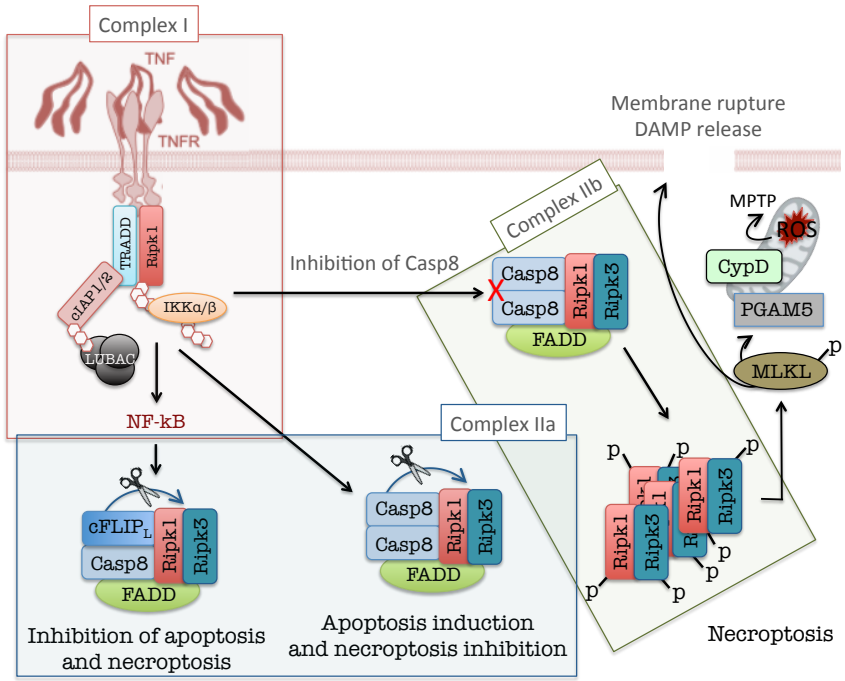

Figure 1.15. TNF-dependent programmed cell death machinery.
The membrane-associated Complex I induces NF-κB activation leading to cFLIPL expression, heterodimerization with caspase 8 and inhibition of both apoptosis and necroptosis. Active caspase 8 in Complex IIa promotes apoptosis and inhibits necroptosis by cleavage of RIPK1 and RIPK3. Upon caspase 8 inactivation (red X), RIPK1 and RIPK3 initiate Complex IIb (necrosome) assembly, amyloid conversion and recruitment of MLKL. This protein acts on the plasma membrane where it mediates membrane rupture with DAMP release and on mitochondria, where it signals to PGAM5, contributing to ROS formation and subsequent MPTP opening mediated by CypD. This leads to mitochondrial dysfunction and sustained ROS production culminating in a necrotic outcome. (Adapted from Ka-Ming Chan F, Luz NF & Moriwaki K, Annu. Rev. Immunol. 2015)

1.6. NRF2 and TNF-dependent necroptosis

There are several independent lines of evidence that suggest a functional link between NRF2 and necroptosis and indicating that activation of NRF2 represses this cell death pathway. Namely, butylated hydroxyanisole (BHA), an NRF2 inducer, suppresses ROS

generation and blocks TNF-dependent necroptosis[235,250], suggesting that this transcription factor acts as a repressor of necroptosis. Furthermore, exogenous GSH attenuates iron-dependent necrosis[226], leading to the hypothesis that the mechanisms via which NRF2 activation counter necroptosis probably involves an increase in cellular glutathione[142].

There is also a functional link between the NRF2-dependent antioxidant pathway and MPTP, which is closed under physiological conditions[251]. In response to pro-oxidant stimuli including ischemia-reperfusion and cytotoxic agents, the MPTP opens irreversibly, eliminating mitochondrial $\Delta\psi_m$ and ATP producing capacity[251]. One of the proteins involved in MPTP opening is GSK-3β[252,253], a kinase that phosphorylates and inhibits NRF2 activation[254,255]. GSK-3β inhibition is cytoprotective via a mechanism involving NRF2 activation and associated with NF-κB inhibition[256]. This suggests that inhibition of NRF2 phosphorylation by GSK-3β reduces mitochondrial ROS accumulation and MPTP opening, presumably ameliorating programmed cell death and tissue damage.

A key component in the necroptosis pathway that was shown to have a link to NRF2 is PGAM5, the protein downstream of MLKL and upstream of MPTP opening[220]. Interestingly, PGAM5 forms a ternary complex containing NRF2 and Keap1 that is localized to mitochondria, contributing to the repression of NRF2-dependent gene expression. Thus, PGAM5, by anchoring the Keap1-NRF2 complex to outer membrane of mitochondria, may facilitate the coordination between mitochondrial function and regulation of NRF2-dependent antioxidant gene expression[257].

Together, these studies reveal that oxidative stress leads to mitochondrial damage through the activation of the necroptotic pathway, and that this mechanism may be countered by the transcriptional regulation of protective genes mediated by NRF2.

1.7. Thesis overview

The general goal of this thesis is to characterize the pathophysiological effects of labile heme in the context of inflammatory agonists leading to necroptosis and understand how these are countered by NRF2. We aimed at uncovering the protective mechanisms via which this redox sensitive transcription factor blocks necroptosis, confers tissue damage control and establishes disease tolerance to systemic infections associated with hemolysis. Manipulation of signal transduction pathways that modulate the oxidative status might unravel a general mechanism for tissue damage control and disease tolerance in different inflammation models.

1.8. References

1. Bernard C. Leçons sur les phénomènes de la vie communs aux animaux et aux végétaux. (J.B. Baillière et fils, 1878).
2. Cannon WB. Organization for physiological homeostasis. Physiol. Rev. 9, 399–431 (1929).
3. Medzhitov, R. Origin and physiological roles of inflammation. Nature 454, 428–35 (2008).
4. Medzhitov, R. Inflammation 2010: New Adventures of an Old Flame. Cell 140, 771–776 (2010).
5. Medzhitov, R., Schneider, D. S. & Soares, M. P. Disease Tolerance as a Defense Strategy. Science (80-.). 335, 936–941 (2012).
6. Råberg, L., Graham, A. L. & Read, A. F. Decomposing health: tolerance and resistance to parasites in animals. Philos. Trans. R. Soc. Lond. B. Biol. Sci. 364, 37–49 (2009).
7. Soares, M. P., Teixeira, L. & Moita, L. F. Disease tolerance and immunity in host protection against infection. Nat. Publ. Gr. 17, 83–96 (2017).
8. Soares, M. P., Gozzelino, R. & Weis, S. Tissue damage control in disease tolerance. Trends in Immunology 35, 483–494 (2014).
9. Martin, S. J. Cell Death and Inflammation: The case for IL-1 family cytokines as the canonical DAMPs of the immune system. FEBS J. 283, 2599–2615 (2016).
10. Brenner, C., Galluzzi, L., Kepp, O. & Kroemer, G. Decoding cell death signals in liver inflammation. J. Hepatol. 59, 583–594 (2013).
11. Roca, F. J. & Ramakrishnan, L. TNF dually mediates resistance and susceptibility to mycobacteria via mitochondrial reactive oxygen species. Cell 153, 521–534 (2013).
12. Yang, C. T. et al. Neutrophils exert protection in the early tuberculous granuloma by oxidative killing of mycobacteria phagocytosed from infected macrophages. Cell Host Microbe 12, 301–312 (2012).

13. Okada, S. Iron-induced tissue damage and cancer: The role of reactive oxygen species-free radicals. Pathol. Int. (1996).
14. Sciences, B., Via, E., College, V. & Tech, V. Antioxidants and Phase 2 Enzymes in Macrophages : Regulation by Nrf2 Signaling and Protection Against Oxidative and Electrophilic Stress. 463–474 (2008). doi:10.3181/0711-RM-304
15. Soares, M. P. & Ribeiro, A. M. Nrf2 as a master regulator of tissue damage control and disease tolerance to infection. Biochem. Soc. Trans. 43, 663–8 (2015).
16. Hayes, J. D. & Dinkova-kostova, A. T. The Nrf2 regulatory network provides an interface between redox and intermediary metabolism. Trends Biochem. Sci. 1–20 (2014). doi:10.1016/j.tibs.2014.02.002
17. Holmstro, K. M. et al. Nrf2 impacts cellular bioenergetics by controlling substrate availability for mitochondrial respiration. (2012). doi:10.1242/bio.20134853
18. Higgins, L. G. & Hayes, J. D. Chemico-Biological Interactions The cap ' n ' collar transcription factor Nrf2 mediates both intrinsic resistance to environmental stressors and an adaptive response elicited by chemopreventive agents that determines susceptibility to electrophilic xenobi. Chem. Biol. Interact. 192, 37–45 (2010).
19. Tebay, L. E. et al. Mechanisms of activation of the transcription factor Nrf2 by redox stressors, nutrient cues and energy status, and pathways through which it attenuates degenerative disease. Free Radic. Biol. Med. (2015). doi:10.1016/j.freeradbiomed.2015.06.021
20. Wild, A. C., Moinova, H. R. & Mulcahy, R. T. Regulation of □ -Glutamylcysteine Synthetase Subunit Gene Expression by the Transcription Factor Nrf2 *.
21. Pompella, A., Visvikis, A., Paolicchi, A., Tata, V. De & Casini, A. F. The changing faces of glutathione , a cellular protagonist. 66, 1499–1503 (2003).
22. Harvey CJ, Thimmulappa RK, Singh A, Blake DJ, Ling G, Wakabayashi N, Fujii J, Myers A, B. S. Nrf2-regulated glutathione recycling independent of biosynthesis is critical for cell survival during oxidative stress. Free Radic Biol Med. 46, 443–453 (2009).
23. Wakabayashi, N. et al. Protection against electrophile and oxidant stress by induction of the phase 2 response : Fate of cysteines of the Keap1 sensor modified by inducers. 2–7 (2004).
24. Benedict, A. L. & Knatko, E. V. The indirect antioxidant sulforaphane protects against thiopurine-mediated photooxidative stress. 2457–2466 (2012). doi:10.1093/carcin/bgs293
25. Hawkes, H. K., Karlenius, T. C. & Tonissen, K. F. Biochimica et Biophysica Acta Regulation of the human thioredoxin gene promoter and its key substrates : A study of functional and putative regulatory elements. BBA - Gen. Subj. 1840, 303–314
26. Abbas, K. et al. Nitric oxide activates an Nrf2 / sulfiredoxin antioxidant pathway in macrophages. Free Radic. Biol. Med. 51, 107–114
27. Wu, K. C., Cui, J. Y. & Klaassen, C. D. Beneficial role of Nrf2 in regulating NADPH generation and consumption. Toxicol. Sci. 123, 590–600 (2011).
28. Lee, J. M., Calkins, M. J., Chan, K., Kan, Y. W. & Johnson, J. a. Identification of the NF-E2-related factor-2-dependent genes conferring protection against oxidative stress in primary cortical astrocytes using oligonucleotide microarray analysis. J. Biol. Chem. 278, 12029–12038 (2003).
29. Xie, Q. W., Kashiwabara, Y. & Nathan, C. Role of transcription factor NF-kappa B/Rel in induction of nitric oxide synthase. J. Biol. Chem. 269, 4705–4708 (1994).
30. Anrather, J., Racchumi, G. & Iadecola, C. NF- kB Regulates Phagocytic

NADPH Oxidase by Inducing the Expression of gp91 phox. (2006). doi:10.1074/jbc.M506172200
31. Itoh, K. et al. Keap1 represses nuclear activation of antioxidant responsive elements by Nrf2 through binding to the amino-terminal Neh2 domain. Genes Dev. 13, 76–86 (1999).
32. Suzuki, T., Motohashi, H. & Yamamoto, M. Toward clinical application of the Keap1-Nrf2 pathway. Trends Pharmacol. Sci. 34, 340–6 (2013).
33. Kensler, T. W., Wakabayashi, N. & Biswal, S. Cell survival responses to environmental stresses via the Keap1-Nrf2-ARE pathway. Annu. Rev. Pharmacol. Toxicol. 47, 89–116 (2007).
34. Sykiotis, G. P. & Bohmann, D. Stress-Activated Cap ' n ' collar Transcription Factors in Aging and Human Disease. 1–23 (2010).
35. Rada, P. et al. SCF/{beta}-TrCP promotes glycogen synthase kinase 3-dependent degradation of the Nrf2 transcription factor in a Keap1-independent manner. Mol. Cell. Biol. 31, 1121–33 (2011).
36. Wu, T. et al. Hrd1 suppresses Nrf2-mediated cellular protection during liver cirrhosis. Genes Dev. 28, 708–722 (2014).
37. Cullinan, S. B. et al. Nrf2 is a direct PERK substrate and effector of PERK-dependent cell survival. Mol. Cell. Biol. 23, 7198–209 (2003).
38. Pekovic-Vaughan, V. et al. The circadian clock regulates rhythmic activation of the NRF2/glutathione-mediated antioxidant defense pathway to modulate pulmonary fibrosis. Genes Dev. 28, 548–60 (2014).
39. Page, A. et al. Marburgvirus Hijacks Nrf2-Dependent Pathway by Targeting Nrf2-Negative Regulator Keap1. CellReports 6, 1026–1036 (2006).
40. Edwards, M. R. et al. The Marburg Virus VP24 Protein Interacts with Keap1 to Activate the Cytoprotective Antioxidant Response Pathway. CellReports 6, 1017–1025 (2014).
41. Gjyshi, O. et al. Kaposi ' s Sarcoma-Associated Herpesvirus Induces Nrf2 during De Novo Infection of Endothelial Cells to Create a Microenvironment Conducive to Infection. (2014). doi:10.1371/journal.ppat.1004460
42. Kosmider, B. et al. Nrf2 protects human alveolar epithelial cells against injury induced by influenza A virus. Respir. Res. 13, 43 (2012).
43. Kesic, M. J., Simmons, S. O., Bauer, R. & Jaspers, I. Free Radical Biology & Medicine Nrf2 expression modi fi es in fl uenza A entry and replication in nasal epithelial cells ☆. 51, 444–453
44. Olagnier, D. et al. Cellular Oxidative Stress Response Controls the Antiviral and Apoptotic Programs in Dengue Virus-Infected Dendritic Cells. 1–18 (2014). doi:10.1371/journal.ppat.1004566
45. Carvajal-yepes, M. et al. Hepatitis C Virus Impairs the Induction of Cytoprotective Nrf2 Target Genes by Delocalization of Small Maf Proteins. 8941–8952 (2011). doi:10.1074/jbc.M110.186684
46. Nairz, M. et al. Nitric oxide-mediated regulation of ferroportin-1 controls macrophage iron homeostasis and immune function in Salmonella infection. J. Exp. Med. 210, 855–73 (2013).
47. Harvey, C. J. et al. Targeting Nrf2 Signaling Improves Bacterial Clearance by Alveolar Macrophages in Patients with COPD and in a Mouse Model. (2011).
48. Dardenne, C. et al. Nrf2 , a PPAR c Alternative Pathway to Promote CD36 Expression on Inflammatory Macrophages : Implication for Malaria. (2011). doi:10.1371/journal.ppat.1002254
49. Larsen, R., Gouveia, Z., Soares, M. P. & Gozzelino, R. Heme cytotoxicity and the pathogenesis of immune-mediated inflammatory diseases. Front. Pharmacol. 3, 77 (2012).
50. Ferreira, A. et al. Sickle hemoglobin confers tolerance to plasmodium infection. Cell 145, 398–409 (2011).
51. Gozzelino, R., Jeney, V. & Soares, M. P. Mechanisms of cell protection by

heme oxygenase-1. Annu. Rev. Pharmacol. Toxicol. 50, 323–354 (2010).
52. Ademolue, T. W., Amodu, O. K. & Awandare, G. A. Sickle cell trait is associated with controlled levels of heme and mild pro-inflammatory response during acute malaria infection. Clin. Exp. Immunol. 283–292 (2017). doi:10.1111/cei.12936
53. Jeney, V. et al. Control of disease tolerance to malaria by nitric oxide and carbon monoxide. Cell Rep. 8, 126–36 (2014).
54. Fourquet, S., Biard, D. & Toledano, M. B. Activation of NRF2 by Nitrosative Agents and H 2 O 2 Involves. (2010). doi:10.1074/jbc.M109.051714
55. Ferreira, A., Balla, J., Jeney, V., Balla, G. & Soares, M. P. A central role for free heme in the pathogenesis of severe malaria: the missing link? J. Mol. Med. (Berl). 86, 1097–111 (2008).
56. Pamplona, A. et al. Heme oxygenase-1 and carbon monoxide suppress the pathogenesis of experimental cerebral malaria. Nat. Med. 13, 703–10 (2007).
57. Martin, D. et al. Regulation of heme oxygenase-1 expression through the phosphatidylinositol 3-kinase/Akt pathway and the Nrf2 transcription factor in response to the antioxidant phytochemical carnosol. J. Biol. Chem. 279, 8919–29 (2004).
58. Thimmulappa, R. K. et al. Identification of Nrf2-regulated genes induced by the chemopreventive agent sulforaphane by oligonucleotide microarray. Cancer Res. 62, 5196–203 (2002).
59. Gozzelino, R. et al. Metabolic Adaptation to Tissue Iron Overload Confers Tolerance to Malaria. Cell Host Microbe 693–704 (2012).
60. Thimmulappa, R. K. et al. Nrf2 is a critical regulator of the innate immune response and survival during experimental sepsis. 116, (2006).
61. Athale, J. et al. Nrf2 promotes alveolar mitochondrial biogenesis and resolution of lung injury in Staphylococcus aureus pneumonia in mice. Free Radic. Biol. Med. 53, 1584–94 (2012).
62. Nairz, M., Sonnweber, T., Schroll, A., Theurl, I. & Weiss, G. The pleiotropic effects of erythropoietin in infection and inflammation. Microbes Infect. 14, 238–246 (2012).
63. Chapple, S. J. et al. Bach1 differentially regulates distinct Nrf2-dependent genes in human venous and coronary artery endothelial cells adapted to physiological oxygen levels. Free Radic. Biol. Med. 92, 152–162 (2016).
64. Ward, J. P. T. Oxygen sensors in context. Biochim. Biophys. Acta - Bioenerg. 1777, 1–14 (2008).
65. Semenza, G. L. Hypoxia-inducible factors in physiology and medicine. Cell 148, 399–408 (2012).
66. Toth, R. & Warfel, N. Strange Bedfellows: Nuclear Factor, Erythroid 2-Like 2 (Nrf2) and Hypoxia-Inducible Factor 1 (HIF-1) in Tumor Hypoxia. Antioxidants 6, 27 (2017).
67. Pan, Y. et al. Multiple Factors Affecting Cellular Redox Status and Energy Metabolism Modulate Hypoxia-Inducible Factor Prolyl Hydroxylase Activity In Vivo and In Vitro. Mol. Cell. Biol. 27, 912–925 (2006).
68. Kim, T. H. et al. NRF2 blockade suppresses colon tumor angiogenesis by inhibiting hypoxia-induced activation of HIF-1?? Cancer Res. 71, 2260–2275 (2011).
69. Oh, E.-T. et al. NQO1 inhibits proteasome-mediated degradation of HIF-1α. Nat. Commun. 7, 13593 (2016).
70. Yeligar, S. M., Machida, K. & Kalra, V. K. Ethanol-induced HO-1 and NQO1 are differentially regulated by HIF-1?? and Nrf2 to attenuate inflammatory cytokine expression. J. Biol. Chem. 285, 35359–35373 (2010).
71. Ke, B. et al. KEAP1-NRF2 complex in ischemia-induced hepatocellular damage of mouse liver transplants. J. Hepatol. 59, 1200–1207 (2013).
72. Hardie, D. G., Ross, F. a. & Hawley, S. a. AMPK: a nutrient and energy

sensor that maintains energy homeostasis. Nat. Rev. Mol. Cell Biol. 13, 251–262 (2012).
73. Kaspar, J. W., Niture, S. K. & Jaiswal, A. K. Nrf2:INrf2 (Keap1) signaling in oxidative stress. Free Radic. Biol. Med. 47, 1304–1309 (2009).
74. Zimmermann, K. et al. Activated AMPK boosts the Nrf2 / HO-1 signaling axis — A role for the unfolded protein response. Free Radic. Biol. Med. 88, 417–426 (2015).
75. Li, F. Y. L. et al. Endothelium-selective activation of AMP-activated protein kinase prevents diabetes mellitus-induced impairment in vascular function and reendothelialization via induction of heme oxygenase-1 in mice. Circulation 126, 1267–1277 (2012).
76. Brocker C, Thompson DC, V. V. The role of hyperosmotic stress in inflammation and disease. Biomol Concepts. 3, 345–364 (2012).
77. Jantsch J, Schatz V, Luft FC, Titze J, Kopp C, Siegert I, Maronna A, Wendelborn D, Linz , Binger KJ, Gebhardt M, Heinig M, R. N. & C Ku, T. J. Cutaneous Na + Storage Strengthens the Antimicrobial Barrier Function of the Skin and Boosts Macrophage-Driven Host Defense. Cell Metab. 493–501 (2015). doi:10.1016/j.cmet.2015.02.003
78. Fraek, M., Beck, F. & Neuhofer, W. Sirt1 resists advanced glycation end products-induced expressions of fibronectin and TGF-β1 by activating the Nrf2/ARE pathway in glomerular mesangial cells. (2012). doi:10.1097/CCM.0b013e31824e1186
79. Kang, E. S. et al. Up-regulation of aldose reductase expression mediated by phosphatidylinositol 3-kinase/Akt and Nrf2 is involved in the protective effect of curcumin against oxidative damage. Free Radic. Biol. Med. 43, 535–545 (2007).
80. Xia, X. et al. NFAT5 protects astrocytes against oxygen–glucose–serum deprivation/restoration damage via the SIRT1/Nrf2 pathway. J. Mol. Neurosci. 61, 96–104 (2017).
81. Huang, K. et al. Sirt1 resists advanced glycation end products-induced expressions of fibronectin and TGF-??1 by activating the Nrf2/ARE pathway in glomerular mesangial cells. Free Radic. Biol. Med. 65, 528–540 (2013).
82. Ding, Y.-W. et al. SIRT1 exerts protective effects against paraquat-induced injury in mouse typeï¿½II alveolar epithelial cells by deacetylating NRF2 inï¿½vitro. Int. J. Mol. Med. 1–10 (2016). doi:10.3892/ijmm.2016.2503
83. Hasday, J. D. & Singh, I. S. Fever and the heat shock response: distinct, partially overlapping processes. Cell Stress Chaperones 5, 471–80 (2000).
84. Schett, G., Steiner, C.-W., Xu, Q., Smolen, J. S. & Steiner, G. TNFalpha mediates susceptibility to heat-induced apoptosis by protein phosphatase-mediated inhibition of the HSF1/hsp70 stress response. Cell Death Differ. 10, 1126–1136 (2003).
85. Xiao, X. et al. HSF1 is required for extra-embryonic development, postnatal growth and protection during inflammatory responses in mice. EMBO J. 18, 5943–5952 (1999).
86. Schett, G. et al. Activation of Fas inhibits heat-induced activation of HSF1 and up-regulation of hsp70. FASEB J. 13, 833–842 (1999).
87. Murapa, P., Ward, M. R., Gandhapudi, S. K., Woodward, J. G. & D'Orazio, S. E. F. Heat shock factor 1 protects mice from rapid death during listeria monocytogenes infection by regulating expression of tumor necrosis factor alpha during fever. Infect. Immun. 79, 177–184 (2011).
88. Yan, L. et al. Mouse heat shock transcription factor 1 de ® ciency alters cardiac redox homeostasis and increases mitochondrial oxidative damage. EMBO J. 21, 5164–5172 (2002).
89. Dayalan Naidu, S., Kostov, R. V. & Dinkova-Kostova, A. T. Transcription factors Hsf1 and Nrf2 engage in crosstalk for cytoprotection. Trends Pharmacol. Sci. 36, 6–14 (2015).

90. Prestera, T. et al. Parallel induction of heme oxygenase-1 and chemoprotective phase 2 enzymes by electrophiles and antioxidants: regulation by upstream antioxidant-responsive elements (ARE). Mol. Med. 1, 827–837 (1995).
91. Maines, M. D. & Ewing, J. F. Stress response of the rat testis: in situ hydridization and immunohistochemical analysis of heme oxygenase-1 (HSP32) induction by hyperthermia. Biol Reprod 54, 1070–1079 (1996).
92. Chen, H. et al. Heat shock protein 27 downregulates the transferrin receptor 1-mediated iron uptake. Int. J. Biochem. Cell Biol. 38, 1402–16 (2006).
93. Almeida, D. V. et al. Induction of phase II enzymes and hsp70 genes by copper sulfate through the electrophile-responsive element (EpRE): Insights obtained from a transgenic zebrafish model carrying an orthologous EpRE sequence of mammalian origin. Fish Physiol. Biochem. 36, 347–353 (2010).
94. Komatsu, M. et al. The selective autophagy substrate p62 activates the stress responsive transcription factor Nrf2 through inactivation of Keap1. Nat. Cell Biol. 12, 213–23 (2010).
95. Samarasinghea B, Walesa CTK, Taylora FR, J. A. Heat Shock Factor 1 Confers Resistance to Hsp90 Inhibitors through p62/SQSTM1 Expression and Promotion of Autophagic Flux. Biochem Pharmacol. 87, 445–455 (2014).
96. Hensen, S. M. M., Heldens, L., Van Genesen, S. T., Pruijn, G. J. M. & Lubsen, N. H. A delayed antioxidant response in heat-stressed cells expressing a non-DNA binding HSF1 mutant. Cell Stress Chaperones 18, 455–473 (2013).
97. Hensen, S. M. M. et al. Activation of the antioxidant response in methionine deprived human cells results in an HSF1-independent increase in HSPA1A mRNA levels. Biochimie 95, 1245–1251 (2013).
98. Higa, A. & Chevet, E. Redox signaling loops in the unfolded protein response. Cell. Signal. 24, 1548–1555 (2012).
99. Martin, D. et al. Unspliced X-box-binding protein 1 (XBP1) protects endothelial cells from oxidative stress through interaction with histone deacetylase 3. J. Biol. Chem. 289, 30625–30634 (2014).
100. Yamamoto, K. et al. Human HRD1 promoter carries a functional unfolded protein response element to which XBP1 but not ATF6 directly binds. J. Biochem. 144, 477–486 (2008).
101. Kaser, A. et al. XBP1 Links ER Stress to Intestinal Inflammation and Confers Genetic Risk for Human Inflammatory Bowel Disease. Cell 134, 743–756 (2008).
102. van 't Wout, E. F. A. et al. Virulence Factors of Pseudomonas aeruginosa Induce Both the Unfolded Protein and Integrated Stress Responses in Airway Epithelial Cells. PLoS Pathog. 11, e1004946 (2015).
103. Richardson, C. E., Kooistra, T. & Kim, D. H. An essential role for XBP-1 in host protection against immune activation in C. elegans. Nature 463, 1092–5 (2010).
104. Weitzman, M. D. & Weitzman, J. B. What's the damage? The impact of pathogens on pathways that maintain host genome integrity. Cell Host Microbe 15, 283–294 (2014).
105. Bouvard, V. et al. Carcinogenicity of malaria and of some polyomaviruses. Lancet Oncol. 13, 339–340 (2012).
106. Hanahan, D. & Weinberg, R. A. Hallmarks of cancer: The next generation. Cell 144, 646–674 (2011).
107. Shiloh, Y. & Ziv, Y. The ATM protein kinase: regulating the cellular response to genotoxic stress, and more. Nat. Rev. Mol. Cell Biol. 14, 197–210 (2013).
108. Figueiredo, N. et al. Anthracyclines induce DNA damage response-mediated protection against severe sepsis. Immunity 39, 874–884 (2013).
109. Biagiotti, S. et al. Dexamethasone improves redox state in ataxia

telangiectasia cells by promoting an NRF2-mediated antioxidant response. 283, 3962–3978 (2016).
110. Otterbein, L. E. et al. Heme oxygenase-1 and carbon monoxide modulate DNA repair through ataxia-telangiectasia mutated (ATM) protein. Proc. Natl. Acad. Sci. U. S. A. 108, 14491–14496 (2011).
111. Dutra, F. F. & Bozza, M. T. Heme on innate immunity and inflammation. Front. Pharmacol. 5, 1–20 (2014).
112. Dixon, S. J. & Stockwell, B. R. The role of iron and reactive oxygen species in cell death. Nat. Chem. Biol. 10, 9–17 (2014).
113. Dixon, S. J. et al. Ferroptosis: an iron-dependent form of nonapoptotic cell death. Cell 149, 1060–72 (2012).
114. Agbor, T. A. et al. The oxido-reductase enzyme glutathione peroxidase 4 (GPX4) governs SalmonellaTyphimurium-induced neutrophil transepithelial migration. Cell. Microbiol. 16, 1339–1353 (2014).
115. Doll, S. & Conrad, M. Iron and ferroptosis: A still ill-defined liaison. IUBMB Life 1–12 (2017). doi:10.1002/iub.1616
116. Yang, W. S. & Stockwell, B. R. Ferroptosis: Death by Lipid Peroxidation. Trends Cell Biol. 26, 165–176 (2016).
117. Carlson, B. A. et al. Glutathione peroxidase 4 and vitamin E cooperatively prevent hepatocellular degeneration. Redox Biol. 9, 22–31 (2016).
118. Sun, X. et al. Activation of the p62-Keap1-NRF2 pathway protects against ferroptosis in hepatocellular carcinoma cells. Hepatology 63, 173–184 (2016).
119. Brault, C. et al. Glutathione peroxidase 4 is reversibly induced by HCV to control lipid peroxidation and to increase virion infectivity. Gut 1–11 (2014). doi:10.1136/gutjnl-2014-307904
120. Levine, B. & Kroemer, G. Autophagy in the Pathogenesis of Disease. Cell 132, 27–42 (2008).
121. Kroemer, G., Mari??o, G. & Levine, B. Autophagy and the Integrated Stress Response. Mol. Cell 40, 280–293 (2010).
122. Vasconcellos, L. R. C. et al. Protein aggregation as a cellular response to oxidative stress induced by heme and iron. (2016). doi:10.1073/pnas.1608928113
123. Arnoult, D., Carneiro, L., Tattoli, I. & Girardin, S. E. The role of mitochondria in cellular defense against microbial infection. Semin. Immunol. 21, 223–232 (2009).
124. Filomeni, G., De Zio, D. & Cecconi, F. Oxidative stress and autophagy: the clash between damage and metabolic needs. Cell Death Differ. 22, 377–388 (2015).
125. Chang, A. L., Ulrich, A., Suliman, H. B. & Piantadosi, C. A. Redox regulation of mitophagy in the lung during murine Staphylococcus aureus sepsis. Free Radic. Biol. Med. 78, 179–189 (2015).
126. East, D. A. et al. PMI: A Δψm independent pharmacological regulator of mitophagy. Chem. Biol. 21, 1585–1596 (2014).
127. Xiao, L. et al. The mitochondria-targeted antioxidant MitoQ ameliorated tubular injury mediated by mitophagy in diabetic kidney disease via Nrf2/PINK1. Redox Biol. 11, 297–311 (2017).
128. Fang, E. F. et al. Tomatidine enhances lifespan and healthspan in C. elegans through mitophagy induction via the SKN-1/Nrf2 pathway. Sci. Rep. 7, 46208 (2017).
129. Schieber, M. & Chandel, N. S. ROS Function in Redox Signaling and Oxidative Stress. CURBIO 24, R453–R462 (2014).
130. Chandel, N. S. Essay Evolution of Mitochondria as Signaling Organelles. Cell Metab. 22, 204–206 (2015).
131. Dixon SJ, S. B. The role of iron and reactive oxygen species in cell death. Nat. Chem. Biol. 9–17 (2013). doi:10.1038/nchembio.1416

132. Gupta, S. C. et al. Upsides and Downsides of Reactive Oxygen Species for Cancer: The Roles of Reactive Oxygen Species in Tumorigenesis, Prevention, and Therapy. Antioxid. Redox Signal. 16, 1295–1322 (2012).
133. Yana, M. H., Wang, X. & Zhu, X. Mitochondrial defects and oxidative stress in Alzheimer disease and Parkinson disease. Free Radical Biology and Medicine 62, 90–101 (2013).
134. Kaspar, J. W., Niture, S. K. & Jaiswal, A. K. Nrf2:INrf2 (Keap1) signaling in oxidative stress. Free Radic. Biol. Med. 47, 1304–9 (2009).
135. Tebay, L. E. et al. Mechanisms of activation of the transcription factor Nrf2 by redox stressors, nutrient cues, and energy status and the pathways through which it attenuates degenerative disease. Free Radic. Biol. Med. 88, 108–146 (2015).
136. Schmidt, H. H. H. W. et al. Antioxidants in Translational Medicine. Antioxid. Redox Signal. 23, 1130–43 (2015).
137. Kovac, S. et al. Nrf2 regulates ROS production by mitochondria and NADPH oxidase. Biochim. Biophys. Acta - Gen. Subj. 1850, 794–801 (2015).
138. Bedard, K. & Krause, K.-H. The NOX family of ROS-generating NADPH oxidases: physiology and pathophysiology. Physiol. Rev. 87, 245–313 (2007).
139. Brewer, A. C. et al. Free Radical Biology & Medicine Nox4 regulates Nrf2 and glutathione redox in cardiomyocytes in vivo. Free Radic. Biol. Med. 51, 205–215
140. Dinkova-Kostova, A. T. & Abramov, A. Y. The emerging role of Nrf2 in mitochondrial function. Free Radic. Biol. Med. 1–10 (2015). doi:10.1016/j.freeradbiomed.2015.04.036
141. Kovac, S. et al. Nrf2 regulates ROS production by mitochondria and NADPH oxidase. Biochim. Biophys. Acta - Gen. Subj. 1850, 794–801 (2015).
142. Dinkova-Kostova, A. T. & Abramov, A. Y. The emerging role of Nrf2 in mitochondrial function. Free Radic. Biol. Med. 88, 179–88 (2015).
143. Zorov, B. D. B., Filburn, C. R., Klotz, L., Zweier, J. L. & Sollott, S. J. Reactive Oxygen Species (ROS) -induced ROS Release : A New Phenomenon Accompanying Induction of the Mitochondrial Permeability Transition in Cardiac Myocytes. (2000).
144. Zhang, J. Teaching the basics of autophagy and mitophagy to redox biologists-Mechanisms and experimental approaches. Redox Biol. 4, 242–259 (2015).
145. Holmström, K. M., Kostov, R. V & Dinkova-kostova, A. T. The multifaceted role of Nrf2 in mitochondrial function. Curr. Opin. Toxicol. 1, 80–91 (2016).
146. Anedda, A., López-bernardo, E., Suleiman, M. S., Manuel, O. & Cadenas, S. The transcription factor Nrf2 promotes survival by enhancing the expression of uncoupling protein 3 under conditions of oxidative stress. Free Radic. Biol. Med. (2013).
147. Ivankovic, D., Chau, K. Y., Schapira, A. H. V & Gegg, M. E. Mitochondrial and lysosomal biogenesis are activated following PINK1/parkin-mediated mitophagy. J. Neurochem. 136, 388–402 (2016).
148. Xiao, L. et al. Redox Biology The mitochondria-targeted antioxidant MitoQ ameliorated tubular injury mediated by mitophagy in diabetic kidney disease via Nrf2 / PINK1. Redox Biol. 11, 297–311 (2016).
149. Zhu, J., Wang, K. Z. Q. & Chu, C. T. After the banquet Mitochondrial biogenesis, mitophagy, and cell survival. Autophagy 1663–1676 (2013).
150. Zhang, Y. J., Wu, K. C. & Klaassen, C. D. Genetic Activation of Nrf2 Protects against Fasting- Induced Oxidative Stress in Livers of Mice. 1–10 (2013). doi:10.1371/journal.pone.0059122
151. Janhavi Athalea, Allison Ulrichb, Nancy Chou MacGarveya, Raquel R. Bartzb, Karen E. Welty-Wolfa, Hagir B. Sulimanb, C. A. P. Nrf2 promotes alveolar mitochondrial biogenesis and resolution of lung injury in

Staphylococcus aureus pneumonia in mice. Free Radic. Biol. Med. 53, 1584–1594 (2012).
152. Suliman, H. B., Welty-Wolf, K. E., Carraway, M., Tatro, L. & Piantadosi, C. a. Lipopolysaccharide induces oxidative cardiac mitochondrial damage and biogenesis. Cardiovasc. Res. 64, 279–88 (2004).
153. Suliman, H. B., Welty-wolf, K. E., Sue, M., Tatro, L. & Piantadosi, C. A. Lipopolysaccharide induces oxidative cardiac mitochondrial damage and biogenesis. 64, 279–288 (2004).
154. Piantadosi, C. a et al. Heme oxygenase-1 couples activation of mitochondrial biogenesis to anti-inflammatory cytokine expression. J. Biol. Chem. 286, 16374–85 (2011).
155. Macgarvey, N. C. et al. Activation of Mitochondrial Biogenesis by Heme Oxygenase-1 – mediated NF-E2 – related Factor-2 Induction Rescues Mice from Lethal Staphylococcus aureus Sepsis. doi:10.1164/rccm.201106-1152OC
156. Cherry, A. D., Suliman, H. B., Bartz, R. R., Piantadosi, C. A. & Carolina, N. Peroxisome Proliferator-activated Receptor □ Co-activator 1- ⎁ as a Critical Co-activator of the Murine Hepatic Oxidative Stress Response and Mitochondrial Biogenesis in Staphylococcus aureus Sepsis *. 41–52 (2014). doi:10.1074/jbc.M113.512483
157. Korolnek, T. & Hamza, I. Macrophages and iron trafficking at the birth and death of red cells. 2893–2898 (2015). doi:10.1182/blood-2014-12-567776.BLOOD
158. Soares, M. P. & Weiss, G. The Iron age of host – microbe interactions. 1482–1500 (2015).
159. Soares, M. P. & Bozza, M. T. Red alert: Labile heme is an alarmin. Curr. Opin. Immunol. 38, 94–100 (2016).
160. Ezraty, B. & Ezraty, B. The ' liaisons dangereuses ' between iron and antibiotics The ' liaisons dangereuses ' between iron and antibiotics. doi:10.1093/femsre/fuw004
161. Stocker, R., Yamamoto, Y., Mcdonagh, A. F., Glazer, A. N. & Ames, B. N. Bilirubin is an Antioxidant of Possible Physiological Importance Published by : American Association for the Advancement of Science Stable URL : http://www.jstor.org/stable/1698769 Accessed : 07-06-2016 09 : 41 UTC. 235, 1043–1046 (1987).
162. Brouard, S. et al. Heme Oxygenase-1-derived Carbon Monoxide Requires the Activation of Transcription Factor NF- □ B to Protect Endothelial Cells from Tumor Necrosis Factor- ⎁ -mediated Apoptosis *. doi:10.1074/jbc.M108317200
163. Arosio, P., Carmona, F., Gozzelino, R., Maccarinelli, F. & Poli, M. The importance of eukaryotic ferritins in iron handling and cytoprotection. 1–15 (2015). doi:10.1042/BJ20150787
164. Gozzelino, R. & Soares, M. P. Coupling Heme and Iron Metabolism via Ferritin H Chain. Antioxid Redox Signal 1754–1769 (2014). doi:10.1089/ars.2013.5666
165. Wegiel, B., Hauser, C. J. & Otterbein, L. E. Heme as a danger molecule in pathogen recognition. Free Radic. Biol. Med. 89, 651–661 (2015).
166. Fernandez, P. L. et al. Heme amplifies the innate immune response to microbial molecules through spleen tyrosine kinase (Syk)-dependent reactive oxygen species generation. J. Biol. Chem. 285, 32844–51 (2010).
167. Zhang, Q. et al. Circulating mitochondrial DAMPs cause inflammatory responses to injury. Nature 464, 104–107 (2010).
168. Burzyn, D. et al. A Special Population of Regulatory T Cells Potentiates Muscle Repair. Cell 155, 1282–1295 (2013).
169. Schiering, C. et al. The alarmin IL-33 promotes regulatory T-cell function in the intestine. Nature (2014). doi:10.1038/nature13577

170. Yuan, S., Treuting, P. M. & Rudensky, A. Y. A Distinct Function of Regulatory T Cells in Tissue Protection. Cell 162, 1078–1089 (2015).
171. Cassat, J. E. & Skaar, E. P. Iron in infection and immunity. Cell Host Microbe 13, 509–19 (2013).
172. Mideo, N., Reece, S. E., Smith, A. L. & Metcalf, C. J. E. The Cinderella syndrome: why do malaria-infected cells burst at midnight? Trends Parasitol. 29, 10–16 (2013).
173. Jiang, N., Tan, N. S., Ho, B. & Ding, J. L. Respiratory protein – generated reactive oxygen species as an antimicrobial strategy. (2007). doi:10.1038/ni1501
174. Foster, R. C. Hemin Lyses Malaria Parasites. 667–669 (1981).
175. Fortes, G. B. et al. Heme induces programmed necrosis on macrophages through autocrine TNF and ROS production. Blood 119, 2368–2375 (2012).
176. Dutra, F. F. et al. Hemolysis-induced lethality involves inflammasome activation by heme. Proc. Natl. Acad. Sci. U. S. A. 111, E4110-8 (2014).
177. Scorza, T. Robust erythrophagocytosis leads to macrophage apoptosis via a hemin-mediated redox imbalance : Role in hemolytic disorders Robust erythrophagocytosis leads to macrophage apoptosis via a hemin-mediated redox imbalance : role in hemolytic disorders. doi:10.1189/jlb.0510249
178. Gladwin, M. T. & Ofori-Acquah, S. F. Erythroid DAMPs drive inflammation in SCD. Blood 123, 3689–3690 (2014).
179. Donnell, A. O. et al. Muscle cell injury , haemolysis and dark urine in children with falciparum malaria in Papua New Guinea. (2006). doi:10.1016/j.trstmh.2005.11.015
180. Seixas, E. et al. Heme oxygenase-1 affords protection against noncerebral forms of severe malaria. Proc. Natl. Acad. Sci. U. S. A. 106, 15837–42 (2009).
181. Andrade, B. B. et al. Heme Impairs Prostaglandin E2 and TGF- β Production by Human Mononuclear Cells via Cu/Zn Superoxide Dismutase: Insight into the Pathogenesis of Severe Malaria. J. Immunol. (2010). doi:10.4049/jimmunol.0904179
182. Cohen, J. The immunopathogenesis of sepsis. Nature 885–891 (2002).
183. Larsen, R. et al. A Central Role for Free Heme in the Pathogenesis of Severe Sepsis. (2010).
184. Brauckmann, S. et al. Lipopolysaccharide-induced hemolysis : Evidence for direct membrane interactions. 1–9 (2016). doi:10.1038/srep35508
185. Piagnerelli, M., Boudjeltia, K. Z., Vanhaeverbeek, M. & Vincent, J. Red blood cell rheology in sepsis. 1052–1061 doi:10.1007/s00134-003-1783-2
186. Arias, M., Quijano, J. C., Haridas, V., Gutterman, J. U. & Lemeshko, V. V. Red blood cell permeabilization by hypotonic treatments , saponin , and anticancer avicins. BBA - Biomembr. 1798, 1189–1196 (2010).
187. Sojo L, Wagner AM, O. J. & R, C. Hemolyzed plasma samples in diabetic ketoacidosis (DKA). J. Endocrinol. Invest. 4, 3–4 (2005).
188. Cochrane, J., Bland, L. & Noble, M. Intravascular Hemolysis and Septicemia due to Clostridium perfringens Emphysematous Cholecystitis and Hepatic Abscesses. 13–15 doi:10.1155/2015/523402
189. Il, S. U. S., Ose, T. A. B., Oy, D. I. R. & Hakraborti, A. B. S. A. C. Protoporphyrin IX-induced structural and functional changes in human red blood cells , haemoglobin and myoglobin. (2004).
190. Kumar, A. A., Bhaskar, E., Palamaner, G., Shantha, S. & Abraham, G. Rhabdomyolysis in Community Acquired Bacterial Sepsis – A Retrospective Cohort Study. 1–5 (2009). doi:10.1371/journal.pone.0007182
191. Martins, R. et al. Heme drives hemolysis-induced susceptibility to infection via disruption of phagocyte functions. (2016). doi:10.1038/ni.3590
192. Eiter, C. H. D. R. et al. Cell-free hemoglobin limits nitric oxide bioavailability in sickle-cell disease. doi:10.1038/nm799

193. Grunig, D. et al. Oxidative stress in sickle cell disease : An overview of erythrocyte redox metabolism and current antioxidant therapeutic strategies. Free Radic. Biol. Med. 65, 1101–1109 (2013).
194. Liu, M. et al. Transcription factor Nrf2 is protective during ischemic and nephrotoxic acute kidney injury in mice. Kidney Int. 76, 277–285 (2009).
195. Tan, R. J. et al. Keap1 hypomorphism protects against ischemic and obstructive kidney disease. Nat. Publ. Gr. 1–14 (2016). doi:10.1038/srep36185
196. Keleku-lukwete, N. et al. Amelioration of inflammation and tissue damage in sickle cell model mice by Nrf2 activation. doi:10.1073/pnas.1509158112
197. Belcher, J. D. et al. Heme oxygenase-1 is a modulator of inflammation and vaso-occlusion in transgenic sickle mice. doi:10.1172/JCI26857.A
198. Soares, M. P. et al. Heme Oxygenase-1 Modulates the Expression of Adhesion Molecules Associated with Endothelial Cell Activation. J Immunol (2004). doi:10.4049/jimmunol.172.6.3553
199. Azizi, G. et al. Autoimmunity in Primary Antibody deficiencies. Int Arch Allergy Immunol 14194, 180–193 (2016).
200. Lee, J., Chan, K., Wai, Y. & Johnson, J. A. Targeted disruption of Nrf2 causes regenerative immune-mediated hemolytic anemia. 1–6 (2004).
201. Chan, F. K., Luz, N. F. & Moriwaki, K. Programmed Necrosis in the Cross Talk of Cell Death and Inflammation. doi:10.1146/annurev-immunol-032414-112248
202. Buttke, T. M. & Sandstrom, P. A. Oxidative stress as a mediator of apoptosis. 7–10 (1994).
203. Berghe, T. Vanden, Linkermann, A. & Jouan-lanhouet, S. Regulated necrosis: the expanding network of non-apoptotic cell death pathways. Nat. Rev. Mol. Cell Biol. 15, 135–147 (2014).
204. Vandenabeele, P., Galluzzi, L., Vanden Berghe, T. & Kroemer, G. Molecular mechanisms of necroptosis: an ordered cellular explosion. Nat. Rev. Mol. Cell Biol. 11, 700–714 (2010).
205. Pasparakis, M. & Vandenabeele, P. Necroptosis and its role in inflammation. Nature 517, 311–320 (2015).
206. Brault, M. & Oberst, A. Controlled detonation: Evolution of necroptosis in pathogen defense. Immunol. Cell Biol. (2016). doi:10.1038/icb.2016.117.This
207. Chan, F. K.-M., Luz, N. F. & Moriwaki, K. Programmed Necrosis in the Cross Talk of Cell Death and Inflammation. Annu. Rev. Immunol. 1–28 (2014). doi:10.1146/annurev-immunol-032414-112248
208. Kuriakose, T. et al. ZBP1/DAI is an innate sensor of influenza virus triggering the NLRP3 inflammasome and programmed cell death pathways. Sci. Immunol. 1, ssg2045 (2016).
209. Thapa, R. J. et al. DAI Senses Influenza A Virus Genomic RNA and Activates RIPK3-Dependent Cell Death. Cell Host Microbe 20, 674–681 (2016).
210. Micheau, O., Boveresses, C. & Epalinges, C.-. Induction of TNF Receptor I-Mediated Apoptosis via Two Sequential Signaling Complexes. 181–190 (2002).
211. Ling L, Cao Z, Goeddel DV. NF-kB-inducing kinase activates IKK-a by phosphorylation of Ser-176. Proc. Natl. Acad. Sci. 3792–3797 (1998).
212. Kreuz, S., Siegmund, D., Scheurich, P. & Wajant, H. NF-kB Inducers Upregulate cFLIP , a Cycloheximide-Sensitive Inhibitor of Death Receptor Signaling. Mol. Cell. Biol. 3964–3973 doi:10.1128/MCB.21.12.3964
213. Papa, S. et al. Gadd45 β mediates the NF- κ B suppression of JNK signalling by targeting MKK7 / JNKK2. (2004). doi:10.1038/ncb1093
214. Harper, N., Hughes, M., Macfarlane, M. & Cohen, G. M. Fas-associated Death Domain Protein and Caspase-8 Are Not Recruited to the Tumor

Necrosis Factor Receptor 1 Signaling Complex during Tumor Necrosis Factor-induced Apoptosis *. doi:10.1074/jbc.M303399200
215. Lin, Y., Devin, A., Rodriguez, Y. & Liu, Z. Cleavage of the death domain kinase RIP by Caspase-8 prompts TNF-induced apoptosis. 2514–2526 (1999).
216. Formation, R. et al. RIP1 / Caspase-8 Containing Intracellular Cell Death Complex Differentially Regulated by cFLIP Isoforms. Mol. Cell 449–463 (2011). doi:10.1016/j.molcel.2011.06.011
217. He, S. et al. Receptor interacting protein kinase-3 determines cellular necrotic response to TNF-alpha. Cell 137, 1100–11 (2009).
218. Li, J. et al. The RIP1 / RIP3 Necrosome Forms a Functional Amyloid Signaling Complex Required for Programmed Necrosis. 339–350 (2012). doi:10.1016/j.cell.2012.06.019
219. Dondelinger, Y. et al. MLKL compromises plasma membrane integrity by binding to phosphatidylinositol phosphates. Cell Rep. 7, 971–81 (2014).
220. Wang, Z., Jiang, H., Chen, S., Du, F. & Wang, X. The Mitochondrial Phosphatase PGAM5 Functions at the Convergence Point of Multiple Necrotic Death Pathways. Cell 148, 228–243 (2011).
221. Jorgensen, I., Rayamajhi, M. & Miao, E. A. Programmed cell death as a defence against infection. Nat. Rev. Immunol. (2017). doi:10.1038/nri.2016.147
222. Chan, F. K. M. et al. A Role for Tumor Necrosis Factor Receptor-2 and Receptor-interacting Protein in Programmed Necrosis and Antiviral Responses. J. Biol. Chem. 278, 51613–51621 (2003).
223. Cho, Y. S. et al. Phosphorylation-Driven Assembly of the RIP1-RIP3 Complex Regulates Programmed Necrosis and Virus-Induced Inflammation. Cell 137, 1112–1123 (2009).
224. Duprez, L. et al. RIP kinase-dependent necrosis drives lethal systemic inflammatory response syndrome. Immunity 35, 908–18 (2011).
225. Harris, P. A. et al. Discovery of Small Molecule RIP1 Kinase Inhibitors for the Treatment of Pathologies Associated with Necroptosis. ACS Med. Chem. Lett. (2013).
226. Goldstein, L., Teng, Z. P., Zeserson, E., Patel, M. & Regan, R. F. Hemin induces an iron-dependent, oxidative injury to human neuron-like cells. J. Neurosci. Res. 73, 113–121 (2003).
227. Laird, M. D., Wakade, C., Alleyne, C. H. & Dhandapani, K. M. Hemin-induced necroptosis involves glutathione depletion in mouse astrocytes. Free Radic. Biol. Med. 45, 1103–1114 (2008).
228. Ramachandran A, McGill MR, Xie Y, Ni HM, Ding WX, J. H. The Receptor Interacting Protein Kinase 3 is a Critical Early Mediator of Acetaminophen-induced Hepatocyte Necrosis in Mice. Hepatology 58, 1–18 (2013).
229. Roychowdhury, S., Mcmullen, M. R., Pisano, S. G., Liu, X. & Nagy, L. E. Absence of receptor interacting protein kinase 3 prevents ethanol-induced liver injury. Hepatology 57, 1773–1783 (2013).
230. Günther C, He GW, Kremer AE, Murphy JM, Petrie EJ, Amann K, Vandenabeele P, Linkermann A, Poremba C, Schleicher U, D. C. & Krautwald S, Neurath MF, Becker C, W. S. The pseudokinase MLKL mediates programmed hepatocellular necrosis independently of RIPK3 during hepatitis. J. Clin. Invest. 126, 4068–4071 (2016).
231. Afonso, M. B. et al. Activation of necroptosis in human and experimental cholestasis. Cell Death Dis. 7, e2390 (2016).
232. Linkermann, A. et al. Two independent pathways of regulated necrosis mediate ischemia-reperfusion injury. Proc. Natl. Acad. Sci. U. S. A. 110, 12024–9 (2013).
233. Linkermann, A. et al. Rip1 (Receptor-interacting protein kinase 1) mediates necroptosis and contributes to renal ischemia/reperfusion injury. Kidney Int.

81, 751–761 (2012).
234. Marshall, K. D., Christopher, P., Huttemann, M. & State, W. Necroptosis : is there a role for mitochondria ? 1–5 (2014). doi:10.3389/fphys.2014.00323
235. Lin, Y. et al. Tumor Necrosis Factor-induced Nonapoptotic Cell Death Requires Receptor-interacting Protein-mediated Cellular Reactive Oxygen Species Accumulation *. J. Biol. Chem. 8, 10822–10829 (2004).
236. Vanlangenakker, N. et al. cIAP1 and TAK1 protect cells from TNF-induced necrosis by preventing RIP1 / RIP3-dependent reactive oxygen species production. Cell Death Differ. 18, 656–665 (2011).
237. Goossens V, Stangé G, Moens K, Pipeleers D, G. J. Regulation of Tumor Necrosis Factor-Induced mitochondria and reactive oxygen species-dependent cell death by the electron flux through the electron transport chain complex I. Antioxid. Redox Signal. (1999).
238. Imai, Y., Kanao, T., Sawada, T., Kobayashi, Y. & Moriwaki, Y. The Loss of PGAM5 Suppresses the Mitochondrial Degeneration Caused by Inactivation of PINK1 in Drosophila. 1, 1–14 (2010).
239. Kanamaru, Y., Sekine, S., Ichijo, H. & Takeda, K. The Phosphorylation-Dependent Regulation of Mitochondrial Proteins in Stress Responses. doi:10.1155/2012/931215
240. Wieder, S. Y. et al. Mitochondrial Division Is Requisite to RAS-Induced Transformation and Targeted by Oncogenic MAPK Pathway Inhibitors Article Mitochondrial Division Is Requisite to RAS-Induced Transformation and Targeted by Oncogenic MAPK Pathway Inhibitors. Mol. Cell 57, 521–536 (2015).
241. Dowding, J. M. et al. Cerium oxide nanoparticles protect against A b -induced mitochondrial fragmentation and neuronal cell death. 21, 1622–1632 (2014).
242. Wang, Z., Jiang, H., Chen, S., Du, F. & Wang, X. The mitochondrial phosphatase PGAM5 functions at the convergence point of multiple necrotic death pathways. Cell 148, 228–43 (2012).
243. Wang, Z., Jiang, H., Chen, S., Du, F. & Wang, X. The mitochondrial phosphatase PGAM5 functions at the convergence point of multiple necrotic death pathways. Cell 148, 228–43 (2012).
244. Zhang, L. et al. Necrostatin-1 Attenuates Ischemia Injury Induced Cell Death in Rat Tubular Cell Line NRK-52E through Decreased Drp1 Expression. 24742–24754 doi:10.3390/ijms141224742
245. Halestrap, A. P. What is the mitochondrial permeability transition pore ? J. Mol. Cell. Cardiol. 46, 821–831 (2009).
246. Baines, C. P. et al. Loss of cyclophilin D reveals a critical role for mitochondrial permeability transition in cell death. 167, 626–629 (2005).
247. Nakagawa, T., Shimizu, S. & Watanabe, T. Cyclophilin D-dependent mitochondrial permeability transition regulates some necrotic but not apoptotic cell death. Nature 434, 652–658 (2005).
248. Schinzel, A. C. et al. Cyclophilin D is a component of mitochondrial permeability transition and mediates neuronal cell death after focal cerebral ischemia. Proc. Natl. Acad. Sci. U. S. A. 102, 12005–10 (2005).
249. Lim, S. Y., Davidson, S. M., Mocanu, M. M., Yellon, D. M. & Smith, C. C. T. The cardioprotective effect of necrostatin requires the cyclophilin- D component of the mitochondrial permeability transition pore. Cardiovasc Drugs Ther. 21, 467–469 (2007).
250. Hayes JD, Chanas SA, Henderson CJ, McMahon M, Sun C, MofTatt GJ,Wolfrz CR, Y. M. The Nrf2 transcription factor contributes both to the basal expression of glutathione Stransferases in mouse liver and to their induction by the chemopreventive synthetic antioxidants, butylated hydroxyanisole and ethoxyquin. Biochem. Soc. Trans. 33–41 (2000).
251. Miura, T. & Tanno, M. Mitochondria and GSK-3b in cardioprotection against

ischemia/reperfusion injury. Cardiovasc. Drugs Ther. 24, 255–263 (2010).
252. Juhaszova, M. et al. Glycogen synthase kinase-3beta mediates convergence of protection signaling to inhibit the mitochondrial permeability transition pore. J. Clin. Invest. 113, 1535–1549 (2004).
253. Gomez, L., Paillard, M., Thibault, H., Derumeaux, G. & Ovize, M. Inhibition of GSK3b by postconditioning is required to prevent opening of the mitochondrial permeability transition pore during reperfusion. Circulation 117, 2761–2768 (2008).
254. Rada, P. et al. Structural and Functional Characterization of Nrf2 Degradation by the Glycogen Synthase Kinase 3/ β-TrCP Axis. Mol. Cell. Biol. 32, 3486–3499 (2012).
255. Salazar, M., Rojo, A. I., Velasco, D., De Sagarra, R. M. & Cuadrado, A. Glycogen synthase kinase-3β inhibits the xenobiotic and antioxidant cell response by direct phosphorylation and nuclear exclusion of the transcription factor Nrf2. J. Biol. Chem. 281, 14841–14851 (2006).
256. Liu, T. et al. Limb ischemic preconditioning protects against contrast-induced acute kidney injury in rats via phosphorylation of GSK-3β. Free Radic. Biol. Med. 81, 170–182 (2015).
257. Lo, S.-C. & Hannink, M. PGAM5 tethers a ternary complex containing Keap1 and Nrf2 to mitochondria. Exp. Cell Res. 314, 1789–803 (2008).

Chapter 2:

Results

"However vast the darkness, we must supply our own light."
(Stanley Kubrick)

2.1. NRF2 is essential to establish disease tolerance to malaria.

We used a well-recognized experimental model of *Plasmodium* infection in which >90% of wild type C57BL/6 mice survive the blood stage of *Plasmodium chabaudi chabaudi* (*Pcc*) infection, via a mechanism that relies on both resistance and disease tolerance mechanisms[1,2]. *Pcc* infection in C57BL/6 mice was associated with the induction of *NAD(P)H quinone dehydrogenase 1* (*Nqo1*) and *glutathione s-transferase* (*Gst)* gene expression in the liver, as assessed by qRT-PCR (*Figure 2.1a,b*). Up regulation of these genes was ablated in NRF2-deficient ($Nrf2^{-/-}$) C57BL/6 mice, as compared to C57BL/6 wild-type ($Nrf2^{+/+}$) controls, demonstrating that the NRF2-dependent antioxidant pathway is activated in response to the blood stage of *Plasmodium* infection (*Figure 2.1a,b,c*). Expression of Heme oxygenase 1 (*Hmox1)* and *Ferritin Heavy Chain* (*FtH*) was induced at comparable levels in the liver of $Nrf2^{-/-}$ *vs.* $Nrf2^{+/+}$ mice in response to *Plasmodium* infection (*Figure 2.1c,d*). This suggests that, in the absence of NRF2, the aforementioned genes are probably regulated via the induction of other transcription factors.

Plasmodium infection was associated with a more pronounced decrease in body weight (*Figure 2.1e*) and temperature (*Figure 2.1f*), as well as with a higher incidence of mortality (*Figure 2.1g*) in $Nrf2^{-/-}$ *vs.* $Nrf2^{+/+}$ mice. Percentage of infected RBCs in circulation, assessed during the course of infection, was similar in $Nrf2^{-/-}$ *vs.* $Nrf2^{+/+}$ *mice* (*Figure 2.1h*). Together, these data demonstrate that Nrf2 is essential to establish disease tolerance to the blood stage of *Plasmodium* infection.

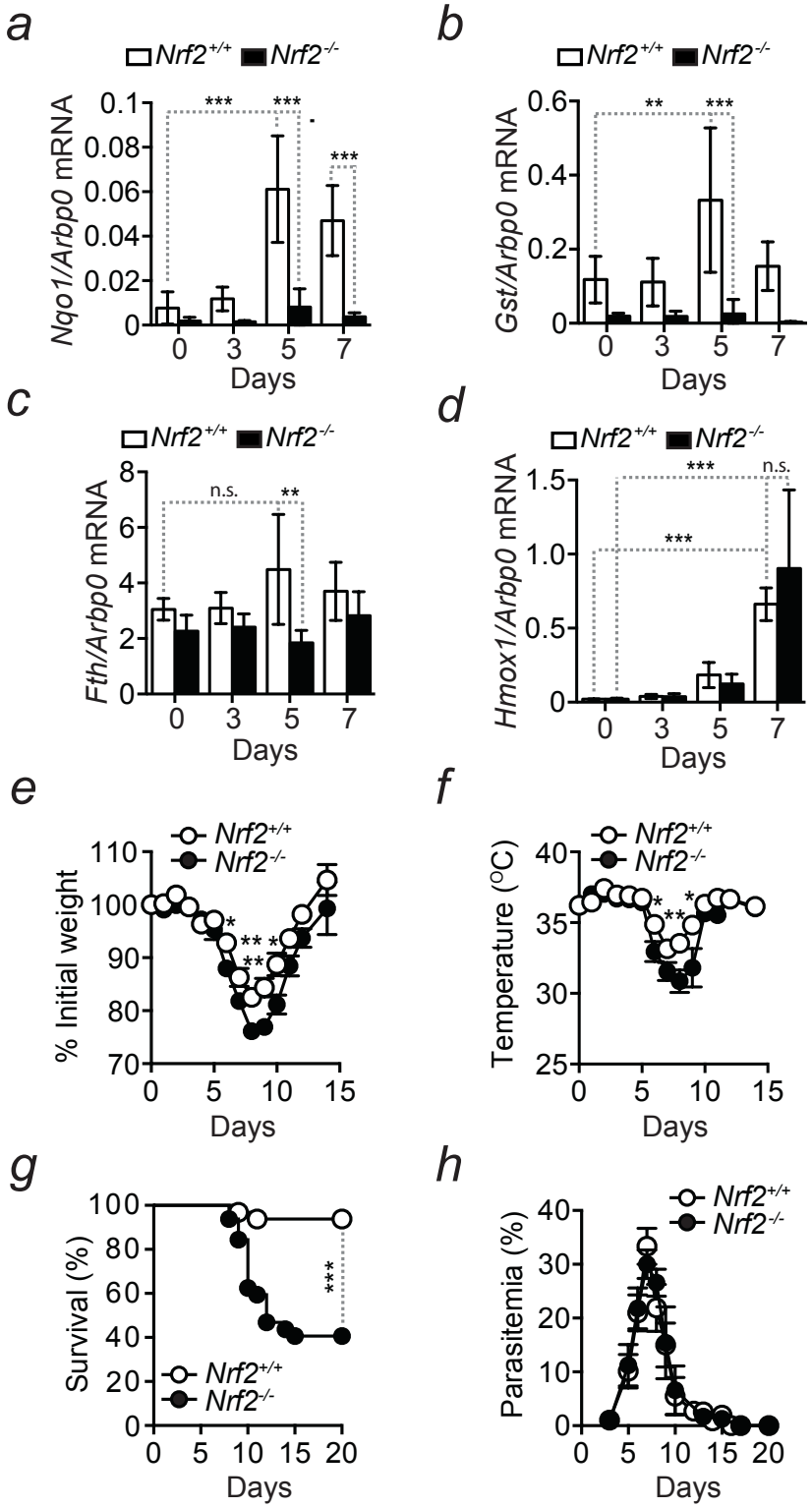
a
Nrf2+/+ Nrf2-/-
Nqo1/Arbp0 mRNA
0.1
0.08
0.06
0.04
0.02
0
***
***
***
0 3 5 7
Days
b
Nrf2+/+ Nrf2-/-
Gst/Arbp0 mRNA
0.6
0.4
0.2
0
**
***
0 3 5 7
Days
c
Nrf2+/+ Nrf2-/-
Fth/Arbp0 mRNA
8
6
4
2
0
n.s.
**
0 3 5 7
Days
d
Nrf2+/+ Nrf2-/-
Hmox1/Arbp0 mRNA
1.5
1.0
0.5
0
***
***
n.s.
0 3 5 7
Days
e
Nrf2+/+
Nrf2-/-
% Initial weight
110
100
90
80
70
0 5 10 15
Days
f
Nrf2+/+
Nrf2-/-
Temperature (°C)
40
35
30
25
0 5 10 15
Days
g
Survival (%)
100
80
60
40
20
0
***
Nrf2+/+
Nrf2-/-
0 5 10 15 20
Days
h
Nrf2+/+
Nrf2-/-
Parasitemia (%)
40
30
20
10
0
0 5 10 15 20
Days

Figure 2.1. NRF2 confers disease tolerance to malaria infection.

(a-d) Liver *Nqo1, Gst, Fth* and *Hmox1* mRNA levels, normalized to *Arbp0*, in non-infected *Nrf2*$^{+/+}$ and *Nrf2*$^{-/-}$ mice (0) and in *Nrf2*$^{+/+}$ and *Nrf2*$^{-/-}$ mice at days 3, 5 or 7 after *Pcc* infection. Data is represented as mean ± STD from n=4-5 mice per genotype, one experiment. One-way ANOVA. (e) Percentage of initial weight and (f) temperature in *Pcc*-infected *Nrf2*$^{+/+}$ and *Nrf2*$^{-/-}$ mice, relative to non-infected controls (day 0). Data pooled from three independent experiments with similar trend (n=16 mice per genotype), represented as mean ± SEM. Mann-Whitney U Test. (g) Percent survival of *Pcc*-infected *Nrf2*$^{+/+}$ and *Nrf2*$^{-/-}$ mice, pooled from six independent experiments with similar trend (n=31-32 mice per genotype). Log-Rank Test. (h) Percentage of infected RBC in *Nrf2*$^{+/+}$ and *Nrf2*$^{-/-}$ mice throughout the course of *Pcc* infection, pooled from six independent experiments (n=27-31 mice per genotype), represented an as mean ± SEM. n.s.: non significant, *p< 0.05, **p< 0.01, ***p<0.001.

Lethality of *Plasmodium* infection in *Nrf2*$^{-/-}$ mice was associated with the development of multi-organ damage, revealed by the accumulation of lactate dehydrogenase (LDH, general tissue damage), alanine aminotransferase (ALT; liver damage), aspartate aminotransferase (AST; liver damage), creatinine kinase (CK; muscle damage) and creatinine (kidney damage) as well as urea (kidney damage) in the plasma (Figure 2.2).

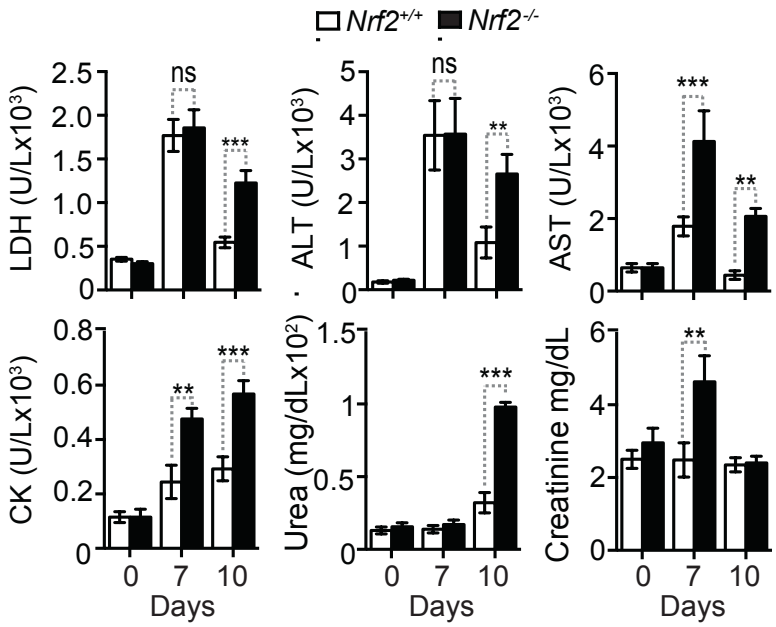

Figure 2.2. NRF2 protects against multi-organ damage/dysfunction in malaria infection.
Serological analysis of general tissue damage marker LDH and specific-tissue damage markers ALT and AST (liver), CK (muscle), Urea and Creatinine (kidney) in *Nrf2*$^{+/+}$ and *Nrf2*$^{-/-}$ mice before (day 0) and at days 7 and 10 after *Pcc* infection. Data pooled from four independent experiments with similar trend (n=10-20 mice per group), represented as mean ± SEM. One-way ANOVA. n.s. non significant, *p< 0.05, **p< 0.01, ***p<0.001.

Histological analysis confirmed that *Nrf2*$^{-/-}$ mice develop more severe liver, kidney and heart damage, observed by the number of necrotic foci as a consequence of *Pcc* infection, when compared to *Nrf2*$^{+/+}$ mice (Figure 2.3).

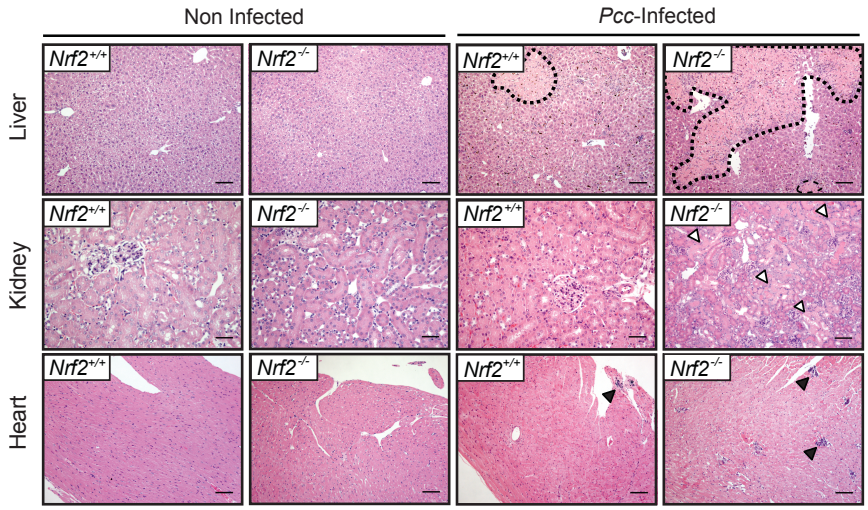

Figure 2.3. NRF2 provides tissue damage control to malaria infection.
Liver, kidney and heart sections stained with H&E from control (non infected) *Nrf2*$^{+/+}$ and *Nrf2*$^{-/-}$ mice and collected 10 days after *Pcc* infection. Dotted lines indicate areas of hepatocyte necrosis. White arrows indicate kidney tubular cell necrosis and black arrows display areas of cardiomyocyte necrosis. Images are representative of two independent experiments, n=8-10 mice per genotype. Scale bar = 100μm.

Tissue damage was associated with the accumulation of DAMPs in the extracellular space[3,4]. *Nrf2*$^{-/-}$ mice display increased levels of

extracellular DNA, as monitored by liver intravital imaging[5] (*Figure 2.4a,b*) as well as detectable levels of circulating mitochondrial DNA in the plasma (*Figure 2.4c*).

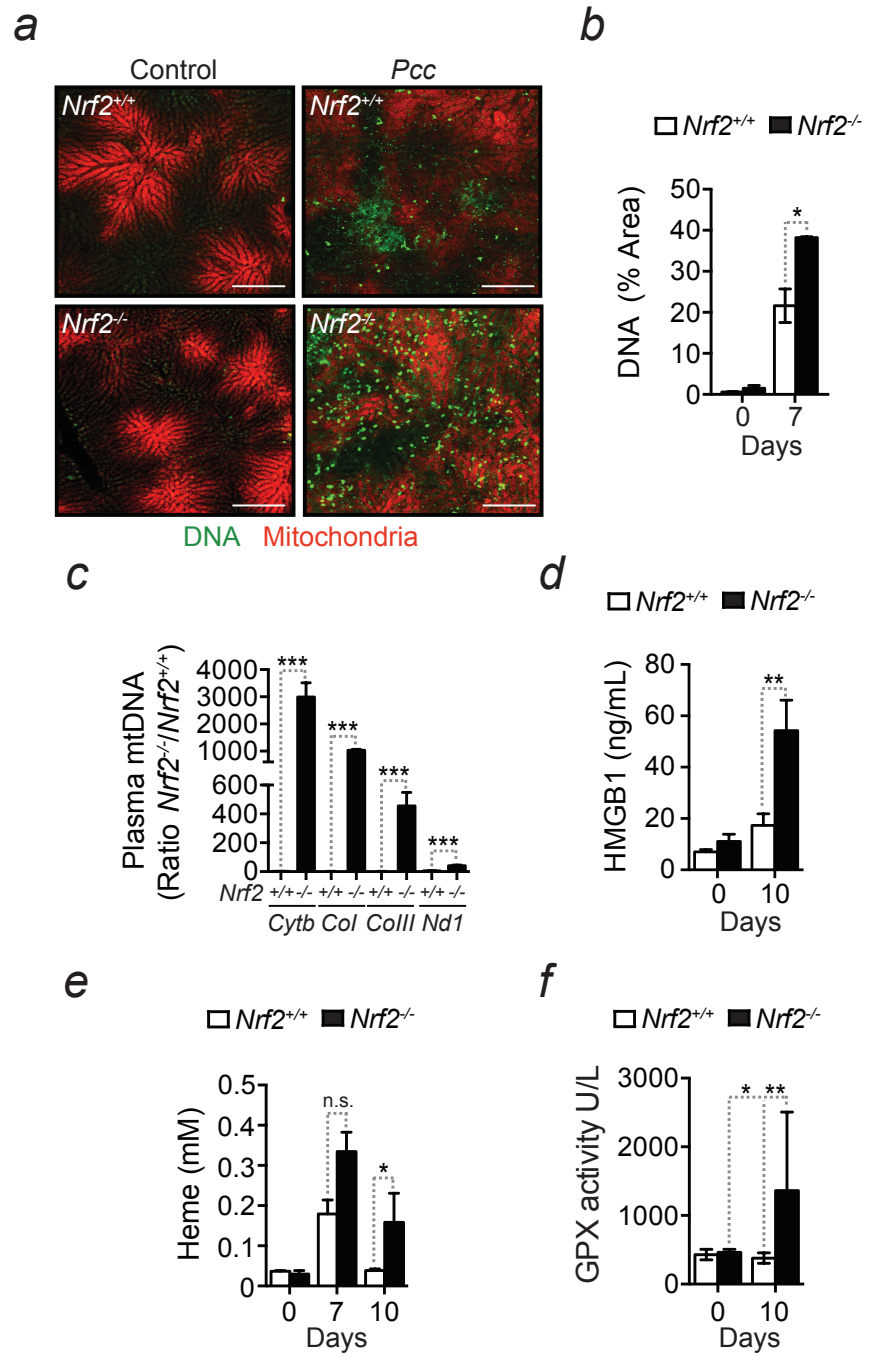

Figure 2.4. NRF2 prevents DAMP release and oxidative stress in malaria infection.

(a) Extracellular DNA (green) monitored by liver intravital microscopy 7 days after *Pcc* infection and in non-infected (control) *Nrf2*$^{+/+}$ and *Nrf2*$^{-/-}$ mice (red: mitochondria). Scale bar = 200 μm. (b) Quantification of liver extracellular DNA from two independent experiments (n=4 mice per group, 4 different areas analyzed), represented as mean % area ± SEM. Mann Whitney U Test. (c) Levels of circulating mtDNA, i.e. *cytochrome b* (*Cytb*), *mitochondrial encoded cytochrome c oxidase I* and III (*mt-CoI*, *mt-CoIII*), and *NADPH dehydrogenase* (*Nd1)* copies in the plasma of infected *Nrf2*$^{+/+}$ and *Nrf2*$^{-/-}$ mice at day 10 post-*Pcc* infection. Data pooled from two independent experiments with similar trend (n=9 mice per group), is represented as mean ± SEM. (d) HMGB1 levels in the plasma of non-infected (Day 0) and infected *Nrf2*$^{+/+}$ and *Nrf2*$^{-/-}$ mice at day 10 post-*Pcc* infection. Data pooled from two independent experiments (n=4-10 mice per group), represented as mean ± SEM. Mann Whitney U Test. (e) Heme levels in the plasma of non-infected (Day 0), or infected *Nrf2*$^{+/+}$ and *Nrf2*$^{-/-}$ mice at days 7 and 10 after *Pcc* infection. Data from one experiment (n=4-6 mice per group) represented as mean ± STD. Mann Whitney U Test. (f) GPX levels in the plasma of non-infected (Day 0) and infected *Nrf2*$^{+/+}$ and *Nrf2*$^{-/-}$ mice 10 days after *Pcc* infection. Data from one experiment (n=4-6 mice per group), represented as mean ± SD. Mann Whitney U Test. n.s.: non significant, *p< 0.05, **p< 0.01, ***p<0.001.

Moreover, higher levels of High Mobility Group Box 1 (HMGB1) (*Figure 2.4d*) were detected in the plasma of *Nrf2*$^{-/-}$ mice as well as higher concentrations of labile heme (*Figure 2.4e*), when compared to infected *Nrf2*$^{+/+}$ mice. Additionally, infected *Nrf2*$^{-/-}$ mice display increased GPX activity in the plasma when compared to their wild-type counterparts, a *proxy* for systemic oxidative stress[6] (*Figure 2.4f*).

We have also found higher levels of circulating cytokines IL-1b, IL-6, MCP-1, MIP-1α, RANTES and IL-10 in the plasma of *Pcc*-infected *Nrf2*$^{-/-}$ *vs Nrf2*$^{+/+}$ mice (*Figure 2.5*).

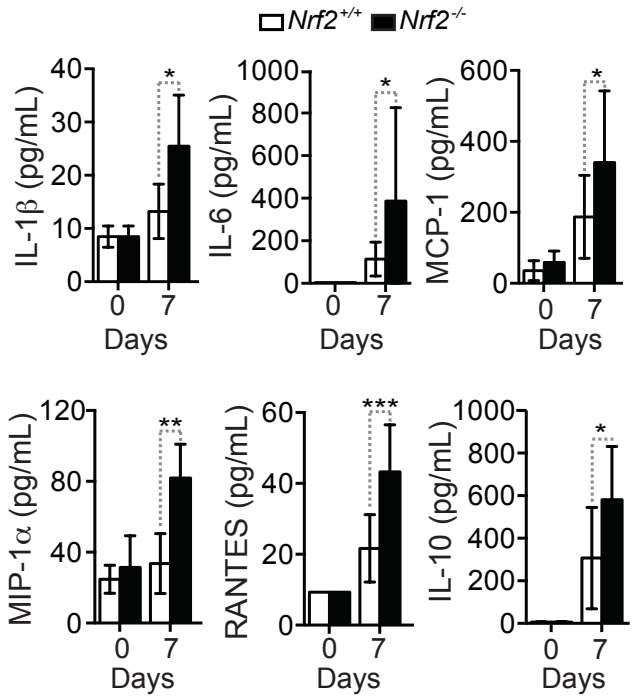

Figure 2.5. NRF2 counters inflammation in malaria infection. Cytokine levels in the plasma of non-infected controls (day 0) and infected *Nrf2*$^{+/+}$ and *Nrf2*$^{-/-}$ mice 7 days post-*Pcc* infection. Data is represented as mean ± STD from n=4-6 mice per genotype, one experiment. Mann Whitney U Test. *p< 0.05, **p< 0.01, ***p<0.001.

Overall, these observations demonstrate that the stress response regulated by NRF2 limits the release of DAMPs into circulation, presumably by controlling the systemic oxidative stress leading to tissue damage, organ dysfunction and necrosis upon *Plasmodium* infection, therefore limiting the extent of inflammatory cytokine secretion and overall inflammation. Therefore, by providing tissue damage control, NRF2 counters disease severity and confers disease tolerance to malaria infection.

2.2. NRF2 is essential to establish disease tolerance to polymicrobial sepsis.

As polymicrobial bloodstream infections are often associated with more or less severe hemolysis[7,8] and NRF2 is protective in the context of different models of sepsis[9,10], we hypothesized that the stress response regulated by NRF2 contributes to the establishment of disease tolerance to sepsis. Thus, we tested this hypothesis specifically for systemic polymicrobial infections leading to sepsis using cecal ligation and puncture (CLP) as experimental model[11].

We have observed that most *Nrf2*$^{-/-}$ mice succumbed to CLP, under experimental conditions that were not lethal to *Nrf2*$^{+/+}$ mice (*Figure 2.6a*), which is consistent with previous observations[9]. However, the survival advantage of *Nrf2*$^{+/+}$ *vs. Nrf2*$^{-/-}$ mice was not associated with differences in pathogen load, as assessed 16 hours after CLP for aerobic and anaerobic bacteria in different organs (*Figure 2.6b*). Of note, body weight (*Figure 2.6c*) and temperature (*Figure 2.6d*) were similar in *Nrf2*$^{-/-}$ *vs. Nrf2*$^{+/+}$ mice subjected to CLP. Finally, CLP in *Nrf2*$^{+/+}$ mice was associated with the induction of *Fth mRNA* expression in the kidney, as assessed by qRT-PCR (*Figure 2.6e*). Upregulation of this gene was ablated in NRF2-deficient (*Nrf2*$^{-/-}$) mice, as compared to wild-type controls, demonstrating that the NRF2-dependent antioxidant pathway is activated in response to polymicrobial sepsis.

Mortality of *Nrf2*$^{-/-}$ mice subjected to CLP was associated with organ damage, as assessed serologically (*Figure 2.7a*) and confirmed by histological analysis (*Figure 2.7b*), through observation of widespread hepatocellular degeneration. This was not apparent however, in the kidney, lung and heart of *Nrf2*$^{-/-}$ mice subjected to CLP (*Figure 2.8*).

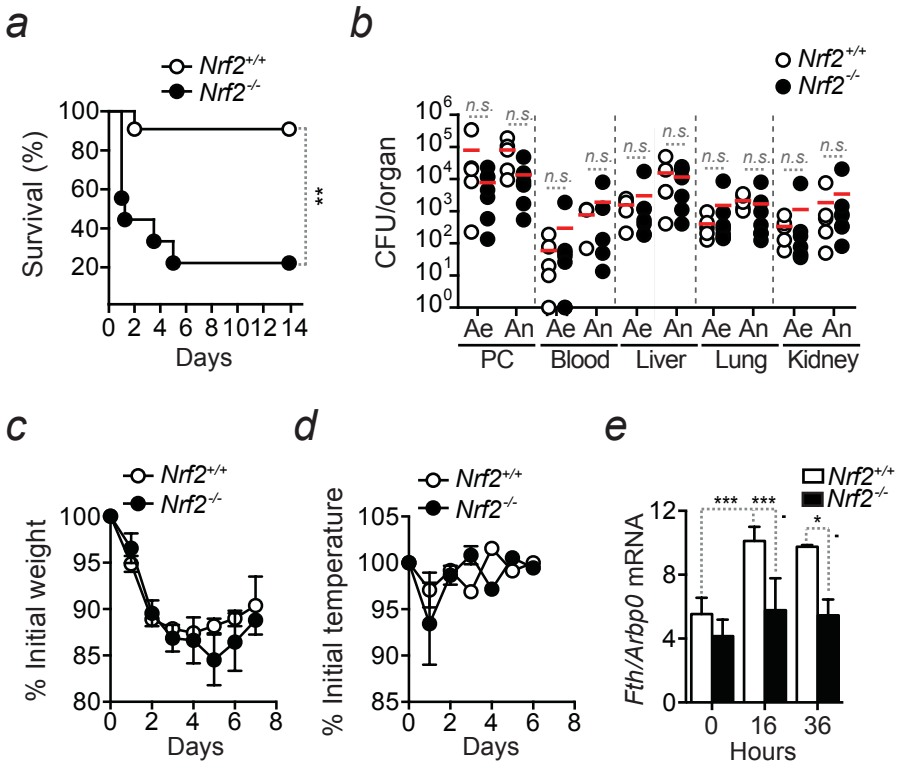

Figure 2.6. NRF2 provides disease tolerance to polymicrobial sepsis.

(a) Survival of *Nrf2*$^{+/+}$ and *Nrf2*$^{-/-}$ mice subjected to CLP in three independent experiments with similar trend (n=9-11 mice *per* genotype). Log-Rank Test. (b) Colony forming units (CFU) of aerobic (Ae) and anaerobic (An) bacteria, 16 hours after CLP in *Nrf2*$^{+/+}$ and *Nrf2*$^{-/-}$ mice. Data pooled from two independent experiments (n=5-6 mice per genotype). Mann Whitney U Test. PC: peritoneal cavity. Percentage of initial (c) weight and (d) temperature in *Nrf2*$^{+/+}$ and *Nrf2*$^{-/-}$ mice subjected to CLP, relative to non-infected controls (day 0). Data pooled from three independent experiments with similar trend (n=9-11 mice per genotype), represented as mean ± SEM. (e) Kidney *Fth* mRNA levels, normalized to *Arbp0*, in control *Nrf2*$^{+/+}$ and *Nrf2*$^{-/-}$ mice (0) and in *Nrf2*$^{+/+}$ and *Nrf2*$^{-/-}$ mice 16 and 36h after CLP. Data is represented as mean ± STD from n=3-8 mice per genotype, one to two experiments. One-Way ANOVA. n.s.: non significant, *p< 0.05, **p< 0.01, ***p<0.001.

Accumulation of mitochondrial DNA (*Figure 2.7c*) and HMGB1 (*Figure 2.7d*) in the plasma was higher in *Nrf2*$^{-/-}$ septic mice as compared to *Nrf2*$^{+/+}$ septic mice after CLP.

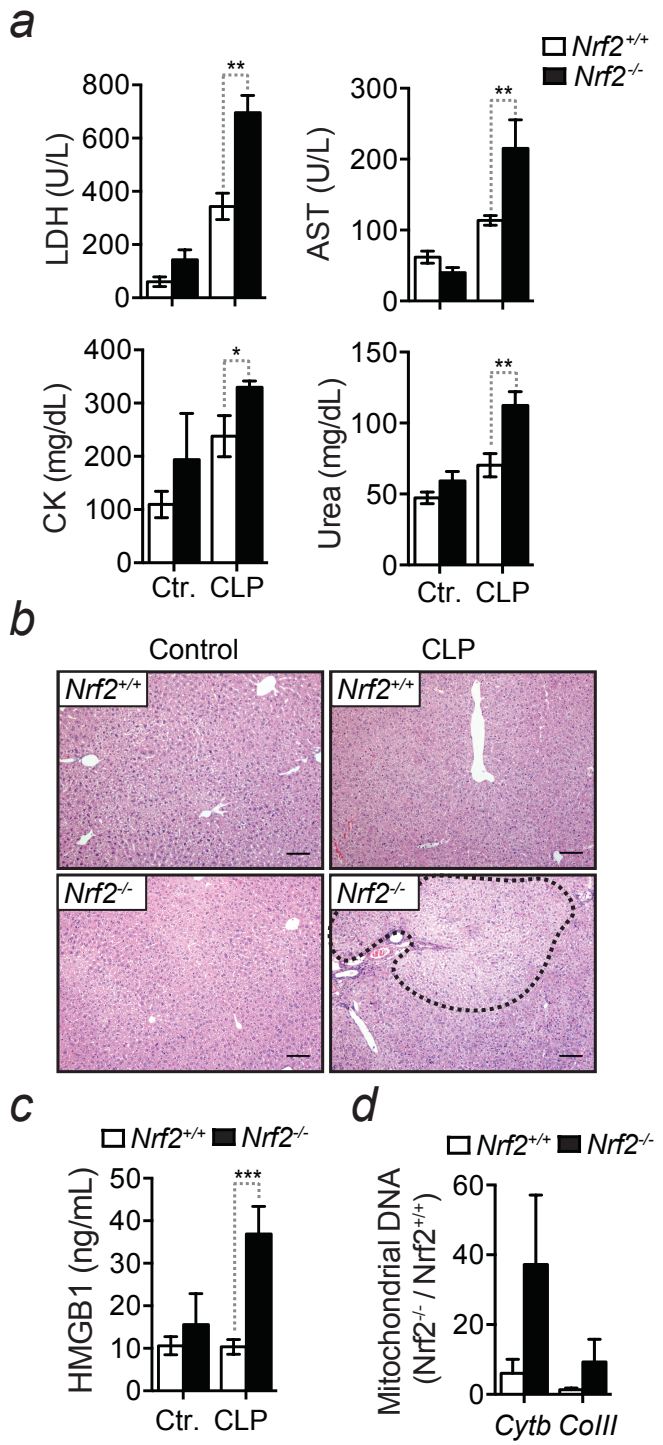

Figure 2.7. NRF2 confers tissue damage control in polymicrobial sepsis.

(a) Serological markers of tissue damage (LDH), liver (ALT), muscle (CK) and kidney (Urea) in plasmas from *Nrf2*$^{+/+}$ and *Nrf2*$^{-/-}$ mice collected before (Ctr.) and 16h after CLP. Data pooled from one to two independent experiments with similar trend (n=5-7 mice per group for CK and Urea; n=7-10 mice per group for LDH and AST). Data represented as mean ± SEM. Mann-Whitney U Test. (b) H&E staining of liver sections from naïve *Nrf2*$^{+/+}$ and *Nrf2*$^{-/-}$ mice (Control) and 16h after CLP. Images correspond to one experiment, n=5-7 mice per group. Dotted line indicates area of hepatocellular degeneration. Scale bar = 100μm. (c) HMGB1 concentration in the plasma of non-infected (Ctr.) and infected *Nrf2*$^{+/+}$ and *Nrf2*$^{-/-}$ mice, 16h after CLP. Data from one experiment (n=7 mice per group) is represented as mean ± STD. Mann-Whitney U Test. (d) Levels of circulating mtDNA in the plasma of mice subjected to CLP, 16h after procedure. Data, pooled from two independent experiments with similar trend (n=5-10 mice per genotype), is represented as mean ± STD. *p< 0.05, **p< 0.01, ***p<0.001.

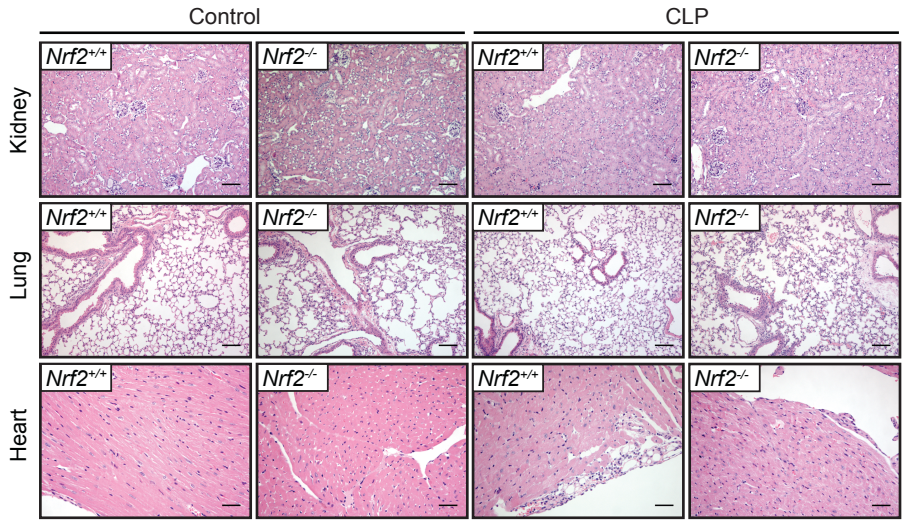

Figure 2.8. NRF2 provides tissue damage control mainly in the liver upon polymicrobial sepsis.

H&E staining of kidney, lung and heart sections from non-infected (control) and infected *Nrf2*$^{+/+}$ and *Nrf2*$^{-/-}$ mice, 16 hours after CLP. Images are representative of n=7 mice per genotype in one experiment. Scale bar = 100 μm.

There were also increased levels of circulating cytokines MCP-1, MIP-1β, MIP-2, RANTES or IL-10 in the plasma of *Nrf2*$^{-/-}$ mice and a similar trend for IL-1α, IL-1β, IL-6, MIP-1α, IL-12 and MIG (*Figure 2.9*), when compared to *Nrf2*$^{+/+}$ mice, 16 hours after being subjected to CLP.

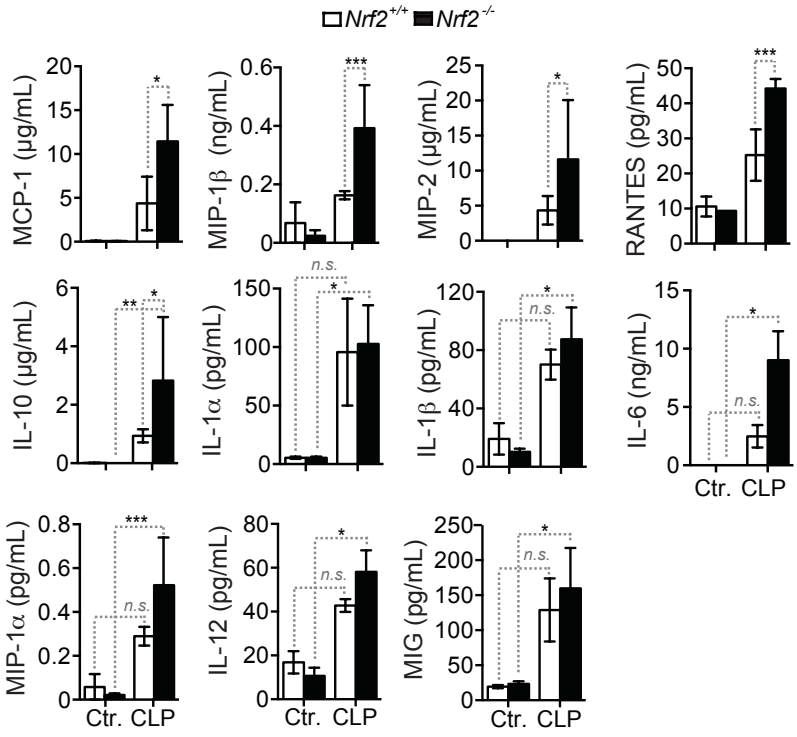

Figure 2.9. NRF2 counters inflammation upon polymicrobial sepsis.

Cytokine levels in the plasma of non-infected (Ctr.) and 16 hours after CLP in *Nrf2*$^{+/+}$ and *Nrf2*$^{-/-}$ mice. Data is represented as mean ± STD from n=3-5 mice per genotype, one experiment. Mann Whitney U Test. n.s.: non significant, *p< 0.05, **p< 0.01, ***p<0.001.

Taken together, our data reveal that NRF2 establishes disease tolerance to polymicrobial infection via a tissue damage control mechanism limiting DAMP release and, presumably, preventing an

unfettered inflammatory response leading to sepsis, which is consistent with previous reports[9].

2.3. NRF2 confers tissue damage control after sterile hemolysis.

We then asked what is the contribution of heme in the pathophysiology of hemolytic infections and whether NRF2 activation is protective against sterile intravascular hemolysis. Induction of acute hemolysis through the administration of Phenylhidrazine (PHZ) was lethal to *Nrf2*$^{-/-}$ mice and not to *Nrf2*$^{+/+}$ mice (*Figure 2.10a*), despite similar levels of hemolysis (*Figure 2.10b*) and heme accumulation in the plasma (*Figure 2.10c*). PHZ administration was, however, linked to the release of mtDNA, significantly higher in the plasma of *Nrf2*$^{-/-}$ mice when compared to their wild-type counterparts (*Figure. 2.10d*). Mortality of *Nrf2*$^{-/-}$ mice was not associated with a significant reduction of body weight (*Figure. 2.10e*) or temperature (*Figure. 2.10f*), when compared to *Nrf2*$^{+/+}$ mice.

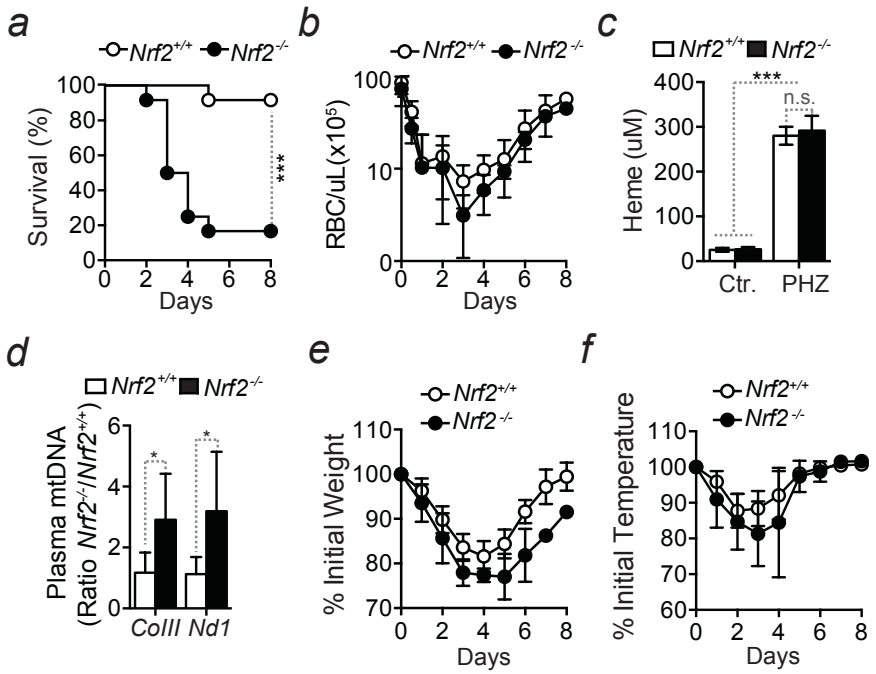

Figure 2.10. NRF2 protects against lethality associated with severe acute hemolysis.
(a) Relative survival of *Nrf2*$^{+/+}$ and *Nrf2*$^{-/-}$ mice subjected to acute intravascular hemolysis, induced by PHZ administration. Data was pooled from three independent experiments with similar trend (n=12 mice per genotype). Log-Rank Test. (b) Mean number of circulating RBC ± STD in the same mice as (a). (c) Heme levels in the plasma of control (Ctr.) or after PHZ administration, when temperature of PHZ-treated *Nrf2*$^{-/-}$ mice was below 27^{o}C (around 24h after second injection). Data from one experiment (n=3-4 mice per group) is represented as mean ± STD. Mann-Whitney U Test. (d) Levels of circulating mtDNA, i.e. *mitochondrial encoded cytochrome c oxidase* III (*mt-CoIII*) and *NADPH dehydrogenase* (*Nd1)* copies in the plasma of control and infected *Nrf2*$^{+/+}$ and *Nrf2*$^{-/-}$ mice, when temperature of PHZ-treated *Nrf2*$^{-/-}$ mice was below 27^{o}C (around 24h after second injection). Data pooled from two independent experiments with similar trend (n=5-7 mice per group) is represented as mean ± SEM. Mann-Whitney U Test. Percentage of initial (e) weight and (f) temperature in *Nrf2*$^{+/+}$ and *Nrf2*$^{-/-}$ mice receiving PHZ, relative to controls (day 0). Data from three independent experiments with similar trend (n=12 mice per genotype) was pooled and is represented as mean ± SEM. n.s.: non significant, *p< 0.05, **p< 0.01, ***p<0.001.

Administration of PHZ led to severe tissue damage in liver and kidney from *Nrf2*$^{-/-}$ mice when compared to their wild-type counterparts. Deletion of NRF2 was associated with higher number of necrotic foci in the liver and multiple areas of tubular cell necrosis, completely absent in the kidney of NRF2 proficient mice. Interestingly, both *Nrf2*$^{-/-}$ and *Nrf2*$^{+/+}$ mice extensively accumulate hemoglobin inside kidney tubular cells, but only knockout cells undergo necrosis followed by detachment of these cells into the tubule lumen (*Figure 2.11*).

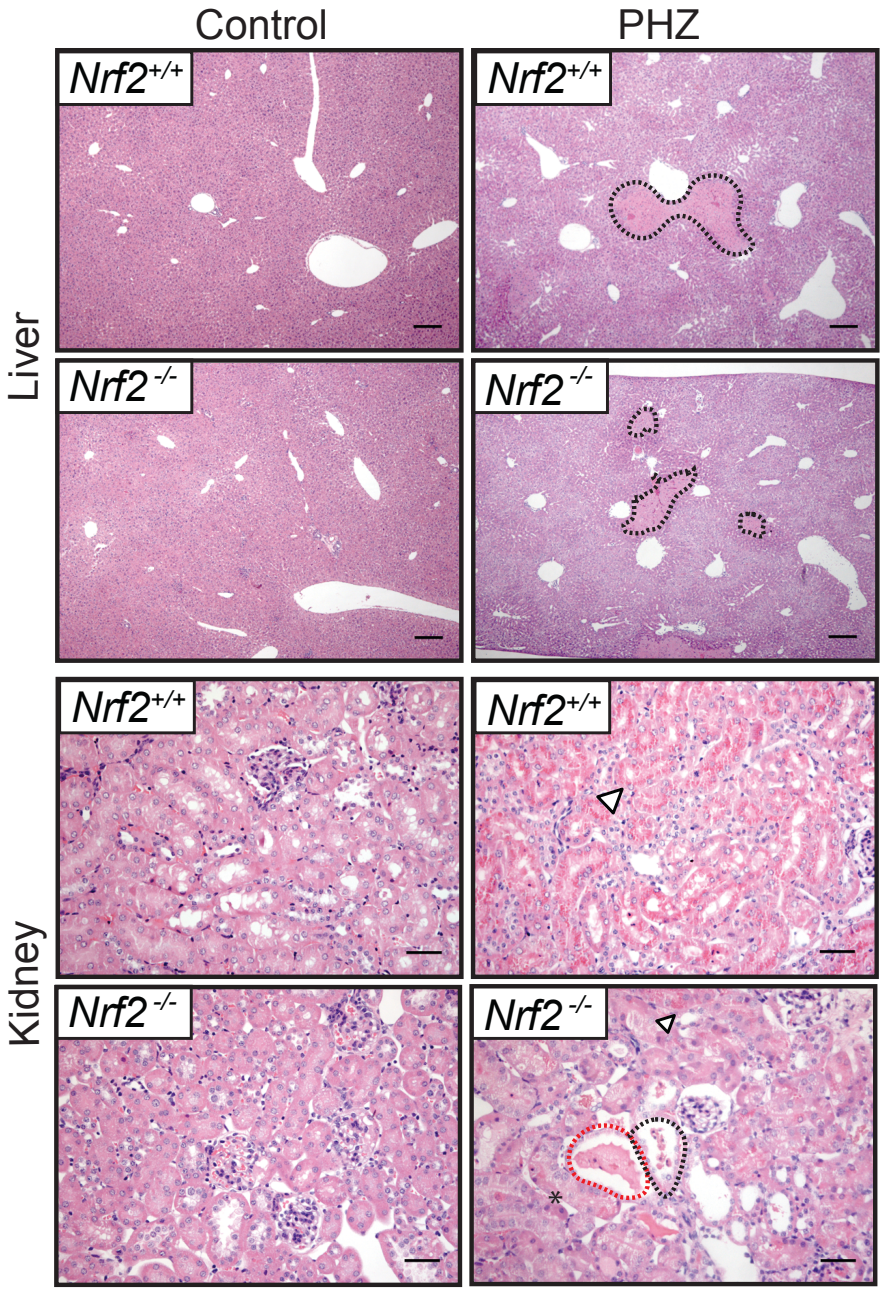

Figure 2.11. NRF2 provides tissue damage control after acute sterile hemolysis.

H&E staining of liver and kidney sections from control (non-treated) *Nrf2*$^{+/+}$ and *Nrf2*$^{-/-}$ mice or from mice receiving the second injection of PHZ 24h before harvesting the organs. Images are representative of one experiment, 4 mice per group. Black dotted line indicate areas of hepatocyte necrosis in

the liver and necrotic tubular cells detached to the lumen of the kidney tubule; red dotted line shows hemoglobin cast; white arrow points to tubular cells filled with hemoglobin and asterisk marks necrotic kidney tubular cells. Scale bar = 200 μm (liver) and 50 μm (kidney).

We then asked whether NRF2 acts directly to counter the pathogenic effects of heme, a byproduct of hemolysis. Heme administration to transgenic OKD48 mice, expressing a NRF2-luciferase reporter[12], was associated with induction of luciferase activity (*Figure 2.12a,b*), demonstrating that heme activates NRF2 *in vivo*. Heme administration led to increased mortality in *Nrf2*$^{-/-}$ mice (*Figure 2.12c*) and to a more pronounced loss of body weight (*Figure 2.12d*) and temperature (*Figure 2.12e*), as compared to *Nrf2*$^{+/+}$ mice. Interestingly, heme administration was associated with extracellular DNA accumulation in the liver of *Nrf2*$^{-/+/+}$ mice (*Figure 2.12f,g*).

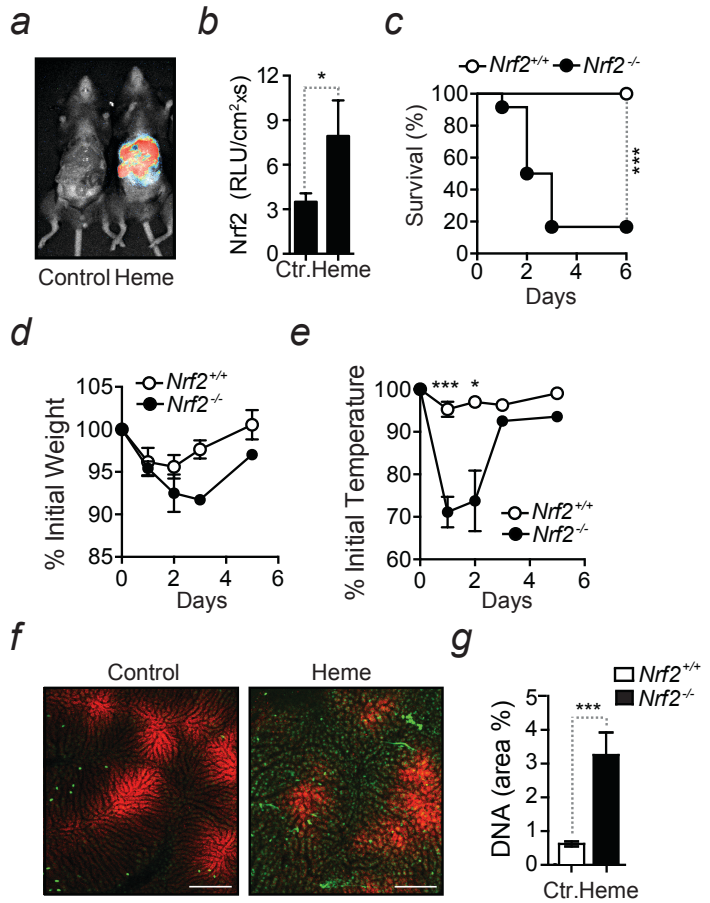

Figure 2.12. NRF2 protects against the cytotoxic effects of labile heme.

(a) Luciferase activity in reporter OKD48 mice, 6 hours after PBS (Control) or heme injection (40mg/Kg). Image is representative of 4-8 mice per group in two independent experiments. (b) Quantification of luciferase activity of mice in (a). Data is represented as mean ± STD. Mann-Whitney U Test. (c) Relative survival of *Nrf2*$^{+/+}$ and *Nrf2*$^{-/-}$ mice subjected to heme administration. Data was pooled from three independent experiments with similar trend (n=12 mice per genotype). Log-Rank Test. Percentage of (d) initial weight and (e) temperature in *Nrf2*$^{+/+}$ and *Nrf2*$^{-/-}$ mice receiving heme. Data from one experiment (n=4 mice per genotype) is represented as mean ± STD. Mann-Whitney U Test. (f) Representative images captured by liver intravital microscopy showing extracellular DNA (green) and mitochondrial TMRM (red) in the liver of *Nrf2*$^{+/+}$ mice receiving PBS or heme 24 hour before. Scale bar = 200 μM. (g) Mean % of liver extracellular DNA ± STD, detected by intravital microscopy. Data in (f) and (g) was pooled from two independent experiments (n=4 mice per group, 4 different areas analyzed). Mann-Whitney U Test. *p< 0.05, **p< 0.01, ***p<0.001.

In contrast to PHZ-induced hemolysis, antibody-induced RBC depletion (*Figure. 2.13a*) was not associated with the accumulation of heme in the plasma (*Figure. 2.13b*), with the activation of NRF2 in transgenic OKD48 mice (*Figure. 2.13c*), nor with increased mortality of *Nrf2*$^{-/-}$ *vs. Nrf2*$^{+/+}$ mice (*Figure. 2.13d*).

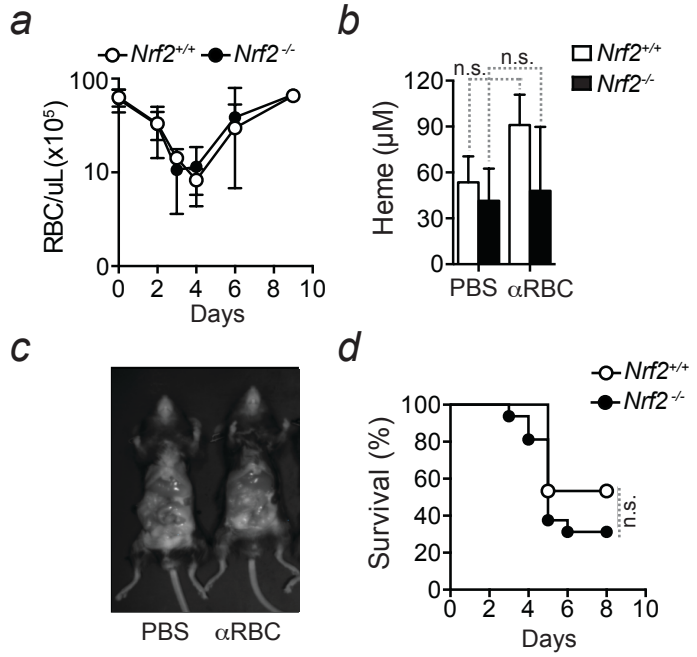

Figure 2.13. NRF2 specifically protects against hemolysis, not RBC depletion.
(a) Number of circulating RBC in *Nrf2*$^{+/+}$ and *Nrf2*$^{-/-}$ mice receiving αRBC serum. Data from four independent experiments with similar trend (n=15-16 mice per genotype) was pooled and is represented as mean ± STD. (b) Heme concentration in the plasma of *Nrf2*$^{+/+}$ and *Nrf2*$^{-/-}$ mice, 4 days after the first administration of αRBC serum. Data from one experiment (n=3-4 mice per genotype) is represented as mean ± STD. Mann-Whitney U Test. (c) Bioluminescence imaging in OKD48 reporter mice, 24h after the first administration of αRBC serum. Images are representative of 2-3 mice genotype. (d) Relative survival of *Nrf2*$^{+/+}$ and *Nrf2*$^{-/-}$ mice receiving αRBC serum. Data polled from four independent experiments with similar trend (n= 15-16 mice per group). Log-Rank Test. n.s.: non significant, *p< 0.05, **p< 0.01, ***p<0.001.

Together, these observations highlight the role of NRF2 in countering the deleterious effects of labile heme generated upon hemolysis, by protecting against necrosis and providing tissue damage control in the context or not of bloodstream infections.

2.4. NRF2 regulates the anti-oxidant response targeting the mitochondria.

When exposed *in vitro* to heme plus TNF, primary mouse hepatocytes increased NRF2 protein expression (*Figure 2.14a*), nuclear translocation (*Figure 2.14b,c*) and transcriptional activity (*Figure 2.14d*). However, while heme alone led to an augmented NRF2 protein expression (*Figure 2.14a*) and nuclear translocation (*Figure 2.14b,c*), it did not induce NRF2 transcriptional activity (*Figure 2.14d*). Moreover, TNF failed *per se* to induce NRF2 protein expression (*Figure 2.14a*), nuclear translocation (*Figure 2.14b,c*) or transcriptional activity (*Figure 2.14d*). Interestingly, our data reveals that heme primes hepatocytes to activate antioxidant NRF2-dependent gene expression in response to TNF, consistent with our

previous observation that heme primes hepatocytes to accumulate ROS in response to TNF[13,14,1].

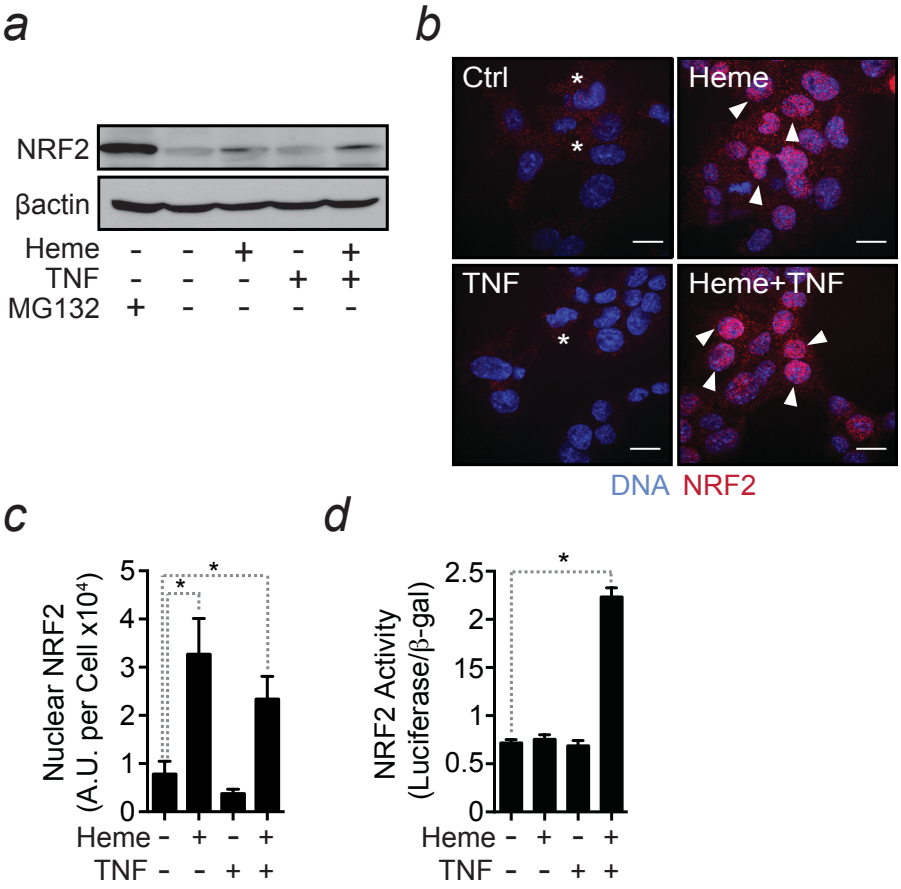

Figure 2.14. Heme synergizes with TNF to induce NRF2 expression but not transcriptional activity.

(a) NRF2 protein expression detected by western blot in whole cell lysates from Hepa1-6 cells not treated (-) or treated (+) with MG132, heme, TNF or heme and TNF. Image is representative of three independent experiments with similar trend. (b) NRF2 protein detected by immunofluorescence (red) in Hepa1-6 cells not treated or treated with heme, TNF or heme plus TNF. (Blue: DNA). Images are representative of three independent experiments. Asterisk indicates cytoplasmic NRF2 and arrowheads nuclear NRF2. Scale: 10μm. (c) Quantification of NRF2 nuclear translocation in Hepa1-6 cells treated as in (a) and (b). Data represents the mean integrated density per cell, from five fields per treatment per experiment in three independent experiments ± STD. Mann-Whitney U Test. (d) NRF2 transcriptional activity in Hepa1-6 cells transiently transfected with an NRF2-luciferase reporter and treated as in (a-c). Data from two independent experiments is

represented as mean ± STD. Mann-Whitney U Test. *p< 0.05, **p< 0.01, ***p<0.001.

Under experimental conditions not cytotoxic to *Nrf2*$^{+/+}$ primary hepatocytes, heme and TNF induced *Nrf2*$^{-/-}$ hepatocytes to undergo programmed cell death (PCD) (*Figure 2.15a*). Cytotoxicity in *Nrf2*$^{-/-}$ hepatocytes was accompanied by the accumulation of high levels of ROS (*Figure 2.15b,e*), including mitochondrial superoxide (mtO_2^-) (*Figure 2.15c,f*) and with mitochondrial membrane (Δψm) hyperpolarization (*Figure 2.15c,g*).

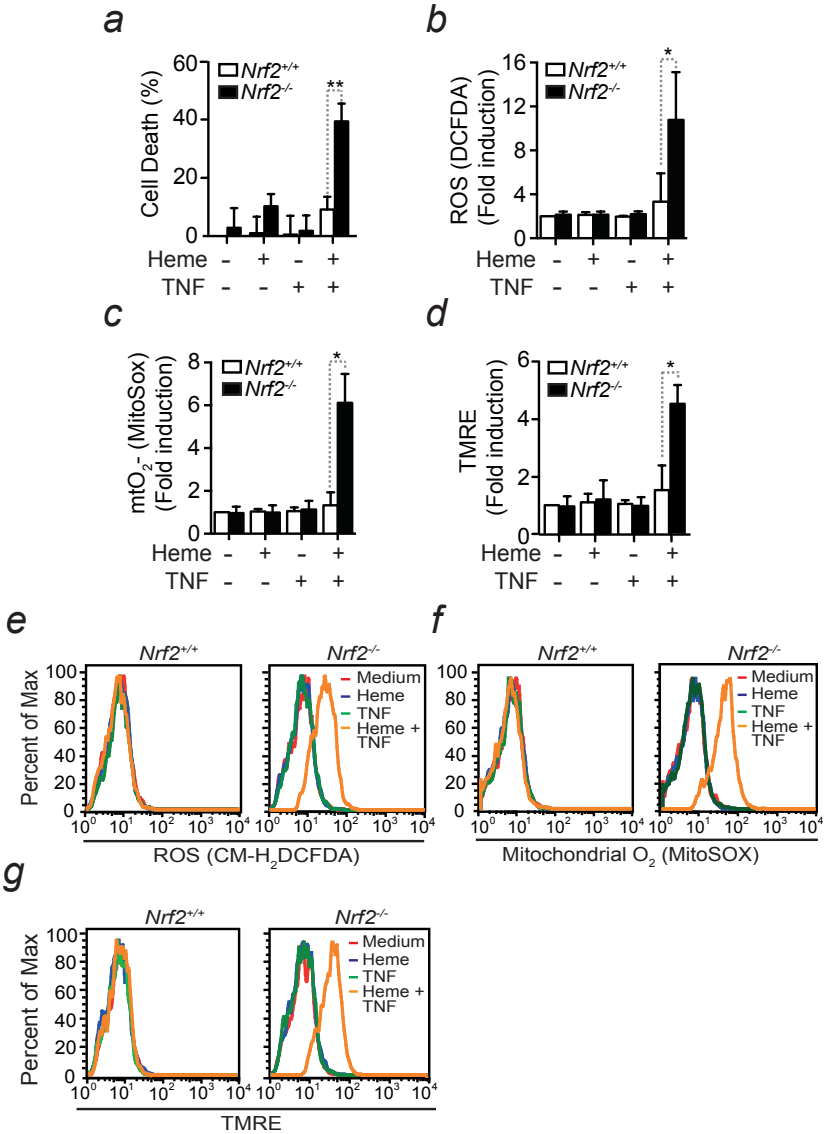

Figure 2.15. NRF2 protects against mitochondrial dysfunction, mitochondrial ROS production and cell death in response to heme and TNF.

(a) Percentage of cell death in *Nrf2*$^{+/+}$ and *Nrf2*$^{-/-}$ primary hepatocytes treated (+) or not (-) with heme, TNF or heme plus TNF and collected 8h after heme treatment. Data is represented as mean ± STD from 6 wells in one out of three independent experiments with similar trend. One-Way ANOVA. Levels of (b,e) intracellular ROS, (c,f) mitochondrial superoxide and (d,g) mitochondrial membrane potential in primary mouse hepatocytes, treated as in (a). Data in (b-d) represents the pool of four independent experiments with the same trend and is displayed as mean ± STD and data in (e-g) displays one from the four independent experiments in (b-d). One-Way ANOVA. *p< 0.05, **p< 0.01, ***p<0.001.

These data show that NRF2 preserves mitochondrial integrity and protects against PCD in response to heme and TNF via a mechanism associated with reduced production/accumulation of mitochondrial O_2^-.

To further investigate the role of mitochondrial O_2^- in the induction of hepatocyte PCD after heme and TNF treatment, we used the mitochondrial O_2^- scavenger, MitoTempo. This mitochondria-specific antioxidant protected primary *Nrf2*$^{-/-}$ (*Figure 2.16a*) or *Nrf2*$^{+/+}$ (*Figure 2.17a*) hepatocytes from undergoing PCD in response to heme and TNF. This suggests that mitochondrial O_2^- plays a central role in the mechanism via which heme sensitizes hepatocytes to undergo PCD in response to TNF and that NRF2 is protective against the production and/or accumulation of mitochondrial ROS. Of note, MitoTempo reduced to basal levels the overall ROS production in *Nrf2*$^{-/-}$ (*Figure 2.16b,d*) or *Nrf2*$^{+/+}$ (*Figure 2.17b,c*) hepatocytes exposed to heme and TNF. This antioxidant effect was similar to the one observed using the glutathione precursor N-acetyl cysteine (NAC) (*Figure 2.16b,d; Figure 2.17b,c*), a well-known general antioxidant, suggesting that mitochondrial O_2^- is the predominant form of ROS generated in hepatocytes exposed to heme and TNF.

MitoTempo preserved mitochondrial Δψm in primary *Nrf2*$^{-/-}$ (*Figure 2.16c,e*) or *Nrf2*$^{+/+}$ (*Figure 2.17d,e*) hepatocytes exposed to heme and TNF, to a similar extent as NAC. This demonstrates that the mechanism via which NRF2 supports mitochondrial integrity involves the repression of mitochondrial O_2^- production/accumulation, which is consistent with the notion that this transcription factor regulates a metabolic response sustaining mitochondrial structure and function[15,16].

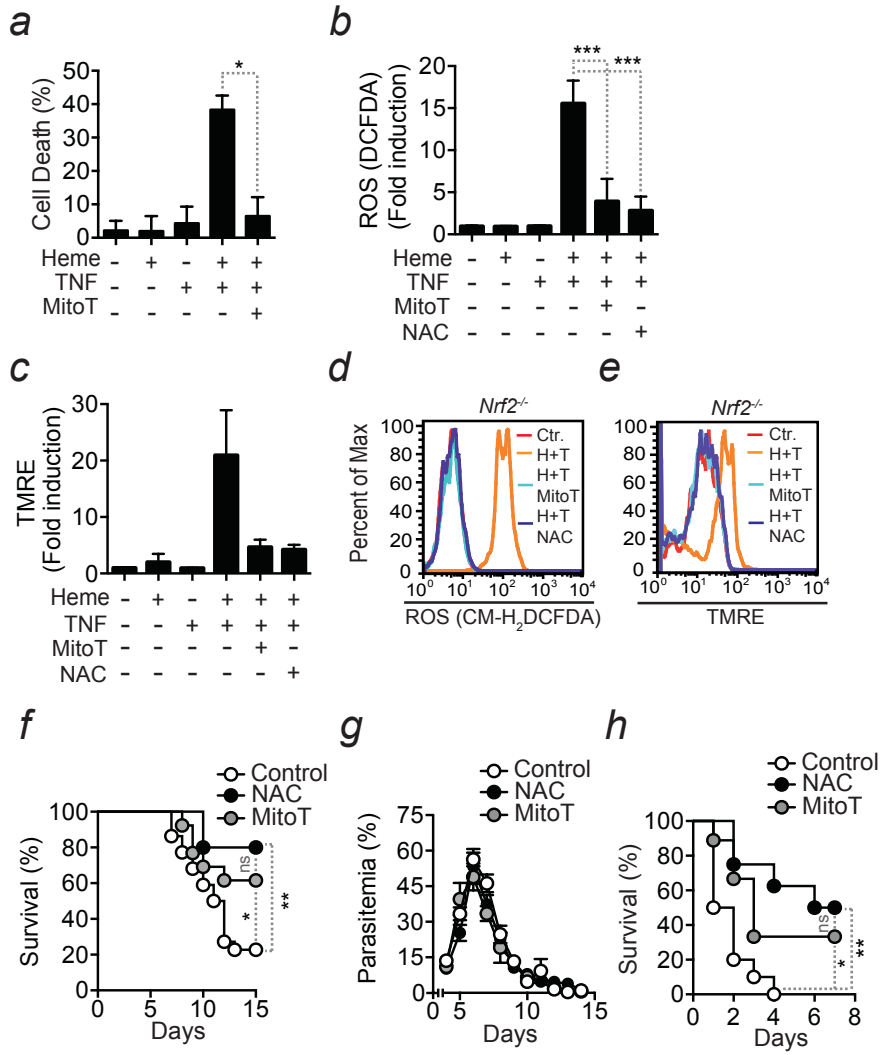

Figure 2.16. NRF2 protects against heme and TNF-mediated cytotoxicity via a mechanism associated with reduced production/accumulation of mitochondrial ROS.
(a) Percentage of cell death in primary mouse *Nrf2*$^{-/-}$ hepatocytes, treated (+) or not (-) with heme and/or TNF and MitoTempo (MitoT) and collected 8h after heme treatment. Data represented as mean ± STD from 6 replicate wells in one out of two independent experiments with the same trend. One-Way ANOVA. (b,d) Intracellular ROS and (c,e) Mitochondrial membrane potential in primary mouse *Nrf2*$^{-/-}$ hepatocytes, treated as in (a) and when indicated (+) with NAC. Data in (b) and (c) corresponds to the pool of three and two independent experiments with the same trend, respectively, and is represented as mean ± STD, relative to untreated (-) controls. One-Way ANOVA. Data in (d) and (e) displays one from the two to three independent experiments in (b) and (c). (f) Relative survival of *Pcc*-infected *Nrf2*$^{-/-}$ mice receiving PBS (Control) versus mice receiving MitoTEMPO (MitoT) or NAC. Data was pooled from three to four independent experiments with similar trend (n=10-23 mice per group). Log-Rank Test. (g) Mean percentage of infected RBC ± SEM, pooled from three to four independent experiments (n=10-23 mice per genotype). (h) Relative survival of *Nrf2*$^{-/-}$ mice receiving heme and treated with PBS (Control), MitoTEMPO (MitoT) or NAC. Data was pooled from two independent experiments with similar trend (n=8-10 mice per group). Log-Rank Test. n.s.: non significant, *p< 0.05, **p< 0.01, ***p<0.001.

We then asked whether NRF2 is acting as an antioxidant *in vivo*. MitoTempo administration to *Nrf2*$^{-/-}$ mice was protective against *Pcc* infection (*Figure 2.16f*) as well as against heme administration (*Figure 2.16h*) to a similar extent to the protection conferred by NAC (*Figure 2.16f,h*). The protective effect of both MitoTempo and NAC against *Plasmodium* infection was not associated with modulation of host pathogen load (*Figure 2.16g*). These results suggest that NRF2 protects against heme toxicity generated during the blood stage of *Plasmodium* infection via an antioxidant mechanism protecting the mitochondria.

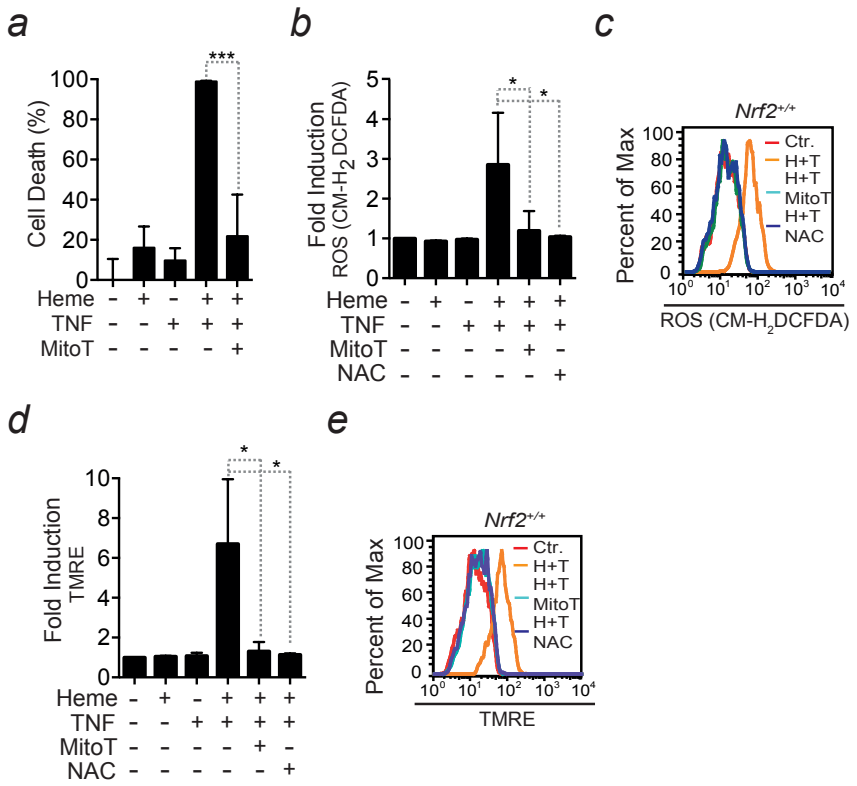

Figure 2.17. Heme and TNF synergize to produce mitochondrial ROS and mitochondrial dysfunction, leading to cell death.

(a) Percentage of cell death in primary mouse *Nrf2*$^{+/+}$ hepatocytes, treated (+) or not (-) with heme and/or TNF and MitoTempo (MitoT) and collected 16h after heme treatment. Data represented as mean ± STD from 6 replicate wells in one out of two independent experiments with the same trend. One-Way ANOVA. (b,d) Intracellular ROS and (c,e) Mitochondrial membrane potential in primary mouse *Nrf2*$^{+/+}$ hepatocytes, treated as in (a) and when indicated (+) with NAC. Data in (b) and (c) corresponds to the pool of three and two independent experiments with the same trend, respectively, and is represented as mean ± STD, relative to untreated (-) controls. Data in (d) and (e) displays one from the two to three independent experiments in (b) and (c). One-Way ANOVA. *p< 0.05, **p< 0.01, ***p<0.001.

2.5. Labile heme sensitizes hepatocytes to undergo TNF-dependent necroptosis.

Induction of cell death in response to heme and TNF was partially rescued by Necrostatin-1 (Nec-1), suggesting that heme sensitizes hepatocytes to undergo PCD via RIPK1-dependent mechanism (*Figure 2.18a*). Primary hepatocytes from RIPK3 deficient (*Ripk3*$^{-/-}$) mice were also protected against heme and TNF (*Figure 2.18b*).

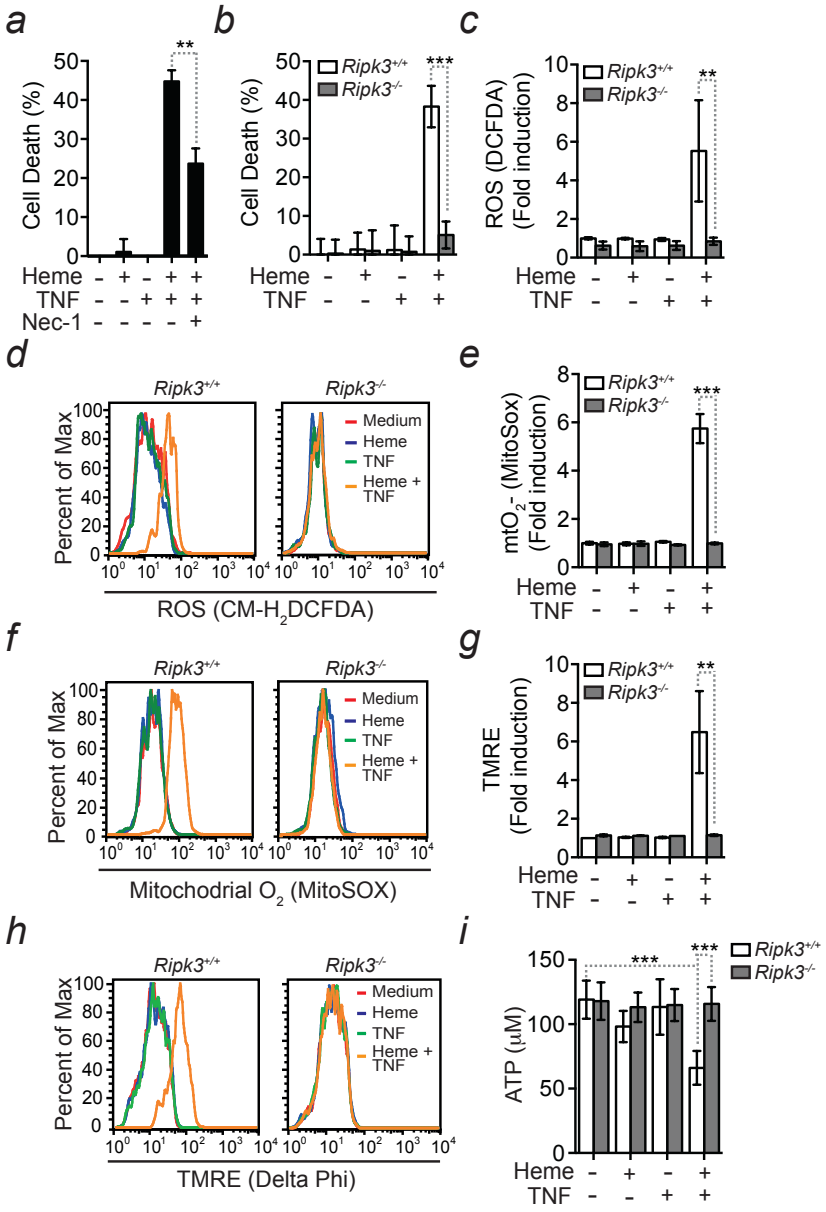

Figure 2.18. Labile heme synergizes with TNF to trigger Ripk3-dependent necroptosis and mitochondrial dysfunction in hepatocytes.

(a) Percentage of cell death in primary hepatocytes isolated from wild-type mice and treated (+) or not (-) with heme, TNF or heme plus TNF and, when indicated (+), with Nec1. Data represented as mean ± STD from 5 wells in one out of two independent experiments with the same trend. One-Way ANOVA. (b) Percentage of cell death in primary *Rip3*$^{+/+}$ and *Ripk3*$^{-/-}$ mouse hepatocytes, treated (+) or not (-) with heme, TNF or heme plus TNF. Data represented as mean ± STD from 5 wells in one out of two independent experiments with the same trend. Relative induction and corresponding histograms of (c,d) intracellular ROS, (e,f) mitochondrial superoxide and (g,h) mitochondrial membrane potential. Data represented as mean ± STD from one out of four independent experiments with the same trend. One-Way ANOVA. (i) Cellular ATP content in *Rip3*$^{+/+}$ and *Ripk3*$^{-/-}$ mouse primary hepatocytes treated (+) or not (-) with heme, TNF or heme plus TNF. Data represented as mean ± STD from one out of two to four independent experiments with the same trend. One-Way ANOVA. *p< 0.05, **p< 0.01, ***p<0.001.

Ablation of PCD in *Ripk3*$^{-/-}$ hepatocytes was associated with protection against intracellular ROS production/accumulation (*Figure 2.18c,d*), including mitochondrial O_2^- (*Figure 2.18e,f*) as well as with maintenance of mitochondrial Δψm, preventing hyperpolarization (*Figure 2.18g,h*).

Heme and TNF reduced the intracellular ATP content of wild-type primary hepatocytes (*Figure 2.18i*), but not of *Ripk3*$^{-/-}$ cells (*Figure 2.18i*). This reveals that heme and TNF interfere with mitochondrial function via a RIPK3-dependent mechanism, consistent with the notion that RIPK3 regulates cellular metabolism[17].

Knockdown of *Mlkl* or *Pgam5* using specific shRNAs (*Figure 2.19a*) protected mouse hepatoma Hepa1-6 cells from undergoing PCD in response to heme and TNF (*Figure 2.19b,c*). This was associated with inhibition of intracellular ROS production/accumulation (*Figure 2.19d,e*), including mitochondrial O_2^- (*Figure 19f,g*) as well as with maintenance of mitochondrial Δψm

(*Figure 2.19h,i*). These results demonstrate that heme primes hepatocytes to undergo PCD via the canonical necroptosis signal transduction pathway involving RIPK1, RIPK3 and MLKL. This signal transduction pathway acts upstream of the outer mitochondria membrane PGAM5[18] to promote mitochondrial O_2^- production/accumulation[19] and mitochondrial dysfunction leading to necrotic cell death[20].

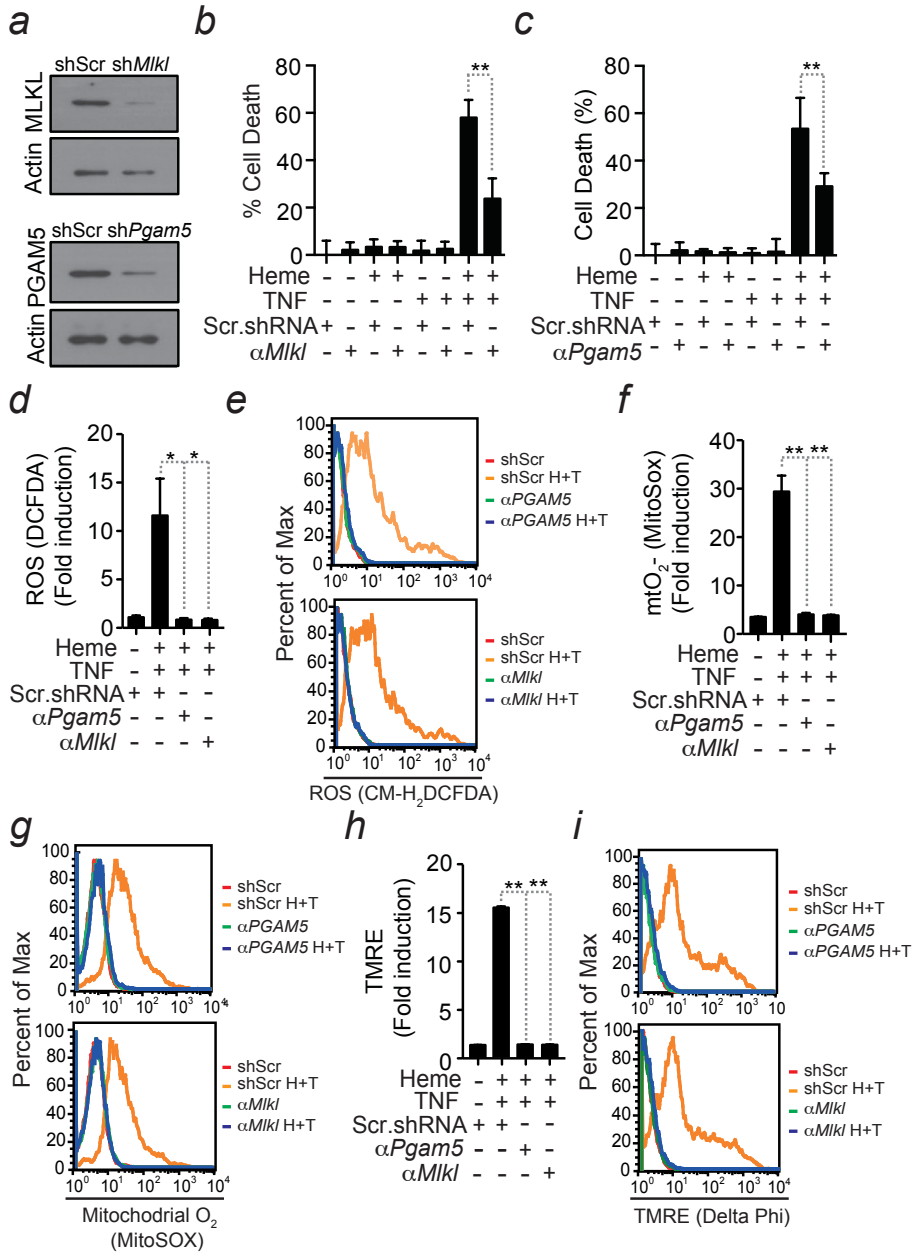

Figure 2.19. Labile heme synergizes with TNF to trigger MLKL and PGAM5-dependent mitochondrial dysfunction and cell death in hepatocytes.
(a) Detection of MLKL and PGAM5 protein expression by western blot, in whole cell extracts from Hepa1-6 cells transduced with a RecAd. encoding a control (scrambled) shRNA (Scr.shRNA) or a RecAd. encoding shRNAs targeting mouse *Mlkl* (sh*Mlkl*) or *Pgam5* (sh*Pgam5*). (b, c) Percentage of cell death in in Hepa1-6 cells treated (+) or not (-) with heme, TNF or heme plus TNF and, when indicated (+), transduced with RecAd. encoding shRNAs targeting (b) mouse *Mlkl* (sh*Mlkl*) or (c) *Pgam5* (sh*Pgam5*). Data represented as mean ± STD from one out of two independent experiments with the same trend. One-Way ANOVA. Relative induction and representative histograms of (d,e) intracellular ROS production, (f,g) mitochondrial superoxide generation and (h,i) increase of mitochondrial membrane potential in Hepa1-6 cells treated as in (b, c). Data is represented as mean ± STD from two independent experiments with the same trend. One-Way ANOVA. *p< 0.05, **p< 0.01, ***p<0.001.

2.6. NRF2 regulates a cytoprotective response that inhibits necroptosis.

We reasoned that if NRF2 acts as a physiologic counter regulator of necroptosis, than genetic loss of function of components of the necroptosis signal transduction pathway should protect *Nrf2*$^{-/-}$ primary hepatocytes from heme sensitization to TNF-dependent necroptosis. Heme and TNF failed to induce primary *Nrf2*$^{-/-}$*Ripk3*$^{-/-}$ hepatocytes to undergo necroptosis, as compared to primary *Nrf2*$^{-/-}$ *Ripk3*$^{+/+}$ hepatocytes (*Figure 2.20a*). Blocking PCD was associated with preservation of homeostatic levels of intracellular ROS production/accumulation (*Figure 2.20b,e*), including mitochondrial O_2^- (*Figure 2.20c,f*) as well as with maintenance of mitochondrial Δψm (*Figure 2.20d,g*) in *Nrf2*$^{-/-}$*Ripk3*$^{-/-}$ vs *Nrf2*$^{-/-}$*Ripk3*$^{+/+}$ hepatocytes. Our data suggests that NRF2 acts as a physiologic counter regulator of heme and TNF-induced necroptosis *in vitro*.

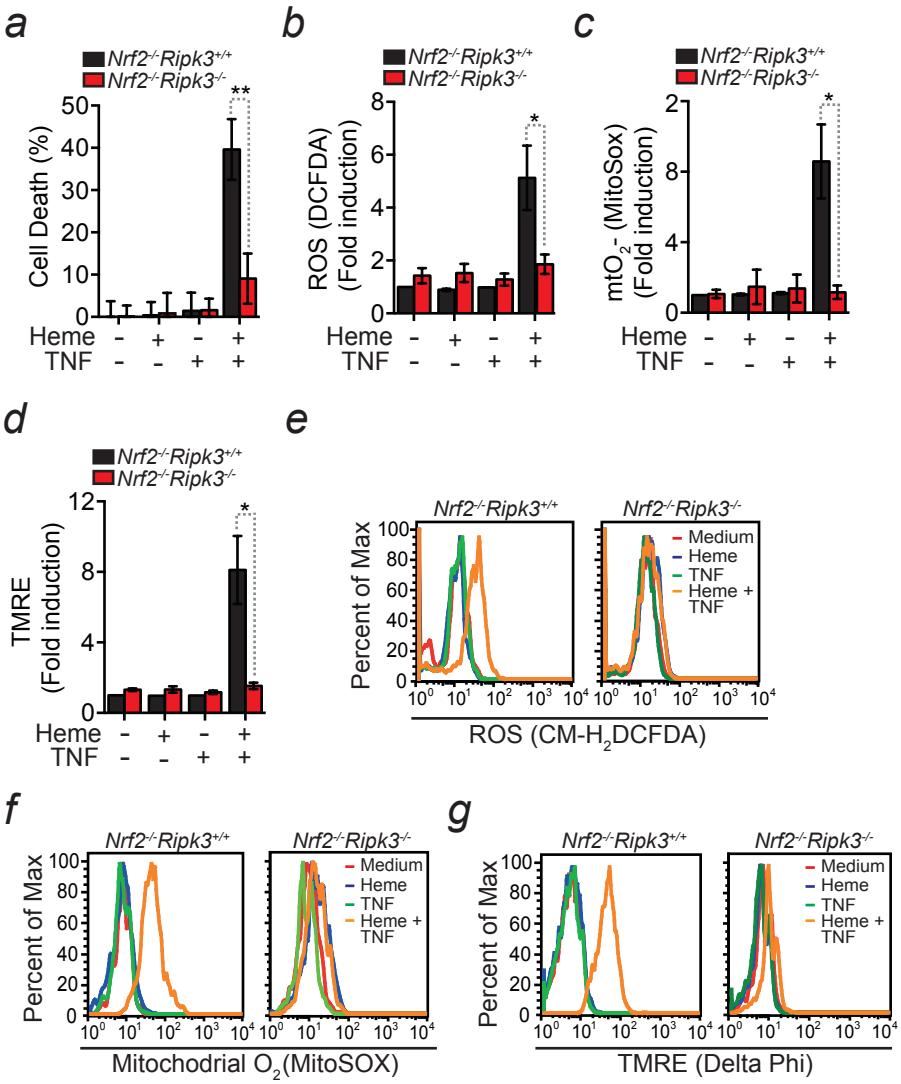

Figure 2.20. NRF2 protects against Rikp3-dependent programmed cell death by blocking mitochondrial ROS production and mitochondrial dysfunction in vitro.

(a) Percentage of cell death in primary *Nrf2*$^{-/-}$*Rip3*$^{+/+}$ and *Nrf2*$^{-/-}$*Ripk3*$^{-/-}$ mouse hepatocytes, treated (+) or not (-) with heme, TNF or heme plus TNF. Data represented as mean ± STD from 6 wells in one out of two independent experiments with the same trend. One-Way ANOVA. Relative induction and corresponding representative histograms of (b,e) intracellular ROS, (c,f) mitochondrial superoxide and (d,g) mitochondrial membrane potential in *Nrf2*$^{-/-}$*Rip3*$^{+/+}$ and *Nrf2*$^{-/-}$*Ripk3*$^{-/-}$ mouse primary hepatocytes treated (+) or not (-) with heme, TNF or heme plus TNF. Data represented

as mean ± STD from a pool of three independent experiments with the same trend. One-Way ANOVA. *p< 0.05, **p< 0.01, ***p<0.001.

As NRF2 acts as a physiologic counter regulator of necroptosis *in vitro,* we hypothesized that genetic loss of function of components of the necroptosis signal transduction pathway should bypass the requirement for the protective effect of NRF2 against infectious or sterile intravascular hemolysis *in vivo*. In contrast to *Nrf2*$^{-/-}$*Ripk3*$^{+/+}$ mice, *Nrf2*$^{-/-}$*Ripk3*$^{-/-}$ mice were protected against PHZ administration (*Figure 2.21a*). Of note, deletion of the *Ripk3* allele *per se* had no impact on the outcome of acute hemolysis in *Nrf2*$^{+/+}$*Ripk3*$^{-/-}$ *vs.* *Nrf2*$^{+/+}$*Ripk3*$^{+/+}$ mice (*Figure 2.21a*). This suggests that NRF2 acts as a physiologic counter regulator of necroptosis to confer protection against sterile intravascular hemolysis.

Genetic loss of function of components of the necroptosis signal transduction pathway also bypassed the requirement for NRF2 in the establishment of disease tolerance to sepsis, as assessed in *Nrf2*$^{-/-}$ *Ripk3*$^{-/-}$ *vs. Nrf2*$^{-/-}$*Ripk3*$^{+/+}$ mice subjected to CLP (*Figure 2.21b*). This protection was not associated with modulation of pathogen load, as assessed for aerobic and anaerobic bacteria in different organs of *Nrf2*$^{-/-}$*Ripk3*$^{+/+}$ *vs. Nrf2*$^{-/-}$*Ripk3*$^{-/-}$ mice (*Figure 2.21c*), 16h after CLP. Of note, deletion of the *Ripk3* allele had no impact *per se* on the outcome of CLP in *Nrf2*$^{+/+}$*Ripk3*$^{-/-}$ *vs. Nrf2*$^{+/+}$*Ripk3*$^{+/+}$ mice (*Figure 2.21b*). Severe hepatocellular degeneration was ablated in livers from *Nrf2*$^{-/-}$*Ripk3*$^{-/-}$ vs *Nrf2*$^{-/-}$*Ripk3*$^{+/+}$ mice, collected 16h post-CLP, as assessed by histological analysis (*Figure 2.21d*). This suggests that NRF2 acts as a physiologic counter regulator of necroptosis to confer disease tolerance to sterile hemolysis and polymicrobial sepsis.

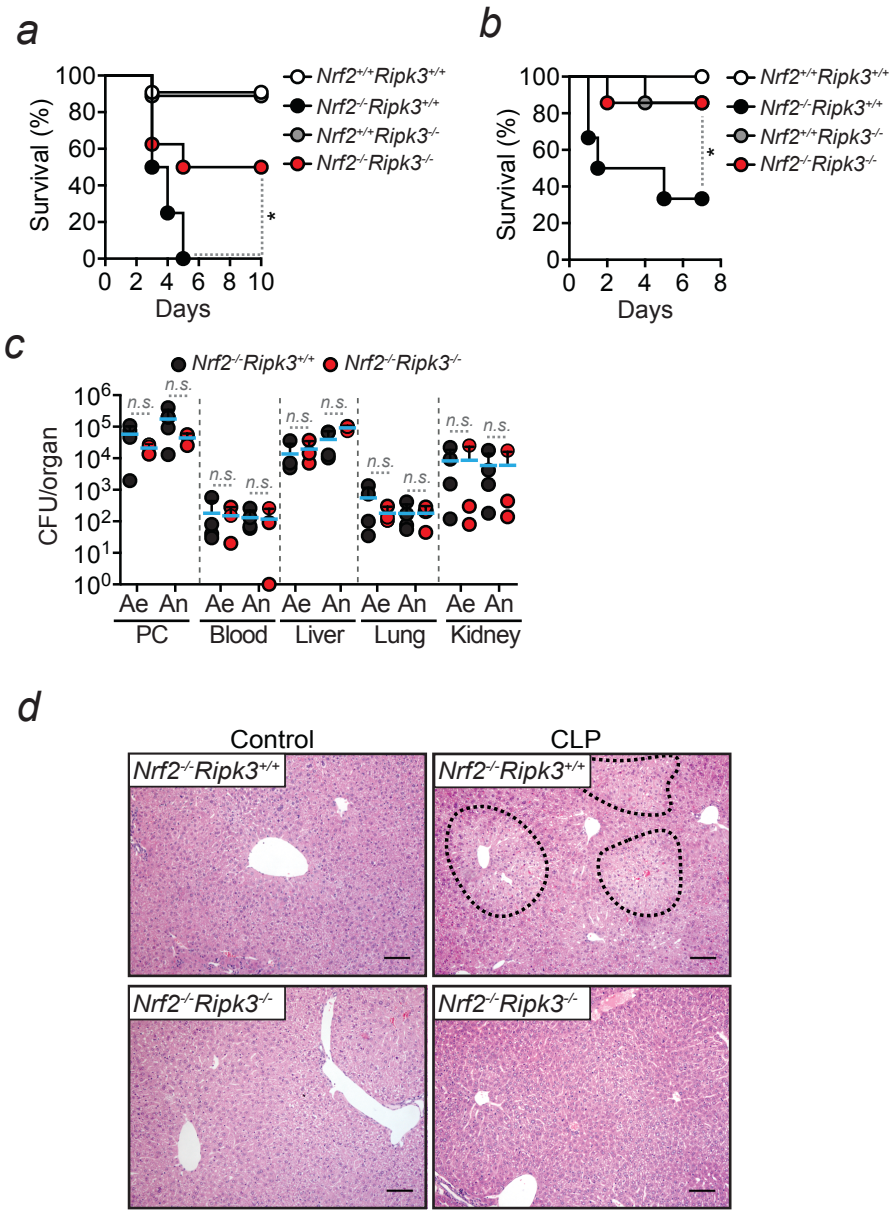

Figure 2.21. NRF2 acts as a cytoprotective molecule against Ripk3-induced damage in vivo after acute hemolysis and sepsis.

(a) Relative survival of *Nrf2*$^{+/+}$*Rip3*$^{+/+}$, *Nrf2*$^{-/-}$*Rip3*$^{+/+}$, *Nrf2*$^{+/+}$*Rip3*$^{-/-}$ and *Nrf2*$^{-/-}$ *Ripk3*$^{-/-}$ mice subjected to acute hemolysis, induced by PHZ administration, in two independent experiments with similar trend (n=8-11 mice per genotype). Log-Rank Test. (b) Relative survival of *Nrf2*$^{+/+}$*Rip3*$^{+/+}$, *Nrf2*$^{-/-}$ *Rip3*$^{+/+}$, *Nrf2*$^{+/+}$*Rip3*$^{-/-}$ and *Nrf2*$^{-/-}$*Ripk3*$^{-/-}$ mice subjected to CLP in two independent experiments with similar trend (n=6-7 mice per genotype). Log-Rank Test. (c) Colony forming units (CFU) of aerobic (Ae) and anaerobic

(An) bacteria 16h after CLP in *Nrf2*$^{-/-}$*Rip3*$^{+/+}$ and *Nrf2*$^{-/-}$*Ripk3*$^{-/-}$ mice. Data pooled from two independent experiments (n=3-4) mice per genotype). PC: peritoneal cavity. Mann-Whitney U Test. (d) H&E staining of the liver of naïve *Nrf2*$^{-/-}$*Rip3*$^{+/+}$ and *Nrf2*$^{-/-}$*Ripk3*$^{-/-}$ mice (Control) and 16h after CLP. Image is representative of (n=7 mice per genotype). Dotted lines indicate areas of hepatocellular degeneration. Scale bar = 100µm. n.s.: non significant, *p< 0.05, **p< 0.01, ***p<0.001.

We then asked whether the establishment of disease tolerance to the blood stage of *Plasmodium* infection also relies on NRF2-driven protection against necroptosis. Pharmacological inhibition of RIPK1 kinase activity using Necrostatin-1 (Nec-1) restored the survival of *Pcc*-infected *Nrf2*$^{-/-}$ mice (*Figure 2.22a*) without interfering with pathogen load, as compared to vehicle treated *Nrf2*$^{-/-}$ mice (*Figure 2.22b*). This demonstrates that NRF2 confers disease tolerance to malaria via a mechanism modulating RIPK1 activation. Deletion of the *Ripk3* allele, however, had no impact on the survival (*Figure 2.22c*) or pathogen load (*Figure 2.22d*) of *Plasmodium*-infected *Nrf2*$^{-/-}$*Ripk3*$^{-/-}$ *vs. Nrf2*$^{-/-}$*Ripk3*$^{+/+}$ mice or *Nrf2*$^{+/+}$*Ripk3*$^{-/-}$ vs *Nrf2*$^{+/+}$*Ripk3*$^{+/+}$ mice.

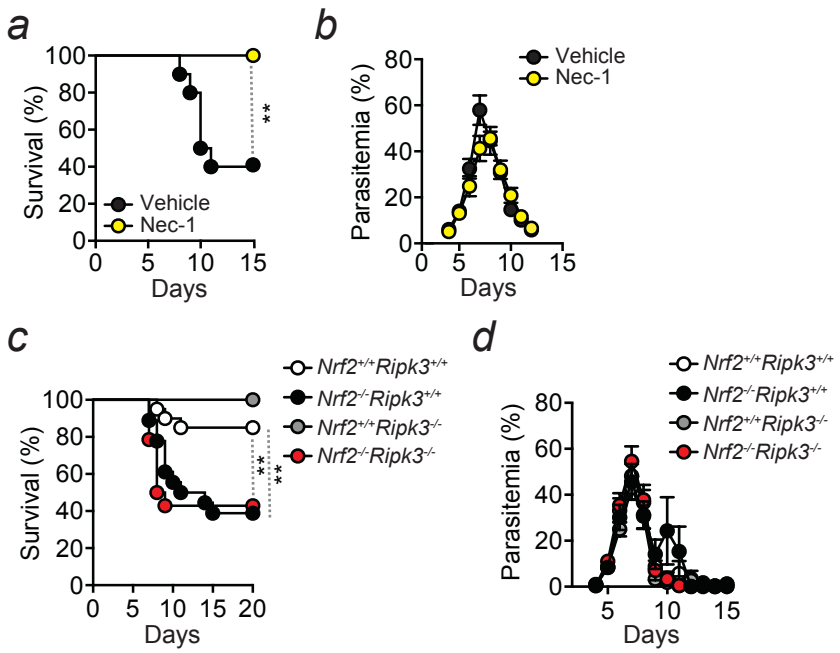

Figure 2.22. NRF2 protects against Ripk1 but not Ripk3-induced lethality in vivo after malaria infection.
(a) Relative survival of *Pcc* infected *Nrf2*$^{-/-}$ mice treated or not (Vehicle) with Nec-1. Data pooled from two independent experiments (n=8-10 mice per group). Log-Rank Test. (b) Percentage of infected RBC in the same mice as (a). Data represented as ± SEM. (c) Relative survival of *Pcc* infected *Nrf2*$^{-/-}$ mice expressing (*Ripk3*$^{+/+}$) or not *Ripk3* (*Ripk3*$^{-/-}$). Data pooled from four independent experiments (n=14-18 mice per genotype). Log-Rank Test. (d) Percentage of infected RBC in the same mice as (a). Data represented an as ± SEM. *p< 0.05, **p< 0.01, ***p<0.001.

We then questioned whether the establishment of disease tolerance to *Plasmodium* infection by NRF2 requires the inhibition of PCD by apoptosis. Deletion of the *Caspase8* allele, however, had no impact on the survival (*Figure 2.23a*) or pathogen load (*Figure 2.23b*) of *Plasmodium* infected *Nrf2*$^{-/-}$*Ripk3*$^{-/-}$*Casp8*$^{-/-}$ *vs.* *Nrf2*$^{-/-}$ *Ripk3*$^{+/+}$*Casp8*$^{+/+}$ mice or *Nrf2*$^{+/+}$*Ripk3*$^{+/+}$*C8*$^{+/+}$ *vs.* *Nrf2*$^{+/+}$*Ripk3*$^{-/-}$*C8*$^{-/-}$ mice.

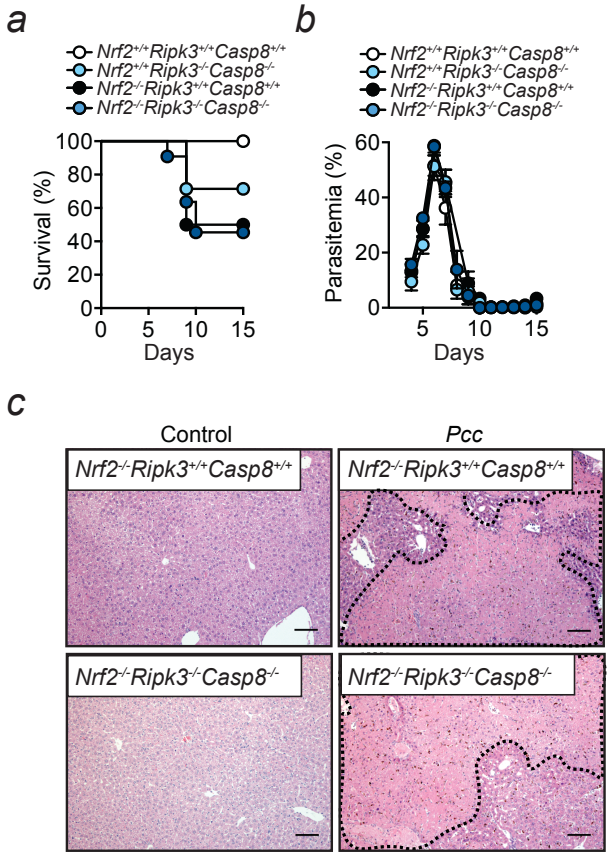

Figure 2.23. NRF2 does not protect against Caspase8 dependent apoptosis in vivo after malaria infection.
(a) Relative survival of *Pcc* infected *Nrf2*$^{-/-}$ mice expressing or not *Ripk3* and *Caspase 8* (*Ripk3*$^{+/+}$*Caspase8*$^{+/+}$ *Ripk3*$^{-/-}$*Caspase8*$^{-/-}$, respectively). Data pooled from two independent experiments (n=4-11 mice per genotype). Log-Rank Test. (b) Percentage of infected RBC in the same mice as (a). Data represented an as ± STD. (c) H&E staining of the liver of naïve mice (Control) and *Pcc* infected *Nrf2*$^{-/-}$ mice expressing *Ripk3* and *Caspase 8* (*Ripk3*$^{+/+}$*Caspase8*$^{+/+}$) or not (*Ripk3/*$^{-/-}$ *Caspase8*$^{-/-}$). Images are representative of one experiment, n=4-5 mice per genotype. Black dotted lines indicate areas of hepatocyte necrosis. Scale bar = 100μm.

Histological analysis confirmed that the extent of liver necrosis in *Plasmodium*-infected *Nrf2*$^{-/-}$*Ripk3*$^{-/-}$*Casp8*$^{-/-}$ was similar to *Nrf2*$^{-/-}$ *Ripk3*$^{+/+}$*Casp8*$^{+/+}$ mice (*Figure 23c*), revealing that NRF2 confers tissue damage control and establishes disease tolerance to malaria via a mechanism that does not involve Caspase8 driven apoptosis.

We afterwards questioned whether NRF2 confers tissue damage control and establishes disease tolerance to malaria via a mechanism involving additional signaling components in the necroptosis pathway. As a candidate, we decided to assess the role of the *peptidyl-prolyl isomerase F* gene (*PPIF*), which encodes the mitochondrial membrane protein Cyclophylin D (CYPD), a key regulator of the mitochondrial permeability transition pore (MPTP) and the induction of regulated necrosis[21,22]. Primary *Ppif* deficient *(Ppif* $^{-/-}$) hepatocytes were refractory to heme and TNF-induced necroptosis (*Figure 2.24a*), an effect associated with maintenance of homeostatic levels of intracellular ROS (*Figure 2.24b,e*), including mitochondrial O_2^- (*Figure 2.24c,f*) as well as with preservation of mitochondrial Δψm (*Figure 2.24d,g*). Deletion of *Ppif* allele *per se* also had no apparent impact *in vivo* on the outcome of sterile hemolysis (*Figure 2.24h*) or *Plasmodium* infection (*Figure 2.24i,j*) in *Nrf2*$^{+/+}$ or *Nrf2*$^{-/-}$ mice, as assessed in *Nrf2*$^{+/+}$*Ppif*$^{+/+}$ *vs. Nrf2*$^{+/+}$*Ppif* $^{-/-}$ mice and *Nrf2*$^{-/-}$*Ppif*$^{+/+}$ *vs. Nrf2*$^{-/-}$*Ppif*$^{-/-}$ mice.

This suggests that heme primes hepatocytes to undergo TNF-induced necroptosis *in vitro* but not *in vivo* via a CYPD-dependent mechanism that promotes mitochondrial O_2^- accumulation and Δψm impairment.

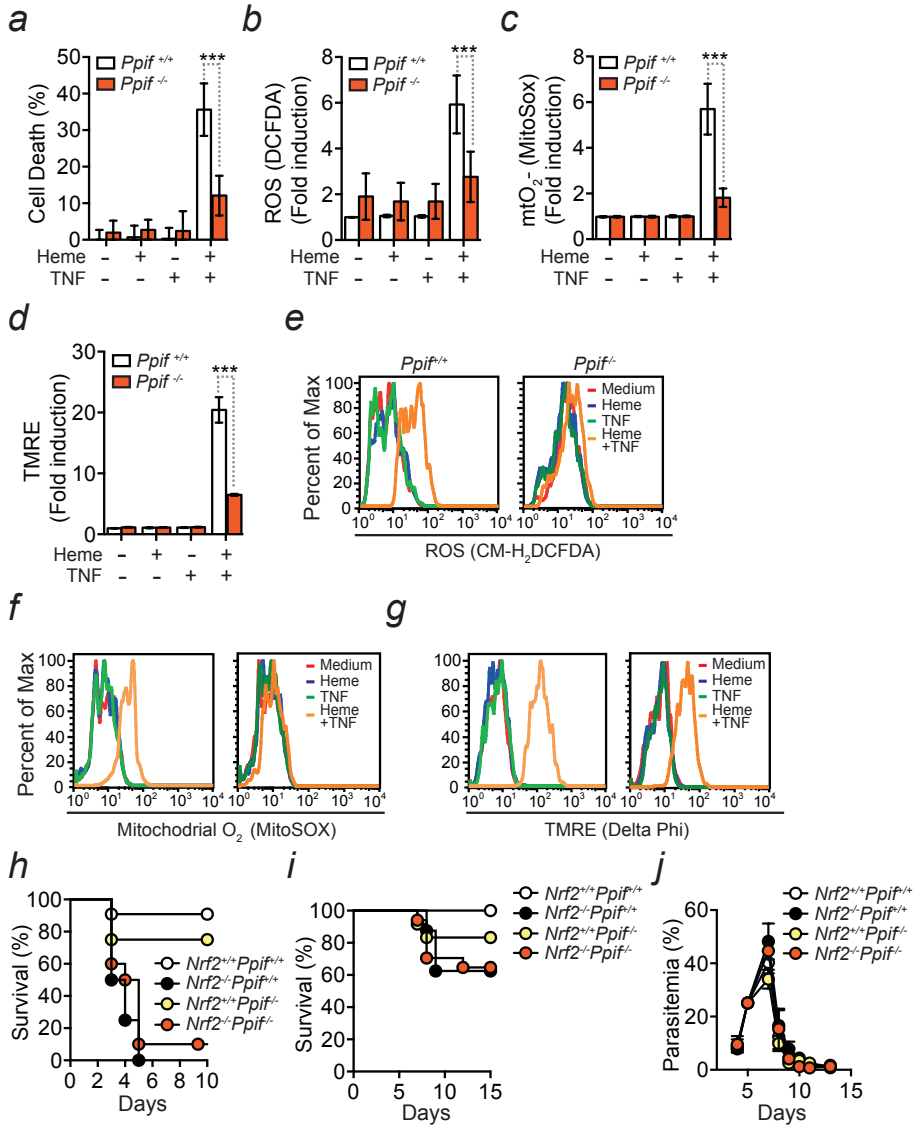

Figure 2.24. CYPD contributes to Heme and TNF-induced PCD and mitochondrial dysfunction in vitro but not in vivo.
(a) Percentage of cell death in *Nrf2*$^{+/+}$ primary mouse hepatocytes expressing or not *CypD* (*Ppif*$^{+/+}$ and *Ppif*$^{-/-}$, respectively) and treated (+) or not (-) with heme plus TNF. Data represented as mean ± STD from 5 wells

in one out of two independent experiments with the same trend. One-Way ANOVA. Relative induction of (b) intracellular ROS, (c) mitochondrial superoxide and (d) mitochondrial membrane potential in *Nrf2*$^{+/+}$ mouse hepatocytes expressing or not *CypD* (*Ppif*$^{+/+}$ and *Ppif*$^{-/-}$, respectively) and treated (+) or not (-) with heme plus TNF. Data represented as mean ± STD from a pool of two to three independent experiments with the same trend. One-Way ANOVA. Histograms corresponding to (e) intracellular ROS, (f) mitochondrial superoxide, (g) mitochondrial membrane potential detected by flow cytometry in primary mouse hepatocytes treated with heme and/or TNF represent one out of two to three independent experiments (b,c,d). (h) Relative survival of PHZ treated *Nrf2*$^{+/+}$*Ppif*$^{+/+,}$ *Nrf2*$^{-/-}$*Ppif*$^{+/+}$ *Nrf2*$^{+/+}$*Ppif*$^{+/+}$ and *Nrf2*$^{-/-}$*Ppif*$^{-/-}$ mice. Data pooled from two independent experiments (n=8-11 mice per genotype). Log-Rank Test. (i) Relative survival of *Pcc* infected *Nrf2*$^{+/+}$*Ppif*$^{+/+,}$ *Nrf2*$^{-/-}$*Ppif*$^{+/+}$ *Nrf2*$^{+/+}$*Ppif*$^{+/+}$ and *Nrf2*$^{-/-}$*Ppif*$^{-/-}$ mice. Data pooled from two independent experiments (n=7-9 mice per genotype). Log-Rank Test. (j) Percentage of infected RBC in the same mice as (i). Data represented as mean ± STD. *p< 0.05, **p< 0.01, ***p<0.001.

We hypothesized that, if *Nrf2*$^{-/-}$*Ripk3*$^{-/-}$ and *Nrf2*$^{-/-}$*Ppif*$^{-/-}$ succumb to *Pcc* similarly to the *Nrf2*$^{-/-}$ mice and if the tissue damage is contributing significantly to lethality after *Pcc* infection, than the extent of tissue damage should be comparable between these genotypes. In fact, deletion of *Ppif* or *Ripk3* alleles in an *Nrf2*$^{-/-}$ background had no impact in rescuing mice from undergoing severe liver necrosis, as assessed in *Nrf2*$^{-/-}$*Ripk3*$^{+/+}$*Ppif*$^{+/+}$ *vs. Nrf2*$^{-/-}$*Ripk3*$^{-/-}$ *Ppif*$^{+/+}$ *vs. Nrf2*$^{-/-}$*Ripk3*$^{+/+}$*Ppif*$^{-/-}$ mice (*Figure 2.25*). These results show that there are two signal transduction pathways driving necroptosis in parallel that involve RIPK3 and CYPD *in vivo* and that NRF2 confers tissue damage control via a mechanism that targets both these pathways.

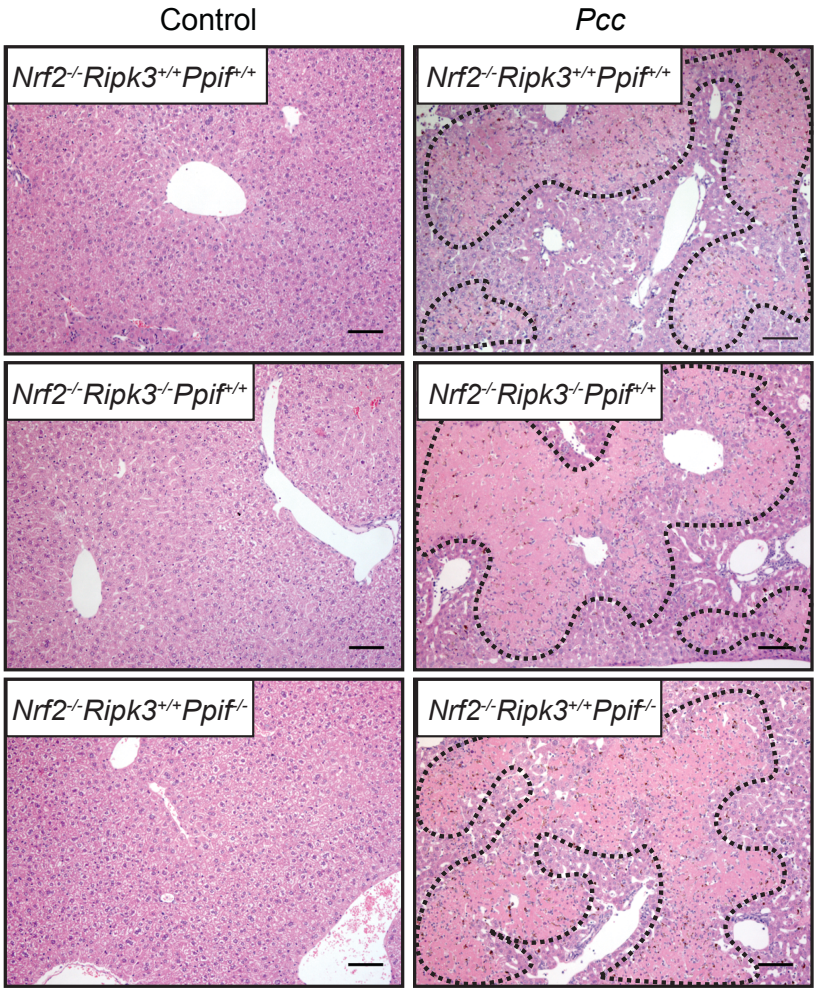

Figure 2.25. NRF2 fails to revert RIPK3 or CYPD-mediated tissue damage in vivo after malaria infection.
(a) H&E staining of liver sections from naïve mice (Control) and *Pcc* infected *Nrf2*$^{-/-}$ mice expressing *Ripk3* or *CypD* (*Ripk3*$^{+/+}$; *Ppif*$^{+/+}$) or not (*Ripk3*$^{-/-}$; *Ppif*$^{-/-}$). Images are representative of one experiment, n=4 mice per group. Black dotted lines indicate areas of hepatocyte necrosis. Scale bar = 100μm.

Combined deletion of *Ppif* and *Ripk3* alleles (*Figure 2.26a*) had no additional impact, as compared deletion of *Ripk3* alone (*Figure 2.21a*), in rescuing *Nrf2*$^{-/-}$ mice from sterile hemolysis, as assessed in *Nrf2*$^{-/-}$*Ripk3*$^{-/-}$*Ppif*$^{-/-}$ *vs.* *Nrf2*$^{+/+}$*Ripk3*$^{-/-}$*Ppif*$^{-/-}$ mice. In contrast,

combined deletion of *Ppif* and *Ripk3* alleles rescued *Nrf2*$^{-/-}$ mice from *Plasmodium* infection (*Figure 2.26b*) without interfering with pathogen load (*Figure 2.26c*), as assessed in *Nrf2*$^{-/-}$*Ripk3*$^{-/-}$*Ppif*$^{-/-}$ *vs.* *Nrf2*$^{-/-}$*Ripk3*$^{+/+}$*Ppif*$^{+/+}$ mice. Of note, combined deletion of the *Ripk3* and *Ppif* alleles had no apparent impact on the outcome of *Plasmodium* infection in *Nrf2*$^{+/+}$ mice, as assessed in *Nrf2*$^{+/+}$*Ripk3*$^{-/-}$ *Ppif*$^{-/-}$ *vs.* *Nrf2*$^{+/+}$*Ripk3*$^{+/+}$*Ppif*$^{+/+}$ mice. Importantly, combined deletion of *Ppif* and *Ripk3* alleles prevented the necrotic outcome of hepatocytes *in vivo* after malaria infection (*Figure 2.26d*).

.

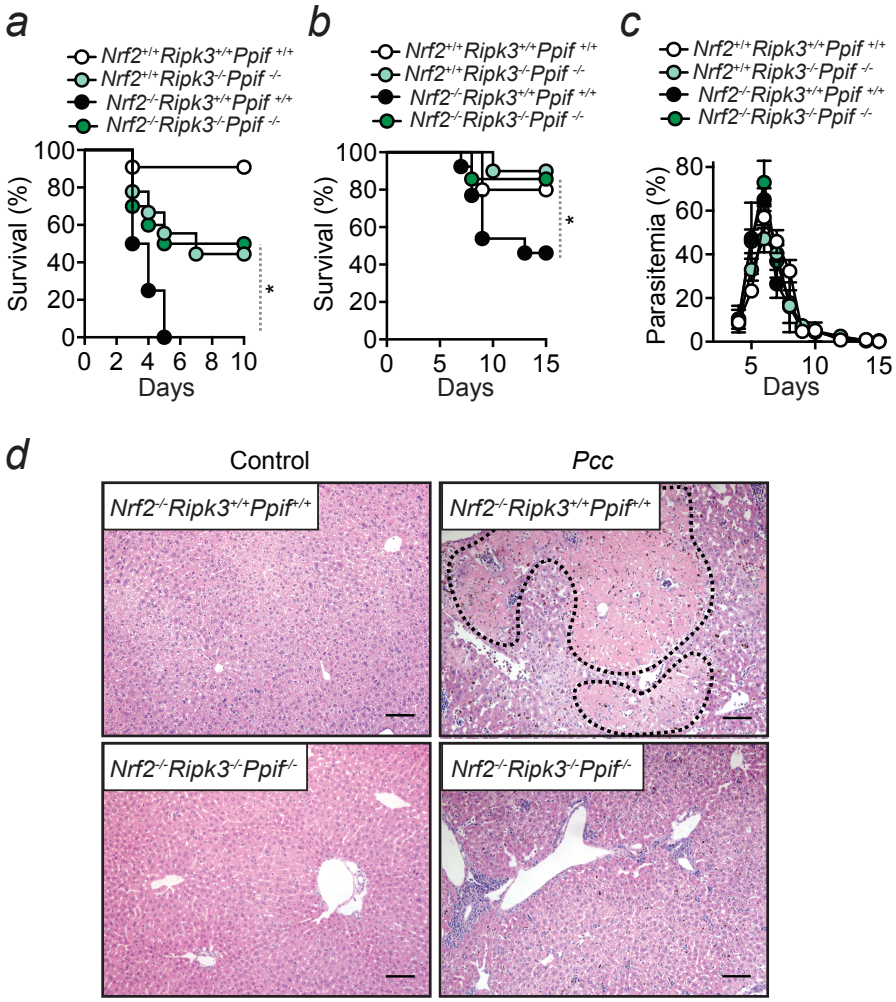

Figure 2.26. NRF2 protects against RIPK3 and CYPD-induced lethality and tissue damage in vivo after malaria infection.
(a) Relative survival of *Nrf2*$^{+/+}$*Ripk3*$^{+/+}$*Ppif*$^{+/+}$, *Nrf2*$^{+/+}$*Ripk3*$^{-/-}$*Ppif*$^{-/-}$, *Nrf2*$^{-/-}$ *Ripk3*$^{+/+}$*Ppif*$^{+/+}$ *and Nrf2*$^{-/-}$ *Ripk3*$^{-/-}$*Ppif*$^{-/-}$ mice treated with PHZ. Data pooled from two independent experiments (n=8-11 mice per genotype). Log-Rank Test. (b) Relative survival of *Pcc* infected *Nrf2*$^{-/-}$ mice expressing or not *Ripk3* and *CypD* (*Ripk3*$^{+/+}$*Ppif*$^{+/+}$ and *Ripk3/*$^{-/-}$*Ppif*$^{+/-}$, respectively). Data pooled from three independent experiments (n=10-14 mice per genotype). Log-Rank Test. (c) Percentage of infected RBC in the same mice as (b). Data represented as mean ± STD. (d) H&E staining liver sections from naïve mice (Control) and *Pcc* infected *Nrf2*$^{-/-}$ mice expressing *Ripk3* and *CypD* (*Ripk3*$^{+/+}$*Ppif*$^{+/+}$) or not (*Ripk3/*$^{-/-}$ *Ppif*$^{-/-}$). Images are representative of three experiments, n=12-14 mice per group. Black dotted lines indicate areas of hepatocyte necrosis Scale bar = 100μm. *p< 0.05, **p< 0.01, ***p<0.001.

Overall, these observations reveal that NRF2 confers tissue damage control and establishes disease tolerance to malaria via a mechanism that targets two signal transduction pathways driving necroptosis involving RIPK3 and CYPD.

2.7. References

1. Seixas, E. et al. Heme oxygenase-1 affords protection against noncerebral forms of severe malaria. Proc. Natl. Acad. Sci. U. S. A. 106, 15837–42 (2009).
2. Gozzelino, R. et al. Metabolic Adaptation to Tissue Iron Overload Confers Tolerance to Malaria. Cell Host Microbe 693–704 (2012).
3. Duprez, L. et al. RIP Kinase-Dependent Necrosis Drives Lethal Systemic Inflammatory Response Syndrome. Immunity 35, 908–918 (2011).
4. Zhang, Q. et al. Circulating mitochondrial DAMPs cause inflammatory responses to injury. Nature 464, 104–7 (2010).
5. Marques, P. E. et al. Hepatic DNA deposition drives drug-induced liver injury and inflammation in mice. Hepatology 348–360 (2014). doi:10.1002/hep.27216
6. Brigelius-Flohé, R. Tissue-specific functions of individual glutathione peroxidases. Free Radic. Biol. Med. 27, 951–965 (1999).
7. Larsen, R. et al. A central role for free heme in the pathogenesis of severe sepsis. Sci. Transl. Med. 2, 51ra71 (2010).
8. Martins, R. et al. Heme drives hemolysis-induced susceptibility to infection via disruption of phagocyte functions. (2016). doi:10.1038/ni.3590
9. Thimmulappa, R. K. et al. Nrf2 is a critical regulator of the innate immune response and survival during experimental sepsis. 116, (2006).
10. Kong, X. et al. Enhancing Nrf2 pathway by disruption of Keap1 in myeloid

leukocytes protects against sepsis. Am. J. Respir. Crit. Care Med. 184, 928–38 (2011).
11. Wichterman, K. a, Baue, a E. & Chaudry, I. H. Sepsis and septic shock--a review of laboratory models and a proposal. J. Surg. Res. 29, 189–201 (1980).
12. Oikawa, D., Akai, R., Tokuda, M. & Iwawaki, T. A transgenic mouse model for monitoring oxidative stress. Sci. Rep. 2, 229 (2012).
13. Gozzelino, R., Jeney, V. & Soares, M. P. Mechanisms of cell protection by heme oxygenase-1. Annu. Rev. Pharmacol. Toxicol. 50, 323–54 (2010).
14. Larsen, R. et al. A Central Role for Free Heme in the Pathogenesis of Severe Sepsis. 71, (2010).
15. Athale, J. et al. Nrf2 promotes alveolar mitochondrial biogenesis and resolution of lung injury in Staphylococcus aureus pneumonia in mice. Free Radic. Biol. Med. 53, 1584–94 (2012).
16. Dinkova-Kostova, A. T. & Abramov, A. Y. The emerging role of Nrf2 in mitochondrial function. Free Radic. Biol. Med. 1–10 (2015). doi:10.1016/j.freeradbiomed.2015.04.036
17. Zhang, D.-W. et al. RIP3, an energy metabolism regulator that switches TNF-induced cell death from apoptosis to necrosis. Science 325, 332–6 (2009).
18. Lo, S.-C. & Hannink, M. PGAM5 tethers a ternary complex containing Keap1 and Nrf2 to mitochondria. Exp. Cell Res. 314, 1789–803 (2008).
19. Wang, Z., Jiang, H., Chen, S., Du, F. & Wang, X. The mitochondrial phosphatase PGAM5 functions at the convergence point of multiple necrotic death pathways. Cell 148, 228–43 (2012).
20. Cho, Y. S. et al. Phosphorylation-driven assembly of the RIP1-RIP3 complex regulates programmed necrosis and virus-induced inflammation. Cell 137, 1112–23 (2009).
21. Javadov, S. & Kuznetsov, A. Mitochondrial permeability transition and cell death: The role of cyclophilin D. Front. Physiol. 4 APR, 1–5 (2013).
22. Nakagawa, T., Shimizu, S. & Watanabe, T. Cyclophilin D-dependent mitochondrial permeability transition regulates some necrotic but not apoptotic cell death. Nature 434, 652–658 (2005).

Chapter 3:

Discussion

"Anything you build on a large scale
or with intense passion invites chaos."
(Francis Ford Coppola)

Labile heme plays a central role in the pathogenesis of severe forms of disease associated with bloodstream infections, as demonstrated for murine experimental models of malaria[1,2,3] and sepsis[4]. Detection of both extracellular hemoglobin[5,6,7] and heme[8,9] is associated with the pathophysiology of both diseases, in both experimental models as well as in human patients[5,6,7,8,9]. However, although the pro-oxidant nature of heme is consistently deleterious[10], several factors like the chronicity and extent of hemolysis might determine the outcomes of the disease in terms of tissue damage and lethality. For example, increased plasma concentrations of labile heme and haptoglobin, the cell-free hemoglobin scavenger, are associated with susceptibility to malaria in human patients[9], whereas in sepsis patients elevated plasma levels of haptoglobin correlate with a lower risk of mortality[7]. As such, the nature of the insult triggering hemolysis, the kinetics of hemoglobin release and oxidation, as well as the inflammatory milieu that accompanies this process is essential for a better understanding of the pathophyological consequences of hemolytic diseases.

Upon hemolysis, circulating cell-free hemoglobin and labile heme are recognized by the immune system as erythroid DAMPs[11], leading to the activation of immune cells and endothelium to an inflammatory, pro-adhesive state that promotes vaso occlusion and tissue injury[12]. Moreover, intravascular hemolysis causes oxidative stress, altering redox balance and amplifying physiological processes that govern blood flow, hemostasis, inflammation, and angiogenesis[12]. In the presence of TNF or other by-products of inflammation, labile heme is highly cytotoxic to both immune[13,14] and parenchymal[15,16,17,18] cells, eventually leading to tissue damage and compromising disease tolerance to bloodstream infections[3,4]. This has been associated with a necrotic phenotype, which was shown to

be extensively linked to the additional release of DAMPs, amplifying the inflammatory response and promoting further tissue damage[19,20].

The pathophysiological consequences of labile heme trigger adaptive stress and damage responses that counter the pathogenic outcomes of hemolysis[12]. Due to the pro-oxidant nature of labile heme[12], the response orchestrated by NRF2 is essential in protecting against oxidative stress[21]. Perhaps the best demonstration that this oxidative stress response is involved in the protection against inflammatory hemolytic diseases is that sickle hemoglobin establishes disease tolerance to malaria via an NRF2-dependent mechanism[22]. The activation of this stress response was shown to counter the pathogenic effects of labile heme in mice[2] and it is most likely to be the case in humans[22].

The work developed in the context of this thesis demonstrates that NRF2 is a critical cytoprotective molecule that counters the deleterious effects of labile heme and establishes disease tolerance to bloodstream infections (Figure 2.1e-h, Figure 2.6a,b). Additionally, our data shows that NRF2 protects against sterile hemolysis (Figure 2.10a-d) and labile heme *per se* (Figure 2.12c-e) suggesting that, in the context of hemolytic infections, this transcription factor provides tissue damage control by specifically countering the cytotoxic effects of labile heme.

Mechanistically, we were able to demonstrate that labile heme sensitizes hepatocytes to accumulate high levels of ROS in response to TNF[4,23,24,10]. This pro-oxidant effect is associated with robust Nrf2 activation, acting as a negative feedback loop, blocking TNF-induced necroptosis (Figure 2.15a) via the inhibition of mitochondrial O_2^- (Figure 2.15c,f) and preserving mitochondrial function (Figure 2.15d,g). This is consistent with the notion that NRF2 regulates an adaptive response to oxidative stress sustaining mitochondrial function[25,26], which we now demonstrate to be critical

in the establishment of disease tolerance to bloodstream infections, as illustrated for malaria (Figure 2.16f,g) as well as to confer protection against sterile hemolysis (Figure 2.16h). In agreement with these findings, we have shown that Nrf2 deficient mice undergo hepatic necrosis upon malaria, accumulate higher levels of DAMPs in circulation in the different models of hemolysis and display increased levels of inflammatory mediators. Together, these data suggests that Nrf2 protects against heme-driven necrosis *in vivo*, blocking the release of DAMPs and ameliorating inflammation.

Unfettered accumulation of mitochondrial O_2^- and the ensuing development of mitochondrial dysfunction in response to heme and TNF are strictly dependent on a signal transduction pathway involving RIPK1, RIPK3, MLKL and PGAM5, as demonstrated by genetic loss of function approach targeting these alleles (Figure 2.18 and Figure 2.19). Signaling via the TNF receptor 1 (TNFR1) emerges from a multimeric complex comprising, among other components, RIPK1 and the heme-oxidized iron regulated protein 2 (IRP2) ubiquitin ligase-1 (HOIL-1L), one of the components of the linear ubiquitin chain assembly complex (LUBAC)[27]. It is possible, therefore, that once transported into the cytosol via specific transporters such as the heme responsive gene 1 (HRG1)[28], heme might interact with HOIL-1L to regulate TNFR1 signaling. This might induce signaling via the RIPK1/3 complex and/or inhibit Caspase-8 activation, favoring the induction of necroptosis. Another possibility is for intracellular heme to be transported into the mitochondria, via specific mitochondrial transporters such as ABCB6[29], promoting lipid peroxidation, ROS accumulation, mitochondrial dysfunction and necrosis. Additionally, because it was shown that heme signals through TLR4 to induce autocrine TNF production in macrophages culminating in necroptosis[30] and that both TNFR1 and TLR4 have been linked to necroptosis[31], it is possible that TNF and heme

synergize in parenchyma cells by signaling to TNFR1 and TLR4 respectively, leading to this explosive type of PCD. The last hypothesis for the mechanism of heme cytotoxicity is that heme-iron might signal through TLR2, a receptor involved in regulating iron deposition in tissues[32] that have been recently shown to sensitize to TNFR1-dependent necroptosis[33]. Of note, HO-1 was shown to be protective to TNF-dependent PCD in primary hepatocytes[34], suggesting that heme catabolism reverts the engagement of the TNF-dependent PCD pathway. Irrespectively of its molecular mechanism of action, labile heme appears to act as a potent pathophysiologic agonist of TNF-induced necroptosis, which is consistent with the observation that Nec1 protects macrophages from heme and TNF-induced PCD[13].

The mechanism via which NRF2 blocks TNF-induced necroptosis relies on the expression of several effector genes, which inhibits the RIPK1, RIPK3, MLKL and PGAM5 signal transduction pathway leading to the accumulation of mitochondrial O_2^- and ultimately to mitochondrial dysfunction (Figure 2.20). Whether these NRF2-regulated effector genes modulate the RIPK1-RIPK3-MLKL-PGAM5 signal transduction pathway or act directly to protect the mitochondria, remains to be established. Perhaps the best link between NRF2 and the pathway to necroptosis is the observation that PGAM5 forms a ternary complex with Keap-1 and NRF2 in the outer mitochondrial membrane, repressing NRF2 activation[35]. The presence of distinct pools of Keap-1 at multiple subcellular locations enables activation of NRF2 in response to specific insults[35]. In this particular context, placing Keap-1 and NRF2 in the mitochondria downstream of the engagement of the necroptosis pathway would justify the protective role of this cytoprotective molecule after heme and TNF at the level of mitochondrial ROS production/accumulation and loss of mitochondrial potential. It is possible, therefore, that the

PGAM5L/Keap-1 complex is targeted by mitochondrial ROS, downstream of RIPK1, RIPK3 and MLKL, to trigger NRF2 activation, leading to the expression of cytoprotective genes and countering necroptosis. An alternative hypothesis would be that the NRF2-Keap1 complex is formed and retained in the cytoplasm through interactions with the cytoskeletal network[36]. Upon heme and TNF-induced mitochondrial ROS production, Keap-1 would sense this cellular redox unbalance, leading to NRF2 nuclear translocation and downstream antioxidant gene expression. In keeping with the notion that heme and TNF induces mitochondrial ROS production countered by NRF2, it was shown in the context of acute bacterial infection that TNF production in leukocytes leads to mitochondrial ROS generation and kidney cell death[37]. Moreover, mitochondrial ROS inhibits GSK3b, a repressor of NRF2 activation[38], presumably allowing the antioxidant pathway to confer tissue damage control to kidney cells[37]. Furthermore, inhibition of GSK-3β blocks the permeability transition pore formation, preventing necrosis[39]. Whether NRF2 provides tissue damage control by blocking mitochondrial ROS and necroptosis via GSK-3β inhibition in the context of hemolytic infections still remains to be established.

In strong support of the notion that the inhibition of heme-driven necroptosis underlies the protective effect of NRF2 *in vivo* is the observation that deletion of the *Ripk3* allele bypasses the requirement for NRF2-driven protection against sterile hemolysis (Figure 2.21a) or the establishment of disease tolerance to sepsis (Figure 2.21b,c). While pharmacologic inhibition of RIPK1 by Nec-1 also bypasses the requirement of NRF2 for establishment of disease tolerance to *Plasmodium* infection (Figure 2.22a,b), this is not the case for deletion of the *Ripk3* allele (Figure 2.22c,d) or even for combined deletion of the *Ripk3* and caspase-8 alleles (Figure 2.23a,b). This suggests that, in the case *Plasmodium* infection, Nrf2

might target an additional component of the regulated necrosis pathway downstream of RIPK1 but not RIPK3, presumably in the mitochondria. Alternatively, inhibition of RIPK1 kinase activity by Nec-1 might be switching its function from mediator of cell death towards a scaffolding function, promoting survival and suppressing inflammation by inhibiting FADD–caspase-8 and RIPK3-MLKL activation[40]. If this proves to be the case, this protective effect of Nec-1 might bypass the absence of Nrf2 by preventing both cell death and inflammation as a consequence of *Plasmodium* infection.

The observation that induction of necroptosis in response to heme and TNF relies on the expression of mitochondrial CypD (Figure 2.24a-g) lead to the hypothesis that CypD may be part of this additional component of the regulated necrosis pathway targeted by Nrf2. Combined deletion of the *Ripk3* and *Ppif* alleles bypasses the requirement of Nrf2 for the establishment of disease tolerance to *Plasmodium* infection (Figure 2.26b,c) suggesting that, in contrast to sterile hemolysis or sepsis which depend solely on RIPK3, the blood stage of *Plasmodium* is associated with the induction of regulated necrosis via a CypD-dependent mechanism, similar to the one eliciting tissue damage associated with ischemia reperfusion injury[41].

Of note, activation of NRF2 in response to viral infections can compromise resistance to infection, therefore acting in a pathogenic manner[42]. This is illustrated for example for the Marburg virus infection, where viral encoded VP24 protein promotes viral replication via a mechanism that targets the ubiquitin ligase activity of the Keap1-associated Cul3–Rbx1 complex and induces NRF2 activation[43,44]. This antagonistic effect of NRF2 is in keeping with the notion that tissue damage control mechanisms establishing disease tolerance to infection are tailor-made for different classes of pathogens[45,46]. This can be particularly relevant to understand the pathologic outcome of co-infections, such viral and bacterial co-

infections[47] where the virus can compromise resistance[48] or disease tolerance[49] to bacteria[48,49]. While the mechanisms via which this occurs are most probably multifactorial, it is tempting to speculate that this could involve viral inhibition of NRF2, which should impair disease tolerance to bacterial infections. This remains however to be established experimentally.

Of note, while a protective effect of NRF2 against bloodstream infections was previously reported, this was attributed to a putative immunoregulatory effect[25,50] exerted, most likely, in macrophages[51,52]. Our data suggests that such immunoregulatory effect may operate indirectly through the cytoprotective effect exerted by NRF2 limiting the release of pro-inflammatory DAMPs, e.g. mitochondrial DNA[53,54,19], HMGB1[55] or labile heme[12]. This does not exclude, however, NRF2 from exerting additional immunoregulatory effects in innate immune cells: either by lowering the levels of secreted pro-inflammatory cytokines[51] synergizing with heme and/or by regulating the sensitivity of death receptor signals[56], NRF2 can contribute to the establishment of disease tolerance to hemolytic bloodstream infections.

In conclusion, we propose that NRF2 acts as a transcriptional repressor of TNF-induced necroptosis and that this cytoprotective effect is critical to confer tissue damage control and establish disease tolerance to bloodstream infections.

References

1. Ferreira, A., Balla, J., Jeney, V., Balla, G. & Soares, M. P. A central role for free heme in the pathogenesis of severe malaria: the missing link? J. Mol. Med. (Berl). 86, 1097–111 (2008).
2. Ferreira, A. et al. Sickle hemoglobin confers tolerance to Plasmodium infection. Cell 145, 398–409 (2011).
3. Pamplona, A. et al. Heme oxygenase-1 and carbon monoxide suppress the pathogenesis of experimental cerebral malaria. Nat. Med. 13, 703–10 (2007).

4. Larsen, R. et al. A Central Role for Free Heme in the Pathogenesis of Severe Sepsis. (2010).
5. Adamzik, M. et al. Free hemoglobin concentration in severe sepsis: methods of measurement and prediction of outcome. Crit. Care 16, R125 (2012).
6. Janz, D. R. et al. Mortality in Patients with Sepsis : an Observational Study. Crit. Care Med. 41, 784–790 (2014).
7. Janz, D. R. et al. Association between haptoglobin, hemopexin and mortality in adults with sepsis. Crit. Care 17, R272 (2013).
8. Gozzelino, R. et al. Metabolic Adaptation to Tissue Iron Overload Confers Tolerance to Malaria. Cell Host Microbe 693–704 (2012).
9. VRR, M. et al. Association between the haptoglobin and heme oxygenase 1 genetic profiles and soluble CD163 in susceptibility to and severity of human malaria. Infect. Immun. 80, 1445–1454 (2012).
10. Larsen, R., Gouveia, Z., Soares, M. P. & Gozzelino, R. Heme cytotoxicity and the pathogenesis of immune-mediated inflammatory diseases. Front. Pharmacol. 3, 77 (2012).
11. Gladwin, M. T. & Ofori-Acquah, S. F. Erythroid DAMPs drive inflammation in SCD. Blood 123, 3689–3690 (2014).
12. Soares, M. P. & Bozza, M. T. Red alert: Labile heme is an alarmin. Curr. Opin. Immunol. 38, 94–100 (2016).
13. Fortes, G. B. et al. Heme induces programmed necrosis on macrophages through autocrine TNF and ROS production. Blood 119, 2368–2375 (2012).
14. Vasconcellos, L. R. C. et al. Protein aggregation as a cellular response to oxidative stress induced by heme and iron. (2016). doi:10.1073/pnas.1608928113
15. Higdon, A. N. et al. Hemin causes mitochondrial dysfunction in endothelial cells through promoting lipid peroxidation: the protective role of autophagy. Am. J. Physiol. Hear. Circ. Physiol. 302, H1394--409 (2012).
16. Balla, J. et al. Endothelial-cell heme uptake from heme proteins: induction of sensitization and desensitization to oxidant damage. Proc. Natl. Acad. Sci. U. S. A. 90, 9285–9 (1993).
17. Larsen, R., Balla, J., Soares, M. P., Silva, G. & Jeney, V. Oxidized Hemoglobin Is an Endogenous Proinflammatory Agonist That Targets Vascular Endothelial Cells * □. 29582–29595 (2009). doi:10.1074/jbc.M109.045344
18. Goldstein, L., Teng, Z. P., Zeserson, E., Patel, M. & Regan, R. F. Hemin induces an iron-dependent, oxidative injury to human neuron-like cells. J. Neurosci. Res. 73, 113–121 (2003).
19. Duprez, L. et al. RIP Kinase-Dependent Necrosis Drives Lethal Systemic Inflammatory Response Syndrome. Immunity 35, 908–918 (2011).
20. Pasparakis, M. & Vandenabeele, P. Necroptosis and its role in inflammation. Nature 517, 311–320 (2015).
21. Keleku-lukwete, N. et al. Amelioration of inflammation and tissue damage in sickle cell model mice by Nrf2 activation. doi:10.1073/pnas.1509158112
22. Ademolue, T. W., Amodu, O. K. & Awandare, G. A. Sickle cell trait is associated with controlled levels of heme and mild pro-inflammatory response during acute malaria infection. Clin. Exp. Immunol. (2017). doi:10.1111/cei.12936
23. Gozzelino, R., Jeney, V. & Soares, M. P. Mechanisms of cell protection by heme oxygenase-1. Annu. Rev. Pharmacol. Toxicol. 50, 323–54 (2010).

24. Gozzelino, R. & Soares, M. P. Coupling Heme and Iron Metabolism via Ferritin H Chain. Antioxid Redox Signal 1754–1769 (2014). doi:10.1089/ars.2013.5666

25. Athale, J. et al. Nrf2 promotes alveolar mitochondrial biogenesis and resolution of lung injury in Staphylococcus aureus pneumonia in mice. Free Radic. Biol. Med. 53, 1584–94 (2012).

26. Dinkova-Kostova, A. T. & Abramov, A. Y. The emerging role of Nrf2 in mitochondrial function. Free Radic. Biol. Med. 1–10 (2015). doi:10.1016/j.freeradbiomed.2015.04.036

27. Elton, L. et al. MALT1 cleaves the E3 ubiquitin ligase HOIL-1 in activated T cells, generating a dominant negative inhibitor of LUBAC-induced NF-κB signaling. FEBS J. 283, 403–412 (2016).

28. Rajagopal, A. et al. Haem homeostasis is regulated by the conserved and concerted functions of HRG-1 proteins. Nature 453, 1127–31 (2008).

29. Krishnamurthy, P. C. et al. Identification of a mammalian mitochondrial porphyrin transporter. Nature 443, 586–589 (2006).

30. Fortes, G. B. et al. Heme induces programmed necrosis on macrophages through autocrine TNF and ROS production. Blood 119, 2368–75 (2012).

31. Petrie, E. J., Hildebrand, J. M. & Murphy, J. M. Insane in the membrane: a structural perspective of MLKL function in necroptosis. Immunol Cell Biol 95, (2016).

32. Meyer, P. N. et al. Hemochromatosis protein (HFE) and tumor necrosis factor receptor 2 (TNFR2) influence tissue iron levels: elements of a common gut pathway? Blood Cells. Mol. Dis. 29, 274–285 (2002).

33. Siegmund, D., Kums, J., Ehrenschwender, M. & Wajant, H. Activation of TNFR2 sensitizes macrophages for TNFR1-mediated necroptosis. Cell Death Dis. 1–10 (2016). doi:10.1038/cddis.2016.285

34. Sass, G., Shembade, N. D. & Tiegs, G. Tumour necrosis factor alpha (TNF)-TNF receptor 1-inducible cytoprotective proteins in the mouse liver: relevance of suppressors of cytokine signalling. Biochem J 385, 537–544 (2005).

35. Lo, S.-C. & Hannink, M. PGAM5 tethers a ternary complex containing Keap1 and Nrf2 to mitochondria. Exp. Cell Res. 314, 1789–803 (2008).

36. Kensler, T. W., Wakabayashi, N. & Biswal, S. Cell survival responses to environmental stresses via the Keap1-Nrf2-ARE pathway. Annu. Rev. Pharmacol. Toxicol. 47, 89–116 (2007).

37. Kalayarasan, S. et al. Protective effect of mitochondria-targeted antioxidants in an acute bacterial infection. J. Biol. Chem. 13, 401–426 (2013).

38. Rada, P. et al. SCF/{beta}-TrCP promotes glycogen synthase kinase 3-dependent degradation of the Nrf2 transcription factor in a Keap1-independent manner. Mol. Cell. Biol. 31, 1121–33 (2011).

39. Juhaszova, M. et al. Glycogen synthase kinase-3beta mediates convergence of protection signaling to inhibit the mitochondrial permeability transition pore. J. Clin. Invest. 113, 1535–1549 (2004).

40. Chan, F. K.-M., Luz, N. F. & Moriwaki, K. Programmed Necrosis in the Cross Talk of Cell Death and Inflammation. Annu. Rev. Immunol. 1–28 (2014). doi:10.1146/annurev-immunol-032414-112248

41. Linkermann, A. et al. Two independent pathways of regulated necrosis mediate ischemia-reperfusion injury. Proc. Natl. Acad. Sci. U. S. A. 110, 12024–9 (2013).

42. Soares, M. P. & Ribeiro, A. M. Nrf2 as a master regulator of tissue damage

control and disease tolerance to infection. Biochem. Soc. Trans. 43, 663–8 (2015).

43. Edwards, M. R. et al. The Marburg Virus VP24 Protein Interacts with Keap1 to Activate the Cytoprotective Antioxidant Response Pathway. CellReports 6, 1017–1025 (2014).

44. Page, A. et al. Marburgvirus Hijacks Nrf2-Dependent Pathway by Targeting Nrf2-Negative Regulator Keap1. CellReports 6, 1026–1036 (2006).

45. Medzhitov, R., Schneider, D. S. & Soares, M. P. Disease Tolerance as a Defense Strategy. Science (80-.). 335, 936–941 (2012).

46. Soares, M. P., Teixeira, L. & Moita, L. F. Disease tolerance and immunity in host protection against infection. Nat. Publ. Gr. 17, 83–96 (2017).

47. Robinson, K. M. et al. The role of IL-27 in susceptibility to post-influenza Staphylococcus aureus pneumonia. Respir. Res. 16, 10 (2015).

48. Jamieson, A. M., Yu, S., Annicelli, C. H. & Medzhitov, R. Influenza Virus-Induced Glucocorticoids Compromise Innate Host Defense against a Secondary Bacterial Infection. Cell Host Microbe 7, 103–114 (2010).

49. amieson AM, Pasman L, Yu S, Gamradt P, Homer RJ, Decker T, M. R. Role of tissue protection in lethal respiratory viral-bacterial coinfection. Science (80-.). 340, 1230–1234 (2013).

50. Thimmulappa, R. K. et al. Nrf2-dependent protection from LPS induced inflammatory response and mortality by CDDO-Imidazolide. Biochem. Biophys. Res. Commun. 351, 883–889 (2006).

51. Kobayashi, E. H. et al. Nrf2 suppresses macrophage inflammatory response by blocking proinflammatory cytokine transcription. Nat. Commun. 7, 11624 (2016).

52. Harvey, C. J. et al. Targeting Nrf2 Signaling Improves Bacterial Clearance by Alveolar Macrophages in Patients with COPD and in a Mouse Model. (2011).

53. Krysko, D. V et al. Emerging role of damage-associated molecular patterns derived from mitochondria in inflammation. Trends Immunol. 32, 157–64 (2011).

54. Zhang, Q. et al. Circulating mitochondrial DAMPs cause inflammatory responses to injury. Nature 464, 104–7 (2010).

55. Wang, H. et al. HMG-1 as a late mediator of endotoxin lethality in mice. Science (80-.). 285, 248–252 (1999).

56. Morito, N. et al. Nrf2 regulates the sensitivity of death receptor signals by affecting intracellular glutathione levels. Oncogene 22, 9275–81 (2003).

Experimental Procedures

“If you're not failing every now and again, it's a sign you're not doing anything very innovative.”
(Woody Allen)

Mice

Experimental procedures involving mice were approved by the Ethics Committee of the Instituto Gulbenkian de Ciência (license: A009/2011) and the "Direção Geral de Alimentação e Veterinária" (license: 0420/000/000/2012) *as per* Portuguese (Decreto-Lei nº 113/2013) and European (Directive 2010/63/EU) legislations. Mice were bred and maintained under specific pathogen free (SPF) conditions at the Instituto Gulbenkian de Ciência (12h day/night; fed *ad libidum*). C57BL/6 *Nrf2*$^{-/-}$ mice (Itoh et al., 1997) were obtained originally from the RIKEN BioResource Center (RBRC01390; Koyadai, Tsukuba, Ibaraki, Japan). C57BL/6 *Ripk3*$^{-/-}$ mice (Newton et al., 2004) were obtained from Vishva Dixit (Genentech, USA). C57BL/6 *Ripk3*$^{-/-}$*Caspase8*$^{-/-}$ mice (Oberst et al., 2011) were obtained from Igor Brodsky (University of Pennsylvania, Philadelphia, USA) with permission from Douglas Green (St. Jude Children's Research Hospital, Memphis, USA). C57BL/6 *Ppif*$^{-/-}$ mice (Basso et al., 2005) were obtained from Jackson Laboratories (022308). C57BL/6 *OKD48* reporter mice (Oikawa et al., 2012) were obtained from RIKEN BioResource Center (RBRC05704). *Nrf2*$^{+/+}$ and *Nrf2*$^{-/-}$ mice were breed in homozygosity and offspring was co-housed immediately from weaning. *Rip3k*$^{-/-}$ and *Ppif*$^{-/-}$ mice were intercrossed with *Nrf2*$^{-/-}$ mice to obtain *Nrf2*$^{-/-}$*Rip3k*$^{-/-}$, *Rip3k*$^{-/-}$*Ppif*$^{-/-}$, *Nrf2*$^{-/-}$*Ppif*$^{-/-}$ and *Nrf2*$^{-/-}$*Rip3k*$^{-/-}$*Ppif*$^{-/-}$ mice. *Rip3k*$^{-/-}$*Caspase8*$^{+/-}$ mice were intercrossed with *Nrf2*$^{-/-}$*Rip3k*$^{-/-}$ mice to generate *Nrf2*$^{-/-}$*Rip3k*$^{-/-}$*Caspase8*$^{+/-}$ mice, subsequently intercrossed to generate *Nrf2*$^{-/-}$*Rip3k*$^{-/-}$*Caspase8*$^{+/+}$ and *Nrf2*$^{-/-}$*Rip3k*$^{-/-}$*Caspase8*$^{-/-}$ mice. Mice were genotyped by PCR using the following primers: *Nrf2:* 5'-TGGACGGGACTATTGAAGGCTG-3', 5'-GCGGATTGACCGTAATGGGATAGG-3', 5'-GCCGCCTTTTCAGTAGATGGAGG-3'; *Ripk3*: 5'-CGCTTTAGAAGCCTTCAGGTTGAC-3', 5'-

GCCTGCCCATCAGCAACTC-3', 5'-CCAGAGGCCACTTGTGTAGCG-3'; *Caspase 8*: 5'-CCAGGAAAAGATTTGTGTCTA-3', 5'-GGCCTTCCTGAGTACTGTCACCTGT-3'; *Ppif*: 5'-ATTTGTCACGTCCTGCACGA CG-3', 5'-AGCCAGCCGACCAATAAAG-3', 5'-AGCCAGCCGACCAATAAAG-3', 5'-GTTCCCGGAGGAAGAGTTC-3'; *OKD48*: 5'-ATCACCAGAACACTCAGTGG-3', 5'-TAG CGCTTCATAGCTTCTGC-3', 5'-CTAGGCCACAGAATTGAAAGATCT-3', 5'-GTAG GTGGAAATTCTAGCATCATCC-3'.

Reagents

CM-H2DCFDA (Molecular Probes, C6827), MitoSox (Molecular Probes, M36008), Tetramethylrhodamine, Methyl Ester, Perchlorate (TMRM, Molecular Probes T668), Tetramethylrhodamine Ethyl Ester (TMRE; Molecular Probes, T669), Sytox Green (ThermoFisher, S7020), Giemsa (VWR; 350864X), heme (i.e. hemin; iron protoporphyrin; Sigma, H5533; Frontier Scientific, FSIH651-9), mouse recombinant TNF (mTNF, R&D System, 410-MT-010), N-acetyl cysteine (NAC; Sigma, A9165), MitoTEMPO (Santa Cruz Biotechnologies, SC-221945), Necrostatin-1 (Nec-1, Enzo Life Sciences; BML-AP309-0020), Phenylhydrazine hydrochloride (PHZ, Aldrich, 114715), anti-mouse RBC polyclonal antiserum (Cedarlane, UK; 007CLA3840), MG132 (Calbiochem; 133407-82-6), Gelatin (G1393 Sigma) and Luciferin (Promega, PROME1605) were used as indicated in the results section.

Plasmodium infection

Mice were infected by intraperitoneal (i.p.) inoculation of $2x10^6$ *Plasmodium chabaudi chabaudi* (*Pcc*; AS strain) infected RBCs, essentially as described (Seixas et al., 2009). Host survival and parasitemia, i.e. percentage of infected RBCs detected in Giemsa stained blood smears, were monitored daily for two weeks, as described (Seixas et al., 2009).

Cecal ligation and puncture (CLP)

CLP was performed under isoflurane anesthesia (Anaesthesia AutoFlow System, EZ-AF9000, PLEXX BV), essentially as described (Larsen et al., 2010; Rittirsch et al., 2009). Briefly, the procedure consists of a 30% cecum ligation and a 23 Gauge (G) needle double puncture, with controlled feces extrusion. Mice received 0.9% saline (40 mL/kg, i.p.) immediately after the procedure and Imipenem/Cilastatin (25mg/kg i.p.), starting 2 hours after procedure and then every 12 hours for 3 days). Body weight (Compact balance CS-series T317.1, Roth) and temperature (Bioseb, France, Rodent Thermometer BIO-TK8851) were monitored daily for up to 7 days and survival up to 14 days. Pathogen load was quantified, essentially as described (Larsen et al., 2010; Rittirsch et al., 2009). Briefly, 16 hours after CLP blood was collected through heart puncture using heparinized needles, peritoneal fluid was obtained by lavage (5 mL; sterile PBS) and organs were harvested, rinsed and homogenized in sterile PBS under a dounce tissue grinder (Sigma, D8938). Serial dilutions were plated onto Trypticase™Soy Agar II supplemented with 5% Sheep Blood plates (Becton Dickinson, 254053) and incubated (24 hours at 37°C) under aerobic (Air; 5% CO_2) or

anaerobic conditions using a tight container equipped with the GasPak™ anaerobe container system (Becton Dickinson, 260678). Anaerobic conditions were confirmed using BBL™ Dry Anaerobic Indicator Strips (Becton Dickinson, 271051).

In Vivo **Treatments**

NAC was dissolved in PBS, pH was adjusted to 7.4 with 5M NaOH and administered (15 mg/kg in 200µL every 12 hour, i.p.) starting at 4 days post-*Pcc* infection until day 15 or starting 2 days prior to heme administration and during 8 days thereafter. MitoTEMPO was dissolved in PBS and administered (2.5mg/kg, 200µL every 12 hours, i.p.) as for NAC. Necrostatin-1 was dissolved in DMSO to a final concentration of 20mg/ml, diluted in sterile PBS and administered (1.25 mg/kg, 200µL every 24 hours, i.p.) starting at 4 days post-*Pcc* infection until day 15. Heme was dissolved in 0.2 M HCl, and pH was adjusted to 7.4 with sterile 0.2 M NaOH. Stock solution was diluted in sterile PBS right before administration (20mg/Kg for *Nrf2*$^{+/+}$ vs *Nrf2*$^{-/-}$ mice, or 40mg/Kg for reporter OKD48 mice, i.p.). Intravascular hemolysis was induced by freshly prepared Phenylhydrazine (PHZ) dissolved in sterile PBS (pH adjusted to 7.4 with sterile 0.2M NaOH) and administered (100mg/Kg and 50 mg/Kg 14 hours thereafter, i.p.), essentially as described (Dutra et al., 2014). Antibody-mediated hemolysis was induced by the administration of an anti-mouse RBC polyclonal antiserum (40µL per mouse, i.p) diluted in sterile PBS to a final volume of 100µL, every other day for 5 days (3x in total). Number of circulating RBC was quantified daily by flow cytometry (FACSCalibur Analyzer, Becton Dickinson) using coulter beads (Cytognos) and analyzed using FlowJo software (Tree Star Inc.).

Cell culture, cytotoxicity and flow cytometry based assays

Primary mouse hepatocytes were isolated, essentially as described (Gonçalves et al., 2007; Gozzelino et al., 2012) and cultured (37°C; 95% humidity, 21% O_2; 5% CO_2) in William's medium (Gibco, 32551-020), supplemented with 4% FBS, 20 U/mL penicillin and 20 U/mL streptomycin. Cytotoxicity was assessed by crystal violet vital staining, essentially as described (Gozzelino et al., 2012; Larsen et al., 2010). Briefly, 24h after isolation and seeding onto gelatin-coated (10% solution, Gelatin, Sigma, G1393) 96-well plates (Costar; 3596), primary hepatocytes were washed in PBS and pulsed with heme (5 μM) in HBSS (Gibco; 24020-117) for 1 hour. Cells were subsequently exposed or not to mouse recombinant TNF (5ng/mL) in William's medium (Life Technologies; 32551-020), supplemented with 4% Fetal Bovine Serum (FBS, Gibco, 10500-064), 20 U/mL penicillin and 20 U/mL streptomycin (Gibco; 15140-122). In experiments using primary *Nrf2*$^{-/-}$ hepatocytes, exposure to TNF was 8 hours. Hepa1-6 cells (C57BL/6 mouse liver hepatoma; ATCC® CRL1830™) were cultured (37°C; 95% humidity, 21% O_2; 5% CO_2) in DMEM (Gibco, 21885), supplemented with 10% FBS, 20 U/mL penicillin and 20 U/mL streptomycin. Briefly, cells were seeded in 96-well plates (Costar; 3596) and grown to confluence. For cytotoxicity assay, cells were washed in HBSS, pulsed with heme (40 μM in HBSS; 1 hour) and stimulated or not with mouse recombinant TNF (50ng/mL) in DMEM supplemented with 10% FBS, 20 U/mL penicillin and 20 U/mL streptomycin for 8h. Both primary cells and cell line were pre-treated, when indicated, 4 hours before heme and/or TNF treatments with N-acetyl cysteine (NAC, 10mM) or MitoTEMPO (25μM) in DMEM. After treatment medium was removed by a quick flick of the wrist and 1% Crystal Violet (Sigma, C3886) solution in 20% EtOH (50μL) was added (1 hour) for primary hepatocytes or 30

minutes for Hepa1-6 cells; RT). Crystal Violet solution was removed by a quick flick of the wrist, plates were dried overnight (with wells facing down on a paper towel) and dye was dissolved in 50% acetic acid (50µL). Optical density was measured in a microplate reader (Victor^3, Perkin Elmer) at λ_{595nm}. Cell death was calculated by subtracting to 100 the percentage of surviving cells ((ODcells-ODblank)/AverageODcontrol x 100). ROS accumulation was quantified using CM-H2DCFDA (10µM), mitochondrial superoxide using MitoSox (10µM) and mitochondrial membrane potential using TMRM (10µM) probes. Briefly, after heme and/or TNF treatment, cells were washed in PBS (70g, 2 minutes; RT). Cellular pellet was re-suspended in 200µL probe solution in PBS (15 minutes, 37^{o}C), washed in PBS (70g, 2 minutes; RT) and re suspended in PBS (150 µL). Fluorescence was quatified by flow cytometry using a low-power air-cooled 15mW blue (I_{488nm}) argon laser and a band-pass filter of $I_{530/30nm}$ on FACSCalibur Analyzer (Becton Dickinson). Data analysis was carried out with FlowJo software (Tree Star Inc.).

Recombinant adenovirus

Recombinant adenovirus for *PGAM5* and *MLKL* or LacZ adenovirus was added to Hepa1-6 cells (500pfu/per cell) at the time of seeding (2.4x10^5 cells/well) in 6-well plates (Costar; 3516) in DMEM (Gibco, 21885). Medium was changed after 6h and experiments were carried out after 72h.

Histopathology

Mice were sacrificed with CO_2 and perfused *in toto* with cold PBS after blood collection via heart puncture. Organs were harvested,

fixed in buffered 10% formalin, processed for paraffin embedding, sectioned at 3μm (3 sections per slide) and stained with hematoxylin and eosin (H&E). Slides were analyzed with a Leica DM LB2 light microscope.

Liver Intravital Microscopy

Confocal intravital microscopy was performed, essentially as described (Marques et al., 2015). Briefly, mice were anesthetized (i.p.) with a mixture of ketamine (125 mg/kg; Imalgene1000, Merial) plus Xylazine (12.5 mg/kg; Rompun, Bayer) in a final volume of 120-160μL/mouse. The liver was surgically exposed onto an acrylic stage fitting an inverted Zeiss Meta microscope equipped with a 10x objective. Sytox Green (100μM) and Tetramethylrhodamine methyl ester (TMRM; 0.5mg/mL) were administered (100μL in PBS, i.v.) 10 minutes before imaging. Image quantification was performed using ImageJ software.

Luciferase Reporter Assays

OKD48 reporter mice received heme (20mg/Kg in PBS, i.p.) or anti-mouse RBC polyclonal antiserum (2x; 48 hours apart; 40μL/mouse, i.p.). Luciferase activity was determined 6 hours after heme and 24 hours after anti-mouse RBC polyclonal antiserum administration, essentially as described (Jeney et al., 2014). Briefly, mice were anesthetized (Ketamine/Xylazine i.p., 120 mg/kg and 16 mg/kg, respectively) before luciferin administration (100mg/Kg in PBS, i.p.). Abdominal skin was removed 5 minutes later and luciferase activity was monitored by whole-mice imaging using an electron-multiplying charge-coupled device (EM-CCD) photon-counting camera

(ImagEM; Hamamatsu). Analysis was performed using Fiji software. *In vitro* luciferase reporter assays were performed in Hepa1-6 cells ($50x10^3$ cells/well) in 6-well plates (Costar; 3516) and transfected with Lipofectamine according to manufacturer's instructions, with 5ug of total DNA (Nrf2 plasmid). The treatments were performed 48h after using heme (40uM, 1h in HBSS) and/or TNF (50ng/ml, 2h in DMEM) for the time indicated followed by lysis with the Luciferase 5X buffer (Luciferase Assay System, Promega, E1501). Luciferase activity was measured using a microplate reader (Victor^3, Perkin Elmer) at λ_{560nm}. Data was normalized to LacZ, i.e. Luc/b-Gal.

Immunofluorescence

Hepa 1-6 cells were seeded onto coverslips in 24 well plates (Costar, 3526) and grown to confluence (37^{o}C, 95% humidity, 21% O_2 and 5% CO_2) in DMEM supplemented with 10% FBS, 20 U/mL penicillin and 20 U/mL streptomycin. Cells were washed with PBS, fixed in 4% paraformaldehyde (5 minutes, RT), washed in PBS, blocked (1% BSA, 0.1% Goat Serum, 0.05% Triton in PBS, 1 hourour, RT). Cells were incubated with rabbit anti-Nrf2 antibody (1:500, Cell Signaling, NRF2; D1Z9C; 12721) for 2 hours at RT or ON at 4^{o}C in blocking solution in a humidified chamber. After washing with blocking solution (3x; 5 minutes, mild agitation), cells were incubated with Cy5 labeled goat anti-rabbit polyclonal antibody (1:1000, A10523, Life Technologies) in blocking solution (1 hour, RT) in a humidified chamber. Cells were washed (3x in PBS 1X) and then quickly rinsed in water before mounting (20µL Mowiol, 81381, Aldrich) containing Dabco (Dabco® 33-LV, Sigma Aldrich, 290734) to which 1 µL 4',6-diamidino-2-phenylindole (DAPI, Life Technologies, D1306) was added to stain DNA. Images were

acquired on a Yokogawa CSU-X Spinning Disk confocal microscope, with a 100x 1.4NA oil immersion objective, using the λ_{685nm} filter (Cy5/Far red Filter and λ_{460nm} (DAPI filter) laser lines and a Andor iXon+ EMCCD camara. Images were processed using Fiji software (automated analysis for immunofluorescence). Briefly, values of Integrated Density per image (around 5 images per treatment with ~20cells per image) were obtained in the Cy5 channel minus the DAPI channel to quantify Cy5 and DAPI co-localization. Number of nuclei was counted to normalize to the number of cells (IndDen/Cell).

Immunoblotting

Hepa 1-6 cells were grown to confluence in 6-well plates (Costar; 3516), treated with heme (40 μM in HBSS; 1 hour) and/or TNF (50ng/mL in DMEM; 2 hours). As positive control, Hepa1-6 cells were treated with MG132 (10μM in DMEM; 6 hours). After scraping, cells were lysed in SDS Loading Buffer (50μL per well, Cell Signaling, 7722) and sonicated (NISONIX Sonicator XL2020) for 2x 10 seconds on ice with a 5 second interval (intensity 5/6). After boiling (95°C; 5 minutes), cells were chilled on ice for 2 minutes and centrifuged (full speed at RT for 10 minutes). Supernatants were transferred to a new tube and proteins were quantified using NanoDrop (NanoDrop 1000, ThermoScientific - Protein 260/280). Cell lysates were loaded on a 10% polyacrylamide gel (50-100μg) and ran in a SDS-PAGE system (BioRad). Proteins were transferred (12V, 90 minutes) to a PVDF membrane (BioRad, 1620177) in a Trans-Blot® Turbo™ Transfer System (Biorad). Membranes were blocked for in 5% milk solution in TBST (50 mM Tris, 150 mM NaCl and 0.05% Tween 20 in water, pH 7.6) for 1 hour at RT. Subsequently, membranes were incubated with rabbit anti-Nrf2

monoclonal antibody (1:1000, Cell signaling, 12721) in TBST (4°C, overnight). For loading control, membranes were incubated with mouse anti-actin monoclonal antibody (1:1000, Santa Cruz Biotechnology, SC8432). Membranes were washed (3x in TBST) and incubated (1 hour; RT) with horseradish peroxidase (HRP)-conjugated donkey anti-rabbit IgG (H+L) (1:20000, Pierce; 31458) or goat anti-mouse IgG (1:1000, Santa Cruz Biotechnology, Sc-2031) in milk solution (5% milk in TBST). Peroxidase activity was visualized using the ECL Western Blotting Substrate (Pierce; 32209) according to the manufacturer's instructions and of the signal detected on photoradiographs (Super RX 18x24 500E, Fujifilm). Digital images were obtained with an image scanner followed by Fiji software analysis.

Real-Time PCR

Mice were sacrificed at day 7 and 10 after *Pcc* infection and at 16 and 36h after CLP. Control mice (*Pcc* day 0, CLP 0h) were not subjected to any infection or surgical procedure. Total RNA was isolated from the whole liver and kidneys using TRIzol (Invitrogen Life Technologies; 15596026) and the RNeasy Mini Kit (RNeasy Plus Mini Kit 50, QIAGEN, 50974134). RNA was quantified using NanoDrop (NanoDrop 1000, ThermoScientific) and used to synthesize cDNA for PCR with Transcriptor First Strand cDNA Synthesis Kit (Roche, 04897030001). cDNA samples were transcribed into mRNA copies by qRT-PCR using SYBR Green PCR mix (iTaq Universal SYBR Green Supermix, BioRad, 1725124). Transcript number was calculated from the threshold cycle (Ct) of each gene with a 2 DDCT method (relative number) and normalized to *Arbp0* expression. The primer sequences used were: *NAD(P)H*

quinone dehydrogenase 1 (*NQO1*) 5'-CCGAACACAAGAAGCTGGAAGCTG-3', 5'-AGGCAAATCCTGCTACGAGCAC-3'; *Glutathione S-transferase* (*GST*) 5'-AGCCATTCTCAACTACATCGCCAC-3', 5'-GGGGGACATAATACCAATTGCCCAATC-3'; *Ferritin Heavy Chain* (*FtH*) 5'-ATGCCGAGAAACTGATGAAGCTGC-3', 5'-TGCACACTCCATTGCATTCAGCC-3'; *Heme oxygenase 1* (*Hmox1*) 5'-AAGGAGGTACACATCCAAGCCGAG-3', 5'-GATATGGTACAAGGAAGCCATCACCAG-3'.

Serology

Blood samples were collected by cardiac puncture in heparinized tubes (Heparina LEO PHARMA 5.000 UI/ml) centrifuged (2×5 minutes, 1600g, 4°C) and plasma was stored (-80°C). Aspartate aminotransferase (AST, EASTR-100), alanine aminotransferase (ALT, EALT-100), lactate dehydrogenase (LDH, D2DH-100), creatine kinase (CK, ECPK-100), creatinine (DICT-500), urea (DIUR-100) and glutathione peroxidase (Gpx, EGPX-100) activity were measured by spectrophotometry (microplate reader Victor^3, Perkin Elmer), according to the manufacturers instructions (Bioassay Systems). Plasma HMGB1 was measured by ELISA according to manufacturer instructions (IBL International; ST51011). DNA was isolated from plasma using DNeasy Blood & Tissue kit (Qiagen; 69504) and DNA concentration was determined by spectrophotometer. Mitochondrial DNA in plasma was quantified by qRT-PCR using the following primers: *Cytochrome b* (*Cytb*) 5'-CTTAGCCATACACTACACATCAG-3' and 5'-ATCCATAATATAAGCCTCGTCC-3'; *Mitochondrial encoded cytochrome c oxidase III* (*mt-COX3*) 5´-

ACGAAACCACATAAATCAAGCC-3´ and 5'-TAGCCATGAAGAATGTAGAACC-3´, *Mitochondrial encoded cytochrome c oxidase I* (*mt-COX1*) 5'-TTCGGAGCCTGAGCGGGAAT-3´ and 5'-ATGCCTGCGGCTAGCACTGG-3´. *NADH dehydrogenase* (*Nd1*) 5'-AGCCTCAAACTCCAAATACTC-3´ and 5'-CCCTGATACTAATTCTGATTCTCC-3´. Relative DNA copy number in plasma was calculated using the threshold cycle (Ct) for each gene in *Nrf2*$^{-/-}$ mice normalized to *Nrf2*$^{+/+}$ mice with a 2^CT method (Zhang et al., 2010). Plasma IL-1α, IL-1β, IL-6, TNF-α, IL-10, IL-12, IP-10, KC, MCP1, MIP-1α, MIP-1β, MIP2, MIG, RANTES, VEGF were measured by Luminex technology using the MAGPIX® system (Merck/Millipore) combined with the MILLIPLEX® MAP magnetic bead-based multi-analyte panels (Merck Millipore, MCYTOMAG-70K). Data analysis was performed by MILLIPLEX® Analyst 5.1 software. Total heme was quantified in plasma using the formic acid assay (Kuross et al., 1988). Briefly, samples were diluted in H_2O in 96 well plates (Costar, 3596) and heme concentration was determined by comparison to a hemin standard curve (0.5-16 µM in H_2O). Formic acid (150 µL/well; 98-100%, Merck) was added and absorbance measured at λ_{405nm} using a microplate reader (Victor^3 Multilabel Readers, Perkin Elmer).

Statistical Analysis

Survival curves were represented as Kaplan-Meier plots and statistical significance was evaluated with the Log Rank (Mantel-Cox) test. Comparison of the means of three or more groups was performed using one-way ANOVA with *a posteriori* Tukey test, when data assumed Gaussian distribution. Otherwise, a group comparison

was carried out, applying the Kruskal-Wallis test, followed by pairwise Mann-Whitney U tests, for assessment of significance between every two groups with p value adjusted using Bonferroni correction. Weight, temperature and parasitemia (line plots) were compared between genotypes using pairwise T-tests. Outliers were identified by the Grubbs' test from the GraphPad software, available online (http:// graphpad.com/quickcalcs/Grubbs1.cfm). All tests were performed using GraphPad v.5.0a software (Prism) and a level of significance was set at *$p < 0.05$, **$p < 0.01$*, ***$p < 0.001$, n.s. $p > 0.05$.

Appendix 1

"The more unknowable the mystery,
the more beautiful it is."
(David Lynch)

Involvement of the p62/NRF2 signal transduction pathway on erythrophagocytosis

Inês B. Santarino[1], Michelle S. Viegas[2], **Ana M. Ribeiro[3]**, Miguel P. Soares[3] and Otília V. Vieira[1*] ***(Adapted)***

Manuscript submitted to the journal Scientific Reports

[1]CEDOC, NOVA Medical School | Faculdade de Ciências Médicas, Universidade NOVA de Lisboa, 1169- 056 Lisboa, Portugal.
[2]CNC - Center for Neuroscience and Cell Biology, University of Coimbra, Largo Marquês de Pombal, 3004-517 Coimbra, Portugal.
[3]Instituto Gulbenkian de Ciência, Oeiras, Portugal, Rua da Quinta Grande, 6, 2780-156, Oeiras, Portugal
* Corresponding author.
Mailing address: CEDOC, NOVA Medical School | Faculdade de Ciências Médicas, Universidade NOVA de Lisboa, 1169-056 Lisboa, Portugal. Phone: (+351) 218 803 100. E-mail: otilia.vieira@nms.unl.pt

Key words: aged Red Blood Cells, phagocytosis, phagolysosome biogenesis, aged Red Blood Cells degradation, p62 and Nrf2.

Introduction

Removal of damaged red blood cells (RBC) from the circulation occurs through erythrophagocytosis, by tissue-resident macrophages in the spleen, liver and bone marrow[1–4]. The rapid removal of damaged RBC from the circulation is important for maintenance of iron/heme homeostasis, as the majority of iron required to sustain erythropoiesis is derived from senescent RBC, and defects in erythrophagocytosis can lead to anemia and iron overload[4].

Previous work has identified receptor-ligand interactions and signaling pathways engaged during erythrophagocytosis. Phagocytic cells recognize damaged RBC by a range of senescence markers such as phosphatidylserine (PS), decreased levels of sialic acid, CD47 and binding of autologous immunoglobulins and opsonins[5]. Furthermore, some receptors involved in RBC clearance have also been established. Several in vitro studies have shown that the recognition of PS on the cell surface by stabilin-2 is important for RBC clearance, while others suggested that clearance of agRBC by macrophages is likely dependent on scavenger receptors rather than specific PS receptors[2,6,7]. However, the engulfment of RBC under physiological conditions is likely to involve a myriad of receptors including the Fc and complement-receptors.

Upon RBC recognition, macrophage actin cytoskeleton and cell surface remodeling takes place allowing the formation of a specialized phagosome known as the erythrophagosome. Following scission from the plasma membrane, phagosomes undergo a maturation process involving a programmed change of their membrane and luminal composition resulting from a highly coordinated series of sequential membrane fusion and fission events with components of the endocytic pathway. Fusion with early-

endosomes followed by interactions with late-endosomes and lysosomes culminates in conversion of the phagosome into a lysosome-like organelle - the phagolysosome. It is within this organelle that RBC undergo degradation allowing for the reutilization of their components[4,8–10].

Beyond the involvement of vesicular traffic machinery, some autophagy players are also involved in phagolysosome biogenesis, including the microtubule-associated protein 1 light chain 3 (LC3), an autophagy effector recruited to single-membrane phagosomes in a process termed LC3-Associated Phagocytosis (LAP). There is strong evidence to suggest that LAP facilitates rapid phagosome maturation while contributing to the degradation of engulfed phagocytic particles and modulation of immune responses[11–13]. In contrast to canonical autophagy, defined by the formation of a double-membrane autophagosome, LAP is associated with the recruitment of LC3 to single-membrane phagosomes carrying different types of cargo in an Atg5, Atg7 and Beclin1-dependent manner, independently of the Mammalian Target of Rapamycin (mTor)-regulated ULK-ATG13-FIP200 complex[11,14]. Rubicon, an adaptor protein, was also identified as being required for LAP but not for autophagy[12]. NADPH oxidase-2 (NOX2) has also been identified as having a LAP-specific role[12,15]. It should be noted that this brief description of phagosomal maturation is a gross oversimplification of a highly complex and precisely choreographed process.

Although several studies have focused on intracellular mechanisms of heme trafficking during hemophagocytosis[16,17], few have addressed the molecular mechanisms underlying maturation and degradation of phagosomes containing RBC. We have recently shown that phagosomes containing RBC cells mature slower than phagosomes containing IgG-opsonized particles[18], which is in

keeping with the notion that that maturation of the phagosome in macrophages depends on the nature of the ingested cargo[19].

The present study was designed to identify the molecular machinery involved in maturation of phagosomes containing RBC. Of note, while erythrophagocytosis takes place mainly in erythrophagocytic macrophages it can also occur in non-professional phagocytes such as hepatic sinusoidal endothelial cells[2,20,21]. The process has some similarities with efferocytosis that occurs in pathological states like atherosclerosis and in which the non-professional phagocytes are smooth muscle cells of the arterial intima. In previous work we generated a smooth-muscle cell line that stably expressed Fcγ-RIIA receptors and described its use in studies of erythrophagocytosis[18]. Here we report mechanistic details of erythrophagocytosis by this non-professional phagocytic cell line as well as by primary bone marrow- derived mouse macrophages (BMDM). We show that beyond LC3, proteins associated with selective autophagy such as p62/SQSTM1 (Sequestosome 1), NBR1 (Neighbor of Braca 1 gene) and NDP52 (Nuclear dot protein 52)[22–24] are recruited to phagosomal membranes. The most striking phenotype was observed for p62 that associates preferentially with phagosomes containing RBC rather than to phagosomes containing IgG-opsonized particles. Moreover, we demonstrate that p62 is critical for RBC degradation. We also show that erythrophagocytosis of RBC drives the translocation of the transcription factor Nuclear factor E2-related factor 2 (NRF2) to the nucleus with subsequent up-regulation of p62 expression levels. In addition, NRF2 absence affects RBC degradation and p62 levels suggesting a link between these two molecular players in RBC degradation.

Results

The type of phagocytic particle determines the association of p62 with phagosomal membranes

We started by studying LAP in the non-professional phagocytes. Damaged RBC were prepared by incubation in PBS (20% hematocrit) for 4 days at 37°C, a treatment that originates PS-exposure on the outer leaflet of the RBC membrane, resembling what happens to RBC during storage[25], or eryptosis – a programmed cell death mechanism similar to apoptosis in nucleated cells[26]. Phagocytosis of RBC was compared to phagocytosis of IgG-opsonized particles, the most studied phagocytic model. IgG-opsonized particles are known to be internalized via Fc-receptors. After exposing phagocytes to RBC or IgG-coated latex beads, LC3 association with phagosomal membranes was assessed by confocal microscopy after immunostaining the endogenous protein. Immediately after phagocytosis, LC3B-II associated with phagosomes containing both particles, as evidenced by LC3 rims surrounding RBC and opsonized latex beads (Fig. 1A-B´). Both types of phagosomes showed a rapid and transient association of LC3 with their membranes, with peaks reaching a maximum of about 80 % (78.7 ± 2.3 %) for RBC and about 70 % (71.0 ± 6.5%) for opsonized beads, at 0 min chase. These results are in keeping with those reported by other groups showing that LC3 can be detected on phagosomes shortly after they are formed while LC3- decorated autophagosomes can take hours to form[11,27]. LC3 gradually dissociated from both types of phagosomes, probably due to recycling from the phagosomal membranes (Fig. 1C). Since our phagocytic assays were performed in serum-free medium and

canonical autophagy is activated under conditions of starvation[28], we tested whether nutrient deprivation was responsible for LC3 association with phagosomes containing RBC. As shown in Suppl. Fig. 1, no differences in the LC3-phagosomal association pattern were observed when phagocytic cells were kept in the presence or absence of serum, suggesting that LAP machinery is independent of the nutritional status of the phagocytes, as previously described[11,13].

Beyond LC3, phagosomal processing and autophagy share other players and mechanisms[12,29–32]. Therefore, we attempted to ascertain whether there was ubiquitination of phagosomal proteins in phagosomes containing both types of phagocytic particles. Indeed, phagosomes containing either RBC or IgG-coated beads were associated with poly- and/or mono-ubiquitinated membrane proteins (Fig. 1D-E´). The time-course for the appearance of this tag in phagosomal membranes (Fig. 1F) showed that shortly after ingestion non-professional phagocytes presented a large fraction (around 60% for both particles) of phagosomes positive for ubiquitinated components with some differences in the kinetics of signal loss over the maturation time.

To get more insight into the autophagy-related molecular machinery involved in phagolysosome biogenesis, we looked at the phagosomal acquisition of p62, NBR1 and NDP52. These are receptors/adaptors which share the ability to simultaneously interact with the lipidated form of LC3, LC3-II, and ubiquitinated substrates[31]. We started by testing intracellular distribution of p62 during both types of phagocytosis, a universal receptor for ubiquitinated cargo under physiological and pathological conditions[7,23,33–35]. Pulse-chase experiments revealed that phagosomes containing RBC displayed a completely different pattern of p62 association compared to IgG-

opsonized beads (Fig. 1G-H). Phagosomes containing RBC showed similar kinetics for acquisition of p62 and ubiquitinated proteins while phagosomes containing IgG opsonized particles showed only modest levels of p62 over time (compare Fig. 1I and Fig. 1F). That difference was not due to changes in expression levels of total p62 in phagocytic cells challenged with the two phagocytic particles as confirmed by western blot (Fig. 1J and K).

Next, we analyzed the association of NBR1 with phagosomal membranes. As seen in Fig. 1L-M', NBR1 was recruited to both types of phagosomes. The time course of NBR1 dissociation from membranes of phagosomes that contained RBC was slightly different from the time course of NBR1 dissociation from phagosomes containing IgG-opsonized particles (Fig.1N). NBR1 dissociation from phagosomal membranes of IgG-coated beads was not observed even for the longest chase time tested. This may be due to a compensatory mechanism for the absence of p62 on the phagosomal membranes of IgG-coated beads.

Finally, we performed immunostaining for NDP52 to assess its acquisition by both types of phagocytic particles (Fig. 1O-P'). Phagosomes containing IgG-opsonized particles showed a transient NDP52 association with around 69% (68.64 ± 1.19%) of positive-phagosomes at 0 min and about 29% (28.69 ± 12.51%) at 60 min chase. Phagosomes containing RBC also showed a transient NDP52 association but this autophagy effector remained associated with these phagosomes for longer periods of time compared with those carrying IgG-opsonized beads (Fig. 1Q).

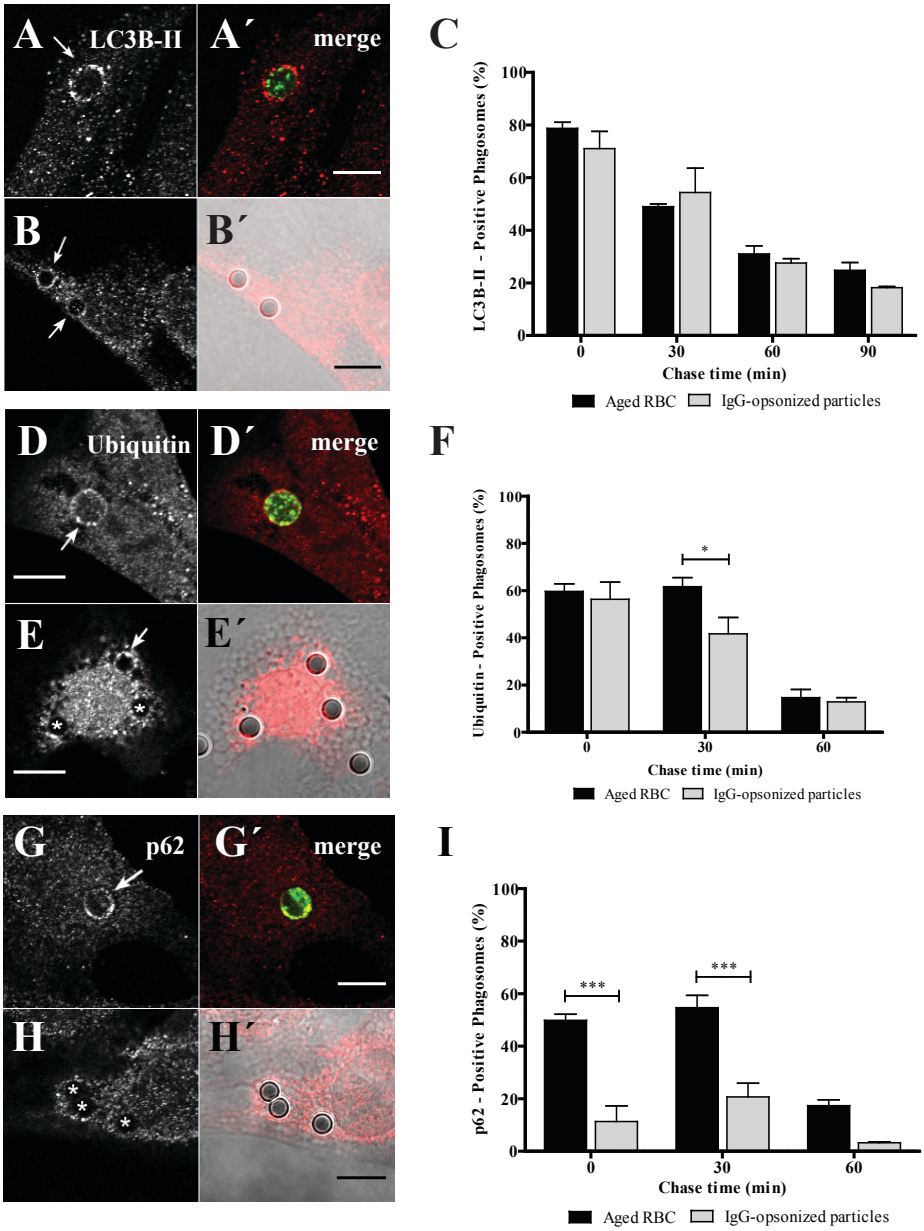

(Figure continues on the next page)

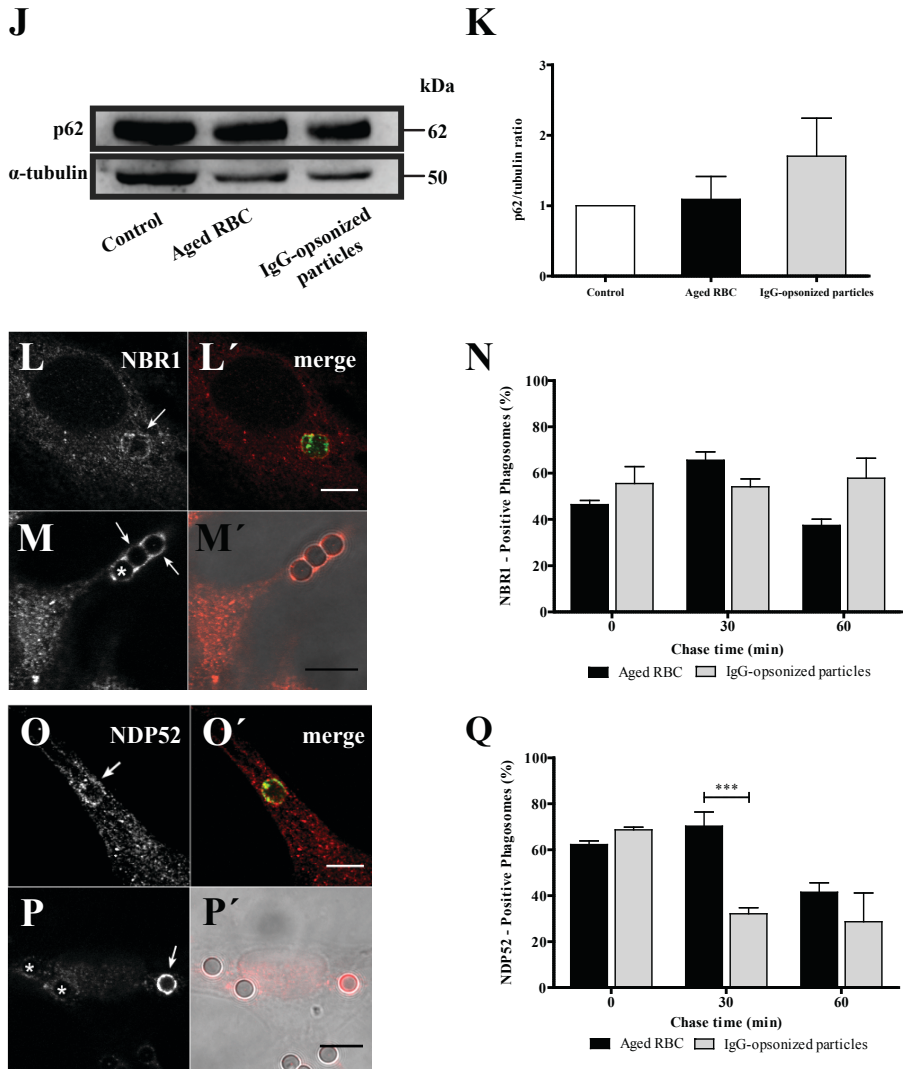

Figure 1. Acquisition of LC3 and autophagy adaptor proteins by phagosomes in non-professional phagocytes.

Phagocytes were challenged with RBC (A, A', D, D', G, G', L, L', O and O') or with IgG-opsonized particles (B, B', E, E', H, H', M, M', P and P') and then immunostained for the endogenous LC3B, ubiquitin, p62, NBR1 and NDP52 as indicated in the different figure panels. A, B, D, E, G, H, L, M, O and P are immunofluorescence images. A', B', D', E', G', H', L', M', O' and P' are the composite of the immunofluorescence image with the phagocytic particles visualized in green (RBC stained with CFSE) or by differential interference contrast (DIC, IgG-opsonized particles). In A-B' and G-H' images were acquired at 0 min chase time. In D-E', L-M' and O-P' the

images were acquired at 30 min chase time. Arrows indicate positive- and asterisks (*) indicate negative- phagosomes for the indicated endogenous protein. Bars, 10 μm. C, F, I, N and Q, Graphs showing the percentage of positive phagosomes for LC3, ubiquitin and the different adaptor proteins. Quantifications were performed in non-professional phagocytes exposed to the different phagocytic particles for 30 min and chased for the times indicated in the graph abscissa. The values are means ± SEM of, at least, three independent experiments. At each time point, at least, 50 phagosomes were analyzed. *, $p<0.05$; ***, $p<0.001$ comparing differences between phagosomes with RBC and with IgG- opsonized particles.
(J) p62 levels in cell lysates of non-professional phagocytes exposed for 30 min to RBC or to IgG-opsonized particles. α-tubulin was used as loading control. (K) Ratio of p62/tubulin of quantified bands in cells exposed or not (control) to RBC or IgG-opsonized particles. Three independent experiments were performed.

p62 and NBR1 are recruited to the phagocytic cups.

Since LAP and the autophagy receptors/adaptors tested in this work were acquired by the phagosomes at very early stages of phagocytosis, we enquired whether they were already present when the phagosomes were positive for F-actin. Phagosome formation is preceded by a dynamic set of events that induce actin cytoskeleton rearrangement in order to support pseudopod extension at sites of particle engulfment. This reorganization leads to a localized cup-shaped protrusion of the plasma membrane, the “phagocytic cup” (Figs. 2 and 3). This structure is enriched in actin filaments responsible for generation of the forces that alter the local shape of the cell surface. In the case of phagocytosis of RBC, membrane protrusions are formed upon actin polymerization, with particle sinking followed by the formation of the phagosome, through a process between complement-mediated phagocytosis and micropinocytosis[36] making the visualization of the phagocytic cups difficult, as can be observed in Fig. 2A (blue arrows in the XZ view point to F-actin). In contrast, in phagocytosis of IgG-opsonized

particles, the actin cups are perfectly visualized (Fig. 3).

To assess how early the autophagy receptors/adaptors associate with the phagocyte particles, phagocytes were exposed to RBC and IgG-opsonized beads, fixed and co-stained for F-actin with Phalloidin and p62, LC3B-II, NBR1 or NDP52. Notably, p62 was found to be present in nascent RBC-containing phagosomes, co-localizing with F-actin as shown in Fig. 2A and absent in phagosomes containing IgG- opsonized particles, Fig. 3A, confirming the selectivity of this adaptor for RBC-containing phagosomes (Fig. 1I). As seen in Fig. 2B and D and Fig. 3B and D, LC3 and NDP52 were not co-localized with F-actin in any of the phagocytic particles incubated with phagocytes suggesting that they were acquired by the phagosomal membranes after actin dissociation and when phagosome maturation starts. NBR1 was present in the phagocytic cups of RBC and IgG-opsonized particles (Fig. 2C and Fig. 3C). Thus, during the phagocytic process, p62 and NBR1 were acquired earlier that NDP52 and LC3, suggesting that the former proteins could be involved in the recruitment of the latter.

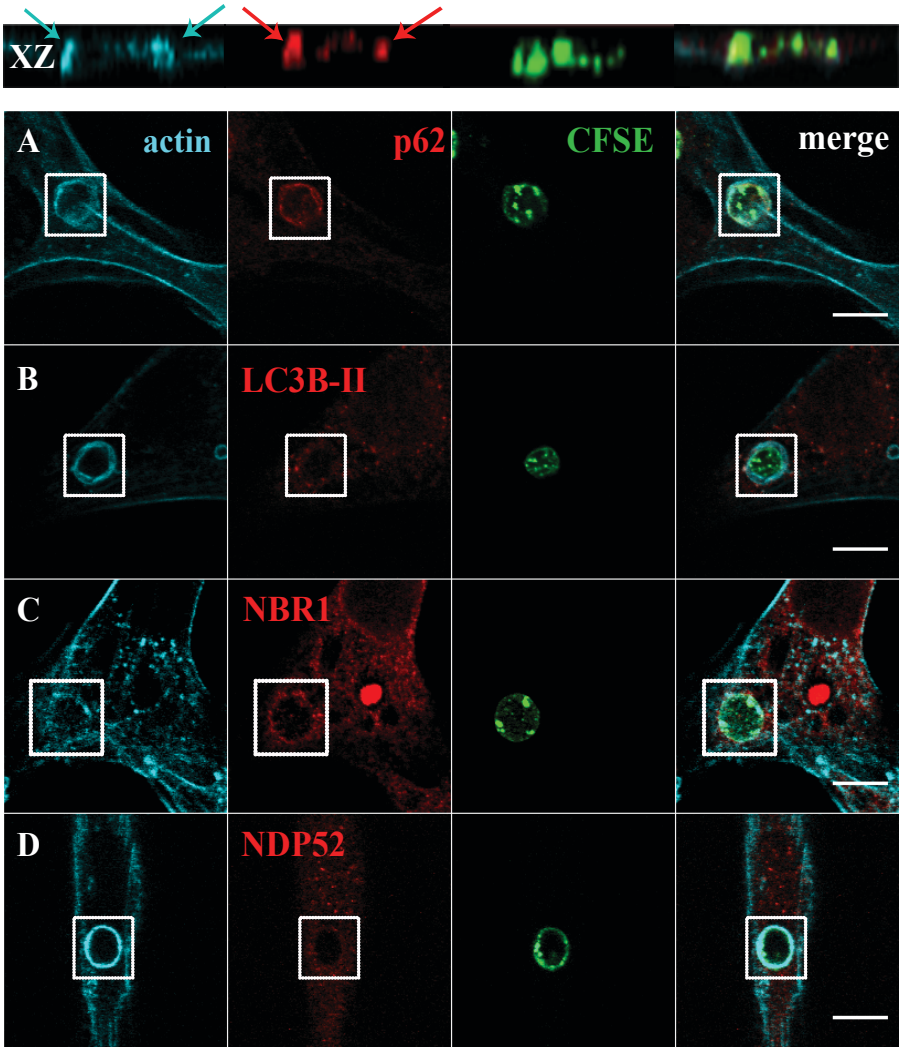

Figure 2. Co-localization of LC3 and autophagy adaptor proteins with F-actin in phagosomes containing RBC.
Non-professional phagocytes were fed with RBC for 30 min, fixed, and stained for F-actin with Phalloidin and for the endogenous LC3 or autophagy adaptors. A-D are representative images, obtained by confocal microscopy, of cells co-stained for F-actin and p62 (A), LC3 (B), NBR1 (C) or NDP52 (D). In A, side views (XZ) are merges of ten vertical sections of confocal stacks. Arrows indicate the nascent phagosome positive for F-actin (blue) and p62 (red). The first column represents cells stained for F-actin. The second column represents cells stained for the endogenous p62, LC3, NBR1 or NDP52. The third column shows internalized RBC stained with CFSE. The fourth column represents merged images of F-actin with LC3 or autophagy adaptors and internalized RBC. The regions outlined by

the boxes are nascent phagosomes. Bars, 10 μm.

Ubiquitin is involved in the recruitment of the autophagy adaptors to the phagosomal membranes.

Since p62, NBR1 and NDP52 have ubiquitin binding domains and ubiquitination occurs during phagocytosis (Fig. 1D-F), we addressed the role of ubiquitin in the recruitment of these adaptors to phagosomes. First, we determined whether ubiquitin was associating with phagocytic cups. As observed in Fig. 4A and B ubiquitin associated with phagocytic cups, visualized by F-actin staining, suggesting that phagosomal ubiquitination could be involved in the recruitment of p62, NBR1 and NDP52. An E1 ubiquitin-activating enzyme inhibitor, PYR-41[37] reduced the percentage of ubiquitin-positive phagosomes containing RBC by 37.0% and by 47.0% for IgG-opsonized particles, when compared with control cells (Fig. 4C). Although inhibition of ubiquitination by PYR-41 of phagosomal membranes was not complete, the effect obtained was sufficient to affect the association of p62 (Fig. 4D), NBR1 (Fig. 4E) and NDP52 (Fig. 4F) with phagosomes containing RBC. The inhibitory effect of PYR-41 in the ubiquitination of phagosomal membranes containing IgG-opsonized particles was only observed for NDP52 recruitment to the phagosomal membranes (Fig. 4E and F). Together, these results suggest a new and differentiating role for ubiquitin in phagocytosis.

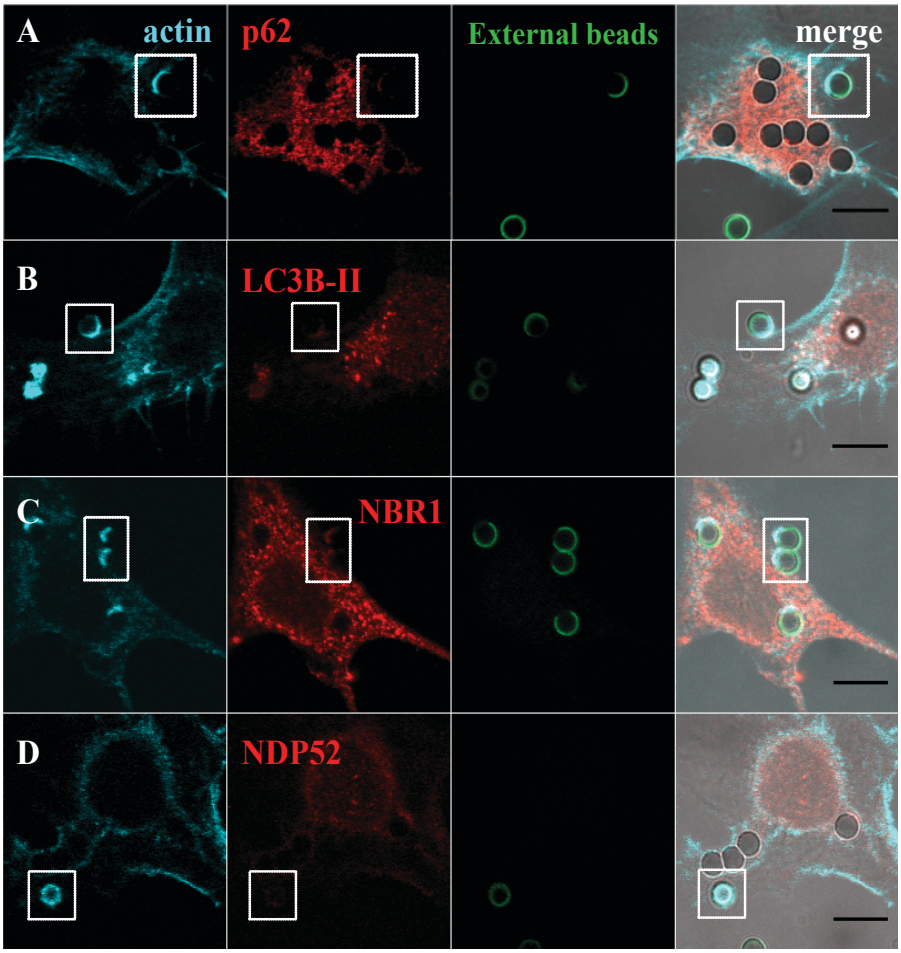

Figure 3. Co-localization of LC3 and autophagy effectors in phagocytic cups of IgG-opsonized particles.

Non-professional phagocytes were fed with IgG-opsonized beads for 30 min, fixed, and co-stained for F-actin with Phalloidin and for the endogenous LC3 or autophagy adaptors. A-D are representative images of cells co-stainined for F-actin and p62 (A), LC3 (B), NBR1 (C) or NDP52 (D). The first column represents cells stained for F-actin. The second column represents cells stained for the endogenous p62, LC3, NBR1 or NDP52. The third column shows non-internalized beads stained with an anti-human IgG antibody conjugated with FITC. The fourth column represents merged images of F-actin with LC3 or autophagy adaptors and the opsonized latex beads (external and internal beads visualized by DIC). The regions outlined by the boxes are phagocytic cups formed upon the recognition of IgG-opsonized particles by the Fc-receptors. Bars, 10 μm

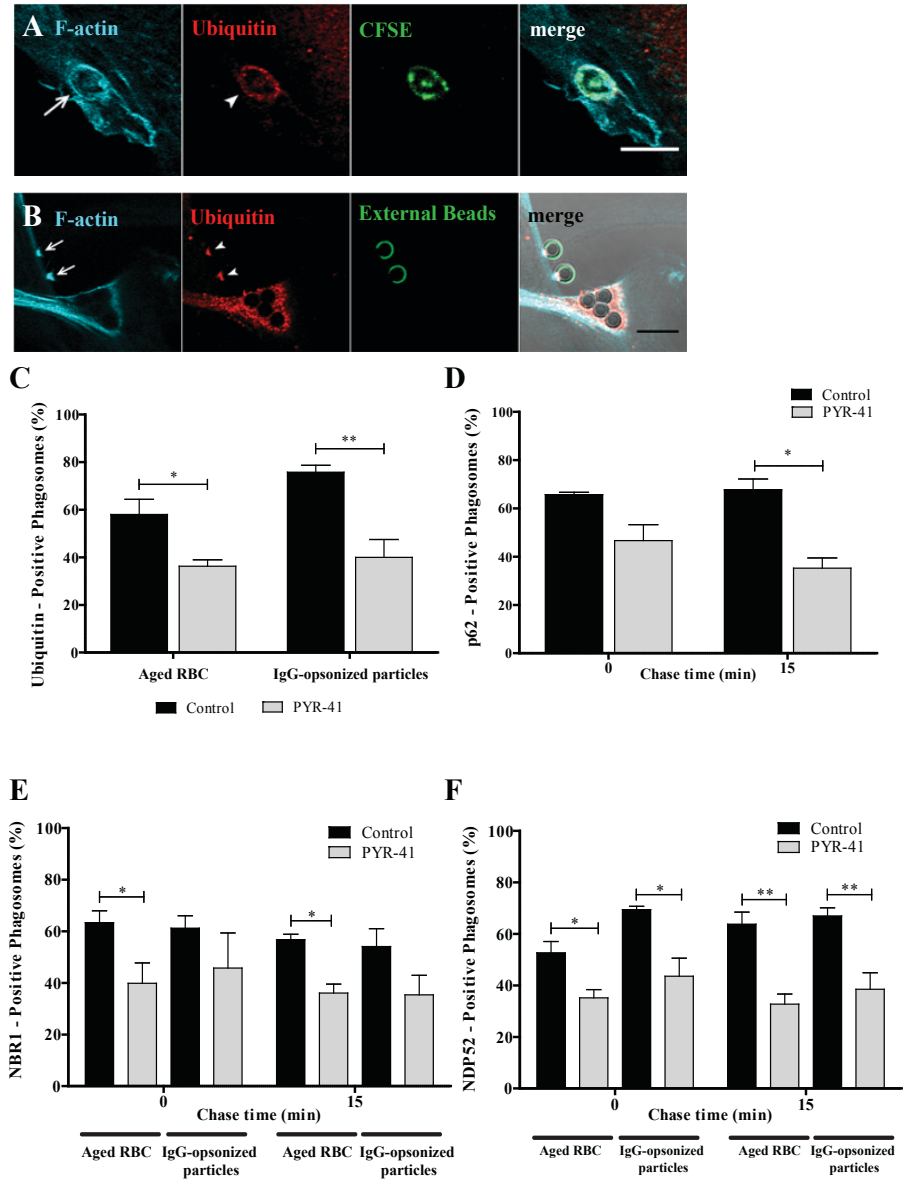

Figure 4. Functional relevance of ubiquitin on the recruitment of autophagy effectors to phagosomes.

Non-professional phagocytes were fed with RBC or IgG-opsonized particles for 30 min, fixed, and co-stained for F-actin and ubiquitin. Representative image of a nascent phagosome (A) and a phagocytic cup (B) positive for actin (first panels) and ubiquitin (second panels). The third panels show internalized RBC labelled with CFSE and non-internalized beads stained with an anti-human IgG antibody conjugated with FITC. The fourth panels

are composites of the 1st, 2nd and 3rd panels. Arrows and arrowheads indicate actin- and ubiquitin- positive phagosome, respectively. Bars, 10 μm. (C) Effect of PYR-41 in the ubiquitination of both RBC- and IgG-opsonized particles-containing phagosomes. Phagocytes were cultured and treated as described in Material and Methods section. (D) Quantification of PYR-41 effect on the acquisition of p62 by RBC- containing phagosomes. (E-F) Quantification of PYR-41 effect on the acquisition of the autophagy adaptor proteins, NBR1 and NDP52, respectively, by RBC- and IgG-opsonized particles-containing phagosomes. The values are means ± SEM of, at least, three independent experiments. At each time point, at least, 50 phagosomes were analyzed. *, $p<0.05$; **, $p<0.01$ comparing differences between adaptor-positive phagosomes containing RBC or IgG-opsonized particles in absence and in presence of the inhibitor PYR-41.

The role of p62 in phagocytosis of IgG-opsonized particles and RBC was compared in mouse BMDM. As shown in Fig. 5A-C the results for wild type BMDM exhibit a pattern that is very similar to the one described above for non-professional phagocytes with p62 associated mainly with RBC-containing phagosomes irrespective of the total p62 levels (Fig. 5D and E). Similarly, p62 associates with phagosomal membranes at very early stages of the phagocytic process in BMDM (Fig.5 F). This suggests that the role of p62 is conserved in professional and non-professional phagocytes. Due to the residual levels of p62 detected in phagosomes containing IgG-opsonized particles we explored in further detail the role of p62, focusing only on RBC-containing phagosomes using mouse BMDM silenced for p62 or BMDM from p62 deficient mice (*p62*$^{-/-}$). Because p62 recruitment to the phagosomal membranes preceded that of LC3 (Fig. 2A and B), we assessed the requirement of the former in the phagosomal association of the latter. Figure 5G compares LC3 dissociation from phagosomal membranes of *p62*$^{+/+}$ and *p62*$^{-/-}$ BMDM and shows that in *p62*$^{-/-}$ BMDM LC3 did not dissociate from these membranes over the periods of time examined, as compared to

p62$^{+/+}$ BMDM. As p62 can interact with NBR1 and NDP52[38], we also enquired whether recruitment of these autophagy effectors to phagosomes was dependent on p62. As shown in Fig. 5H and I, neither NBR1 nor NDP52 association with phagosomal membranes required p62. Interestingly, the effect of p62 absence in LAP (Fig. 5G) delaying LC3 dissociation/degradation from the phagosomal membranes, seemed to have consequences in phagosome maturation and degradation. Phagolysosome biogenesis was assessed by the acquisition of the lysosomal membrane marker LAMP-1 in p62 silenced cells, in which p62 expression was reduced by 70.4 ± 0.08% assessed by qPCR and by Western blot (see Suppl. Fig. 2). As can be observed in Fig. 6A-C, the percentage of LAMP-1-positive phagosomes in p62 silenced cells was lower when compared to the phagosomes in control cells (23.8 ± 6.3% compared with 50.2 ± 9.1%, respectively, at 0 min chase time). This effect on phagolysosome biogenesis can have an impact in the RBC degradation which in turn can lead to a defective uptake and subsequent damage. Indeed, the absence of p62 imapaired RBC degradation (Fig. 6D and E). Control and p62-silenced cells were challenged with CFSE- labeled RBC for 15 min and then followed by live-cell confocal microscopy for 300 min. In control cells, the internalized RBC underwent efficient degradation after 60 min chase (assessed by the loss of fluorescence and disappearance of RBC by DIC, Fig.6 D and E upper panels, respectively). In contrast, the absence of p62 led to the failure of RBC degradation showed by the persistence of these RBC even after 300 min chase (Fig. 6D and E lower panels). These results suggest that p62 is critical for phagosomal maturation and further degradation of RBC.

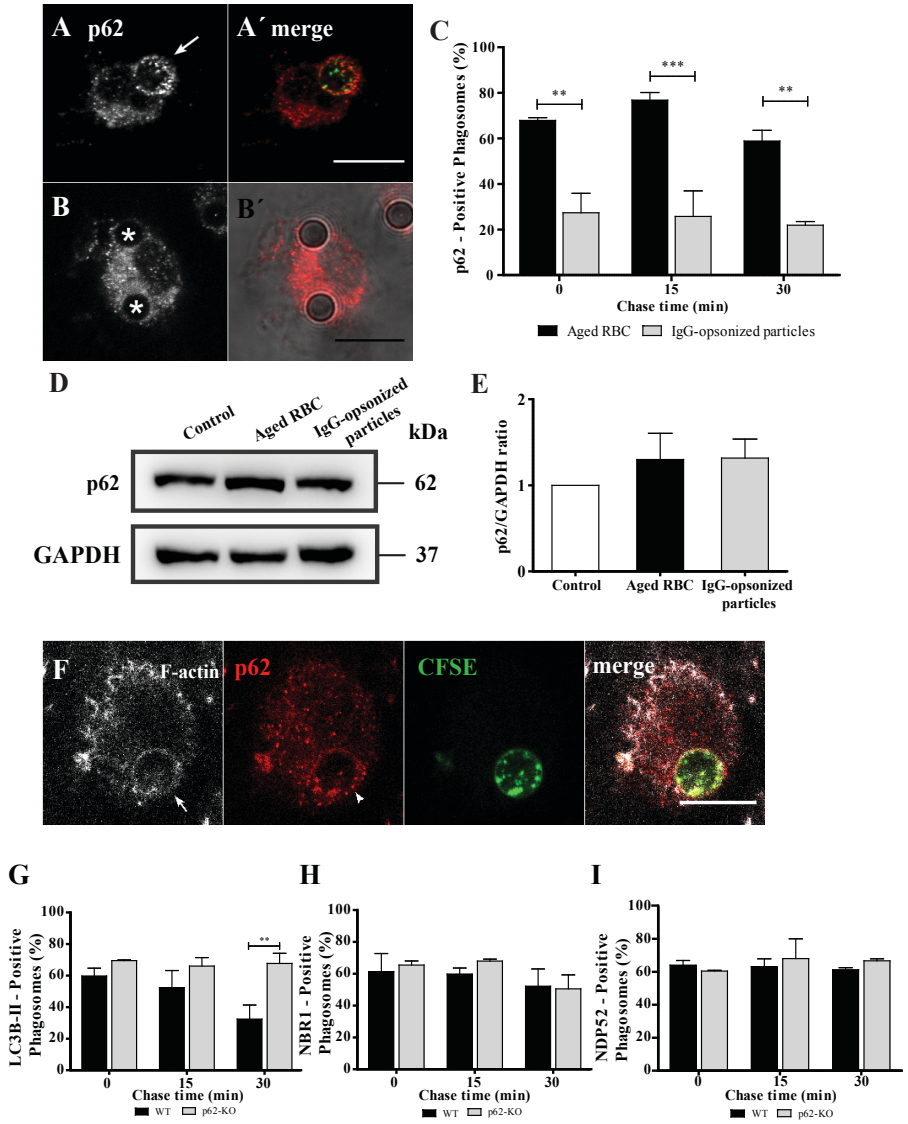

Figure 5. Effect of p62 in the recruitment of LC3, NBR1 and NDP52 to phagosomes containing RBC cells in BMDM.

After pulse-chase experiments with RBC or IgG-opsonized particles, WT-BMDM cells were fixed and stained for p62. (A) WT-BMDM containing a p62-positive phagosome at 15 min chase time. (A') Corresponding merged image showing the internalized RBC stained with CFSE. (B) WT-BMDM containing p62-negative phagosomes at 15 min chase time. (B') Corresponding merged image showing the internalized IgG-opsonized particles in DIC. (C) Quantification of p62 positive-phagosomes. (D) p62 levels in total cell lysates of WT- BMDM exposed for 15 min to RBC or IgG-opsonized particles. GAPDH was used as loading control. (E) Ratio of

p62/GAPDH of quantified bands in cells exposed or not to RBC, IgG-opsonized particles. Three independent experiments were performed. (F) Representative image of RBC-containing phagosome positive for actin (in white) and p62 (in red). Arrow and arrowhead indicate actin- and p62-positive phagosome, respectively. Quantification of LC3- (G), NBR1- (H) and NDP52- (I) positive phagosomes in WT- BMDM (black bars) and p62-KO- BMDM (grey bars). The values are means ± SEM of, at least, three independent experiments. At each time point, at least, 50 phagosomes were analyzed. **, p<0.01; ***, p<0.001 comparing differences between p62-positive phagosomes containing RBC and IgG-opsonized particles or differences between of LC3-positive phagosomes in WT- and p62-KO-BMDM.

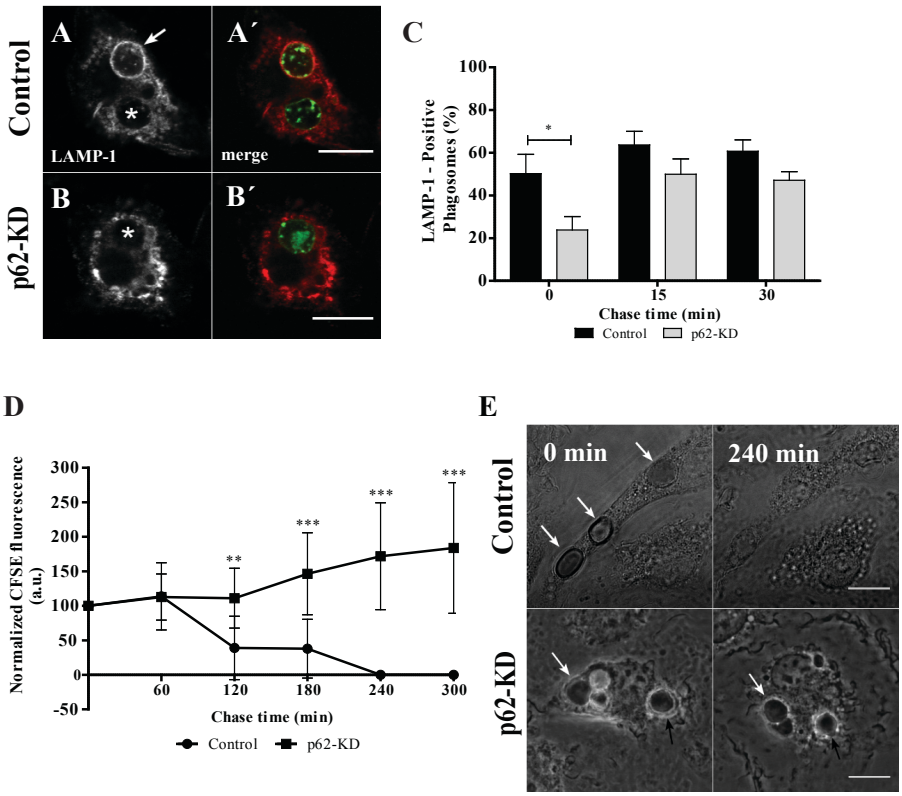

Figure 6. Functional relevance of p62 in RBC degradation.
After pulse-chase experiments with RBC, control- and p62-silenced BMDM were fixed and stained for LAMP- 1. (A) Control-BMDM containing LAMP1-positive and LAMP1-negative phagosomes at 0 min chase time. (B) p62-KD-BMDM containing a LAMP-1-negative phagosome at 0 min chase time. (A´, B') Corresponding merged images showing the internalized RBC stained with CFSE. Arrow indicates a LAMP-1-positive phagosome and

asterisks (*) indicate LAMP-1-negative phagosomes. (C) Quantification of LAMP-1-positive phagosomes in WT-BMDM (black bars) and p62-KD-BMDM (grey bars). The values are means ± SEM of, at least, three independent experiments. At each time point, at least, 50 phagosomes were analyzed. *, $p<0.05$, comparing differences between WT- and p62-KD-BMDM. (D, E) Time-lapse experiments of WT- and p62-KD- BMDM challenged with CFSE labeled-RBC for 15 min (0 min chase time) and followed for 300 min further to assess phagosome degradation. Phagosome degradation (D) was measured by the disappearance of fluorescence and the phagosome assessed by DIC (E). Bars, 10 μm. The values are means ± SD of 10 different phagosomes. **, $p<0.01$; ***, $p<0.001$ comparing differences between WT- BMDM and p62-KD-BMDM. (E) DIC images at 0 min and 240 min chase time of WT- BMDM and p62-KD-BMDM. Arrows point to RBC- containing phagosomes.

Erythrophagocytosis is associated with p62-dependent NRF2 activation.

The transcription factor NRF2 that under cellular stress conditions, namely oxidative stress, is translocated to the nucleus and promotes transcription of several genes responsible for cytoprotection[39]. Under basal conditions NRF2 is ubiquitinated by Kelch-like ECH-associated protein 1 (KEAP1)-Cul3-E3 ubiquitin ligase complex and targeted to the 26S proteasome for degradation. Oxidative stress represses KEAP1 binding to the Cul3–Rbx1 complex, allowing newly transcribed NRF2 to undergo nuclear translocation and to trigger the transcription of effector genes providing metabolic adaptation to oxidative stress[39–41] NRF2 can also become activated via a non-canonical mechanism: phosphorylation of Ser351 of the KIR (Keap1-interacting 8 region, aa 346–359) of p62 causing p62's affinity for KEAP1 to significantly increase[42]. Once stabilized, newly transcribed NRF2 translocates to the nucleus where it heterodimerizes with other basic leucine zipper transcription factors, and it upregulates genes containing an antioxidant response element (ARE) in their

promoter [43–45] .

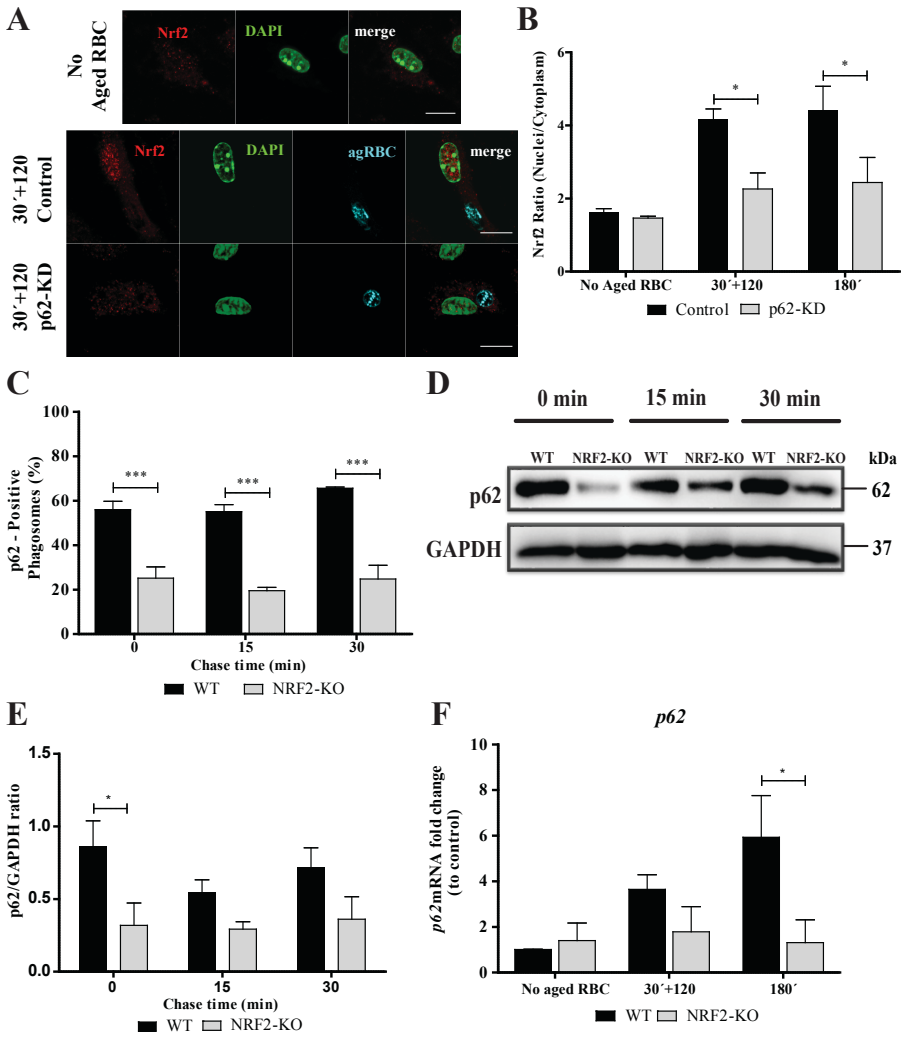

(Figure continues on the next page)

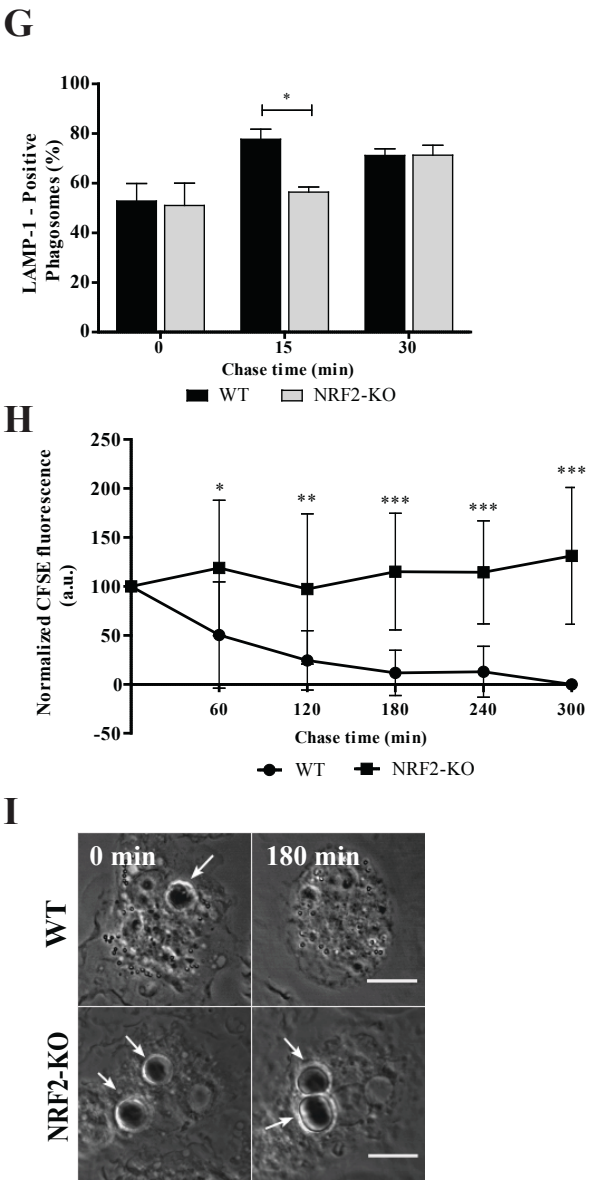

Figure 7. NRF2 is critical for RBC degradation in BMDM.
WT and p62-KD-BMDM were fed with CFSE-stained RBC for 30 min and then chased for 120 min or fed for 180 min. (A) Translocation of NRF2 into the nucleus in WT- and in p62-KD-BMDM, assessed by immunostaining, in the absence (first row) or upon incubation with RBC (second and third rows). The second row represents NRF2-nuclear translocation in WT-BMDM. The third row represents NRF2-nuclear translocation in p62-KD-BMDM. NRF2 staining is represented in red, nucleus in green and

internalized RBC in cyan. The last panels are merged images. Bars, 10 μm. (B) Quantification of NRF2 nuclear translocation expressed as a ratio of the fluorescence intensity between the nucleus and the cytoplasm. *, $p<0.05$ comparing differences between NRF2 fluorescence in WT-BMDM and p62-KD-BMDM challenged with RBC. (C-F) WT- and NRF2-KO-BMDM were challenged with RBC for 15 min (0 min chase) and then chased for the indicated times in the figures. (C) Quantification of p62-positive phagosomes after fixation and immunostaining for the endogenous protein. (D) p62 levels in total cell lysates of WT- and NRF2-KO-BMDM, for short time points. GAPDH was used as loading control. (E) Ratio of p62/GAPDH of quantified bands in cells exposed to RBC. Three independent experiments were performed. (F) WT- and NRF2-KO-BMDM were challenged with RBC for 30 min and then chased for 120 min or fed for 180 min. The expression of p62 gene was assessed by RT-qPCR. Data were normalized to the endogenous Hprt and Pgk1 genes. The values are means ± SEM expression levels of three independent experiments, each measured in two technical replicates. *, $p<0.05$. (G) Quantification of LAMP-1-positive phagosomes after fixation and stained for LAMP-1. The values are means ± SEM expression levels of three independent experiments, each measured in two technical replicates. *, $p<0.05$. (H, I) Time-lapse experiments of WT- and NRF2-KO-BMDM challenged with CFSE labeled-RBC for 15 min (0 min chase time) and followed for 300 min further to assess phagosome degradation. Phagosome degradation was analyzed as described in the legend of Fig.6. The values are means ± SD of 10 different phagosomes. *, $p<0.05$; **, $p<0.01$; ***; $p<0.001$ comparing differences between WT- and NRF2-KO-BMDM. (H) DIC images at 0 min and 180 min chase time of WT- and NRF2-KO-BMDM. Arrows point to RBC-containing phagosomes.

To get more mechanistic insights concerning the role of p62 in erythrophagocytosis we questioned whether erythrophagocytosis was associated with NRF2 nuclear translocation and whether this was dependent on p62. As observed in Fig. 7A and quantified in Fig. 7B, NRF2 translocated to the nucleus only in cells that have internalized RBC. This occurred later in the phagocytic process, reaching maxima at 30 min pulse followed by 120 min chase or at 180 min phagocytosis of RBC suggesting that the translocation of this transcription factor occurs only after fusion of phagosomes with

lysosomes and when RBC degradation was already occurring (Fig. 6C and D). The fluorescence intensities ratio of NRF2 on nuclei and cytoplasm was roughly twofold in WT-BMDM exposed to RBC compared to unstimulated controls (Fig. 7A and B). Interestingly, in absence of p62, NRF2 translocation to the nucleus was reduced by 50%, when compared with control cells (Fig. 7A and grey columns in B). Next, we assessed the role of NRF2 on phagosomal maturation and RBC degradation, using BMDM from Nrf2 deficient (*Nrf2*$^{-/-}$ mice. Through the entire maturation process the percentage of p62-positive phagosomes in *Nrf1*$^{-/-}$ BMDM was reduced (Fig. 7C) when compared with *Nrf2*$^{+/+}$ BMDM. This result could be attributed to the lower levels of p62 in *Nrf2*$^{-/-}$ BMDM when compared with *Nrf2*$^{+/+}$ BMDM as shown in the Western Blot (Fig. 7D) and quantified in Fig. 7E. Thus, in erythrophagocytosis, p62 was required for NRF2 nuclear translocation and once there, this transcription factor controlled the levels of the former. Finally, we assessed whether NRF2 nuclear translocation during erythrophagocytosis was associated with p62 transcription (Fig. 7F). p62 expression increased after NRF2 translocation and absence of NRF2 showed a very significant effect on p62 levels (5.93 ± 2.23 *versus* 1.31 ± 1.23) at 180 min erythrophagocytosis. Altogether, these results strongly suggest the existence of a positive feedback between NRF2 and p62.

Transport of RBC-containing phagosomes to the lysosomes was only slightly affected in *Nrf2*$^{-/-}$ BMDM when compared with *Nrf2*$^{+/+}$ BMDM (Fig. 7G), while the effect on RBC degradation was very striking (Fig. 7H and I). These two outcomes were similar to the results obtained in p62 silenced BMDM (Fig. 6D and E) suggesting that p62 and NRF2 are involved in the same pathway.

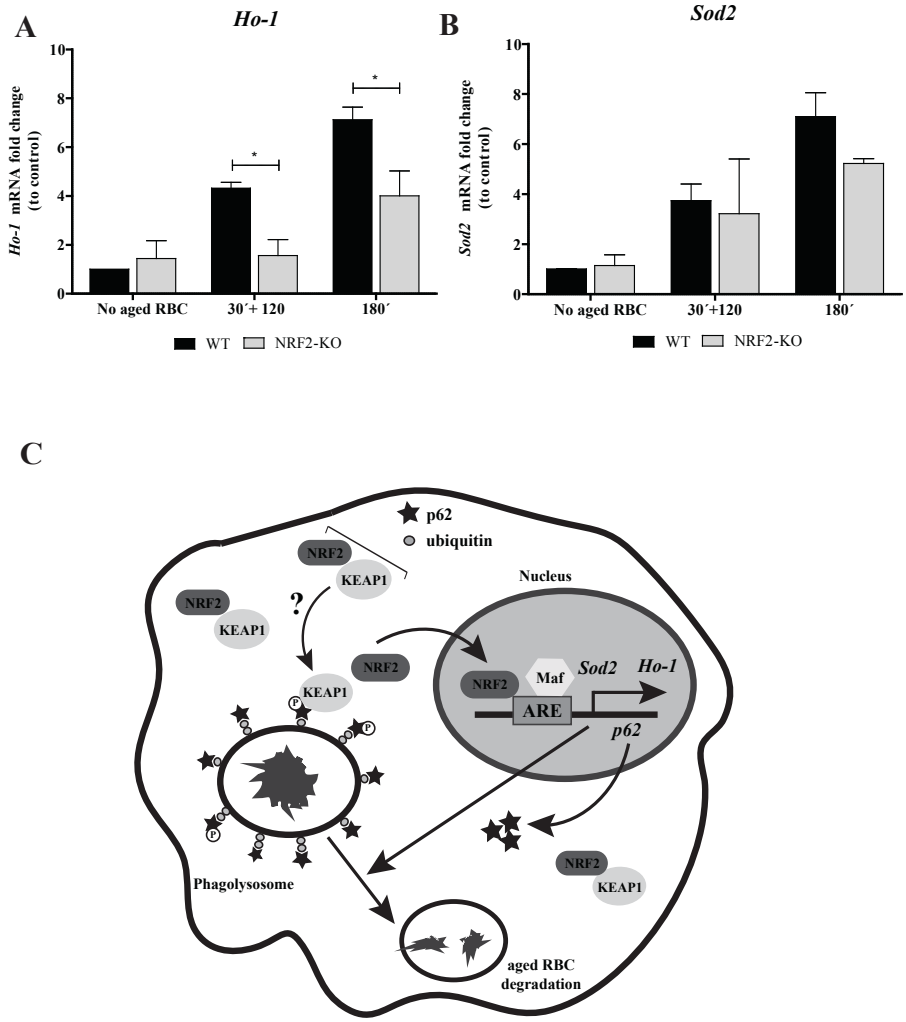

Figure 8. NRF2-target genes expression upon erythrophagocytosis for long time points.

WT and NRF2-KO-BMDM were challenged with RBC for 30 min and then chased for 120 min or fed for 180 min. The expression of HO-1 (A), SOD2 (B) genes was assessed by RT-qPCR. Data were normalized to the endogenous Hprt and Pgk1 genes. The values are means ± SEM expression levels of three independent experiments, each measured in two technical replicates. *, $p<0.05$. (C) Working Model: Our model suggests that degradation of RBC by macrophages is dependent on p62/NRF2 signaling pathway. p62 is recruited to RBC-containing phagosomes shortly after erythrophagocytosis. Then, after phagolysosome formation NRF2 is translocated to the nucleus. This translocation leads to its activation and to

the increase in HO-1, p62 and SOD2 expression. These molecular machinery leads to an oxidative stress impairment promoting RBC degradation.

Since heme is a pro-oxidant molecule, we tested the involvement of NRF2 in the transcription of anti-oxidant genes, including thioredoxin-1, ferritin, glutathione S-transferase, peroxidoxin-1, heme oxygenase 1 (*Hmox1*), catalase, superoxide dismutase (*SOD*) 1 and 2. Among these, only the expression of *HO-1* and *SOD2* were increased after NRF2 translocation in BMDM challenged with RBC (Fig. 8A and B, black bars). As observed in Fig. 8A, in the absence of NRF2 (grey bars) the expression levels of *Hmox1* were reduced compared to WT-BMDM (black bars), after erythrophagocytosis. Although no statistical significances were observed for *SOD2* gene expression (Fig. 8B), it was possible to see a slight difference at 180 min pulse time in *Nrf2*$^{-/-}$ BMDM when compared with *Nrf2*$^{+/+}$ BMDM. Thus, the involvement of NRF2 on *HO-1* and *SOD2* expression can be attributed to the intracellular release of potentially pro-oxidant labile heme, which occurs after RBC degradation within the lysosomes. Accordingly, we conclude that NRF2 is both part of the machinery required for RBC degradation as well as for the anti-oxidative response.

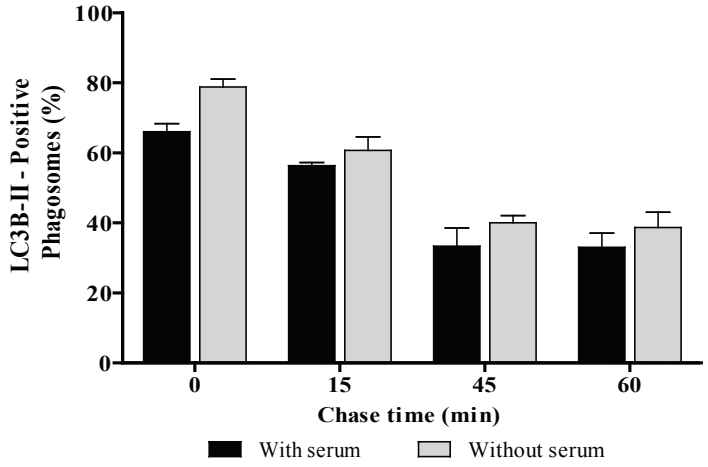

Supplementary Figure 1. Association of LC3 with phagosomal membranes in the absence of serum. Quantification of LC3B-II-positive phagosomes in non-professional phagocytes incubated in medium supplemented (black bars) or not/starved (grey bars) with serum, exposed to RBC and chased for the indicated times. The values are means ± SEM of, at least, three independent experiments. At each time point, at least, 100 phagosomes were analyzed.

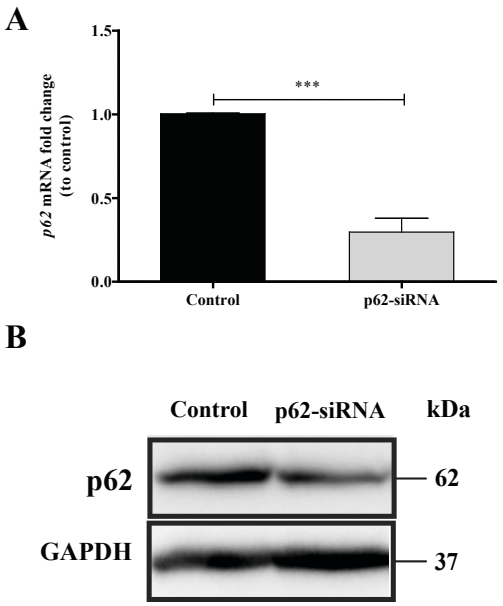

Supplementary Figure 2. Assessment of p62 silencing in BMDM.

(A) p62 mRNA fold change in knockdown versus control cells (transfected with scramble RNAi) was determined by RT-qPCR. Data were normalized to the endogenous HPRT and PGK1 genes. The values are means ± SEM expression levels of four independent experiments, each measured in two technical replicates. ***, $p<0.001$ comparing differences between scramble and knockdown cells. (B) Western Blot of p62 expression levels in knockdown versus control cells (transfected with scramble RNAi). GAPDH was used as loading control.

Discussion

While erythrophagocytosis is critical to the regulation of iron/heme metabolism and maintenance of homeostasis our understanding of the molecular processes underlying the maturation of phagosomes containing RBC and their subsequent degradation by hemophagocytic macrophages is quite rudimentary. In this work we provide some new insights into the biogenesis of phagolysosmes containing RBC, their maturation, and the ordered degradation of RBC in both non-professional and professional phagocytes. We show that the process is complex and involves a convergence of endocytic and autophagic processes. When RBC are phagocytosed, p62 and NRF2 are critical for phagolysosome biogenesis and degradation. Our findings also show that beyond the involvement of LC3, other components of the selective autophagy machinery such as NBR1, NDP52 and p62 are also recruited to the single membrane phagosomes.

Among the selective autophagy machinery tested, the most interesting outcome was observed for p62. This protein is recruited mostly to phagosomes carrying RBC but very weakly to phagosomes containing IgG-opsonized particles, suggesting not only that it has a negligible role in Fc-mediated phagocytosis but also the existence of different types of LAP. The fact that these results were observed in both non-professional and professional phagocytes suggests a conserved role of p62 in RBC-containing phagosomes maturation

and degradation. p62 associates with phagosomal membranes at very early stages of the RBC-phagocytic process, co-localizing with F-actin. We attempted to understand what signals the association of p62 with the phagocytic cups. Among other domains, p62 has a LC3-interacting motif (WXXL/I) called the LC3 recognition sequence (LRS) or the LC3-interacting region (LIR) as well as ubiquitin binding domains[22,46,47]. Our results indicate that p62 is not recruited to phagosomal membranes via interaction with LC3 since this protein associates with the phagosomal membranes after p62 and when F-actin is no longer detected on phagosomes. Using a pharmacological approach, we found that the recruitment of p62 might rely, at least in part, via the interaction of its ubiquitin-binding domain with ubiquitinated components of the phagosomal membranes.

The absence of p62 affects phagolysosome biogenesis with striking effects on RBC degradation. Though p62 has been shown to mediate intracellular xenophagic degradation of bacteria that undergo ubiquitination in response to their escape from phagosomes and subsequent formation of a double membrane organelle[33,35,48], to our knowledge this is the first time that the requirement of p62 for phagocytic cargo degradation within a single membrane organelle is reported. Interestingly, when RBC within the phagolysosome start to be degraded, NRF2 translocates to the nucleus. The translocation of this transcription factor is p62-dependent and in its absence RBC degradation is blocked suggesting that p62 and NRF2 act together to degrade these phagocytic particles. We enquired how and why p62 and NRF2 interact upon erythrophagocytosis. In xenophagy, p62 is translocated to autophagosomes containing invasive *Salmonella* leading to Ser351 phosphorylation in the KIR motif, enhancing the interaction between p62-KEAP1 and consequently NRF2

translocation[49]. Furthermore, under amino acid rich conditions the mammalian Target of Rapamycin Complex 1 (mTORC1) has been identified as one of the kinases responsible for the phosphorylation of p62[42]. Interestingly, NRF2-target genes are induced at the same time that autophagosomes entrap the microbes[49]. Our data, however, reveal a different sequential dynamic of p62 and NRF2 in response to RBC engulfment. In erythrophagocytosis, p62 associates with phagosomal membranes at very early stages while NRF2 is activated later. We propose that once the RBC starts to degrade in the phagolysosome, and their contents are imported into the phagocyte cytosol for storage or recycling, phosphorylation of the p62 residue Ser351 occurs, through an unknown mechanism, culminating with NRF2 translocation to the nucleus and induction of some of its transcriptional targets (Fig.8C). In erythrophagocytosis, we could detect the up-regulation of three well-known NRF2-target genes: p62, Hmox1 and SOD2. The results obtained for p62 confirm the positive feedback that exists between NRF2 and p62 that has been already reported for other experimental settings[43–45]. The up-regulation of the other two genes could result from the products of RBC degradation and reactive oxygen species formation. In erythrophagocytic macrophages, RBC processing is followed by heme release from hemoglobin and its subsequent translocation from the phagolysosome lumen into the cytoplasm, via a mechanism assisted by the heme responsive gene 1 transporter (HRG1)[50,16,51]. Once in the cytosol, the heme catabolism enzyme HO-1 releases iron from the protoporphyrin ring for storage or reuse. Thus, the increase in concentration of cytosolic heme may explain the increase of HO-1 expression. Besides iron extraction from protoporphyrin, HO-1 generates equimolar amounts of biliverdin and carbon monoxide (CO), two anti-oxidant molecules[52,53]. SOD2 up-regulation could be explained by an attempt of the macrophages to scavenge

mitochondrial superoxide and thereby lower oxidative stress. Overproduction of reactive oxygen species has been described to be linked to impaired lysosomal function resulting from changes in cysteine residue of the Atp6v1a1 subunit of vATPase and its subsequent failure in acidifying the lysosomes[54–56]. Since lysosomal pH is a key determinant of lysosomal enzyme activity this could explain why in the absence of NRF2 or p62, RBC are not degraded.

Finally, some autophagy genes (such as Ndp52 and LC3B) as well as Lamp were demonstrated to be upregulated by the NRF2 signaling pathway[57] which in turn can contribute to the rapid degradation of RBC reinforcing the critical role of NRF2 in this process.

Although how the p62/NRF2 pathway modulates the degradation of RBC is far from being elucidated, with this work we reinforce the view that this non-canonical signaling pathway is activated in the absence of oxidative stress or under autophagic conditions[43–45,58,59]. Furthermore, we were able to identify new molecular machinery involved in erythrophagocytosis of RBC, opening new avenues for specific targeting and modulation of this process. This new knowledge may have a critical role in a number of hemolytic disorders associated with defects in RBC function that can lead to premature RBC senescence, such as sickle cell disease. Finally, as PS-exposure on the outer surface of cells is a characteristic of eryptosis and apoptosis, our findings will possibly help to understand in detail the process of apoptotic cells clearance and why this mechanism fails in atherosclerosis and neurodegenerative diseases.

Materials and Methods

Cell culture

Rabbit vascular smooth muscle cells, used as a non-professional phagocytic cell line, were from ATCC (Manassas, VA, USA) and maintained in RPMI-1640 medium (Invitrogen, Carlsbad, CA, USA) containing 10% FBS and 100 U/mL antibiotics. Cells were grown in a humidified incubator at 37oC under 5% CO_2 atmosphere. Cells stably expressing Fcγ-RIIA were generated as described before[18,60]. Cells were plated in 24-multiwell plates at a density of 30 103 cells per well and grown on glass cover slips for 24 h. For experiments with the E1 inhibitor PYR-41 (Calbiochem, San Diego, CA, USA), 20 103 cells were plated per well and 24 h after, the drug was added. L929 cell line (kindly provided by Prof. Ira Tabas, Columbia University, NY, USA) was cultured to produce L-cell conditioned media (LCCM) enriched in M-CSF to differentiate monocytes into macrophages, as previously described[61].

Bone marrow-derived macrophages (BMDM) were obtained from 8-10 week old C57BL/6J wild-type (WT), p62-knockout (kindly provided by Prof. Herbert Virgin, Washington University School of Medicine, St. Louis, MO, USA) and NRF2-KO mice. Primary macrophages were maintained as described 62, but in RPMI- 1640 medium, containing 10% FBS heat inactivated and 30 % LCCM.

Mice were bred and maintained under specific pathogen-free (SPF) conditions, according to protocols approved by local (Instituto Gulbenkian de Ciência) and national (Portuguese Official Veterinary Department; Direcção Geral de Veterinária) ethics committees according to the Portuguese (Decreto-Lei 113/2013) and European (Directive 2010/63/EU) legislations. C57BL/6 *NRF2*$^{-/-}$ mice were provided by the RIKEN BioResource Center (Koyadai, Tsukuba,

Ibaraki, Japan). C57BL/6J wild-type and *NRF2*$^{-/-}$ mice were co-housed from weaning (3-4 weeks old) to the date of the experiments. Red blood cells (RBC) were obtained from human blood collected from healthy volunteers at CNC and CEDOC. Written informed consent was obtained from all volunteers and approved by the Ethical Review Board of the Faculty of Medicine of the University of Coimbra and NOVA Medical School. RBC were isolated and aged as described before[18].

Phagocytosis and phagosomal maturation assays

Aged RBC (RBC) and IgG-opsonized latex beads were prepared as described before[18] as were phagocytosis and phagosomal maturation assessment (pulse-chase) experiments. In pulse-chase experiments the pulse time was 30 min for non-professional phagocytes and 15 min for BMDM, followed by the chase times indicated in the graphs abscissa. Phagocytosis experiments with PYR-41 were performed as follows: the inhibitor was added to phagocytes at final concentrations of 5 and 10 μM, for experiments with RBC and IgG-opsonized particles, respectively, overnight. PYR-41 was present throughout the pulse-chase experiments. When the purpose of the experiment was the visualization of phagocytic cups, the phagocytic cells were challenged with phagocytic particles without synchronization and without lysis of RBC.

RNAi experiments

To knockdown p62 also known as (SQSTM1 or Sequestosome) in BMDM, a siRNA smart pool against p62 and a non-targeting sequence siRNA, scramble, (control) were used (GE Dharmacon, Lafayette, CO, USA). BMDM were transfected with Lipofectamine RNAiMAX (Invitrogen, Carlsbad, CA, USA) according to the manufacturer's instructions. Experiments to assess RBC

degradation were performed 72 h after transfection with siRNAs.

Immunofluorescence and microscopy

Monoclonal antibodies used were: Lysosomal associated membrane protein-1 (LAMP-1) (1:50, Hybridoma Bank, Iowa City, IA, USA), Neighbor of BRCA1 gene1 [NBR1, (1:80, Abnova, Heidelberg, Germany)] and Nuclear factor (erythroid-derived 2)-like 2 [NRF2, (1:50, Cell Signaling, Danvers, MA, USA)]. Polyclonal antibodies used were: LC3B-II (1:100, Cell Signaling, Taipei, Neihu, Taiwan), p62 C-term (1:80, Abgent, San Diego, CA, USA), Nuclear dot protein 52 [NDP52, (1:80, Abcam, Cambridge, UK)], and Ubiquitin (1:50, DAKO, Via Real Carpinteria, CA, USA). For immunoflourescence (IF), cells were fixed with 4% PFA for 30 min, permeabilized using 0.1% Triton X-100 (with 200 nM glycine) for 30 min and blocked with 0.5% Gelatin from cold water fish skin in PBS for 30 min. The exception was for LAMP-1 staining in which cells were permeabilized using methanol for 10 min and for NRF2 in which permeabilization and blocking were performed with 0.25% Triton X-100 and 1% BSA/10% FBS in 1X PBS/0.1% Tween-20, respectively. Then, the cells were incubated with the appropriate primary antibody for 90 min at room temperature (RT), followed by incubation with secondary antibody (1:800, from Jackson Immunoresearch, West Grove, PA, USA) for 1 h at RT. For visualization of phagocytic cups, phalloidin conjugated with Cy5 (1:100, Invitrogen), to stain F-actin, was added with the secondary antibodies. Stained samples were mounted with Mowiol/DABCO (Calbiochem) and analyzed by using a laser scanning confocal microscope (Carl Zeiss, Jena, Germany, LSM 510 software) or a Zeiss Cell Observer with a 63× oil immersion objective (NA = 1.30). The images were analyzed by using LSM Image Browser, Image-J software or Zen software. For live-cell imaging, BMDM were seeded in 35 mm glass bottom microwell petri dishes

(MatTEK Corporation, Ashland, MA, USA) after differentiation and p62-silencing, BMDM were incubated for 15 min with RBC. After this time, non-internalized cells were lysed and the disappearance of Carboxyfluorescein-diacetate-Succinimidyl Ester (CFSE) fluorescence intensity was followed as a function of time under a Carl Zeiss LSM 710 META laser scanning confocal microscope (ZEN software) using a 63× oil immersion objective (NA = 1.30), at 37°C in CO2-independent medium. Fluorescence intensity of RBC containing phagosomes at 15 min pulse was normalized to 100.

Quantitative PCR

p62, SOD2 and HO-1 were assessed by quantitative real-time PCR (qPCR). Total RNA was isolated using the NZY Total RNA Isolation kit (NZYTech, Lisbon, Portugal), and 300 ng were reverse transcribed with iScript® cDNA synthesis kit (Bio-Rad, Hercules, CA, USA), according to the manufacturer's protocols.

Primers sequence: p62, Forward 5´-GTCTTCTGTGCCTGTGCTGGAA -3´, Reverse 5´-TCTGCTCCACCAGAAGATCCCA -3´; HO-1, Forward 5´-AAGGAGGTACACATCCAAGCCGAG -3´, Reverse 5´-GATATGGTACAAGGAAGCCATCACCAG -3´; SOD2, Forward 5´ -TAAGGGTGGTGGAGAACCCAAAGGAG -3´, Reverse 5´-TTATTGAAGCCAAGCCAGCCCCAG -3´; Pgk1, Forward 5´-ATGGATGAGGTGGTGAAAGC -3´, Reverse 5´-CAGTGCTCACATGGCTGACT-3´. Hypoxanthine phosphoribosyltransferase 1, Hprt1, (QIAGEN, Hilden, Germany) and Pgk1 (Sigma-Aldrich, St.Louis, MO, USA) were used as housekeeping genes. The p62, SOD2 and HO-1 mRNA levels were calculated by the Pfaffl method and normalized to both Hprt1 and Pgk1 mRNA levels.

Western blot

For preparation of the total protein cell lysates, cells were lysed and blotted as described 63. The antibodies incubated in TBS were: mouse p62 primary antibody (Clone 2C11, Abnova, Heidelberg, Germany) and ECL mouse HRP-conjugated secondary antibody (GE Healthcare, Little Chalfont, UK); mouse α-Tubulin primary antibody (Sigma-Aldrich) and Goat Anti-mouse HRP-conjugated secondary antibody (Bio- Rad, Hercules, CA, USA); and goat GAPDH primary antibody (Sicgene, Cantanhede, Portugal) and Rabbit Anti-Goat HRP-conjugated secondary antibody (Bio-Rad). Blots were developed with ECL (GE Healthcare). ChemiDocTM Touch Imaging System was used to detect fluorescence and bands quantification was performed using Image Lab software (Bio-Rad).

Statistical analysis

Statistical analysis (t-test or Two-way ANOVA followed by Bonferroni post-test) was performed using the GraphPad PRISM software version. 5.0. $p < 0.05$ (*), $p < 0.01$ (**) and $p < 0.001$ (***) were considered to be statistically significant.

References

1. Gottlieb, Y. et al. Physiologically aged red blood cells undergo erythrophagocytosis in vivo but not in vitro. Haematologica 97, 994–1002 (2012).
2. Lee, S. J., Park, S. Y., Jung, M. Y., Bae, S. M. & Kim, I. S. Mechanism for phosphatidylserine-dependent erythrophagocytosis in mouse liver. Blood 117, 5215–5223 (2011).
3. Fens, M. H. A. M. et al. A role for activated endothelial cells in red blood cell clearance: Implications for vasopathology. Haematologica 97, 500–508 (2012).
4. Soares, M. P. & Hamza, I. Macrophages and Iron Metabolism. Immunity 44, 492–504 (2016).
5. Lutz, H. U. & Bogdanova, A. Mechanisms tagging senescent red blood cells for clearance in healthy humans. Front. Physiol. 4 DEC, 1–15 (2013).
6. Terpstra, V. & van Berkel, T. J. C. Scavenger receptors on liver Kupffer cells mediate the in vivo uptake of oxidatively damaged red blood cells in mice. Blood 95, 2157–2163 (2000).

7. Kim, S. et al. Cross Talk between Engulfment Receptors Stabilin-2 and Integrin v 5 Orchestrates Engulfment of Phosphatidylserine-Exposed Erythrocytes. Mol. Cell. Biol. 32, 2698–2708 (2012).
8. Antonelou, M. H., Kriebardis, A. G. & Papassideri, I. S. Aging and death signalling in mature red cells: From basic science to transfusion practice. Blood Transfus. 8, 39–47 (2010).
9. Kinchen, J. M. & Ravichandran, K. S. Phagosome maturation: going through the acid test. Nat. Rev. Mol. Cell Biol. 9, 781–95 (2008).
10. Vieira, O. V, Botelho, R. J. & Grinstein, S. Phagosome maturation: aging gracefully. Biochem. J. 366, 689–704 (2002).
11. Martinez, J. et al. Microtubule-associated protein 1 light chain 3 alpha (LC3)-associated phagocytosis is required for the efficient clearance of dead cells. Proc. Natl. Acad. Sci. U. S. A. 108, 17396–17401 (2011).
12. Martinez, J. et al. Molecular characterization of LC3-associated phagocytosis reveals distinct roles for Rubicon, NOX2 and autophagy proteins. Nat. Cell Biol. 17, 893–906 (2015).
13. Henault, J. et al. Noncanonical Autophagy Is Required for Type I Interferon Secretion in Response to DNA-Immune Complexes. Immunity 37, 986–997 (2012).
14. Florey, O. & Overholtzer, M. Autophagy proteins in macroendocytic engulfment. Trends in Cell Biology 22, 374–380 (2012). Huang, J. et al. Activation of antibacterial autophagy by NADPH oxidases. Proc. Natl. Acad. Sci. U. S. A. 106, 6226–6231 (2009).
15. White, C. et al. HRG1 is essential for heme transport from the phagolysosome of macrophages during erythrophagocytosis. Cell Metab. 17, (2013).
16. Soares, M. P. & Hamza, I. Macrophages and Iron Metabolism. Immunity 44, 492–504 (2016).
17. Viegas, M. S., Estronca, L. M. B. B. & Vieira, O. V. Comparison of the Kinetics of Maturation of Phagosomes Containing Apoptotic Cells and IgG-Opsonized Particles. PLoS One 7, (2012).
18. Zhou, Z. & Yu, X. Phagosome maturation during the removal of apoptotic cells: receptors lead the way. Trends in Cell Biology 18, 474–485 (2008).
19. Knutson, M. & Wessling-resnick, M. Iron Metabolism in the Reticuloendothelial. 38, 61–88 (2003).
20. Kay, M. M. Mechanism of removal of senescent cells by human macrophages in situ. Proc. Natl. Acad. Sci. U. S. A. 72, 3521–3525 (1975).
21. Bjørkøy, G. et al. p62/SQSTM1 forms protein aggregates degraded by autophagy and has a protective effect on huntingtin-induced cell death. J. Cell Biol. 171, 603–614 (2005).
22. Kirkin, V., Lamark, T., Johansen, T. & Dikic, I. NBR1 cooperates with p62 in selective autophagy of ubiquitinated targets. Autophagy 5, 732–733 (2009).
23. Thurston, T. L. M., Ryzhakov, G., Bloor, S., von Muhlinen, N. & Randow, F. The TBK1 adaptor and autophagy receptor NDP52 restricts the proliferation of ubiquitin-coated bacteria. Nat. Immunol. 10, 1215–1221 (2009).
24. Bosman, G. J. C. G. M. Survival of red blood cells after transfusion: Processes and consequences. Frontiers in Physiology 4 DEC, (2013).
25. Lang, K. S. et al. Mechanisms of suicidal erythrocyte death. Cellular Physiology and Biochemistry 15, 195–202 (2005).
26. Florey, O., Kim, S. E., Sandoval, C. P., Haynes, C. M. & Overholtzer, M. Autophagy machinery mediates macroendocytic processing and entotic cell death by targeting single membranes. Nat. Cell Biol. 13, 1335–43 (2011).

27. Kabeya, Y. et al. LC3, GABARAP and GATE16 localize to autophagosomal membrane depending on form-II formation. J Cell Sci 117, 2805–2812 (2004).
28. Kabeya, Y. et al. LC3, GABARAP and GATE16 localize to autophagosomal membrane depending on form-II formation. J Cell Sci 117, 2805–2812 (2004).
29. Booth, J. W., Kim, M. K., Jankowski, A., Schreiber, A. D. & Grinstein, S. Contrasting requirements for ubiquitylation during Fc receptor-mediated endocytosis and phagocytosis. EMBO J. 21, 251–258 (2002).
30. Deretic, V., Saitoh, T. & Akira, S. Autophagy in infection, inflammation and immunity. Nat Rev Immunol 13, 722–737 (2013).
31. Lee, W. L., Kim, M.-K., Schreiber, A. D. & Grinstein, S. Role of ubiquitin and proteasomes in phagosome maturation. Mol. Biol. Cell 16, 2077–2090 (2005).
32. Romao, S. & M??nz, C. LC3-associated phagocytosis. Autophagy 10, 526–528 (2014).
33. Zheng, Y. T. et al. The adaptor protein p62/SQSTM1 targets invading bacteria to the autophagy pathway. J. Immunol. 183, 5909–5916 (2009).
34. Dupont, N. et al. Shigella Phagocytic Vacuolar Membrane Remnants Participate in the Cellular Response to Pathogen Invasion and Are Regulated by Autophagy. Cell Host Microbe 6, 137–149 (2009).
35. Yoshikawa, Y. et al. Listeria monocytogenes ActA-mediated escape from autophagic recognition. Nat. Cell Biol. 11, 1233–1240 (2009).
36. Hoffmann, P. R. et al. Phosphatidylserine (PS) induces PS receptor-mediated macropinocytosis and promotes clearance of apoptotic cells. J. Cell Biol. 155, 649–659 (2001).
37. Yang, Y. et al. Inhibitors of ubiquitin-activating enzyme (E1), a new class of potential cancer therapeutics. Cancer Res. 67, 9472–9481 (2007).
38. Lamark, T. et al. Interaction Codes within the Family of Mammalian Phox and Bem1p Domain- containing Proteins. J. Biol. Chem. 278, 34568–34581 (2003).
39. Suzuki, T., Motohashi, H. & Yamamoto, M. Toward clinical application of the Keap1-Nrf2 pathway. Trends in Pharmacological Sciences 34, 340–346 (2013).
40. Hayes, J. D. & Dinkova-Kostova, A. T. The Nrf2 regulatory network provides an interface between redox and intermediary metabolism. Trends Biochem. Sci. 39, 199–218 (2014).
41. Dinkova-Kostova, A. T. & Abramov, A. Y. The emerging role of Nrf2 in mitochondrial function. Free Radic. Biol. Med. 88, 179–188 (2015).
42. Ichimura, Y. et al. Phosphorylation of p62 Activates the Keap1-Nrf2 Pathway during Selective Autophagy. Mol. Cell 51, 618–631 (2013).
43. Jain, A. et al. p62/SQSTM1 is a target gene for transcription factor NRF2 and creates a positive feedback loop by inducing antioxidant response element-driven gene transcription. J. Biol. Chem. 285, 22576–22591 (2010).
44. Komatsu, M. et al. The selective autophagy substrate p62 activates the stress responsive transcription factor Nrf2 through inactivation of Keap1. Nat. Cell Biol. 12, 213–223 (2010).
45. Lau, A. et al. A noncanonical mechanism of Nrf2 activation by autophagy deficiency: direct interaction between Keap1 and p62. Mol. Cell. Biol. 30, 3275–3285 (2010).
46. Pankiv, S. et al. p62/SQSTM1 binds directly to Atg8/LC3 to facilitate degradation of ubiquitinated protein aggregates by autophagy*[S]. J. Biol. Chem. 282, 24131–24145 (2007).
47. Noda, N. N., Ohsumi, Y. & Inagaki, F. Atg8-family interacting motif crucial for selective autophagy. FEBS Letters 584, 1379–1385 (2010).

48. Mostowy, S. et al. p62 and NDP52 proteins target intracytosolic Shigella and Listeria to different autophagy pathways. J. Biol. Chem. 286, 26987–26995 (2011).
49. Ishimura, R., Tanaka, K. & Komatsu, M. Dissection of the role of p62/Sqstm1 in activation of Nrf2 during xenophagy. FEBS Lett. 588, 822–828 (2014).
50. Rajagopal, A. et al. Haem homeostasis is regulated by the conserved and concerted functions of HRG-1 proteins. Nature 453, 1127–1131 (2008).
51. White, C. et al. NIH Public Access. 17, 261–270 (2014).
52. Korolnek, T. & Hamza, I. Blood Spotlight Macrophages and iron traf fi cking at the birth and death of red cells. 125, 2893–2898 (2015).
53. Gozzelino, R. & Arosio, P. Iron homeostasis in health and disease. Int. J. Mol. Sci. 17, 2–14 (2016).
54. Feng, Y. & Forgac, M. Inhibition of vacuolar H+-ATPase by disulfide bond formation between cysteine 254 and cysteine 532 in subunit A. J. Biol. Chem. 269, 13224–13230 (1994).
55. Li, Z., Berk, M., McIntyre, T. M., Gores, G. J. & Feldstein, A. E. The lysosomal-mitochondrial axis in free fatty acid-induced hepatic lipotoxicity. Hepatology 47, 1495–1503 (2008).
56. Pivtoraiko, V. N., Stone, S. L., Roth, K. A. & Shacka, J. J. Oxidative stress and autophagy in the regulation of lysosome-dependent neuron death. Antioxid. Redox Signal. 11, 481–496 (2009).
57. Pajares, M. et al. Transcription factor NFE2L2/NRF2 is a regulator of macroautophagy genes. Autophagy 1–15 (2016). doi:10.1080/15548627.2016.1208889
58. Fan, W. et al. Keap1 facilitates p62-mediated ubiquitin aggregate clearance via autophagy. Autophagy 6, 614–621 (2010).
59. Copple, I. M. et al. Physical and functional interaction of sequestosome 1 with Keap1 regulates the Keap1-Nrf2 cell defense pathway. J. Biol. Chem. 285, 16782–16788 (2010).
60. Cardoso, C. M. P., Jordao, L. & Vieira, O. V. Rab10 regulates phagosome maturation and its overexpression rescues Mycobacterium-containing phagosomes maturation. Traffic 11, 221–235 (2010).
61. Warren, M. K. & Vogel, S. N. Bone marrow-derived macrophages: development and regulation of differentiation markers by colony-stimulating factor and interferons. J. Immunol. 134, 982–9 (1985).
62. Oliveira, M. S. et al. Infection with Mycobacterium ulcerans induces persistent inflammatory responses in mice. Infect. Immun. 73, 6299–6310 (2005).
63. Choi, S. Il et al. Lysosomal trafficking of TGFBIp via Caveolae-mediated endocytosis. PLoS One 10, (2015).

Acknowledgements

We would like to thank Prof. Ira Tabas (Columbia University, New York, NY, USA) for providing the L929 cell line, Prof. Herbert Virgin (Washington University, St. Louis, MO, USA) for providing p62-KO mice legs, Dr. H. Girão (CNC.IBILI, Univ. of Coimbra) for the E1-inhibitor, T. Pereira for technical assistance with microscopy and

N. Domingues for collecting the human blood.

This work was supported by the Foundation for Science and Technology of the Portuguese Ministry of Science and Higher Education [HMSP-ICT/0024/2010, co-founded by the European Union (FEDER – Fundo Europeu de Desenvolvimento Regional) through COMPETE – Programa Operacional Factores de Competitividade and QREN – Quadro de Referência Estratégico], iNOVA4Health - UID/Multi/04462/2013, a program financially supported by FCT through national funds and co-funded by FEDER under the PT2020 Partnership Agreement and FCT to OVV.

PhD fellowships references: SFRH/BD/62197/2009, SFRH/BD/90258/2012 and SFRH /BD/51877/2012. PTDC/SAU-TOX/116627/2010, HMSP-ICT/0022/2010, European Community 7th Framework Grant ERC- 2011-AdG 294709-DAMAGECONTROL to MPS.

Author contributions

Conceived and designed the experiments: IBS, MSV, AMR, MPS and OVV; Performed the experiments: IBS, MSV; Analyzed the data: IBS, MSV, MPS and OVV; Contributed reagents/materials/analysis tools: AMR, MPS and OVV; Wrote the paper: IBS, MSV, MPS and OVV.

The authors declare no competing financial interests.

Appendix 2

"If you can dream it, you can do it. Always remember that this whole thing was started with a dream and a mouse."
(Walt Disney)

Nrf2 as a master regulator of tissue damage control and disease tolerance to infection

Miguel P. Soares[*1] and **Ana M. Ribeiro**[*]

Biochem. Soc. Trans. (2015) 43, 663-668;
doi:10.1042/BST20150054 (Adapted)

[*]Instituto Gulbenkian de Ciência, Rua da Quinta Grande, 62, 6, 2780-156 Oeiras, Portugal; [1]To whom correspondence should be addressed: Miguel P. Soares; Inflammation group, Instituto Gulbenkian de Ciência, Rua da Quinta Grande, Oeiras, Portugal, Tel.: +351-214464520, Email: mpsoares@igc.gulbenkian.pt

Key words: Disease tolerance, infection, Nrf2, oxidative stress, tissue damage control.

Resistance to infection defines a defense strategy that limits host disease severity via immune driven mechanisms that target pathogens for expulsion, containment or killing. Disease tolerance defines a distinct defense strategy that limits host disease severity without however, targeting pathogens[1,2,3]. Described originally in plants[4], disease tolerance is operational in flies[5,6,7] and mammals, including in mice[8,9] as well as in humans[10]. The term disease tolerance is used hereby to refer explicitly to the defense strategy defined originally in the plant literature[1,4], which limits host 'damage to functions and structures[4] imposed by infection, without interfering with host pathogen load[1,4].

Disease tolerance is regulated by a number of evolutionarily conserved stress and/or damage responses. These confer tissue damage control, i.e. prevent 'damage to functions and structures' imposed by infection[11,4]. Presumably, stress and/or damage responses evolved from ancestral forms of life where they provided cellular adaptation to environmental changes[12]. Much like resistance mechanisms, these adaptive responses evolved, most probably, under the selective pressure imposed by host microbe interactions.

Resistance mechanisms can elicit, per se, varying levels of cellular stress and damage to the host parenchyma, as illustrated for innate immune responses associated with the production of reactive oxygen species (ROS) and/or reactive nitrogen species (RNS). This is coupled to a countervailing oxidative stress response regulated by nuclear factor-erythroid 2-related factor 2 (Nrf2), a member of the cap'n'collar basic leucine zipper family transcription factor characterized structurally by the presence of Nrf2–ECH homology domains[13]. Other members of this family include NF–E2 p45, NRF1 and NRF3[13].

Mechanisms regulating Nrf2 activation in the context of infection

Engagement of pattern recognition receptors (PRRs) by pathogen-associated molecular patterns (PAMP) activates Nrf2 in innate immune cells such as monocytes/macrophages (Mø). For example, lipopolysaccharide (LPS) recognition by toll-like receptor 4 (TLR4) triggers the transcrip- tion/expression of the inducible form of nitric oxide synthase (iNOS/NOS2), via a mechanism involving the adaptor molecule Myd88 (myeloid differentiation primary response gene 88) and the transcription factor nuclear factor kappa B (NF-κB)[14]. The TLR4–MyD88–NF-κB signal transduction pathway also triggers the transcription/expression of the phagocytic NADPH oxidase (NOX2/gp91phox)[15], which generates intracellular superoxide ($O_2^{\cdot -}$). The NO generated by iNOS reacts with $O_2^{\cdot -}$ and produces peroxinitrate ($ONNO^-$) anions, which targets several thiol-based (S-H) redox systems, including reactive cysteines in the Kelch-like ECH-associated protein 1 (Keap1)[12,16,17] (Figure 1). Keap1 is an adaptor for the cullin (Cul)3– RING (really interesting new gene)-box protein (Rbx)1 ubiquitin ligase complex, which targets Nrf2 constitutively for proteolytic degradation by the 26s proteasome[12].

Under oxidative stress, some of the reactive cysteines of Keap1, i.e. Cys151 are targeted by $ONNO^-$, generating thiol oxidation products and ultimately forming disulfide bonds[18]. These alter the tertiary structure of Keap1, inhibiting its ubiquitin ligase activity and Nrf2 degradation[12,16,17]. The newly transcribed Nrf2 undergoes nuclear translocation and binds to small musculoaponeurotic fibrosarcoma (sMaf) transcription factors, including MafF, MafG and MafK[13], driving the transcription of Nrf2-responsive genes containing DNA antioxidant responsive elements (AREs) in their promoter[12]

(Figure 1). In addition, NF-κB also acts directly on the Nrf2 promoter to induce Nrf2 transcription[12], presumably required to sustain Nrf2-dependent gene expression (Figure 2). It is now clear that other E3 ubiquitin ligase complexes contribute to integrate Nrf2 activation within different forms of cellular stress[12]. These include the Skp1 (S-phase kinase-associated protein 1)–Cul1–F-box (SCF)–β-transducin repeats-containing proteins (β-TrCP) complex (SCFβ-TrCP)[19], which recognizes the Neh6 (Nrf2-ECH homology 6) domain of Nrf2 when phophorylated by the glycogen synthase kinase 3 (GSK3)[19]. Presumably, Nrf2 phosphorylation at the Neh6 domain allows for coupling of different forms of stress sensed by GSK3 with Nrf2 ubiquitination by the SCFβ-TrCP complex and its degradation by the 26s proteasome[12,19] (Figure 1). The HMG (high mobility group)-coA reductase degradation 1 (Hrd1) E3 ubiquitin–protein ligase involved in endoplasmic reticulum- associated protein degradation (ERAD) also controls Nrf2 activation[20]. Hrd1 targets the Nhe4–5 domain of Nrf2 for ubiquitination and degradation by the 26s proteasome[20] (Figure 1). How Hrd1 acts in the context of other components of the endoplasmic reticulum stress response, such as the protein kinase RNA-like ER kinase 1 (PERK1)[21], to regulate Nrf2 is not clear. It is worth noting that Nrf2 activity is controlled to a large extent by its rate of transcription/expression (Figure 1). This is regulated by several transcription factors including NF-κB and Nrf2 itself, as well as clock components that impose a circadian control to Nrf2 activity[22] (Figure 1).

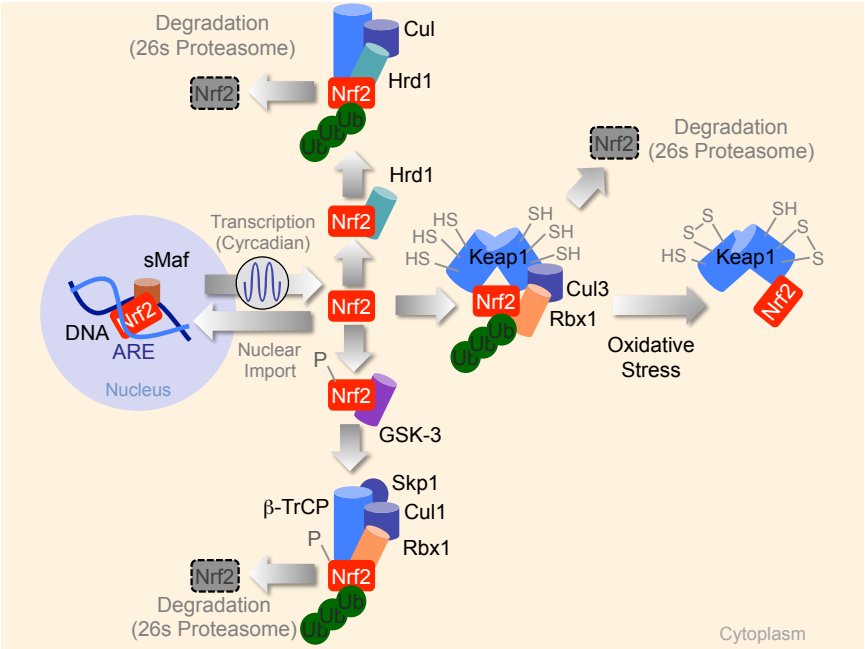

Figure 1. Control of Nrf2 activation by different E3 ubiquitin ligase complexes.

Acronyms are defined throughout the text. When no longer targeted for degradation by E3 ubiquitin ligase complexes, Nrf2 activity is controlled mainly by its rate of transcription, with newly transcribed Nrf2 regulating gene expression. It is the Keap1–Cul3–Rbx1, Hrd1 E3 ubiquitin ligase and SCFβ-TrCP complexes, however that underlies the stress responsive nature of Nrf2 activity.

Nrf2 and resistance to infection

Perhaps the best demonstration that Nrf2 modulates host resistance to infection is provided by the observation that deletion of the Nrf2 allele in mice enhances resistance to Marburg virus infection[23]. This effect is mediated by the Marburg virus encoded VP24 protein, which binds the Kelch domain of Keap1 and inhibits the ubiquitin ligase activity of the Keap1–Cul3–Rbx1 complex, hence inducing Nrf2 activation[23,24]. Several other observations are consistent with the notion that viruses induce host Nrf2 activation in vitro, as suggested

for Kaposi's sarcoma-associated herpes virus[25], as well as for Influenza[26,27] and dengue[28] viruses. However, the pathophysiologic relevance of these observations remains to be elucidated. Conversely, other viruses such as hepatitis C virus, down-regulate Nrf2 activation via a mechanism impairing its nuclear import through delocalization of sMaf proteins[29]. The impact of this phenomenon to the outcome of hepatitis C virus infection is also not clear. Intracellular bacteria also modulate Nrf2 activation, as demonstrated for *Salmonella typhimurium* infection in Mø[30]. Activation of Nrf2 enforces the transcription/expression of Ferroportin-1, an iron exporter that decreases iron cellular content[30]. This limits *Salmonella* access to iron, restraining the proliferation of this intracellular pathogen[30]. Whether Nrf2 acts under pathophysiologic conditions to promote resistance to *Salmonella* infection is likely, but this remains to be formally demonstrated[30]. Pharmacologic activation of Nrf2 by sulforaphane promotes resistance to *Pseudomonas aeruginosa*[31] as well as to *Plasmodium* infection in mice[32].

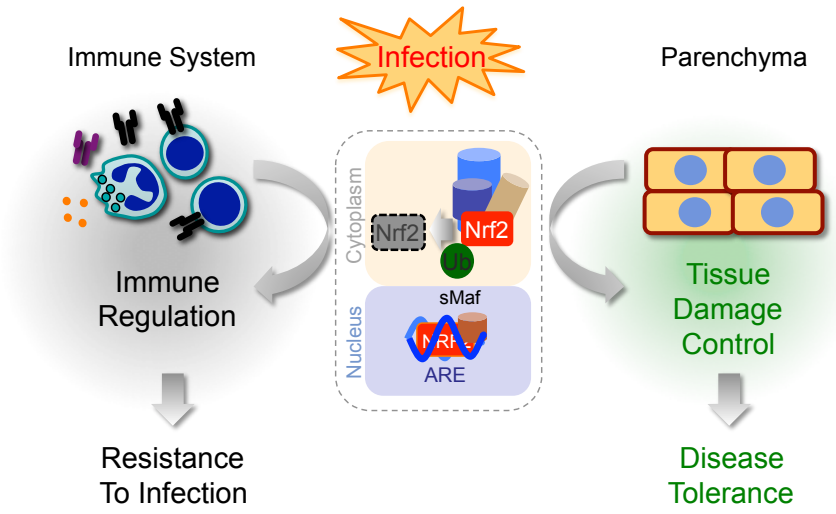

Figure 2. Outcomes of Nrf2 activation.
Upon infection, activation of Nrf2 in different cellular components of the immune system acts in an immunoregulatory manner, which modulates resistance to infection. Activation of Nrf2 in parenchyma tissues provides tissue damage control and disease tolerance to infection. Control of Nrf2 activation is illustrated in the context of a generic E3 ubiquitin ligase complex, detailed under Figure 1.

Nrf2 and disease tolerance to infection

The Nrf2 signal transduction pathway can be co-opted to confer tissue damage control and disease tolerance to systemic infections. One of the mechanisms via which this occurs involves the establishment of a functional crosstalk between the gasotransmitters nitric oxide (NO) and carbon monoxide (CO), as illustrated for *Plasmodium* infection[33,34]. When applied pharmacologically both NO[34,35,36] and CO[33,37,38] suppress the development of experimental cerebral malaria in mice, a lethal form of severe malaria that resembles, in many aspects, human cerebral malaria[39]. This protective effect acts via Nrf2 activation by NO[40], presumably via a mechanism targeting Keap1 at Cys151[12,41]. Nrf2 activation induces HO-1 expression and the production of CO via heme catabolism by HO-1. CO acts as the gasotransmitter suppressing the onset of experimental cerebral malaria[40]. This occurs via a mechanism involving the binding of CO to the prosthetic heme group of cell free hemoglobin generated during the blood stage of *Plasmodium* infection, preventing heme from participating in the pathogenesis of experimental cerebral malaria[40,33,37,38]. The protective effect exerted by the NO->Nrf2->HO-1->CO signal transduction pathway is not associated with modulation of host pathogen load, suggesting that the cross talk established between these two gasotransmitters

confers disease tolerance to *Plasmodium* infection via a mechanism regulated by Nrf2[1,40].

Presumably, the mechanism via which Nrf2 confers tissue damage control and disease tolerance to malaria also involves the expression of Nrf2-responsive genes regulating heme/iron metabolism[42]. These include the iron storage protein Ferritin H chain (FtH)[43,44], which confer tissue damage control and disease tolerance to malaria in mice[10]. There is further evidence that argues strongly for the central role of the Nrf2 signal transduction pathway in the establishment of disease tolerance to *Plasmodium* infection. In a similar manner to humans carrying hemizygous sickle mutations in the beta chain of hemoglobin, transgenic sickle mice are protected from cerebral malaria[37]. This protective effect is exerted irrespectively of parasite load, revealing that sickle hemoglobin can confer disease tolerance to *Plasmodium* infection[1,37]. Sickle hemoglobin induces HO 1 through Nrf2, leading to the production of CO, which confers disease tolerance to malaria[37,38]. Whether this mechanism explains how sickle hemoglobin protects humans from malaria remains to be established but is likely to be the case. It is probable that chronic hemolytic episodes driven by red blood cell mutations act as a general protective mechanism against malaria in human populations, such as illustrated for hemoglobin C[45,46], glucose 6 phosphate dihydrogenase (G6PD) deficiency in males[47], β- or α thalassemia[46] that confer protection against severe anemia caused by *P. falciparum* infection as well as for other red blood cell cytoskeleton or membrane protein defects[48]. Presumably, this protective effect is mediated via different mechanisms that converge at the level of Nrf2 activation. Therefore it is possible that sickle hemoglobin and probably other red blood cell mutations co-evolved with the Nrf2 signal transduction pathway to limit disease severity associated with these mutations while conferring protection against

malaria, such as illustrated for the sickle hemoglobin[37]. There is circumstantial evidence to suggest that Nrf2 confers disease tolerance to systemic infections, other than malaria. Namely, Nrf2 is protective against endotoxic shock[49], severe sepsis triggered by polymicrobial infection[49] and lung injury induced by *Staphylococcus aureus* infection[50] in mice. These salutary effects have been associated mainly with immunoregulation but there is no clear evidence whether Nrf2 modulates pathogen load in these specific experimental settings[49]. We have experimental evidence confirming that Nrf2 prevents the lethal outcome of polymicrobial sepsis in mice, without, however, interfering with pathogen load (A. M. Ribeiro and S. Weis et al., unpublished observation). This suggests that Nrf2 can confer disease tolerance to infection, presumably acting as an immunoregulatory transcription factor in innate immune cells, but likely also in parenchyma cells to provide tissue damage control, although this remains to be fully established.

Mechanisms underlying the protective effect of Nrf2 against infection

There is a general consensus that Nrf2 is protective against systemic infections, via a mechanism targeting NF-κB and modulating pro-inflammatory gene expression in Mø[49,51] (Figure 2). However, Nrf2 activation is required to sustain interleukin (IL)-1β secretion in Mø, via a mechanism involving NLRP3 (NACHT, LRR and PYD domains-containing protein 3) driven caspase 1 activation, an essential step in the processing of pro-IL-1β towards IL-1β secretion[52]. This would argue that Nrf2 promotes, rather than restrains, inflammation. Moreover, Nrf2 induces the expression of the activating transcription factor 3 (ATF3) in Mø, an IL-6 repressor that is protective against LPS but highly deleterious against bacterial infection[53]. This

suggests that Nrf2 can also act in a deleterious manner in the context of systemic bacterial infections (Figure 2). Oxidative stress can trigger parenchyma cells to undergo regulated necrosis[54], leading to tissue damage and organ dysfunction, eventually compromising disease tolerance to infection[11]. Therefore, host protective mechanisms that prevent parenchyma cells from undergoing regulated necrosis, such as those driven by Nrf2, should enforce tissue damage control and disease tolerance to systemic infections[11] (Figure 2). Presumably, this occurs via the expression of Nrf2 regulated effector genes, such as those controlling glutathione synthesis/conjugation[12,17], heme metabolism, i.e. HO-1[55,56,57] iron metabolism, e.g. FtH[58,59], ferroportin-1[30] and/or lipid peroxidation, e.g. biliverdin reductase[60]. Other mechanisms underlying the protective effects of Nrf2 were linked to maintenance of mitochondrial function[50].

Trade-off of the stress response given by Nrf2

Disease tolerance mechanisms do not exert a negative impact on pathogens. As such, stress responses underlying disease tolerance create a situation in which the infected host, although healthy, can transmit the disease. This has probably major consequences on the natural selection of genes regulating stress responses, including Nrf2[61]. Moreover, stress responses preserve core cellular functions at the expense of 'accessory' ones[62,63,64] and therefore must be tightly regulated over time[1]. Nrf2 is no exception to this rule as illustrated by the observation that chronic Nrf2 activation promotes tumorigenesis[65].

Conclusion

The stress response regulated by Nrf2 probably plays a major role in conferring disease tolerance to systemic infections, such as those triggered by bacteria infection and leading to severe sepsis or the one triggered by Plasmodium infection and leading to severe forms of malaria. Viral infections, on the other hand, appear to thrive on host Nrf2 activation, as illustrated by a number of examples in which induction of Nrf2 activity favours virus proliferation. Given the above, it is not clear to what extent the Nrf2 signal transduction pathway may be targeted to treat infectious diseases.

Funding

This work was supported by the Fundação para a Ciência e Tecnologia [grant numbers RECI-IMI-IMU-0038-2012, PTDC/SAU-TOX/116627/2010 and HMSP-ICT/0018/2011 (to M.P.S.) and SFRH/BD/51877/2012 (to A.M.R.)]; and the European Research Council [grant number ERC-2011-AdG 294709-DAMAGECONTROL (to M.P.S.)]

References

1. Medzhitov, R., Schneider, D. S. & Soares, M. P. Disease Tolerance as a Defense Strategy. Science (80-.). 335, 936–941 (2012).
2. Ayres, J. S. & Schneider, D. S. Tolerance of Infections. 271–296 doi:10.1146/annurev-immunol-020711-075030
3. Schneider, D. S. & Ayres, J. S. us about treating infectious diseases. 8, 889–895 (2008).
4. CALDWELL RM, SCHAFER JF, COMPTON LE, P. F. Tolerance to Cereal Leaf Rusts. Science (80-.). (1958).
5. Ayres, J. S. & Schneider, D. S. A signaling protease required for melanization in Drosophila affects resistance and tolerance of infections. PLoS Biol. 6, 2764–2773 (2008).
6. Ayres, J. S., Freitag, N. & Schneider, D. S. Identification of drosophila mutants altering defense of and endurance to Listeria monocytogenes

infection. Genetics 178, 1807–1815 (2008).
7. Ashburner, M. The Bacterial Symbiont Wolbachia Induces Resistance to RNA Viral Infections in Drosophila melanogaster. (2008). doi:10.1371/journal.pbio.1000002
8. Råberg, L., Sim, D. & Read, A. F. Disentangling genetic variation for resistance and tolerance to infectious diseases in animals. Science 318, 812–4 (2007).
9. Seixas, E. et al. Heme oxygenase-1 affords protection against noncerebral forms of severe malaria. Proc. Natl. Acad. Sci. U. S. A. 106, 15837–42 (2009).
10. Seixas, E., Coutinho, A., Cardoso, S., Rebelo, S. & Poli, M. Metabolic Adaptation to Cellular Iron Overload Confers Tolerance to. 1–18
11. Soares, M. P., Gozzelino, R. & Weis, S. Tissue damage control in disease tolerance. Trends in Immunology 35, 483–494 (2014).
12. Hayes, J. D. & Dinkova-kostova, A. T. The Nrf2 regulatory network provides an interface between redox and intermediary metabolism. Trends Biochem. Sci. 1–20 (2014). doi:10.1016/j.tibs.2014.02.002
13. Sykiotis, G. P. & Bohmann, D. Stress-Activated Cap ' n ' collar Transcription Factors in Aging and Human Disease. 1–23 (2010).
14. Nathan, C. No Title.
15. Anrather, J., Racchumi, G. & Iadecola, C. NF- kB Regulates Phagocytic NADPH Oxidase by Inducing the Expression of gp91 phox. (2006). doi:10.1074/jbc.M506172200
16. Itoh, K. et al. Keap1 represses nuclear activation of antioxidant responsive elements by Nrf2 through binding to the amino-terminal Neh2 domain. Genes Dev. 13, 76–86 (1999).
17. Suzuki, T., Motohashi, H. & Yamamoto, M. Toward clinical application of the Keap1-Nrf2 pathway. Trends Pharmacol. Sci. 34, 340–6 (2013).
18. Kensler, T. W., Wakabayashi, N. & Biswal, S. Cell survival responses to environmental stresses via the Keap1-Nrf2-ARE pathway. Annu. Rev. Pharmacol. Toxicol. 47, 89–116 (2007).
19. Rada, P. et al. SCF/{beta}-TrCP promotes glycogen synthase kinase 3-dependent degradation of the Nrf2 transcription factor in a Keap1-independent manner. Mol. Cell. Biol. 31, 1121–33 (2011).
20. Wu, T. et al. Hrd1 suppresses Nrf2-mediated cellular protection during liver cirrhosis. Genes Dev. 28, 708–722 (2014).
21. Cullinan, S. B. et al. Nrf2 is a direct PERK substrate and effector of PERK-dependent cell survival. Mol. Cell. Biol. 23, 7198–209 (2003).
22. Pekovic-Vaughan, V. et al. The circadian clock regulates rhythmic activation of the NRF2/glutathione-mediated antioxidant defense pathway to modulate pulmonary fibrosis. Genes Dev. 28, 548–60 (2014).
23. Page, A. et al. Marburgvirus Hijacks Nrf2-Dependent Pathway by Targeting Nrf2-Negative Regulator Keap1. CellReports 6, 1026–1036 (2006).
24. Edwards, M. R. et al. The Marburg Virus VP24 Protein Interacts with Keap1 to Activate the Cytoprotective Antioxidant Response Pathway. CellReports 6, 1017–1025 (2014).
25. Gjyshi, O. et al. Kaposi ' s Sarcoma-Associated Herpesvirus Induces Nrf2 during De Novo Infection of Endothelial Cells to Create a Microenvironment Conducive to Infection. (2014). doi:10.1371/journal.ppat.1004460
26. Kosmider, B. et al. Nrf2 protects human alveolar epithelial cells against injury induced by influenza A virus. Respir. Res. 13, 43 (2012).
27. Kesic, M. J., Simmons, S. O., Bauer, R. & Jaspers, I. Free Radical Biology & Medicine Nrf2 expression modi fi es in fl uenza A entry and replication in nasal epithelial cells ☆. 51, 444–453
28. Olagnier, D. et al. Cellular Oxidative Stress Response Controls the Antiviral and Apoptotic Programs in Dengue Virus-Infected Dendritic Cells. 1–18

(2014). doi:10.1371/journal.ppat.1004566
29. Carvajal-yepes, M. et al. Hepatitis C Virus Impairs the Induction of Cytoprotective Nrf2 Target Genes by Delocalization of Small Maf Proteins. 8941–8952 (2011). doi:10.1074/jbc.M110.186684
30. Nairz, M. et al. Nitric oxide-mediated regulation of ferroportin-1 controls macrophage iron homeostasis and immune function in Salmonella infection. J. Exp. Med. 210, 855–73 (2013).
31. Harvey, C. J. et al. Targeting Nrf2 Signaling Improves Bacterial Clearance by Alveolar Macrophages in Patients with COPD and in a Mouse Model. (2011).
32. Dardenne, C. et al. Nrf2 , a PPAR c Alternative Pathway to Promote CD36 Expression on Inflammatory Macrophages : Implication for Malaria. (2011). doi:10.1371/journal.ppat.1002254
33. Pamplona, A. et al. Heme oxygenase-1 and carbon monoxide suppress the pathogenesis of experimental cerebral malaria. Nat. Med. 13, 703–10 (2007).
34. Gramaglia, I. et al. Low nitric oxide bioavailability contributes to the genesis of experimental cerebral malaria. 1417–1422 (2006). doi:10.1038/nm1499
35. Cabrales, P., Zanini, G. M., Meays, D., Frangos, J. A. & Carvalho, L. J. M. Nitric Oxide Protection Against Murine Cerebral Malaria Is Associated With Improved Cerebral Microcirculatory Physiology. 203, (2011).
36. Martins, Y. C. et al. Nitric Oxide Synthase Dysfunction Contributes to Impaired Cerebroarteriolar Reactivity in Experimental Cerebral Malaria. (2013). doi:10.1371/journal.ppat.1003444
37. Ferreira, A. et al. Sickle hemoglobin confers tolerance to Plasmodium infection. Cell 145, 398–409 (2011).
38. Ferreira, A., Balla, J., Jeney, V., Balla, G. & Soares, M. P. A central role for free heme in the pathogenesis of severe malaria: the missing link? J. Mol. Med. (Berl). 86, 1097–111 (2008).
39. Newton, C. R. J. C., Warrell, D. A. & M, D. Neurological Manifestations of Falciparum Malaria. 695–702 (1998).
40. Jeney, V. et al. Control of disease tolerance to malaria by nitric oxide and carbon monoxide. Cell Rep. 8, 126–36 (2014).
41. Fourquet, S., Biard, D. & Toledano, M. B. Activation of NRF2 by Nitrosative Agents and H 2 O 2 Involves. (2010). doi:10.1074/jbc.M109.051714
42. Gozzelino, R. & Soares, M. P. Coupling Heme and Iron Metabolism via Ferritin H Chain. Antioxid Redox Signal 1754–1769 (2014). doi:10.1089/ars.2013.5666
43. Pietsch, E. C. Nrf2 Mediates the Induction of Ferritin H in Response to Xenobiotics and Cancer Chemopreventive Dithiolethiones. J. Biol. Chem. 278, 2361–2369 (2003).
44. Iwasaki, K., Mackenzie, E. L., Hailemariam, K. & Sakamoto, K. Hemin-Mediated Regulation of an Antioxidant-Responsive Element of the Human Ferritin H Gene and Role of Ref-1 during Erythroid Differentiation of K562 Cells Hemin-Mediated Regulation of an Antioxidant-Responsive Element of the Human Ferritin H Gene and Ro. (2006). doi:10.1128/MCB.26.7.2845
45. Modiano, D. et al. Haemoglobin C protects against clinical Plasmodium falciparum malaria. 305–308 (2001).
46. Evans, J. A. & Timmann, C. No Title. 20, (2017).
47. Guindo, A., Fairhurst, R. M., Doumbo, O. K., Wellems, T. E. & Diallo, D. A. X-Linked G6PD Deficiency Protects Hemizygous Males but Not Heterozygous Females against Severe Malaria. (2007). doi:10.1371/journal.pmed.0040066
48. Williams, T. N. Human red blood cell polymorphisms and malaria. Curr. Opin. Microbiol. 9, 388–94 (2006).
49. Thimmulappa, R. K. et al. Nrf2 is a critical regulator of the innate immune

response and survival during experimental sepsis. 116, (2006).
50. Athale, J. et al. Nrf2 promotes alveolar mitochondrial biogenesis and resolution of lung injury in Staphylococcus aureus pneumonia in mice. Free Radic. Biol. Med. 53, 1584–94 (2012).
51. Rushworth, S. A., Macewan, D. J., Maria, A. & Connell, O. Lipopolysaccharide-induced expression of NAD(P)H:quinone oxidoreductase 1 and heme oxygenase-1 protects against excessive inflammatory responses in human monocytes. J Immunol. (2008). doi:10.4049/jimmunol.181.10.6730
52. Hill, C. & Carolina, N. Nuclear Factor E2-related Factor-2 (Nrf2) Is Required for NLRP3 and AIM2 Inflammasome Activation *. 2, 17020–17030 (2014).
53. Hoetzenecker, W. et al. ROS-induced ATF3 causes susceptibility to secondary infections during sepsis-associated immunosuppression. (2012). doi:10.1038/nm.2557
54. Berghe, T. Vanden, Linkermann, A. & Jouan-lanhouet, S. Regulated necrosis: the expanding network of non-apoptotic cell death pathways. Nat. Rev. Mol. Cell Biol. 15, 135–147 (2014).
55. Brouard, B. S. et al. Carbon Monoxide Generated by Heme Oxygenase 1 Suppresses Endothelial Cell Apoptosis. (2000).
56. Brouard, S. et al. Heme Oxygenase-1-derived Carbon Monoxide Requires the Activation of Transcription Factor NF- □ B to Protect Endothelial Cells from Tumor Necrosis Factor- ⎵ -mediated Apoptosis *. doi:10.1074/jbc.M108317200
57. Vile, G. F., Waltner, C. & Tyrrell, R. M. Heme oxygenase 1 mediates an adaptive response to oxidative stress in human skin fibroblasts. 2607–2610
58. Pham, C. G. et al. Ferritin Heavy Chain Upregulation by NF- □ B Inhibits TNF ⎵ -Induced Apoptosis by Suppressing Reactive Oxygen Species. 529–542 (2003).
59. Brouard, S., Tobiasch, E., Bach, F. H. & Soares, M. P. No Title. (2017).
60. Stocker, R., Yamamoto, Y., Mcdonagh, A. F., Glazer, A. N. & Ames, B. N. Bilirubin Is an Antioxidant of Possible Physiological Importance. 4–7
61. Vale, P. F., Fenton, A. & Brown, S. P. Limiting Damage during Infection : Lessons from Infection Tolerance for Novel Therapeutics. (2014). doi:10.1371/journal.pbio.1001769
62. Kültz, D. Evolution of the cellular stress proteome : from monophyletic origin to ubiquitous function. J Exp Biol 3119–3124 (2003). doi:10.1242/jeb.00549
63. Do, H. O. W. & Respond, C. M OLECULAR AND E VOLUTIONARY B ASIS. doi:10.1146/annurev.physiol.67.040403.103635
64. López-maury, L., Marguerat, S. & Bähler, J. Tuning gene expression to changing to evolutionary adaptation. (2008). doi:10.1038/nrg2398
65. DeNicola, G. M. et al. Oncogene-induced Nrf2 transcription promotes ROS detoxification and tumorigenesis. Nature 475, 106–9 (2011).

ITQB-UNL | Av. da República, 2780-157 Oeiras, Portugal
Tel (+351) 214 469 100 | Fax (+351) 214 411 277

www.itqb.unl.pt